Forschungszentrum Karlsruhe
Technik und Umwelt

Wissenschaftliche Berichte
FZKA 6524

Effects of Humic Substances on the Migration of Radionuclides: Complexation and Transport of Actinides

Third Technical Progress Report

G. Buckau (Editor)

Institut für Nukleare Entsorgung

Oktober 2000

Forschungszentrum Karlsruhe
Technik und Umwelt

Wissenschaftliche Berichte
FZKA 6524

EFFECTS OF HUMIC SUBSTANCES ON THE MIGRATION OF RADIONUCLIDES: COMPLEXATION AND TRANSPORT OF ACTINIDES

THIRD TECHNICAL PROGRESS REPORT

EC Project No.: FI4W-CT96-0027

(Work Period 01.99 - 12.99)

G. BUCKAU (Editor)

Institut für Nukleare Entsorgung

Forschungszentrum Karlsruhe GmbH, Karlsruhe
2000

Als Manuskript gedruckt

Forschungszentrum Karlsruhe GmbH
Postfach 3640, 76021 Karlsruhe

Mitglied der Hermann von Helmholtz-Gemeinschaft
Deutscher Forschungszentren (HGF)

ISSN 0947-8620

Project Partners:

Partner No. 1 (Coordinator): FZK/INE, D
Partner No. 2: BGS, UK
Partner No. 3: CEA-SGC, F
Partner No. 4: FZR-IfR, D
Partner No. 5: KUL, B
Partner No. 6: LBORO, UK
Partner No. 7: CEA-LSLA, F (Associated to Partner No. 3)
Partner No. 8: GERMETRAD, F (Associated to Partner No. 3)
Partner No. 9: RMC-E, UK
Partner No. 10: NERI, DK
Partner No. 11: GSF-IfH, D (Associated to Partner No. 1)

Duration of the Project:

01.97-12.99

Foreword

The present report describes progress within the third year of the EC-project "Effects of Humic Substances on the Migration of Radionuclides: Complexation and Transport of Actinides". The project is conducted within the EC-Cluster "Radionuclide Transport/ Retardation Processes". Without being a formal requirement of the Commission or co-funding bodies, this report documents results of the project in great technical detail and makes the results available to a broad scientific community. Results of the first and second years of the project are published in an equivalent form [1,2].

The report contains an executive summary written by the coordinator. More detailed results are given by individual contributions of the project partners in 20 annexes. Not all results are discussed or referred to in the executive summary report and thus readers with a deeper interest also need to consult the annexes.

[1] Buckau G. (editor) (1998) "Effects of Humic Substances on the Migration of Radionuclides: Complexation and Transport of Actinides, First Technical Progress Report", Report FZKA 6124, August 1998, Research Center Karlsruhe.

[2] Buckau G. (editor) (1999) "Effects of Humic Substances on the Migration of Radionuclides: Complexation and Transport of Actinides, Second Technical Progress Report", Report FZKA 6324, June 1999, Research Center Karlsruhe.

Content

EXECUTIVE SUMMARY

EFFECTS OF HUMIC SUBSTANCES ON THE MIGRATION OF RADIONUCLIDES: COMPLEXATION AND TRANSPORT OF ACTINIDES

THIRD TECHNICAL PROGRESS REPORT

EC Project No.: FI4W-CT96-0027

(Work Period 01.99 - 12.99)

G. Buckau
(FZK/INE)

Content of Executive Summary

INTRODUCTION

The project started 01.97 and had a duration of three years. This report covers the third year, i.e. the period 01.99 - 12.99. Work has been conducted on all Tasks of the project. (Task 1 ("Sampling and Characterization"); Task 2 ("Complexation"); Task 3 ("Actinide Transport"), Task 4 ("Migration Model Development and Testing") and Task 5 ("Assessment of Impact on Long-Term Safety").

The "First Technical Progress Report" [1] and "Second Technical Progress Report" [2] have been published, covering the achievements of the first and second years, respectively. The present third technical progress report covers the third and final year of the project. Through these technical progress reports, individual contributions of different project partners and results in great technical detail are accessible to the scientific community. The final report [3] gives a summary of results and achievements from the whole project, however, in less detail. For demonstration of the impact of humic colloid mediated actinide transport in the far-field of radioactive waste disposals, three migration case studies have been formulated. The outcome of these migration case studies is given in a separate report [4].

The project encompasses development of the necessary input to judge upon the influence of humic substances on the long-term safety of radioactive waste disposal. The project focuses on long-lived radionuclides with high radiotoxicity, i.e. actinides and technetium, and their behavior in the far-field. To assess the impact of humic substances on the radionuclide migration in the far-field, relevant processes need to be introduced into models. These models rest on a step-wise approach where data of individual processes from relatively well defined systems are tested for their applicability on more complex laboratory systems on natural material (especially batch and column experiments under near-natural conditions). The processes described by models developed from laboratory experiments are limited by the size and time constraints of such studies. Furthermore, large-scale inhomogeneities and deviation from equilibrium in the real, more or less open, system cannot be easily developed through investigations on the laboratory scale. In order to achieve adequate confidence that relevant processes have been regarded in models developed, the real system is also investigated with respect to for example, chemical behavior of actinide analogue trace elements in natural humic colloids and the migration behavior of humic colloids present at a real site. A schematic description of the overall approach of the project is shown in Fig. 1.

Contrary to original intentions and for reasons beyond the reach of the project partners, an encompassed research site in France did not materialize and the Sellafield is not anymore a candidate site for disposal. Sellafield, however, is used as a reference site for such geochemical conditions. Material relevant for the German "Königstein" and "Johanngeorgenstadt" uranium mining and milling sites is also used within the project. Some aspects are investigated on Boom Clay material. The German Gorleben site presently is questioned as a candi-

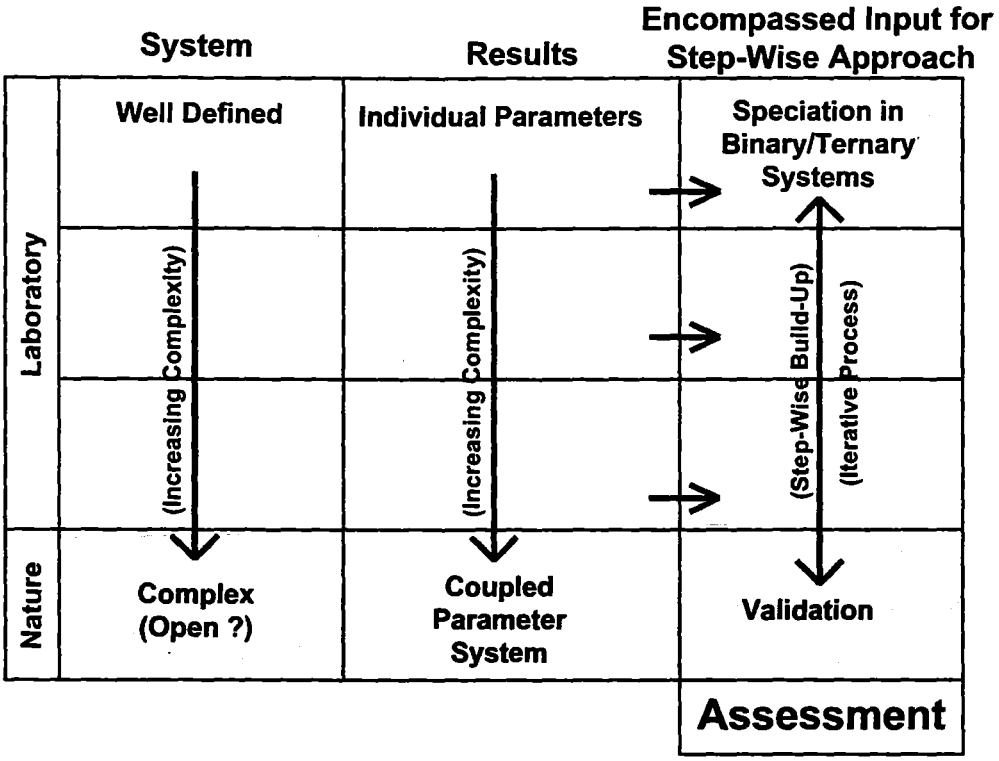

	System	Results	Encompassed Input for Step-Wise Approach	
Laboratory	1. Basic Static Binary/Ternary Systems with Designed/Defined Material	Thermodynamic Data on: - Humate Complexation (Solution) - Humate Complexation (Solid Phase) - Sorption of Humic Substances on Minerals - Kinetics	Speciation in static binary and ternary systems	Iterative Process
	2. Static Batch and Diffusion Exp. with Natural Material	Sorption Data on: - Natural Systems under - Lab-Conditions, including: - Kinetics - Redox	Verification that Data are: - Appropriate, and - Correct	
	3. Dynamic Column Experiments with - Designed/Defined or - Natural Material (Chem-Lab), (Dipole)	Transport Behaviour including: - Kinetics - Redox	Verification that Data are: - Appropriate, and - Correct	
Nature	4. Real (Open) Nat. Analougue In-Situ Kd Geochemical Analysis	Data for: - Natural Geochemical and Hydrological Conditions - Relevant Time-Scales - Geological/Geochemical Transformations	Validation for Natural System: - Lab-Data - Natural Conditions	
			Assessment	

Fig. 1: Schematic description of the overall project approach.

date site. For this site, however, a tremendous amount of data on geology, hydrology and geochemistry, are available. Furthermore, material for laboratory investigations still is available. For these reasons, site-specific work focuses on this site.

The project has been tremendously successful. (1) Material, methods and experimental results have been well documented. (2) The data-base on actinide humate interaction has been extended considerably. (3) For the first time, results from designed laboratory systems and near-natural systems (batch and column experiments) have been brought to a consistent description by introduction of the kinetic concept. (4) Analysis of real aquifer systems has resulted in validated answers to the fate of humic colloids in the far-field. (5) Fundamental process understanding of metal ion humate interaction under laboratory conditions has been improved. (6) Codes have been developed for immediate application to real site predictions.

Humic colloid mediated actinide transport relies on two issues, namely (i) the origin, stability and mobility of humic colloids, and (ii) the interaction between actinide ions and humic colloids. With respect to the first issue, one great achievement has been demonstration that humic colloids in natural groundwater show no significant decomposition or retention, but migrate like ideal tracers until discharged [3]. In one case this was shown to be the case for humic substance introduced 15.000 years ago that until present has migrated as an ideal tracer over a distance of approximately 25 km. In the Gorleben aquifer system, also no indication for decomposition or retention of humic colloids was found. With respect to the second issue, a major achievement has been introduction of a kinetic approach. The outcome is consistency and predictability, including upscaling, of near-natural systems in the laboratory. The question of actinide humate interaction, nevertheless remains an unresolved problem. The reason is that the chemical behavior of actinide ions added under laboratory conditions and the behavior of natural trace metal ions, including naturally occurring actinides, deviate strongly from each other. A great portion of natural trace element constituents of natural humic colloids is found to be practically irreversibly bound, including natural actinide ions. This is of major concern, because selection of input-data for application of the developed codes, therefore remains an unsolved problem.

Application of kinetic data from laboratory investigations results in a considerably enhanced humic colloid mediated actinide migration velocity compared to application of an equilibrium concept (Kd concept) or even worse, ignoring humic colloids. A much greater enhancement of predicted actinide transport, however, is the result of applying data obtained from analysis of natural chemical analogues. In this case, one portion of humate bound actinide ions is found to migrate like an inert tracer. The consequence for safety assessment is that, until otherwise can be proven, humic colloid mediated actinide transport will lead to unhindered transport for a portion of actinide ions. This portion will govern the individual dose from actinide ions in case of a release.

1. OBJECTIVES

The main objective of the project is to determine the influence of humic substances on the migration of radionuclides. For the long-term safety, long-lived highly radiotoxic nuclides are the most relevant. The project therefore focuses on actinide elements and technetium. In order to achieve the main objective a thorough understanding is needed for (i) the complexation of actinides with humic substances, (ii) the influence of humic substances on the sorption properties of sediments, and (iii) the mobility of actinide humic substance species in groundwater.

2. PARTNERS AND PROJECT STRUCTURE

The project had 11 partners and one additional temporary partner. Three partners are associated to other contractors. The partners and their partnership is as follows:

Partner No. 1 (Coordinator): FZK/INE, D

Partner No. 2: BGS, UK

Partner No. 3: CEA-SESD, F

Partner No. 4: FZR-IfR, D

Partner No. 5: KUL, B

Partner No. 6: LBORO, UK

Partner No. 7: CEA-LASO, F, (Associated to Partner No. 3)

Partner No. 8: GERMETRAD, F, (Associated to Partner No. 3)

Partner No. 9: RMC-E, UK

Partner No. 10: NERI, Dk

Partner No. 11: GSF-IfH, D, (Associated to Partner No. 1)

Temporary Contributor: Uni-Mainz (EC-TMR grant FI4W-CT97-5005)

The project is divided into five tasks with a project structure as shown in Fig. 2.

3. SUMMARY OF RESULTS

A brief summary of major achievements during the third (and last) year of the project is given below. Details can be found in the annexes.

Project Management Structure
(Overview)

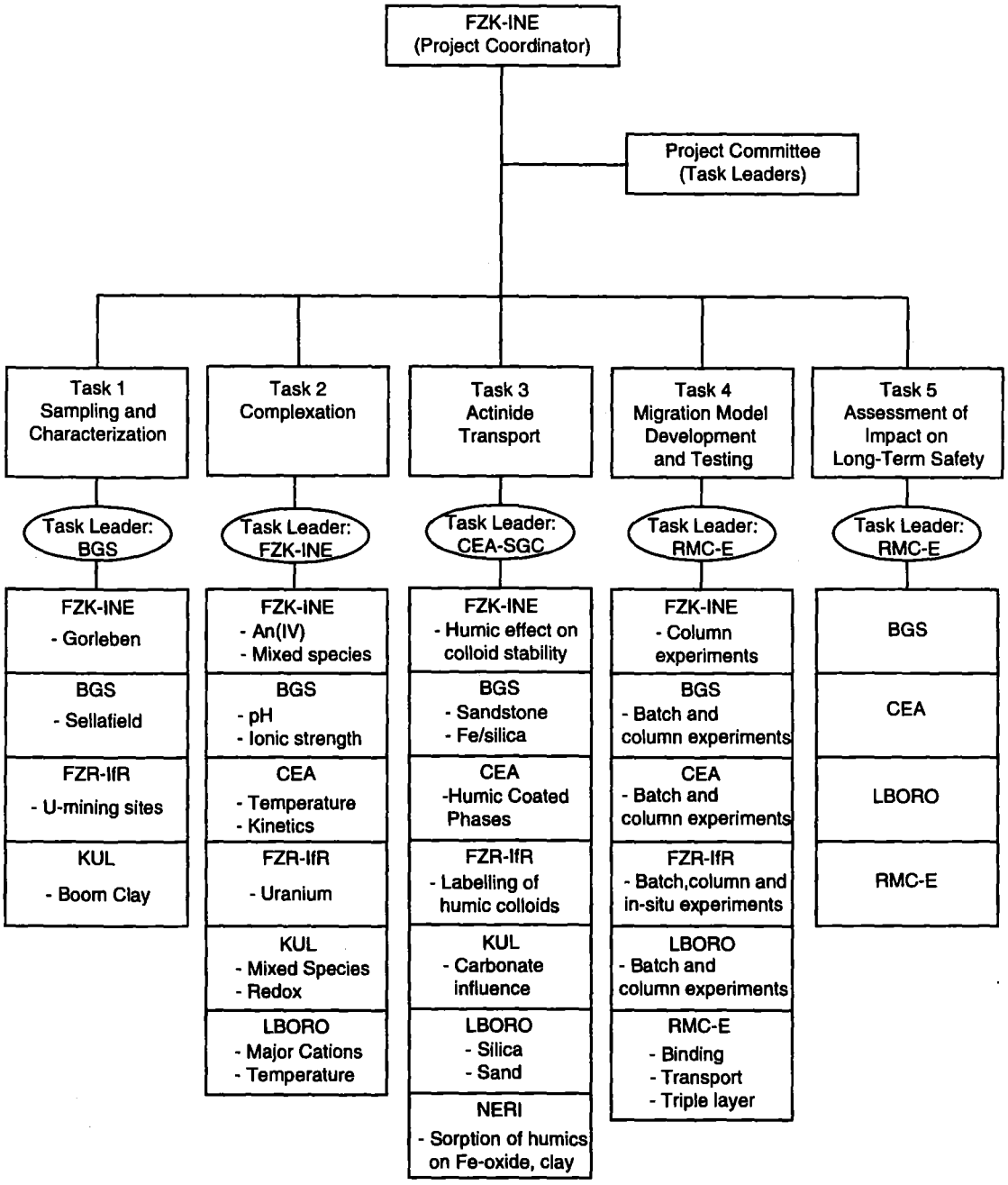

Fig. 2: Project structure

3.1 TASK 1 (Sampling and Characterization)

The objectives of this task are to ensure sampling and appropriate characterization of relevant experimental material, ensure appropriate documentation of the sampling and characterization and thus provide the basis for trustworthy interpretation of results and intercomparison studies between different laboratories. Natural experimental material from Gorleben (D), Sellafield and Derwent Reservoir (UK), Johanngeorgenstadt (D), Königstein (D) and reference sites have been sampled and characterized.

Although this task was formally finalized already in the first year of the project, results have shown the benefit in developing new experimental systems. In this last year of the project, this includes generation and characterization of ^{14}C synthetic humic acid (^{14}C-M1) allowing for direct determination of humic acid distribution and exchange velocity between different phases. A set of columns with different sediments conditioned with one Gorleben groundwater allows insight in the impact of differences in characteristic properties of sediments. This work also reconfirmed the importance of extended (several months) conditioning of near-natural column systems and thorough monitoring of hydraulic and chemical parameters.

Characterization data for the large variety of experimental material can be found in different individual contributions in the foregoing and the present technical progress reports as well as different publications. In addition to this, in Annex 20 some important characteristic data are summarized.

3.2 TASK 2 (Complexation)

The objectives of this task are to provide relevant basic data on actinide/technetium humate complexation and the reduction of the redoxsensitive elements. Considerable progress has been achieved in a number of issues: (i) critical assessment of experimental methods; (ii) humate and fulvate complexation of the trivalent europium ion, the tetravalent neptunium, thorium and technetium ions, and hexavalent uranyl ion; and (iii) actinide desorption kinetics.

There has been a general continuation of the generation of actinide humate complexation data. Most significant achievements are initial data on the tetravalent actinide and technetium humate interaction and more insight in the formation of mixed complexes. The amount of data on the desorption kinetics of actinide ions has grown considerably. Nevertheless, further studies on these issues are required in order to provide the required scientific basis. One example is the desorption kinetics of humic colloid bound actinide ions that is shown to depend on a variety of parameters, including pH, ionic strength and the humic colloid concentration. This experimental basis, however, has not yet allowed establishing adequate process understanding.

For this purpose, characterization of local binding environment by EXAFS and FTIR has been initiated. Further such studies will be required in order to provide the necessary experimental basis for firm and exhaustive conclusions. In addition, further development of possible collective polyelectrolyte properties or humic-humic association/agglomeration is required (cf. task 4 "model development and testing").

3.3 TASK 3 (Actinide Transport)

The objectives of this task are to identify, describe and quantify relevant mechanisms influencing the actinide and technetium transport by batch and column experiments on both defined/designed and natural material. This includes not only migration of actinide elements and technetium on natural material under near-natural conditions and covalently humic acid coated silica beads, but also for example, the sorption of humic acid on mineral surfaces and the influence of humic acid and various minerals on the reduction of redoxsensitive elements.

The transport behavior of uranium, europium and technetium has been investigated by column experiments on Gorleben groundwater and sediments from Gorleben and various sites in Bavaria. The importance of humic colloid mediated transport, as already previously demonstrated for trivalent americium and europium, is verified. Results show that the scavenging function of sediments for actinide ions desorbed from aquatic humic colloids appears largely independent of the type of groundwater equilibrated sediment. Possible impact of grain size and thus the total sediment surface still needs to be verified.

Experiments with a variety of sediments (hematite, goethite, silica, muscovite, kaolinite and aluminum oxide) shows that aquatic humic acid sorbs on fresh sediment surfaces and that specific sediment surface properties, and not only the surface area, are essential for the humic acid sorption. One promising approach is inclusion of the protonation of functional groups of humic acid and sediment surface functional groups. The actinide distribution in binary (no humic acid) ternary systems is investigated. Investigations on the kinetics of equilibration of ternary systems show that irrespective the order of addition of the ternary system components, within less than 24 hours the same species distribution is found.

In addition, the key question concerning the origin, long-term stability and mobility of natural humic colloids in real aquifer systems has been analyzed in real aquifer systems [3]. Geochemical and isotope-geochemical analysis show no indication for decomposition or sorption of humic colloids. This is of great importance because indications of unhindered mobility of humic colloids in column experiments cannot be up-scaled for distances, time-scales and conditions relevant under real conditions. For the assessment of the impact of humic substances this means that it needs to be assumed that humic colloids in the far-field

will remain stable until their discharge with surface water takes place. This also simplifies modeling, because retention of humic colloids can be omitted.

3.4 TASK 4 (Migration Model Development and Testing)

The objectives of this task are to rationalize the state of understanding by establishing numerical models, test these models to ensure their applicability or identify processes still not adequately understood. Following conclusions already during the first project meeting, development of new models for transport modeling was necessary. The major achievement has been to develop and test models taking the above mentioned non-equilibrium in batch and column experiments into account.

In the past, interpretation of actinide transport based on the thermodynamic equilibrium approach and filtering of humic colloids has been subject to major difficulties. Application of such approaches does not allow for comparison of different systems, nor scaling within the same experimental system. The solution was development of a kinetic approach, successfully implemented in the open transport code K1D allowing for incorporation of equilibrium and kinetics of different reactions, as required.

A mechanistic model has been developed based on humic colloids as penetrable dispersed polyelectrolyte microgels where the metal ion complexation is governed by the exchange of metal ions with polyelectrolyte counterions. An important question is the size or molecular weight necessary for reaction energy from the collective polyelectrolyte properties to dominate over the local interaction with functional groups. Furthermore, association/agglomeration as a consequence of local charge neutralization by metal ion complexation may need to be considered. None of presently available metal ion humate complexation models provide process understanding with respect to the observed kinetic processes. Therefore, despite the great progress within the present project, continued efforts on the development of metal ion humate interaction process understanding is required.

3.5 TASK 5 (Assessment of Impact on Long-Term Safety)

Task 5 consists of (i) implementation of the developed migration models into actinide transport code; (ii) development of generic criteria for optimization of the transport code; and (iii) development of migration cases for application of the transport code to real site conditions. The latter is serves the visualization of the impact of humic substances on the predicted migration of actinide ions at different sites making use of different input-data.

Three different migration case studies have been formulated for the Gorleben and Dukovany sandy aquifer sites and for a uranium mining and milling rock pile [4]. The Dukovany migration case is a valley near the Dukovany power plant, 300 m south from a shallow low-level waste repository in the Czech Republic [5]. Exhaustive mineralogical, petrological and geochemical data are available for this shallow site in a sand deposit with some silt and clay. The Dukovany site is very similar to the British low-level disposal site at Drigg in Cumbria.

Transport calculations of Pu in Dukovany are shown in Fig. 3. This figure illustrates the dilemma of predictive actinide transport calculations at real sites. The tool for modeling has been developed and is ready for immediate application. The process understanding, however, is insufficient to decide upon appropriate input data. Calculations on the Dukovany site demonstrate the grave underestimation of Pu migration if humics are ignored. Furthermore, application of equilibrium data (cf. Kd concept) also leads to drastic underestimation of the mobility of plutonium. The same is true for application of the "conservative roof" approach [6]. It is therefore clear that a kinetic approach needs to be applied. However, the dilemma is that (a) laboratory investigations, where plutonium is contacted with groundwater humic colloids under conditions and time-frames that can be applied in the laboratory and (b) dissociation of tetravalent trace metal ions from natural humic colloids, lead to very different results. The overall outcome is that actinide ions possibly irreversibly bound to humic colloids is the main concern, whereas ionic non-humic colloid bound species will show extensive retention.

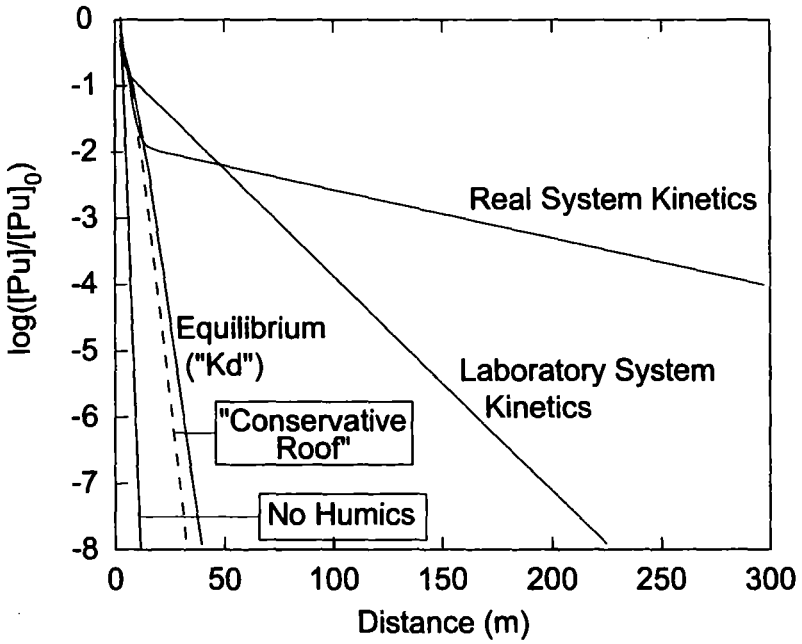

Fig. 3: Development of plutonium concentration in groundwater for a release according to the Dukovany migration case study and application of different approaches reflecting absence of humic substances, the "Conservative roof approach" [6] and differences in kinetics of relevant processes in the presence of humic substances.

4. REFERENCES

[1] Buckau G. (editor) (1998) "Effects of Humic Substances on the Migration of Radionuclides: Complexation and Transport of Actinides, First Technical Progress Report", Report FZKA 6124, August 1998, Research Center Karlsruhe.

[2] Buckau G. (editor) (1999) "Effects of Humic Substances on the Migration of Radionuclides: Complexation and Transport of Actinides, Second Technical Progress Report", Report FZKA 6324, June 1999, Research Center Karlsruhe.

[3] Buckau G. (editor) (2000) "Effects of Humic Substances on the Migration of Radionuclides: Complexation and Transport of Actinides, Final Report, EUR report, in press.

[4] Buckau G., Bryan N. and Schmeide K. (2000) "Effects of Humic Substances on the Migration of Radionuclides: Three Migration Case Studies" (tentative title), FZKA Report, Research Center Karlsruhe, in preparation.

[5] Bryan N. "Humics Project: Dukovany Migration Case Study", RMC-E report R00-041(E), April 2000, RMC Environmental, UK

[6] Hummel W., Glaus M. and Van Loon L.R. (1995) "Binding of Radionuclides by Humic Substances: The Conservative Roof Approach", in: Binding Models Concerning Natural Organic Substances in Performance Assessment, Proceedings of an OECD-NEA Workshop organized in co-operation with the Paul Sherrer Institute, Bad Surzach, Switzerland, 14-16 September 1994.

Annex 1

Actinide transport in column experiments: Influence of humic colloids

(R. Artinger, T. Schäfer and J.I. Kim (FZK/INE))

3rd Technical Progress Report

EC Project:

"Effects of Humic Substances on the Migration of Radionuclides: Complexation and Transport of Actinides"

Project No.: FI4W-CT96-0027

Actinide Transport in Column Experiments: Influence of Humic Colloids

R. Artinger, T. Schäfer and J.I. Kim

Forschungszentrum Karlsruhe, Institut für Nukleare Entsorgung

PO Box 3640, 76021 Karlsruhe, Germany

Actinide transport in column experiments: Influence of humic colloids

R. Artinger, T. Schäfer and J.I. Kim

Forschungszentrum Karlsruhe, Institut für Nukleare Entsorgung
Postfach 3640, 76021 Karlsruhe, Germany

Introduction

In natural aquifers, aquatic humic colloids are ubiquitous and take part in geochemical solid-water-interface reactions. Due to their strong interaction with multivalent actinide ions, humic colloids exert a crucial influence on the mobility of actinides.

The humic colloid-mediated actinide migration can be studied by column experiments, which enable the variation of different parameters like flow velocity and column length. Column experiments with natural sandy sediments and groundwaters rich in humic colloids demonstrate that a fraction of actinides, such as Am(III), U(VI), Np(IV/V) migrates as humic colloid-borne species by the same velocity as a conservative tracer, e.g. tritiated water [1-3]. The fraction of humic colloid-borne actinides is generated by kinetically controlled processes governing the actinide/humic colloid interaction [2, 4] and the redox behavior of actinide ions [5]. From inorganic colloids, such as iron oxides, a mobilization by humic substances is also reported [6]. Where actinide ions interact with inorganic colloids, by surface sorption or incorporation via alteration processes, this humic substances enhanced inorganic colloid transport is of special importance.

The influence of aquatic humic colloids on the migration behavior of tetravalent Th is studied by column experiments with natural sandy sediment and groundwater rich in humic substances, both from the Gorleben aquifer (Lower Saxony, Germany). The influence of the groundwater residence time in the column and the equilibration time of Th with groundwater prior to the injection into a column are investigated. The results are compared with data from other column experiments studying different actinides. Furthermore, first results are presented on the humic stabilized transport of inorganic colloids on low cristalline colloidal Fe(III) phase 2-line ferrihydrite (HFO) in presence of Am(III).

Experimental

Migration experiments were performed under inert gas conditions (Ar + 1 % CO_2) in a glove box using columns of 250 and 500 mm length and 50 mm in diameter, tightly packed with pleistocene aeolian quartz sand sampled from the near aquifer surface at the Gorleben site. Tritiated water, HTO, was used as a conservative tracer to determine the hydraulic properties of the columns. The sand columns were equilibrated with a Gorleben groundwater, indicated as GoHy-532, for more than 1 year. Due to equilibration under 1 % CO_2 partial pressure, the pH shifted to 7.6 compared to 8.9 of the original groundwater. Detailed characterization of the sediment and groundwater can be found elsewhere [7].

Th migration experiments were carried out with flow lenghts of 25 and 75 cm (connecting a 25 and 50 cm column in series) and a Darcy velocity varying from 0.02 to 0.35 m/d. The corresponding migration time was between 6 hours and 17 days. For all experiments, 1 mL of ^{234}Th spiked initial solution with a Th concentration of ~$5 \cdot 10^{-12}$ mol/L was injected into the column. Th was allowed to react with the groundwater GoHy-532 for 0.5 hour to 18 days. Ultrafiltration experiments with a nominal molecular size cutoff from 10^3 to 10^6 Dalton (Filtron Co., Microsep™ Microconcentrators, USA) confirm the quantitative binding (>99 %) of Th onto the humic colloids. The elution of HTO and radionuclides investigated were measured by single fraction analysis by liquid scintillation counting (HTO, ^{234}Th) and by γ spectrometry (^{59}Fe, ^{241}Am, ^{243}Am).

For preparation of radioactive 2-line-ferrihydrite (HFO), the synthesis described by Schwertmann and Cornell [8] was modified using an irradiated 99.99+ % pure iron foil (GoodFellow, Germany). The activated iron foil was dissolved in HNO_3, adding 2.5 g of inactive $Fe(NO_3)_3 \cdot 9H_2O$ salt. HFO was formed by adding 1 M KOH to adjust the pH to 7-8 for 2 hours at room temperature. The purification of HFO was performed by washing up to five times with Milli-Q water (centrifugation, decantation and re-dispersion). By this procedure stabile HFO colloid suspensions were obtained.

HFO colloid migration experiments were carried out using a column length of 25 cm and a Darcy velocity between 0.2 and 0.3 m/d. ^{241}Am was allowed to sorb onto HFO colloids for 1 hour. Afterwards, the ^{241}Am spiked HFO colloids were added to the groundwater GoHy-532 with a contact time between 1h and 18 hours prior to injection into the column. ^{243}Am had reacted previously also for 1 hour with GoHy-532. Fig.1 shows a simplified diagram of this spike procedure prior to injection into the column. Total injected americium (^{241}Am and ^{243}

Am) concentration was $7.7 \cdot 10^{-7}$ mol/L for all experiments. The HFO colloid concentration used for pulse injections was 2.95 mg/L for a molar mass of 89 g HFO/mol Fe and 6.72 mg/L for continuous injection. The total injection volumes were 1 ml for pulse injection and 168.2 ml (~1 pore volume) for continuous injection. In order to determine changes in the humic colloid concentration in eluted groundwater, UV/Vis spectroscopy was performed using a CARY-5E spectrometer (Varian Co., USA). For analysis of the relative humic colloid concentration the absorption signal at 300 nm was used.

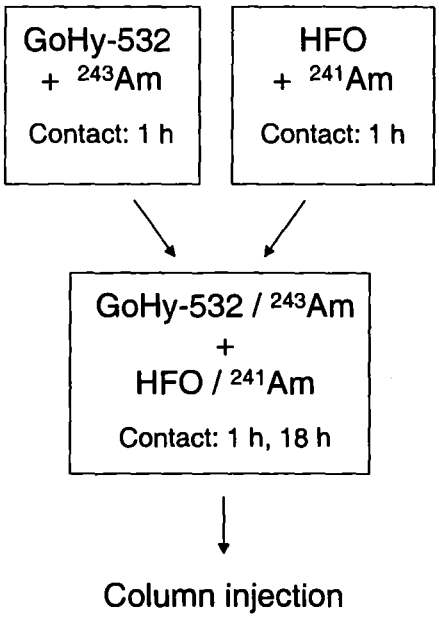

Fig. 1: Simplified diagram of the preparation of Am spiked groundwater GoHy-532 used for HFO colloid migration experiments.

Results and discussion

Th migration experiments

Humic colloid-mediated Th migration was studied varying the groundwater residence time in the column and the equilibration time of Th with groundwater prior to the injection into the column. In Fig. 2, the Th breakthrough curves are shown. In all experiments humic colloid-borne Th migration is about 5 % faster than the groundwater flow velocity. This is attributed

to a pore size exclusion process of humic colloid-bound Th. The fraction of humic colloid-borne Th is increased with increasing equilibration time and decreasing migration time. This is attributed to a kinetically controlled association/dissociation of Th with humic substances and a subsequent sorption onto the sediment surface. This kinetically influenced migration behavior is also observed for Am(III) and U(VI) [9] and discussed in more detail in [10].

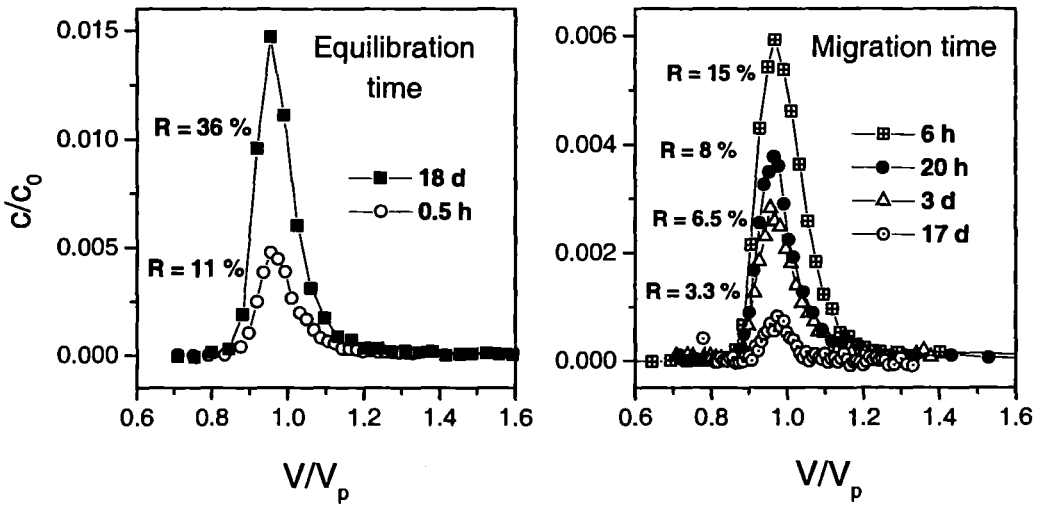

Fig. 2: Th breakthrough curves as a function of the equilibration time of Th with groundwater prior to the injection into the column (left) and the migration time in the column (right). R is the recovery of humic colloid-borne Th.

Depending on the migration and equilibration time of the Th humic colloid complex, the fraction of unimpeded humic colloid-borne Th varies from 3 to 36 %. This Th fraction is comparable to that of Am(III), which was investigated under comparable conditions. Due to the long-term equilibration between groundwater and sediment as well as an almost quantitative recovery of Np(IV) humate colloids [7], retention of humic colloid-borne Th is unlikely. Therefore, one may conclude that Th(IV) is retained by the dissociation from the humic colloid and a subsequent sorption onto the sediment. Accordingly, the dissociation kinetics of Th(IV) from humic colloids seems to be comparable to that of Am(III) under the given groundwater conditions.

Overview of column experiments studying humic colloid-borne actinide migration

Results from column experiments performed at different laboratories studying the humic colloid-borne migration of different actinide ions are shown in Fig. 3. Here, results from the Research Center Karlsruhe (FZK) (partly obtained in cooperation with Research Center Rossendorf and University of Mainz) [2, 7, 9], the Technical University of Munich (TUM) [1, 11, 12] and the National Research Center for Environment and Health (GSF) [1, 13] are shown. The recovery of unimpeded humic colloid-borne actinides (including the lanthanide Eu) in these different column experiments shows a clear dependency with the concentration of actinides bound to humic colloids. All these experiments were performed with groundwaters rich in humic colloids (GoHy-532 and –2227) and a Pleistocene aeolian quartz sand from the Gorleben site. Common features of the experiments are: i) a humic colloid concentration of 60 to 160 mg/L, ii) pH of about 7.5, iii) an equilibration time >2 days between actinide ions and humic colloids and iv) a migration time of 5 to 20 hours. Within this bounds a variation of the recovery of humic colloid-borne actinides is expected. However, the variations shown in Fig. 3 are much larger than expected. As seen in Fig. 3, in general, the recovery of humic colloid-borne actinides increases with increasing concentrations of actinide ions bound to humic colloids. To get a stoichometric relation between the humic colloids and the actinides an average molecule weight of 1000 g/mol is assumed [14]. From this number equimolar conditions may derived at an actinide concentration of about 10^{-4} mol/L. This region of an estimated equivalent stoichiometry of actinides and humic colloids calculated for the different groundwaters is shown in Fig. 3 by the shaded vertical line. At lower actinide concentrations, one humic colloid should be loaded with only one (or none) single actinide ion (single actinide complexation), whereas at higher actinide concentrations one humic colloid should be loaded with more than one actinide ions (multiple actinide complexation). Thereby, the loading is still low enough to maintain stable humic colloids under given groundwater conditions. In case of migration experiments with ^{233}Pa concentrations of about 10^{-11} to 10^{-12} mol/L, the concentration of the simultaneously present mother nuclide ^{237}Np is used. The following can be concluded from Fig. 3:

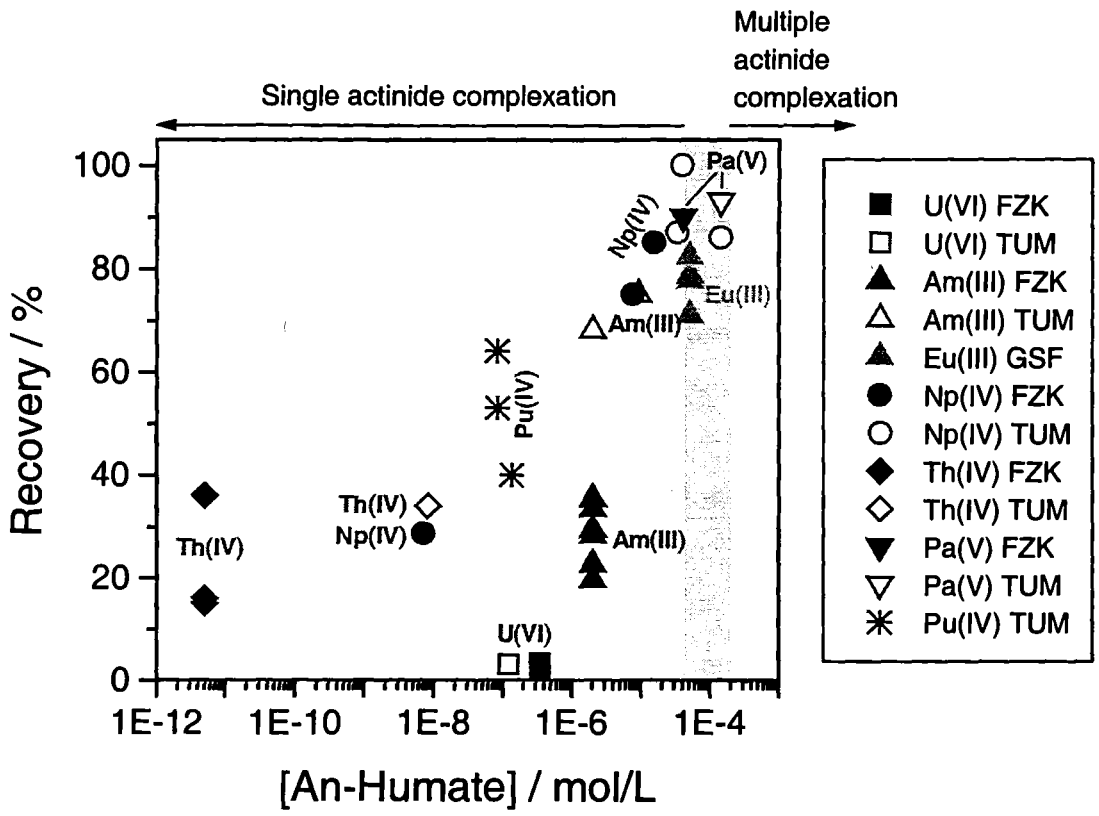

Fig. 3: Recovery of unimpeded humic colloid-borne actinides in column experiments as a function of the actinide concentration bound to humic colloids. The shaded area represents an estimated equivalent stoichiometry of actinides and humic colloids (see text). Migration experiments from the Research Center Karlsruhe (FZK), the Technical University of Munich (TUM) and the National Research Center for Environment and Health (GSF) are shown. Common features of the experiments are: i) a humic colloid concentration of 60 to 160 mg/L, ii) ~pH 7.5, iii) an equilibration time >2 days between actinides and humic colloids and iv) a migration time of 5 to 20 hours.

i) The fraction of humic colloid-borne actinides is comparable for Th(IV), Pa(V) and U(VI) between FZK and TUM. For Np(IV) concentrations $>10^{-5}$ mol/L the fraction of humic colloid-borne Np is also similiar. This agreement between both laboratories emphasizes the capability and reproducibility of column experiments to investigate the humic colloid-borne actinide transport. However, a discrepancy is found for Np(IV), Am(III) and Eu(III), respectively, for the transition from single actinide loading onto the humic colloids to equivalent concentrations with a possible multiple actinide complexation.

ii) A high mobilization of humic colloid-borne actinides (recovery >75 %) is observed for Am(III), Np(IV) and Pa(V) only at actinide concentrations close to an equivalent humic colloid concentration. Contrary to this, the recovery of Am(III) and the tetravalent actinides Th(IV), Np(IV) and Pu(IV) is much lower for low actinide concentrations. Even in the case of a long-term equilibration period of Pu(IV) with humic colloids up to four years, the fraction of colloid-borne Pu is lower than 75 % [12].

iii) The humic colloid-facilitated mobilization of trace amounts of tri- and tetravalent actinides is much higher than that of U(VI).

In summary, the comparison of numerous column experiments reflects the influence of the chemical behavior of the actinide on its humic colloid-borne mobilization. Furthermore, the experiments performed at different laboratories indicate an influence of the concentration of actinide ions bound to humic colloids. It is obvious that a higher actinide concentration may change the nature the humic colloid, e.g. due to charge neutralization effects. Therefore, beside the humic colloid concentration in groundwater and the kinetically controlled association/dissociation of actinides with humic substances, it may also be necessary to take into account the stoichiometric ratio of actinides and humic colloids. Additional experiments are indispensable to study this concentration dependency under well defined conditions and its effect on the humic colloid-borne mobilization of actinides.

Migration of humic stabilized HFO in Gorleben groundwater

The recovery for pulse injections of americium (^{241}Am, ^{243}Am) and HFO (^{59}Fe) are listed in Tab. 1. ^{59}Fe as an indicator for HFO colloids could not be used for pulse injection experiments, due to the effects of dispersion. The migration velocity for Am in the HFO/humic colloid system is up to 6 % higher than for HTO as it is typical for humic colloid borne actinide migration (see above). Higher migration velocities due to the larger colloid size of HFO and a more pronounced effect of pore size exclusion could not be observed. An increase of the equilibrium time of ^{241}Am spiked HFO with ^{243}Am spiked GoHy-532 from 1 hour to 18 hours enhanced the mobility of both americium isotopes. This effect of higher Am recoveries with increasing contact time is comparable with that from previously performed migration experiments without addition of inorganic colloids demonstrating a similar association/dissociation kinetics [2].

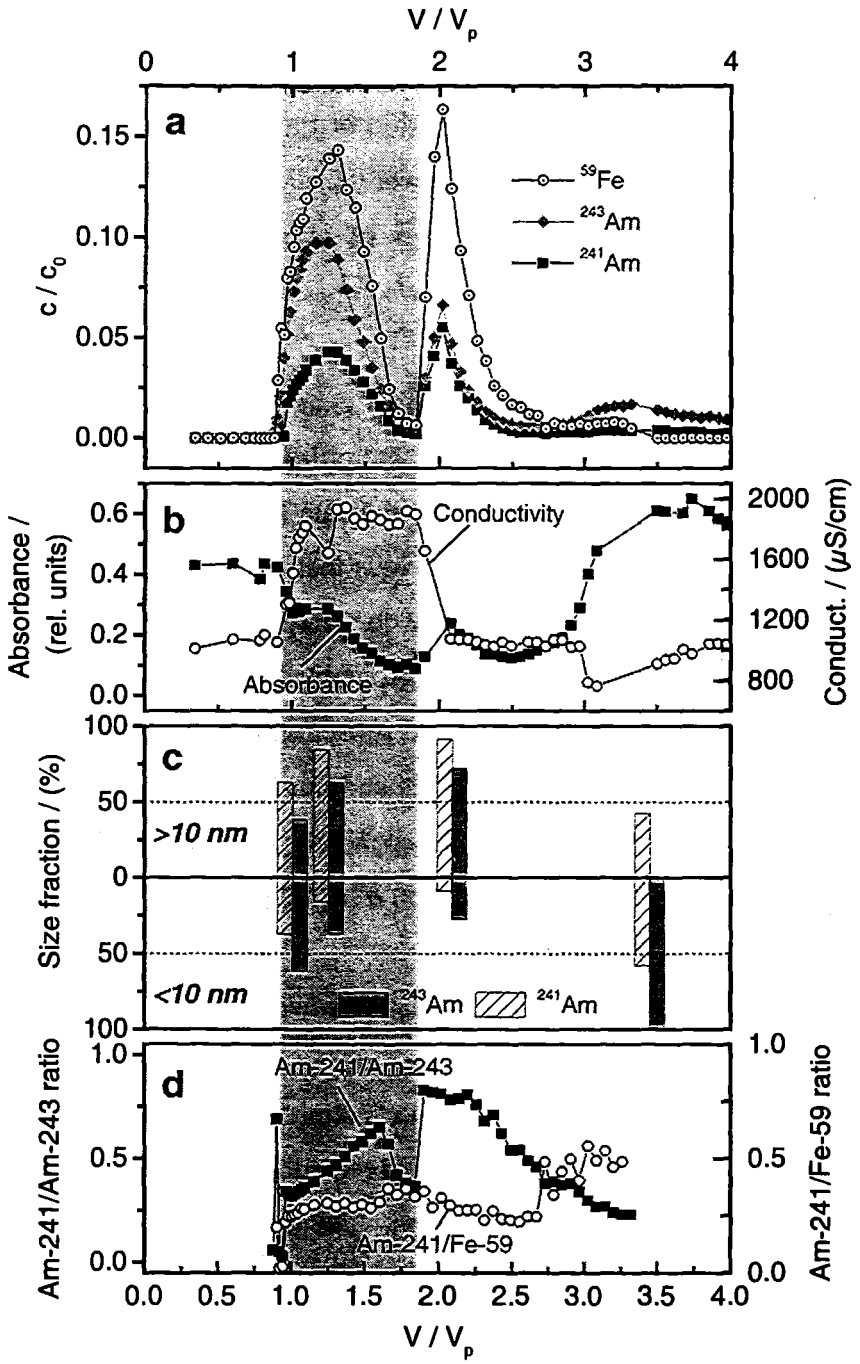

Fig. 4: Column experiment on HFO colloid facilitated Am migration
a) Breakthrough curves of ^{241}Am, ^{243}Am and ^{59}Fe (HFO indicator).
b) Conductivity and absorbance at 300 nm of effluent.
c) Size characterization of eluted ^{241}Am and ^{243}Am determined by ultrafiltration.
d) $^{241}Am/^{243}Am$ and $^{241}Am/^{59}Fe$ isotope ratios in effluent.

Table 1: *Results from HFO/Americium column experiments in GoHy-532 groundwater*

Equilibrium time (h):	Injection type:	Total Recovery ^{241}Am:	Retardation $R_{f(^{241}Am)}$	Total Recovery ^{243}Am:	Retardation $R_{f(^{243}Am)}$	Total Recovery ^{59}Fe:
1h	Pulse	0.5 %	0.97	0.9 %	0.97	n. d.*
18h	Pulse	4.6 %	0.95	7.2 %	0.94	n. d.*
18h	Continuous	4.6 %	-	9.3 %	-	14.6 %

* : not detected

In the continuous injection experiment the sorption and remobilization behavior of HFO and humic colloids was monitored (Fig. 4). Due to insufficient purification of the HFO colloid suspension (KNO_3 residues), the electrical conductivity was increased from ~1 mS/cm in GoHy-532 to 2 mS/cm (Fig. 4b). The increase in ionic strength results in a significant immobilization of HFO and humic substances in the column. For the HFO (^{59}Fe signature) and $^{241/243}$Am breakthrough (^{241}Am, ^{243}Am) no plateau value was reached as it is expected and visible in the conductivity measurements (Fig. 4b). After reaching a first breakthrough maximum a steep decline can be observed in Fig. 4a. Parallel to this, the UV/Vis absorbance at 300 nm changed from 0.4 to 0.1 relative units indicating an immobilization of humic substances in the column. Analysis of this first breakthrough leads to a recovery of 9.1 % ^{59}Fe spiked HFO, 2.5 % ^{241}Am and 5.4% ^{243}Am. At the early beginning of this first breakthrough a single peak with significantly higher ^{241}Am/^{243}Am and ^{241}Am/^{59}Fe ratios is detected (Fig. 4d). This signal indicate an unretarded HFO colloid transport even faster than the mean travel time of humic colloids due to size exclusion from smaller pores.

Changing the permeating fluid to the non-spiked groundwater a decline in ionic strength and a mobilization of HFO and organic colloids are observed. This second breakthrough results in recoveries of 5.5 % HFO, 1.5 % ^{241}Am and 1.9 % ^{243}Am. After three pore volumes, remobilization of humic substances is found as indicated by an increase of the absorbance signal at 300 nm. Parallel to this, for ^{243}Am a third broad breakthrough with a recovery of additional 2.0 % is found. A colloid size of approximately 10 nm (corresponds to a nominal filter pore size of 100 kD) is found to be suitable to discriminate between humic (<10 nm) and HFO colloids. HFO showed a maximum in colloid number in the range of 60-70 nm as determined by Photon Correlation Spectroscopy (PCS). Ultrafiltration of the effluent measured in all three breakthrough sections revealed that the fraction of ^{241}Am bound to

colloids >10 nm is significantly higher than that of ^{243}Am (Fig. 4c). These ultrafiltration results indicate, that a fraction of ^{241}Am remains on HFO colloids throughout the retention period in the column (about 20 h for three pore volumes), which doesn't achieve equilibrium with ^{243}Am initially bound onto humic colloids. This observation is confirmed by the constant ^{241}Am/^{59}Fe isotope ratio.

The lower recovery of ^{241}Am compared to ^{243}Am is attributed to the HFO retention in the column as shown by the total HFO recovery of 14.6 %. Contrary to this, for humic substances no significant interaction with the sediment is expected due to the long-term equilibration procedure. The ^{241}Am/^{243}Am isotope ratio reflects the different breakthrough behavior of the americium isotopes. Accordingly, changes in the ^{241}Am/^{243}Am isotope ratio could be related to the different immobilization and mobilization behavior of the HFO and humic colloids.

From the column migration experiments the following results can by summarized:

i) Initially positively charged HFO colloids are partly mobile in pH neutral Gorleben groundwater GoHy-532 rich in humic substances.
ii) Humic stabilized HFO colloids facilitate the Am migration. A fraction of Am is bound onto HFO colloids, which doesn't achieve equilibrium with the solution within the retention period in the column. The fraction of HFO colloid-borne Am is relatively low compared to the humic colloid-borne Am migration due to the high retention of 85 % of the HFO colloids onto the sediment.
iii) Humic stabilized HFO colloids immobilized in the sandy aquifer can be mobilized by changes in the groundwater conditions.

Conclusion

Column experiments studying the influence of humic colloids on the Th(IV) migration confirm the kinetics of the metal humic colloid association/dissociation as a key issue for the actinide migration behavior. Comparison of numerous actinide migration experiments performed in different laboratories indicates an additional influence, namely the actinide loading onto the humic colloids. Therefore, beside the actinide speciation in groundwater and

the kinetics of the actinide humic colloid interaction, it may also be necessary to take into account the stoichiometric ratio of actinides and humic colloids.

First migration experiments demonstrate the mobility of humic stabilized colloidal 2-line-ferrihydrite (HFO) under near natural conditions. Otherwise, positively charged HFO colloids should not migrate. Am(III) was found to be partly mobilized as HFO colloid-borne species. Therefore, humic substances may intervene in the aquatic subsurface actinide migration not only as immediate actinide carrier but also as stabilizing agent for an inorganic colloid mediated mobilization. Further experiments are in progress to study this influence of humic stabilized inorganic colloids on the actinide migration. The results obtained from actinide migration experiments with groundwaters rich in humic colloids emphasize the complexity of the humic colloid facilitated actinide transport.

References

1. Kim, J.I., Delakowitz, B., Zeh, P., Klotz, D., Lazik, D.: A column experiment for the study of colloidal radionuclide migration in Gorleben aquifer systems. Radiochim. Acta **66/67**, 165 (1994).
2. Artinger, R., Kienzler, B., Schuessler, W., Kim, J.I.: Effects of humic substances on the ^{241}Am migration in a sandy aquifer: Batch and column experiments with Gorleben groundwater/sediment systems. J. Contam. Hydrol. **35**, 261 (1998).
3. Kim, J.I., Delakowitz, B., Zeh, P., Lin, X., Ehrlicher, U., Schauer, C., Probst, T.: Migration behavior of radionuclides. In: Colloid migration in groundwaters: Geochemical interactions of radionuclides with natural colloids. Final report. EUR 16754 EN, European Commission, Luxembourg / Brussels 1996.
4. Rao, L., Choppin, G.R., Clark, S.B.: A study of metal-humate interactions using cation exchange. Radiochim. Acta **66/67**, 141 (1994).
5. Marquardt, C.M., Artinger, R., Zeh, P., Kim, J.I.: Redoxchemistry of Np(V) in a groundwater rich in humic substances. In: Effects of humic substances on the migration of radionuclides: complexation and transport of actinides. Second technical progress report., Buckau, G., Editor, Report FZKA 6324, Research Center Karlsruhe, Karlsruhe 1999, p. 21.

6. Kretzschmar, R., Sticher, H.: Transport of humic-coated iron oxide colloids in a sandy soil: Influence of Ca^{2+} and trace metals. Environ. Sci. Technol. **31**, 4397 (1997).
7. Artinger, R., Seibert, A., Marquardt, C.M., Trautmann, N., Kratz, J.V., Kim, J.I.: Humic colloid-borne Np migration: Influence of the oxidation state. Radiochim. Acta Accepted for publication (2000).
8. Schwertmann, U., Cornell, R.M.: *Iron Oxides in the Laboratory (Preparation and Characterization).* Dr. Chr. Dyllick-Brenzinger ed. 1991, Weinheim: VCH Verlagsgesellschaft mbH. 137.
9. Pompe, S., Artinger, R., Schmeide, K., Heise, K.H., Kim, J.I., Bernhard, G.: Investigation of the migration behavior of uranium in an aquifer system rich in humic substances: laboratory column experiments. In: Effects of humic substances on the migration of radionuclides: complexation and transport of actinides. Second technical progress report., Buckau, G., EditorKarlsruhe 1999, p. 219.
10. Schüßler, W., Artinger, R., Kienzler, B., Kim, J.I.: Conceptual modeling of the humic colloid-borne americium(III) migration by a kinetic approach. Environ. Sci. Technol. Accepted for publication (2000).
11. Kim, J.I., *et al.*: Colloid migration in groundwaters: Geochemical interactions of radionuclides with natural colloids. Report RCM 00394, Technical University Munich, Munich 1994.
12. Kim, J.I., Zeh, P., Runde, W., Mauser, C., Pashalidis, I., Kornprobst, B., Stöwer, C.: Nuklidmigration (Tc-99, Np-237, Pu-238, Am-241) im Deckgebirge und Salzstock des geplanten Endlagerortes Gorleben. RCM 01495, Institute of Radiochemistry, Technical University of Munich, Munich 1995.
13. Klotz, D.: Conditioning of columns and ^{152}Eu migration experiments. In: Effects of humic substances on the migration of radionuclides: complexation and transport of actinides. Second technical progress report., Buckau, G., Editor, Report FZKA 6324, Research Center Karlsruhe, Karlsruhe 1999, p. .
14. Ngo Manh, T.: Unpublished results (2000).

Annex 2

Some Aspects on the Influence of Photochemical Reactions on the Complexation of Humic Acid with Europium(III)

(J.-M. Monsallier, F. J. Scherbaum, G. Buckau and J.I. Kim (FZK/INE))

3rd Technical Progress Report

EC Project:

"Effects of Humic Substances on the Migration of Radionuclides: Complexation and Transport of Actinides"

Project No.: FI4W-CT96-0027

Some Aspects on the Influence of Photochemical Reactions on the Complexation of Humic Acid with Europium(III)

J.M. Monsallier, F.J. Scherbaum, G. Buckau and J.I. Kim

Forschungszentrum Karlsruhe, Institut für Nukleare Entsorgung

PO Box 3640, 76021 Karlsruhe, Germany

SOME ASPECTS ON THE INFLUENCE OF PHOTO-CHEMICAL REACTIONS ON THE COMPLEXATION OF HUMIC ACID WITH EUROPIUM(III)

Jean-Marc Monsallier, Franz J. Scherbaum, Gunnar Buckau and Jae-Il Kim

Forschungszentrum Karlsruhe, Institut für Nukleare Entsorgungstechnik, P.O. Box 3640, 76021 Karlsruhe, Germany

Abstract

Photochemical reactions in the Eu(III)-humic acid system are investigated by fluorescence spectroscopy. For comparison, humic acid without europium is also studied. Irradiation is performed by high energy laser beam. The impact of photodegradation of humic acid is monitored by different indicators showing strong variations in response. The decrease in DOC content with increasing irradiation dose is lower than the decrease in UV/Vis absorption. The highest impact is found for the fluorescence intensity. At 3 kJ/mg humic acid absorbed energy and in absence of europium, fluorescence diminishes by more than 90 %. In the presence of Eu(III), however, fluorescent groups are partly stabilized in this range of absorbed energy. With the photodegradation, smaller entities are observed. The photodegradation of the humic acid leads to a decrease of the europium-humate complexation constant. Furthermore, europium is reduced to the divalent state. The present study shows that for metal ion humic acid complexation studies by laser-fluorescence spectroscopy, great care is needed to avoid significant experimental artifacts, such as photodegradation and metal ion redox reactions.

Introduction

Numerous investigations have been performed on the complexation behavior of humic acid with actinide ions applying a large variety of experimental methods. Depending on the method, the results vary considerably. Time resolved laser fluorescence spectroscopy (TRLFS) has the advantage of direct speciation and allows measurements at the very low metal ion concentrations required for the low solubility of multivalent metal cations. Thereby, spectral information is obtained from excitation, emission and the lifetime of emission. When TRLFS is used to evaluate the metal ion complexation, it is generally assumed that no photodegradation accompanies the excitation of these multi-functional macromolecules. Such photodegradation, however, has been reported for excitation of the Eu- and Tb-humate at 308 and 394 nm using an excimer laser [1]. The objective of the present work is to evaluate photo-chemical reactions induced by laser irradiation and the influence on complexation studies of the Eu(III)-humic acid system by time-resolved laser-induced fluorescence spectroscopy.

In the wavelength range where irradiation is done, humic acid is the dominant light absorber and absorption by other components can be omitted. The dose imposed by the irradiation is expressed in energy absorbed per unit weight humic acid (kJ/mgHA). The resulting photodegradation is measured by different methods. The complexation constant of Eu(III) with non-photodegraded and photodegraded humic acid is determined by means of ultrafiltration.

Experimental

Reagents

The humic acid investigated is Gohy-573(HA), which originates from a groundwater at 139 m depth of the Gorleben aquifer system located in Northern Germany. The purification and characterization of Gohy-573(HA) can be found elsewhere [2]. Its proton exchange capacity (PEC) determined by pH titration under Ar atmosphere is 5.38±0.20 meq/g [2]. Stock solutions are prepared by dissolving a known amount of humic acid in 0.1 M NaOH rapidly followed by dilution with 0.1 $NaClO_4$. The pH is adjusted to 6.0 by addition of $HClO_4$. With few exceptions, 10^{-3} M MES buffer (2-mospholine-ethane sulfonic acid) is used for stabilization of pH. The molar humic acid concentration is obtained by multiplying a given weight concentration (g/L) by the PEC (meq/L) divided by the charge of the metal ion under investigation (z). Thus, for europium(III), the humic acid concentration is expressed as [HA(III)] [3].

Laser Induced Fluorescence Spectroscopy

The laser system used for irradiation of humic acid solution and for laser fluorescence spectroscopy of complexed and non-complexed europium is an excimer pumped dye laser system (Lambda Physics, Compex 205 and Scanmate II). Dye-laser pulse at 394 nm (dye: Qui), 1mJ pulse energy and a pulse duration of 25 ns at FWHM is used for irradiation of the sample solution. The sample cell is a rectangular silica cell (HELLMA). The fluorescence emission light is monitored perpendicular to the laser pulse, spectrally resolved by a polychromator (Acton Research, Spectra Pro 275; entrance slit width: 0.5 mm; grating: 300 lines /mm) and detected by an intensified time gated diode array detector (Princeton Instruments, OSMA IRY 700 GR, 1024 linear arranged Si photo diodes). The experimental equipment operates in a spectral window of 210 nm width with a wavelength resolution of about 1.1 nm. Using a beam splitter, a small fraction of the laser pulse is reflected onto a pyroelectric detector connected to a powermeter (Newport 1835C) to monitor the pulse energy. Reading out and digitizing the data from the diode array detector is controlled by an SI180 camera controller (Spectroscopy Instrument). The system components are synchronized by a digital delay/pulse generator (Stanford Research Systems: DG535) as a master trigger unit. With the software POSMA (Spectroscopy Instruments), a PC is used to control the system and analyze the data. Final emission spectra obtained are the results of 10 to 25 averaged single spectra. The resulting emission spectra are normalized to the average pulse energy.

Ultrafiltration

Ultrafiltration is used to investigate the Eu complexation with photodegraded and non-photodegraded humic acid. This method allows the separation of the non-complexed Eu ion from its humate complex by size fractionation [4]. The filtration system uses a membrane of nominal cut-off 1000 Daltons (Filtron Co., Microsep^{TM} Microconcentrators). Europium concentrations in filtrates are quantified by ICP-MS. A correction is used for the partial retention of the non-complexed Eu ion, and possibly sorption on the membrane (at pH 6.0, 0.1 M $NaClO_4$, 75% of the non-complexed Eu^{3+} ion is found in the filtrate). The Eu species distribution is calculated by the total Eu concentration and the concentration in filtrate, applying the correction factor. Published results [4] show the validity of the method for non-photodegraded humic acid. Alteration of humic acid by photodegradation, including changes in size distribution, could introduce experimental artifacts. As shown in this work, however, this method can be applied also for photodegraded humic acid.

Results and discussion

Humic acid has a broad UV/Vis absorption, increasing strongly towards shorter wavelength without distinct features. It has broad excitation and emission bands and a complex fluorescence decay time dependency. Part of the complexity in fluorescence properties has been attributed to excited state processes (e.g., intramolecular energy transfer) [4,7]. Due to irradiation, a number of different photochemical processes can be induced, including breaking of bonds, change in functional groups and structures that may also change intramolecular interactions. Through examination of UV/Vis absorption and fluorescence, including comparison of fluorescence decay between irradiated and non-irradiated humic acid, information is obtained on structural changes induced by photodegradation.

A) Humic acid solution without europium

Humic acid solution is irradiated at wavelengths of 308 and 394 nm by the pulsed laser system. 308 nm is chosen because at this wavelength the highest dose rate is achieved. 394 nm is chosen because of its relevance for Eu-humate interaction studies. For comparison, an absorbed energy of 3.0 kJ/mg HA reflects the typical situation for measurement of the Eu fluorescence lifetime for speciation purposes under these conditions.

Influence on UV/Vis absorption

In Fig. 1, UV/Vis absorption spectra are shown for humic acid after irradiation at 308 nm with absorbed energy up to 418 kJ/mg humic acid. The UV/Vis absorption decreases over the entire wavelength range and for the highest dose the absorption decreases with almost 80 %.

In Fig. 2 the absorption relative to non-irradiated samples is shown for different irradiation doses, with and without presence of MES buffer. The decrease in absorption is higher around the irradiation wavelength than at shorter and longer wavelengths. Nevertheless the decrease in absorption is relatively uniform and also takes place at shorter wavelengths than that of irradiation. In the presence of MES buffer, the decrease in UV/Vis absorption is lowered compared to samples without the buffer. This indicates that the organic buffer acts as a scavenger for photochemically generated reactive species.

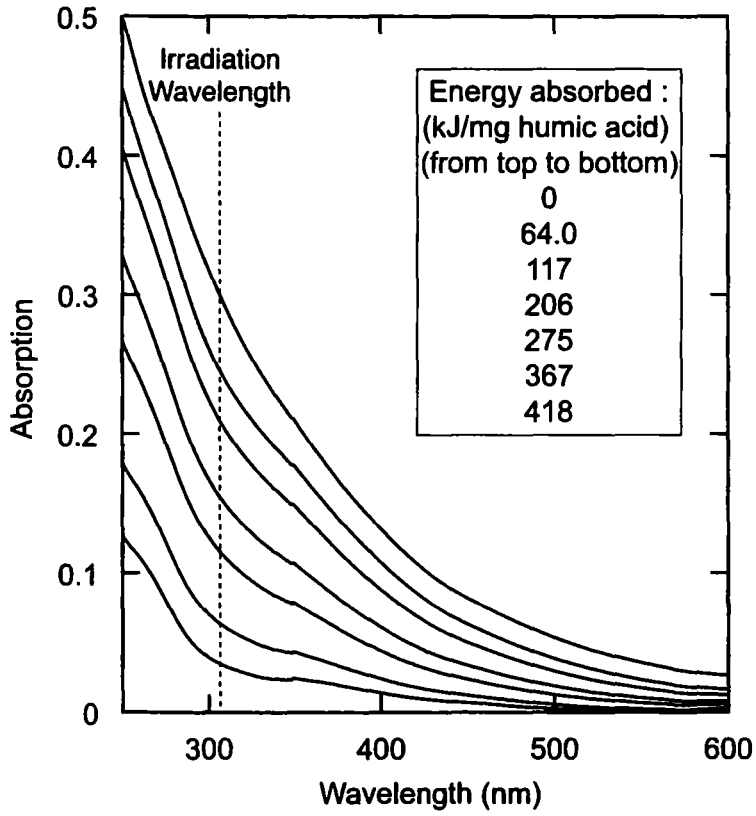

Fig. 1: UV/Vis absorption spectra of humic acid for different absorbed energy from pulsed laser irradiation at 308 nm.

A key question is to which extent UV/Vis absorption can be used as an indicator for decomposition of humic substances. As seen in Fig. 2, the decrease in DOC concentration with increased absorbed irradiation dose is lower than the decrease in UV/Vis absorption. This shows that the decrease in UV/Vis absorption is the result of a variety of photochemical reactions including modification of the electronic structure and bond-breakage. Separate investigations by gel permeation chromatography show the generation of smaller entities.

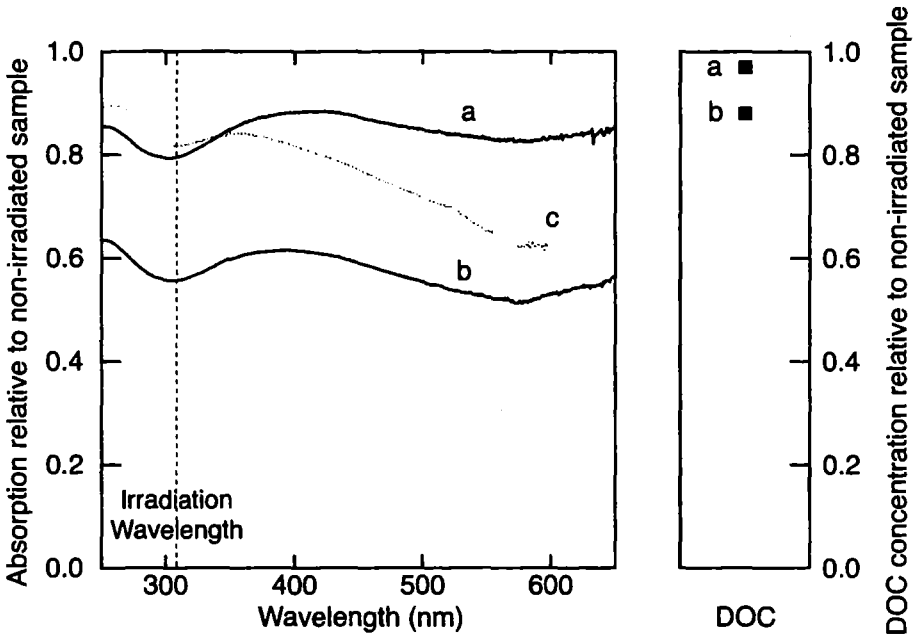

Fig. 2: UV/Vis absorption and DOC concentration relative to non-irradiated samples of humic acid for different absorbed energy from pulsed laser irradiation at 308 nm. Samples a and b are without MES buffer and 28.1 and 66.8 kJ/mg humic acid absorbed irradiation energy, respectively. Sample c is with 10^{-3} mol/L MES buffer and 64.0 kJ/mg humic acid absorbed irradiation energy.

Influence on fluorescence spectrum

The decrease in fluorescence intensity with irradiation is much stronger than the decrease in UV/Vis absorption. In Fig. 3, the fluorescence spectra of humic acid are shown for irradiation at 394 nm. In Fig. 4, the fluorescence emission intensity at 500 nm is shown as a function of the absorbed energy. The fluorescence intensity decreases with increasing absorbed energy. At an absorbed energy of approximately 3.0 kJ/mg HA, the fluorescence intensity is decreased by approximately 95 %, compared to an only marginal decrease in the UV/Vis absorption at 250 nm for the same irradiation dose (cf. Fig. 1).

B) Irradiation of a humic acid solution containing Eu

Influence on the emission spectrum of Eu and humic acid

When exciting a non-complexed Eu^{3+} ion solution at 394 nm, two main bands ($^5D_0 - {}^7F_1$ and $^5D_0 - {}^7F_2$, at 592 and 617 nm, respectively) are observed. Another weak band can also be seen ($^5D_0 - {}^7F_4$ at 697 nm), whereas the other transitions ($^5D_0 - {}^7F_3$, $^5D_0 - {}^7F_5$ and $^5D_0 - {}^7F_6$) are very weak. For the non-complexed Eu^{3+} ion, the band at 592 nm is the most intense. Upon complexation, the peak positions do not change, but the relative intensity of the different bands change and for Eu(III)-humate, the $^5D_0 - {}^7F_2$ (617 nm) band becomes the most intense.

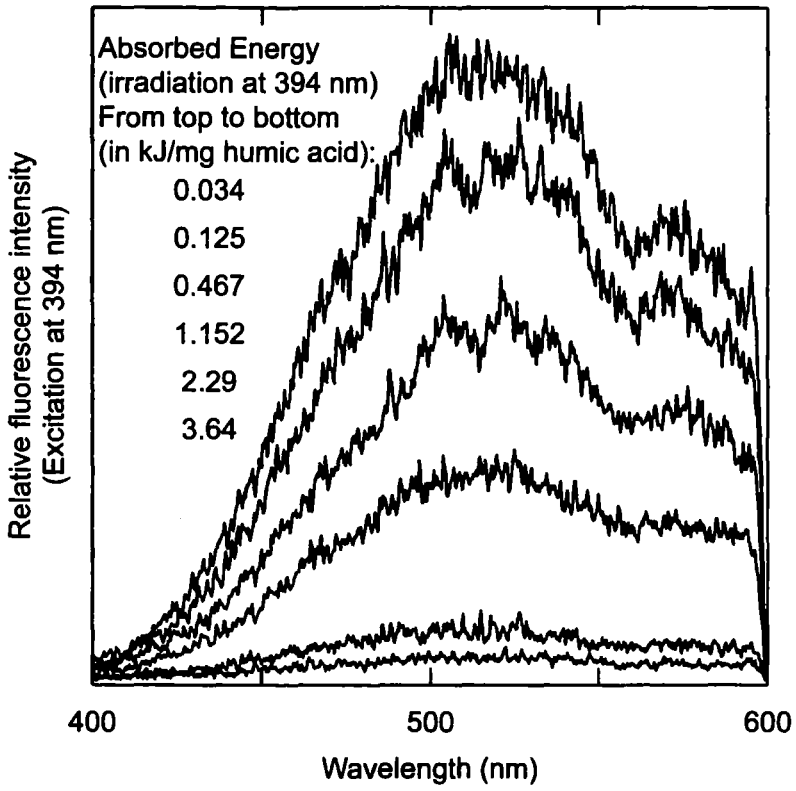

Fig. 3: Influence of irradiation by laser at 394 nm on the fluorescence of humic acid. Fluorescence spectra from excitation at 394 nm are shown for different absorbed irradiation energy.

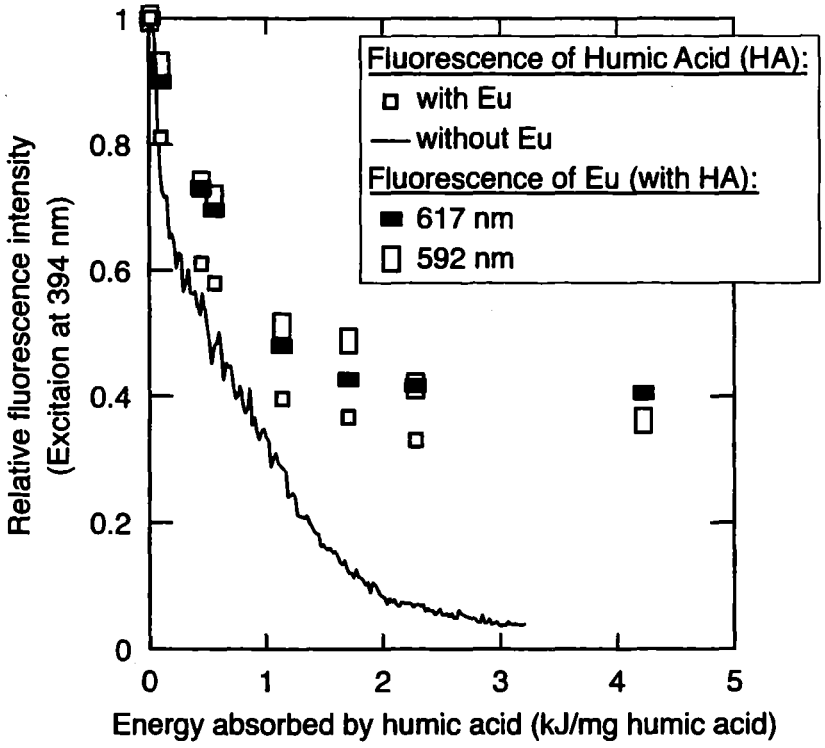

Fig. 4: Decrease in europium fluorescence bands (592 nm and 617 nm)) and humic acid fluorescence at 500 nm with and without europium as a function of absorbed irradiation dose.

Humic acid is complexed with europium at pH 6.0 (buffered with 10^{-3} mol/L MES) in 0.1 mol/L $NaClO_4$. Europium concentrations are equivalent to 20, 40 and 65 % of the fraction of humic acid functional groups that can be complexed under these conditions (the loading capacity) [3]. This ensures that the concentrations of non-complexed europium are negligible in the starting solutions. The solutions are equilibrated for 48 hours prior to irradiation experiments.

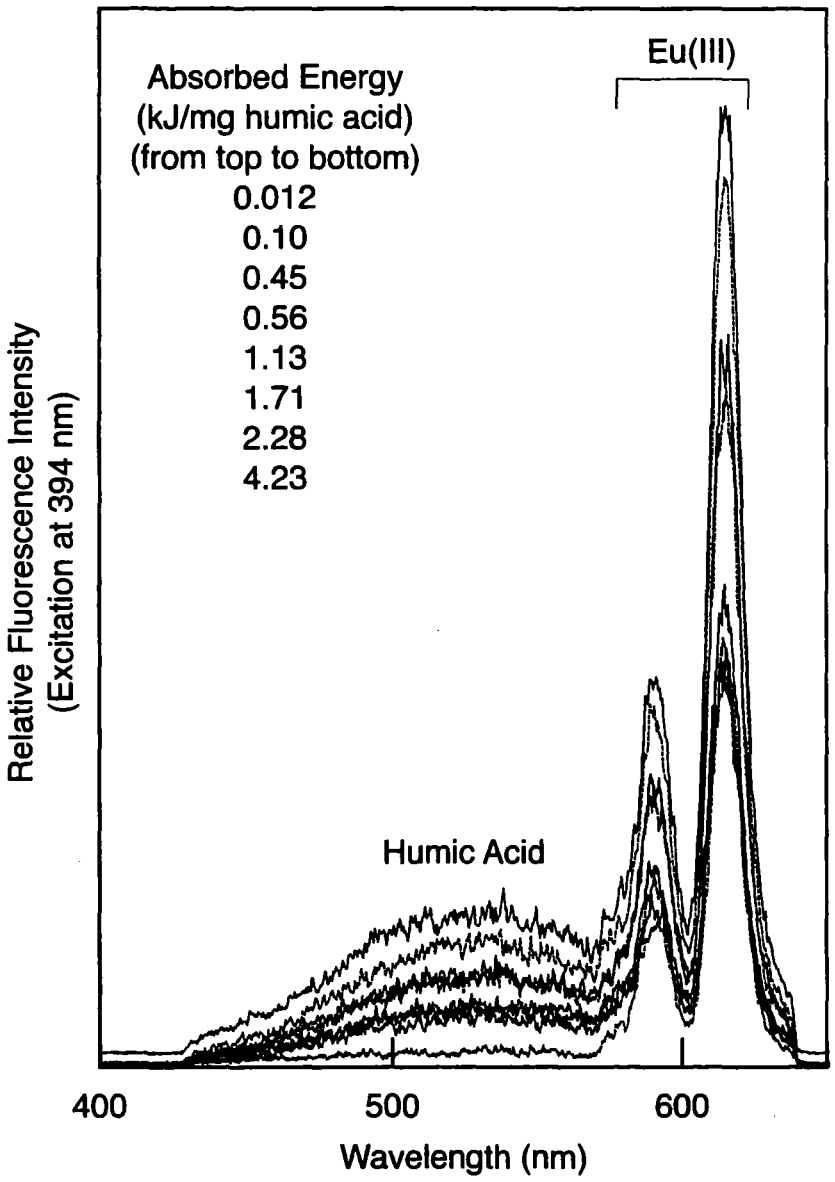

Fig. 5: Fluorescence of europium complexed with humic acid and that of humic acid (500 nm) as a function of absorbed irradiation energy by laser at 394 nm. The europium concentration is equivalent to occupation of 40 % of the fraction of humate sites that can be complexed (loading capacity) under these conditions (pH 6.0, I=0.1 ($NaClO_4$)).

Figure 5 shows the europium and humic acid fluorescence as a function of the absorbed energy at 40 % europium loading. The irradiation energy is delivered by the laser source used

for the fluorescence measurements (394 nm). The fluorescence intensities of both europium bands and that of humic acid decrease with increasing irradiation dose. Irrespective of the absorbed energy, the ratio between the two bands at 592 and 617 nm remains basically constant (2.36±0.17). This observation suggests that during photodegradation, the ratio of free Eu/complexed Eu is not affected. However, the fluorescence intensity of free Eu being much smaller than that of Eu humic acid complex, a small change in the free Eu concentration is difficult to observe by the Eu emission spectrum. Furthermore, to which extent the mode of complexation between humic acid and Eu (III) is affected by degradation of humic acid cannot be determined.

In Fig. 4, the relative fluorescence intensities of humic acid with and without europium as well as the two europium emission bands are shown. The relative fluorescence intensity ratio of the two europium emission bands remains virtually constant with increasing irradiation dose. In absence of europium, the humic acid fluorescence diminishes rapidly and, as discussed above, decreases by approximately 95 % at an absorbed irradiation dose of 3 kJ/mg humic acid. In the presence of europium, the humic acid fluorescence becomes stabilized for absorbed doses above approximately 1 kJ/mg humic acid. The reason for the stabilization of humic acid fluorescence by europium in this range of absorbed energy is not yet clear.

Photolytic generation of Eu(II)

Irradiation with laser light at 394 nm not only leads to changes in the absorption, fluorescence, size distribution and functional group content of humic acid but also leads to the generation of divalent europium. In Fig. 6, the $^5D_0$-$^7F_1$ transition (592 nm) of Eu(III) is shown for photodegraded humic acid in the presence of europium. This spectrum is recorded for the highest europium concentration, i.e. 65 % of the humic acid europium loading capacity and photodegradation by an absorbed energy of 4 kJ/mg humic acid. Around 460 nm a band corresponding to Eu(II) is observed.

Influence on the Eu-humate complexation

Stability constants of europium with non-photodegraded and photodegraded humic acid are determined by the ultrafiltration method at pH 6.0 and I=0.1 M ($NaClO_4$). Separate investigations showed that less than 8 % of europium in the filtrate was complexed, and thus the ultrafiltration method can be applied also to photodegraded humic acid. Degradation of humic acid is done by laser irradiation at 308 nm with an absorbed energy of 80 kJ/mg HA. After laser irradiation, europium is added in concentrations equivalent to 20 and 65 % of the humic acid europium(III) loading capacity. The stability constants are evaluated by the charge neutralization model [3]. The results are summarized in Table 1. For the investigation on the non-photodegraded humic acid, as expected, no influence of the loading is found. The overall average of the europium-humate stability constant is found to be 6.37±0.10, which is in good agreement with values determined for different trivalent f-elements by ultrafiltration and

spectroscopic methods (logß=6.24±0.28 [3]). For the photodegraded humic acid results are different. Again, no significant influence of the loading of humic with europium is found, however, the overall average of the stability constant is much lower, namely 5.19±0.12.

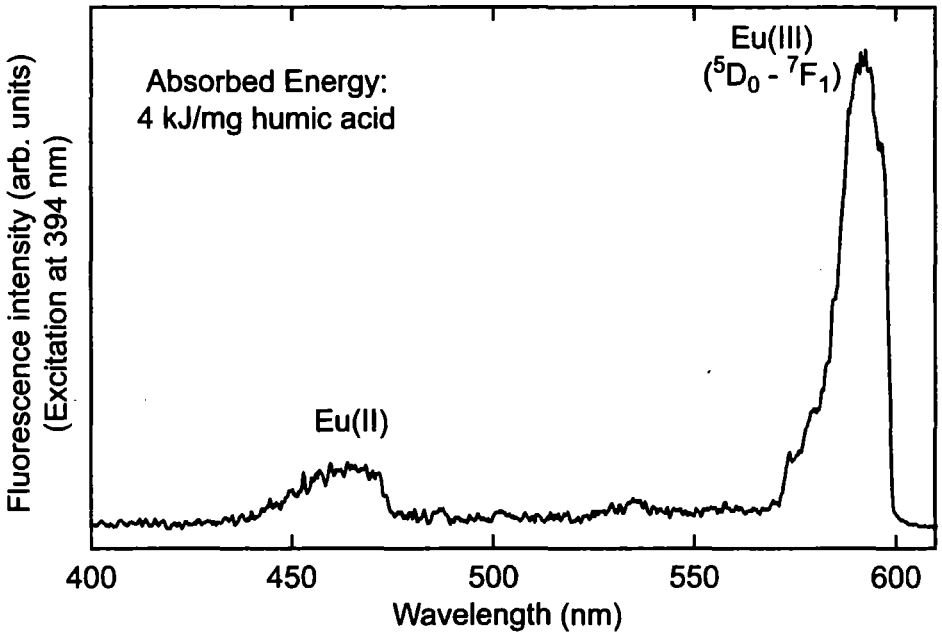

Fig. 6: Photolytic generation of Eu^{2+} in humic acid solution irradiated by laser at 394 nm (4 kJ/mg HA). The europium concentration is equivalent to 65 % of the loading capacity of the humic acid.

Table 1: Europium-humate complexation constants at pH 6.0 (I=0.1 M ($NaClO_4$). Non-photodegraded and photodegraded humic acid is investigated for europium concentrations equivalent to 20 and 65 % of the effective humic acid concentration. No correction is made for the impact of photodegradation on the functional group content*.

Humic Acid	log ß (L/mol)	
	20 % Loading	65 % Loading
Non-photodegraded	6.31 ± 0.06	6.40 ± 0.10
Photodegraded*	5.13 ± 0.11	5.26 ± 0.08

Photodegradation leads to changes both in the functional group content of humic acid and decrease in molecular size. Investigations on different size fractions of humic acid show that with decreasing size the complexation strength decreases [5]. Comparison of the metal ion complexation with humic and with fulvic acid also shows lower complexation strength for the smaller fulvic acid [6]. Simultaneously, photodegradation results in modification of the functional group content. Delineation of the impacts from decrease in the molecular size and change in the functional group content, cannot be performed by the present data.

Summary and Conclusions

The sensitivity of different properties of humic acid towards photodegradation varies strongly. Photodegradation leads to generation of smaller entities. The decrease in dissolved organic carbon is lower that the decrease in UV/Vis absorption. The decrease in fluorescence intensity, however, is much more pronounced that the former two decomposition indicators. Addition of europium leads to stabilization of humic acid towards photodegradation.

Application of laser-induced fluorescence spectroscopy for studying the europium-humate interaction may be subject to considerable experimental artifacts through photochemically induced reactions. These artifacts are due to changes in functional group content and lowering in molecular size of humic acid. Simultaneously, photolytic reduction of europium from the trivalent to the divalent state takes place. Due to the relatively low fluorescence efficiency of europium, significant photolytic impact can occur. This is especially true for high absorbed irradiation doses, for example where europium lifetime measurements are conducted. Therefore, great care is needed to ensure that significant experimental artifacts are avoided where the europium humic acid system is studied.

References

[1] Bidoglio G., Omnetto N., Robouch P. "Kinetic studies on Lanthanide Interactions with Humic Substances by Time Resolved Laser Induced Fluorescence", *Radiochim. Acta*, **52/53**, 1991, 57.

[2] Kim J.I., Buckau G., Li G.H., Duschner H., Psarros N. "Characterization of Humic and Fulvic Acids from Gorleben Groundwater", *Fresenius, J. Anal. Chem.*, **338**, 1990, 245.

[3] Kim J.I., Czerwinski K.R. "Complexation of Metal Ions with Humic Acid: Metal Ion Charge Neutralization Model", *Radiochim. Acta*, **73**, 1996, 5.

[4] Kim J.I., Rhee D.S., Wimmer H., Buckau G., Klenze R., "Complexation of Trivalent Actinide Ions (Am^{3+}, Cm^{3+}) with Humic Acid: A Comparison of Different Experimental Methods", *Radiochim. Acta*, **62**, 1993, 35.

[5] Monsallier J.M. "Influence of Humic Acid Size on Actinide Complexation", Dissertation, Florida State University, 1998.

[6] Buckau G., Kim J.I., Klenze R., Rhee D.S., Wimmer H. "A Comparative Study of the Fulvate Complexation of Trivalent Transuranic Element Ions", *Radiochim. Acta*, **57**, 1992, 105.

Annex 3

Initial Studies on the Complexation of Tetravalent Neptunium with Fulvic Acid

(Ch. Marquardt, V. Pirlet and J.I. Kim (FZK/INE in cooperation with SCK/CEN))

3rd Technical Progress Report

EC Project:

"Effects of Humic Substances on the Migration of Radionuclides: Complexation and Transport of Actinides"

Project No.: FI4W-CT96-0027

Initial Studies on the Complexation of Tetravalent Neptunium with Fulvic Acid

C.M. Marquardt, V. Pirlet* and J.I. Kim

Forschungszentrum Karlsruhe, Institut für Nukleare Entsorgung
PO Box 3640, 76021 Karlsruhe, Germany

* SCK-CEN, Mol Belgium

Initial studies on the Complexation of tetravalent Neptunium with Fulvic Acid

C.M. Marquardt[1], V. Pirlet[2], J.I. Kim[1]

[1]Forschungszentrum Karlsruhe, Institut für Nukleare Entsorgungstechnik,

[2]SCK-CEN, Mol, Belgium

Abstract

For the appraisal of humic colloid facilitated migration of a given tetravalent actinide ion under reducing conditions of aquifer systems, in this work, the tetravalent neptunium ion Np(IV) was chosen for the spectroscopic study of its fulvate complexation behaviour. Fulvic acid was taken because of its solubility at low pH (< 2), at which the Np(IV) undergoes minimal hydrolysis and no carbonate complexation. Two main kind of experiments were carried out by spectroscopic speciation at pH 1 and 1.5, a batch and a titration experiment. The studies were performed in Np(IV) concentration range from 2.5×10^{-6} to 9.7×10^{-5} M and at fulvic acid concentration in the range from 6.5×10^{-4} to 8.5×10^{-3} eq/l. The concentrations of total Np(IV) and Np(IV) in solution were measured by liquid scintillation counting. All other species were estimated by absorption spectroscopy, the uncomplexed Np(IV) at 960 nm and the Np(IV)-fulvate at 967.5 nm with molar absorption coefficients of 162 and 63 L mol^{-1} cm^{-1}, respectively. Additionally, a absorption maximum of complexed Np(IV) is found at 974.5 nm, but nature of this species is unknown up to now. By mixing Np(IV) and FA(IV) a neptunium fulvate aggregate is formed, which alters with time. The reaction between aggregate and species in solution reaches equilibrium after 3 days. The amount of NpFA(IV)-aggregate varies not only with time but also depends on the method (batch or titration) the studies were made. The complexation constant is evaluated by the metal ion charge neutralisation model by taking into account the loading capacity (LC) and the hydrolysis given by the corresponding hydrolysis constants for $NpOH^{3+}$ and $Np(OH)_2^{2+}$ from literature. For pH 1 and 1.5 15 % and 75 % LC were evaluated yielding in log β`s of 7.86 ± 0.09 and 9.18 ± 0.17, respectively. The values both LC and log β show a discrepancy, that cannot explained without further investigations on the Np(IV)-fulvate complexation.

1. Introduction

Neptunium can exist simultaneously in different oxidation states in aqueous solutions. In solutions without reducing components (aerobic), pentavalent neptunium is stable as neptunyl ion (NpO_2^+). But under reducing conditions, as expected in groundwaters of deep geological formations, the NpO_2^+ can be reduced to tetravalent neptunium (Np(IV)). Especially, in humic colloid containing ground waters (Boom Clay, Belgium and Gorleben, Germany), NpO_2^+ is reduced into tetravalent oxidation state [1]. Column experiments with these groundwaters showed that tetravalent Np will be bound onto humic colloids under pH neutral conditions [2]. Consequently, the neptunium migration is facilitated in the tetravalent oxidation state. Hitherto, it is unknown in detail in which form and to which strength the tetravalent neptunium is bound to the humic colloids. But for safety assessment the knowledge of binding mechanisms with all related thermodynamic and kinetic parameters is necessary.

The goal of the present work is to elucidate the complexation (mechanism and strength) of tetravalent neptunium by humic colloids.

One of the biggest problem investigating tetravalent actinide ions is the high tendency for hydrolysis, the reaction with water molecules resulting in monomeric, polymeric and solid species $An(OH)_x^{4-x}$. Due to that, data concerning the complexation of tetravalent actinides with humic substances under environmental conditions are missing in the literature. The hydrolysed species undergoes polymerisation at higher ion concentration resulting in colloid and particle formation. In order to impede such reactions and to facilitate calculations and interpretations, we have started the experiments at low pH in the slight hydrolysed range pH < 1.5). In this acidic pH range the fulvic acid fraction (FA) of the humic colloids can be used as soluble fraction in contrast to non-soluble humic acid fraction. Many earlier studies showed that both humic colloid fractions (humic and fulvic acids) have very similar complexation behaviour [3,4] and studies of one can be compared with each other.

In the present work we have examined the reaction between Np(IV) and fulvic acid at pH 1 and 1.5. For the work purpose, UV-VIS spectroscopy was chosen, as it provides a direct quantification of the species involved in the reaction and the accessibility to the ratio of the free Np(IV) on the complexed Np(IV).

2. Experimental details

All experiments were performed under argon atmosphere to avoid oxidation of Np(IV), at pH 1 and 1.5 in hydrochloric acid solutions at room temperature. The fulvic acid (FA) is initially originated from the Boom Clay interstitial water, sampled in the underground research facility in Mol (Belgium) but was provided in a freeze-dried form by the Institute für Nukleare Entsorgungstechnik (INE, Forschungszentrum-Karlsruhe). The fulvic acid was extracted, isolated, and purified in the frame of the laboratory intercomparison exercise in the MIRAGE project of the CEC [5]. The proton exchange capacity is determined to be 3 meq/g from the first derivative of the titration curve obtained by potentiometric titration. Stocks solutions of FA of different concentrations are prepared by dissolving appropriate amounts of freeze-dried FA in a small volume of 0.1 M NaOH and fixing the appropriate pH with HCl. The FA concentration in the UV-VIS cuvette is determined by Total Organic Carbon (TOC) measurement. The tetravalent Np stock solution is obtained by electrochemical reduction of pentavalent Np solution in 1M HCl. The purity of tetravalent Np stock solution was confirmed by spectroscopy by means of the Np(IV) absorption band at 960 nm and Np(V) absorption band at 980.4 nm. The molar absorption coefficients of 162 [6] and 395 L mol^{-1} cm^{-1} [7] were used to calculate concentrations of Np(IV) and NpO_2^+, respectively. For all solutions UV-VIS spectroscopy was used to study the complexation reactions at the wavelength interval between 920 and 1040 nm (Varian, Cary 5 spectrophotometer). The total Np concentration and the Np concentration in solution were determined by LSC (Liquid scintillation counting, Beckman) with discriminating the β-decay of its daughter Pa-233.

Two main kinds of experimental approaches are carried out at pH 1. First, samples were prepared in a batch method by adding certain volumes of fulvic acid solution to a Np(IV) solution. For each Np/FA ratio one separated cuvette was used. Within this study the Np(IV) ion concentration was maintained constant at about $1.1x10^{-4}$ M while varying the FA concentration from $6.47x10^{-4}$ to $8.47x10^{-3}$ eq/l. Second, complexation was examined by adding Np gradually to a FA solution with a certain concentration in one cuvette (titration method). The Np(IV) ion concentration is varied from $2.5x10^{-6}$ to $9.73x10^{-5}$ M and from $3.48x10^{-6}$ to $6.87x10^{-5}$ M while maintaining the fulvic acid concentration constant at $2.86x10^{-3}$ eq/l. At pH 1.5, two experiments were carried out by varying the FA concentration from $1.52x10^{-4}$ to $5x10^{-3}$ eq/l while the Np is maintained constant at two different concentrations, $3.5x10^{-5}$ and $8x10^{-5}$ M.

When Np was added, an instantaneous aggregation being observed for most of the samples to the fulvic acid solutions. The total and soluble Np and FA concentrations were measured at the end of the experiments by LSC and TOC methods, respectively, which allow to obtain the amount of Np and FA involved in the brownish aggregate by substraction. The aggregation was not observed for very low ratios of $[Np(IV)]_f/[FA(IV)]_t$. After addition of Np(IV) in the different cuvettes and equilibration, the solution was analysed by spectroscopy with a Cary 5 spectrophotometer (VARIAN).

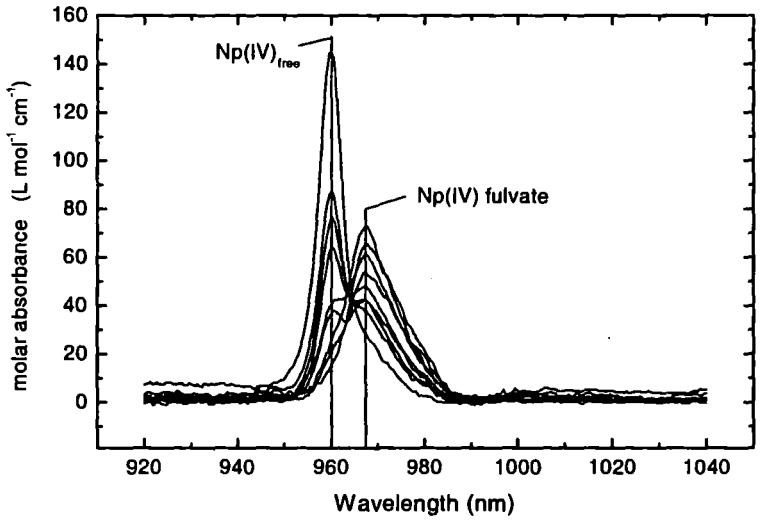

Fig.1: Absorption spectra for the complexation of Np(IV) with fulvic acid at pH 1 (The concentration of Np is kept constant to $1.1x10^{-4}$ M , while varying the FA concentration from $6.47x10^{-4}$ to $8.47x10^{-3}$ eq/l.

3. Results and discussion

3.1 Absorption spectroscopy of Np(IV) in FA(IV) solutions

The spectroscopic speciation was started with samples of different FA concentrations ($6.47x10^{-4}$ to $8.47x10^{-3}$ eq/l) at constant Np concentration of $1.1x10^{-4}$ M (batch method, see appendix: **Table 1**). The obtained spectra are shown in **Figure 1**. In each spectrum two absorption bands can be recognized. The Np(IV) ion absorption band is characterized by a well-known maximum at 960 nm and a FWHM of 6 nm and the absorption of the Np(IV)-fulvate complex appears with a maximum at 967.5 nm and a FWHM of 10.3 nm. By increasing the total FA concentration the Np(IV) ion peak becomes smaller whereas the absorption band of Np(IV) fulvate complex grows due to rising complexation.

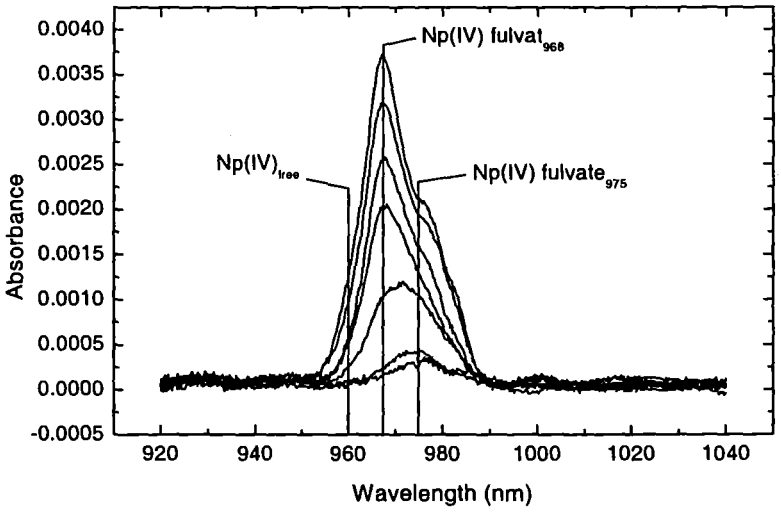

Fig.2: Absorption spectra for the complexation of Np(IV) with fulvic acid at pH 1 (The concentration of fulvic acid is kept constant to $2.8x10^{-3}$ eq/l , while varying the Np concentration from $2.53x10^{-6}$ to $9.73x10^{-5}$ M by a titration method.

In a second experiment the titration as well as the batch method was used for lower ratios of $Np(IV)_t$ to $FA(IV)_t$. By increasing the Np concentration from $2.5x10^{-6}$ to $9.73x10^{-5}$ M in a solution with a constant FA concentration of $2.8x10^{-3}$ eq/l (see appendix: **Table II**), we observed a new absorption band in addition to the peak characteristic of the Np(IV)-fulvate complex at 967.5 nm (designated as $NpFA(IV)_{968}$). This is illustrated in **Figure 2 and 3**. It is assumed that this absorption band with a maximum at 974.5 nm and a FWHM of 14.5 nm is related to another Np(IV) fulvate species and is called $Np(IV)FA_{975}$. Increasing the ratio

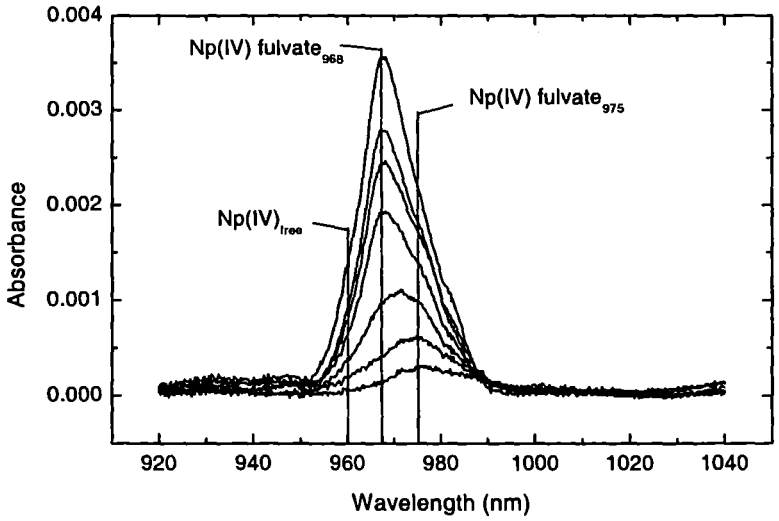

Fig. 3: Absorption spectra for the complexation of Np(IV) with fulvic acid at pH 1 (The concentration of fulvic acid is kept constant to $2.85x10^{-3}$eq/l , while varying the Np concentration from $3.48x10^{-6}$ to $6.87x10^{-5}$ M by a batch experiment (different cuvettes).

$[Np(IV)]_i/[FA]_t$, the absorption band of $NpFA(IV)_{968}$ appears as well.

In order to look at the pH dependency of the fulvate complexation experiments were done at pH 1.5. The spectra (see **Figure 4**) of the solutions at pH 1.5 show the same characteristics with the same band maxima at 960 nm, 967.5 and 974.5 nm for the Np(IV) ion and the two Np(IV)-fulvate complexes, respectively. At pH 1.5, we can expect a higher deprotonation of the fulvic acids and hence, a higher complexation strength of the fulvic acids towards the Np(IV).

3.2 Complexation behaviour and kinetic aspects

After adding Np(IV) to different concentrated FA solutions, parts of the FA aggregates for all the ratios of $[Np(IV)]_i/[FA(IV)]_t$ except at large excess of fulvic acid compared to the Np (about 1000-fold). After the brownish aggregate has deposited on the bottom, UV-VIS spectra of the solution have been recorded regularly with time. As shown in **Figure 5**, a change in the spectrum can be followed with time and an increasing amount of Np(IV) in solution has been measured simultaneously by radiochemical analysis. These observations indicate that obviously most of Np(IV) is bound onto the aggregates and subsequently, free

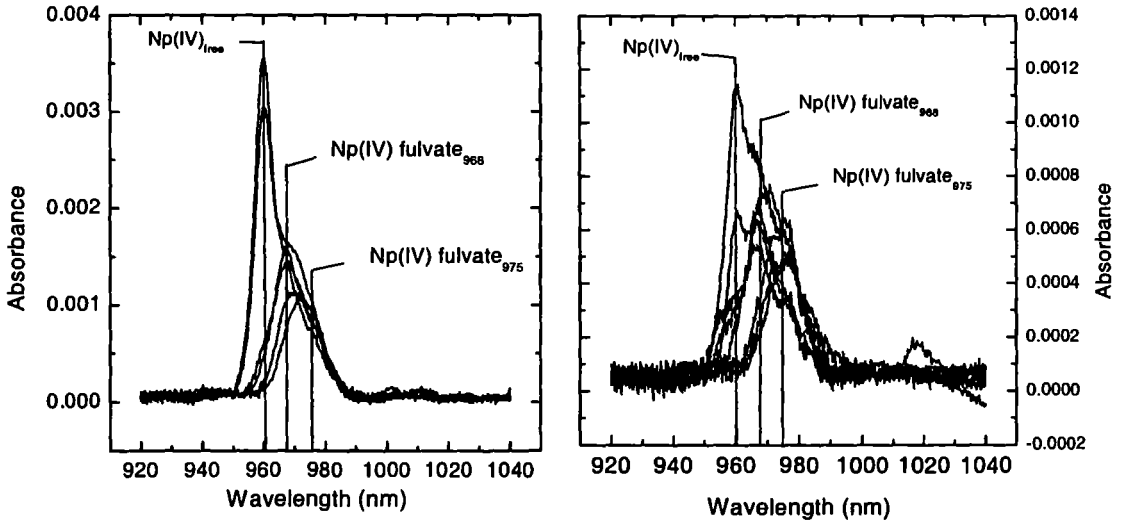

Fig.4: Absorption spectra for the complexation of Np(IV) with fulvic acid at pH 1.5 (The concentration of Np is kept constant at $8x10^{-5}$M for the left graph and $3.3x10^{-5}$M for the right one , while varying the fulvic acid concentration from $1.5x10^{-4}$ to $4.94x10^{-3}$ eq/l.

Np(IV) and Np(IV) fulvate are released into the solution with time. The presence of Np in the aggregated fulvate is confirmed by radiochemical analyses of it. This leads to the conclusion that the aggregated fulvate on one hand is re-dissolved by forming smaller Np(IV) fulvate particles and on the other hand that parts of the Np(IV) ions are able to leave the fulvic molecule. An equilibrium among Np(IV), Np(IV) fulvate in solution and aggregated Np(IV) fulvate is obviously reached after about three days.

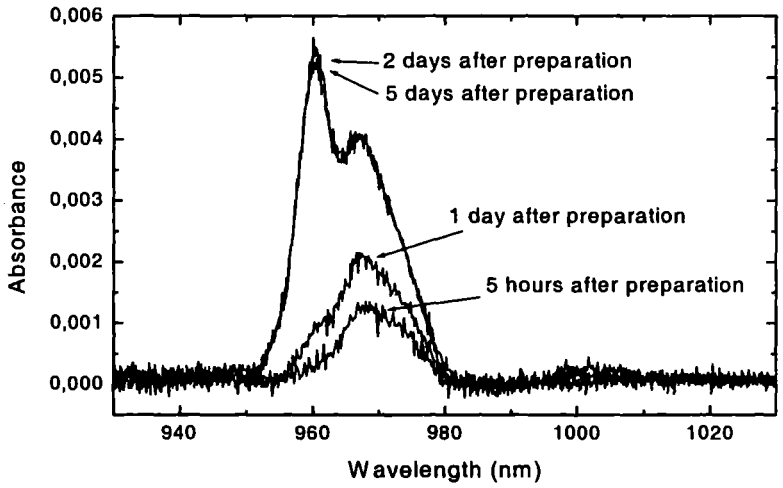

Fig.5: Kinetic evolution of the UV absorption spectrum representing the complexation of Np(IV) with fulvic acid at pH 1 as a function of the time.

Aggregation of the FA implies the saturation of some fulvic acid sites by Np(IV) ions and the formation of less hydrophylic structures by molecular aggregation. The kinetic was different for the experiments of Figure 1 and 2 and depends obviously on the different ratios of $[Np(IV)]_t/[FA]_t$. Adding a small volume of concentrated neptunium solution to a large volume of fulvic acid solution might form a local oversaturation of fulvic acid and hence a fast aggregation takes place. All of the free neptunium, which is not bound to the fulvic can be co-extracted inside the aggregates and only a small absorption of all neptunium species is observed in the spectrum (Fig. 5). With time, the fulvic acid can be rearranged and neptunium is released due to diffusion into the bulk solution. Contrary to this, adding small volumes of concentrated fulvic acid solution to a large volume of neptunium solution seems to prevent local saturation of the fulvic acid and is the better choice for the experiment.

These kinetic aspects seem to be important in the system involving different ratios of Np(IV) ions and fulvic acid and, the way the complexes are prepared. Consequently, the kinetic effects have been taken into account for recording the spectra.

Evaluation of the complexation reactions at pH 1

The total neptunium concentration $[Np]_t$ is known from LSC and α-spectroscopy. Impurities of oxygen can oxidize Np(IV) to NpO_2^+ with time. The amount of NpO_2^+ ($[NpO_2^+]$) is estimated spectroscopically by the absorption band at 980.4 nm and hence, the difference $[Np]_t - [NpO_2^+]$ corresponds to the total Np(IV) concentration ($[Np(IV)]_t$). The NpO_2^+ ion shows no significant interaction with the fulvic acid at such low pH values. In order to facilitate interpretations of the spectra the absorption band of the NpO_2^+ was mathematically substracted from the total spectrum and can not be recognized in the presented figures. As mentioned before, after mixing Np(IV) and FA sometimes the fulvate aggregates as Np(IV)-fulvate. The amount of aggregated neptunium fulvate ($[NpFA(IV)]_{agg}$) was calculated by the difference of $[Np(IV)]_t$ and Np(IV) measured radiometrically in solution ($[Np(IV)]_{aq}$) after aggregation. Parallel to that, the FA concentrations in solution and in the aggregates are obtained by TOC measurements. The concentrations of free Np(IV) and of the Np-species in solution are deduced from the absorption spectra. However, the peak and the corresponding absorbance coefficient of the free Np(IV) ion is well known and give reliable values, whereas the characteristics of the fulvate species had to be find. Each spectrum has been numerical deconvoluted with Gaussian-Lorentzian functions by the GRAMS program (Galactic) resulting in pure spectra of each neptunium species. From the pure species spectrum the molar absorption coefficients are evaluated by the Lambert-Beer-Law $\varepsilon_i = \varepsilon_{0i} \cdot c_m \cdot d$ at each wavelength i for each species m and with concentration of the species c_m, which was known from radiometric measurements. The concentration of neptunium fulvate in solution $[NpFA(IV)]_{aq}$ is calculated by substracting the spectroscopically determined Np(IV) concentration [Np(IV)] from $[Np(IV)]_{aq}$. The absorption coefficient for the NpFA(IV) at 967.5 nm, was calculated to 63 ± 8 L mol^{-1} cm^{-1}. In Table I (appendix) the concentrations of the species are listed.

For better illustration of the data from table 1 and 2 (appendix, batch experiment, pH 1), the relative concentration of free Np(IV), Np(IV) fulvate and aggregated Np(IV) fulvate are plotted in **Figure 6**. It is obvious, that at $[Np(IV)]_t/[FA(IV)]_t$ ratios below 0.10 the total Np(IV) is complexed and $NpFA(IV)_{aggr}$ and $NpFA(IV)_{aq}$ are present in similar concentrations. Above 0.1 the free Np(IV) concentration and $NpFA(IV)_{aq}$ increase, whereas the $NpFA(IV)_{aggr}$ remains roughly constant.

The interaction of Np(IV) with fulvic acid is expressed by this relation in a first approach:

$$Np(IV) + FA(IV) \leftrightharpoons NpFA(IV) \qquad \text{(eq.1)}$$

according to the charge neutralization model described in earlier publications [8], where Np(IV) represents the concentration of uncomplexed Np(IV) ion, Np(IV)FA(IV) the total concentration of the fulvate complex ($Np(IV)FA(IV)_{aggr}$ + $Np(IV)FA(IV)_{aq}$). FA(IV) denotes free fulvic acid concentration, i.e. the uncomplexed functional groups of the fulvic acids given by the following substraction $[FA]_{tot} - [NpFA(IV)]_t$. The molar concentration of binding sites

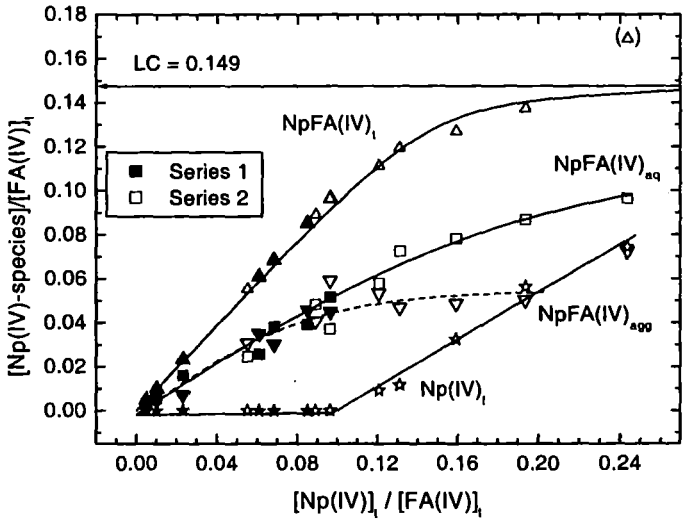

Fig. 6: Relative concentrations of Np(IV) species in fulvic acid solution at pH 1.0. The line for $NpFA(IV)_t$ is fitted according to [10].

($[FA]_{tot}$) can be calculated by multiplying the proton exchange capacity (PEC, (eq/g)) with the weighted amount of FA expressed in g/l.

The tetravalent neptunium is readily hydrolysed, and it is not expected that only the Np^{4+} ion exist in solution at pH 1 and 1.5. Calculations of the hydrolysis of Np(IV) with log β_{11}, β_{12}, β_{13} and β_{14} of 14.5, 28.2, 39.2 and 47.2 gives a species distribution of the Np(IV) at given pH values, which is shown in the table:

pH	Np^{4+}	$NpOH^{3+}$	$Np(OH)_2^{2+}$	$Np(OH)_3^{+}$	$Np(OH)_4$
	mol/l	mol/l	mol/l	mol/l	mol/l
1.0	5.19×10^{-8}	1.64×10^{-6}	8.22×10^{-6}	8.22×10^{-8}	2.6×10^{-12}
	0.5 %	16.4 %	82.2 %	0.8 %	-
1.5	5.76×10^{-9}	5.76×10^{-7}	9.13×10^{-6}	2.89×10^{-7}	2.89×10^{-11}
	0.06 %	5.76 %	91.3 %	2.89 %	-

The values for the hydrolysis are critical selected from literature for β_{11}, β_{12} and calculated with correlation of the constants and the electrostatic interaction energy between the actinide and OH^- ion [9]. The calculations were made by the MINEQL-program. From the data it is obvious, that Np(IV) can be present as hydrolysed species $NpOH^{3+}$ (16.4 %) and $Np(OH)_2^{2+}$(82.2 %) at pH 1. The $Np(OH)_4$ is undersaturated in solution and consequently forms no precipitate, which was confirmed by the experiment.

The absorption band observed at 960 nm is caused by the absorption these hydrolysed species. Unfortunately, no change can be observed in the spectra varying the pH from 0 to 1.5 and consequently, the release of one or two protons from one or two water molecules in the hydrated shell does not change significantly the absorption peak of the Np(IV). But nevertheless, the hydrolysis has to be taken into consideration for calculations of complexation constants. In a first approach we assume that only Np^{4+} reacts with fulvate molecule. The following reactions with the corresponding reaction constants can be considered:

$$Np^{4+} + H_2O \leftrightharpoons Np(OH)^{3+} + H^+ \qquad \log K_{h1} = 0.5 \qquad (2)$$

$$Np^{4+} + 2\,H_2O \leftrightharpoons Np(OH)_2^{2+} + 2H^+ \qquad \log \beta_{h2} = 0.2 \qquad (3)$$

$$Np^{4+} + FA(IV) \leftrightharpoons NpFA(IV) \qquad \log \beta = \text{ to be found} \qquad (4)$$

For fulvate complexation reaction the complexation constant log β is defined according to the law-of-mass-action and the charge neutralization model to:

$$\beta = \frac{[NpFA(IV)]}{[Np^{4+}][FA(IV)]} \qquad (5)$$

with

$$[FA(IV)] = FA(IV)_t\ LC - [NpFA(IV)] \tag{6}$$

The free Np^{4+} concentration is determined by the hydrolysis reactions and rearrangement of equation (1) and (2) gives

$$[Np^{4+}] = \frac{[Np(OH)_2^{2+}][H^+]^2}{\beta_{h2}} \tag{7}$$

$$\beta = \frac{[NpFA(IV)]}{[Np(OH)_2^{2+}][H^+]^2} \cdot \frac{1}{[FA(IV)]_t\, LC - [NpFA(IV)]} \tag{8}$$

No we have to consider that, however, the measured Np absorbance band is the sum of $Np(OH)^{3+}$ and $Np(OH)_2^{2+}$. The ratio between both species should be constant and is fixed by the equilibria between the two hydrolysis reactions (Eq. 2 and 3). If we assume that the hydrolysed species is not involved in interactions with fulvic acid, the mol fraction can be picked directly from the above shown Table. From the measured absorbance the $Np(OH)_2^{2+}$ is calculated by $[Np(OH)_2^{2+}]=\varepsilon\ 0.822/\varepsilon_0$, with 0.822 as the mol fraction of the second hydrolysis species at pH 1.0.

The evaluation of the fulvate complexation has been made only for the experimental results when free Np(IV) could be observed (Table I). The $Np(IV)_f$ ion concentration being not available from the other sets of data. In **Figure 7** the data are plotted according to the neutralization model in a linear relationship with the slope LC.

$$[Np^{4+}] = \frac{[Np^{4+}][FA(IV)]_t}{[Np(IV)FA]} \cdot LC - \frac{1}{\beta} = F \cdot LC - \frac{1}{\beta} \tag{9}$$

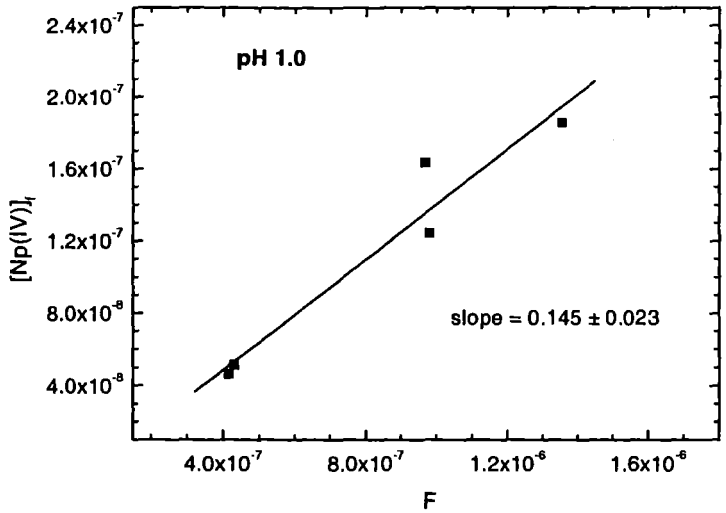

Fig. 7: Evaluation of loading capacity (LC) for Np(IV) fulvate complexation at pH 1.0.

The $[Np^{4+}]$ is calculated by Eq. (7) and for the loading capacity a slope of 0.145 by linear regression is obtained and this result coincides with the saturation curve ($[NpFA(IV)]_t/[FA(IV)]_t$ versus $[Np(IV)]_t/[FA(IV)]_t$) in Figure 6. A numerical solution of this relations is given elsewhere [10].

The reaction stoichiometry can be obtained by rearranging equation (1) in the following way:

$$\log [NpFA(IV)]/[Np^{4+}] = \log \beta + n \log[FA]_{free} \qquad (10)$$

When the ratio $[NpFA(IV)]/[Np^{4+}]$ is plotted versus $[FA]_{free}$ on a log-log scale a linear relationship is obtained with a slope of n. This equation has been applied to our data for the total neptunium fulvate and for only the neptunium fulvate in solution (**Figure 8**). For both data sets a slope near unity (1.12 ± 0.2 and 1.01 ± 0.23) has been found at pH 1.0 for the Np(IV)-fulvate complex and only a insignificant difference between the aggregate and the solution species can be assumed. At higher ratios $Np(IV)_t/FA(IV)_t$ and hence, higher loading of the fulvate, the slope changes, maybe due to more a aggregation of FA molecules. These values were rejected and are not shown in the graph.

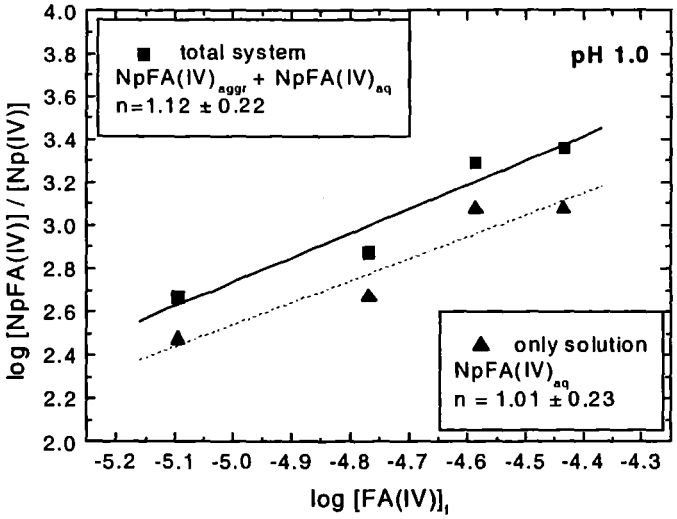

Fig. 8: Validation of the complextion of Np(IV) with fulvic acid at pH 1.0 postulated by Eq. (1). The free fulvate concentration is evaluated by Eq. (6).

For the data a complexation constant log β can now be calculated by equation (8) at pH 1. For the reaction

$$Np^{4+} + FA(IV) \leftrightharpoons NpFA(IV) \qquad (11)$$

a complexing constant of

$$\log \beta = 7.86 \pm 0.09$$

is yielded.

Discussion of experiments at $Np(IV)_t/FA(IV)_t$ ratios < 0.1.

Two remarkable observations (see Fig. 2 and 3) are made at lower $Np(IV)_t/FA(IV)_t$ ratios (<0.1). First, in the absorption spectra no absorbance of the free Np(IV) is observed, but it must be emphasized, that the detection limit of the Np(IV) by absorbance spectroscopy is of about 8 x 10^{-7} mol/L. For the experiment about 0.8-30 % of the applied total Np(IV) concentration are not detectable, and hence, the data cannot be used for calculations of the complexation constant. Second, at ratios lower than 0.01, only one absorbance peak at 974.5 nm is observed and a maximum at 967.5 nm does not exist. But with increasing ratio, corresponding to increasing loading of the fulvate, the absorbance at 968 nm arises and overlays the absorbance at 974.5 nm. From this observation two Np-fulvate species can be assumed, which are denoted as $NpFA(IV)_{968}$ and $NpFA(IV)_{975}$. The spectra were deconvoluted in both absorbance bands, and the yielded absorbances at given $[Np(IV)]_t/[FA(IV)]_t$ ratios are illustrated in **Figure 9.** From this plot the absorbances of $NpFA(IV)_{975}$ complex reach a saturation, whereas the $NpFA(IV)_{968}$-absorbances still increase. The two fulvate species are obviously not dependent of each other and are formed

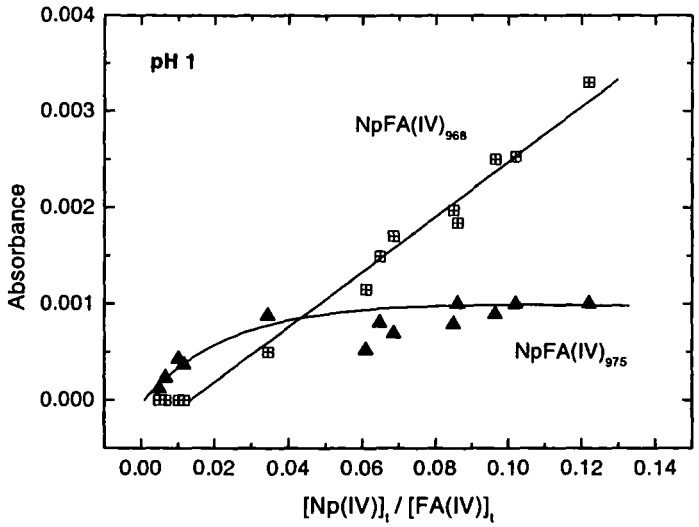

Fig. 9: Absorbances of $NpFA(IV)_{968}$ and $NpFA(IV)_{975}$ depending on the loading of fulvate at pH 1.

simultaneously. For the molar absorption coefficient for the $NpFA(IV)_{975}$ complex, which was calculated from data where $NpFA(IV)_{968}$ is zero, a first rough value of 51 L mol^{-1} L^{-1} was obtained. What kind of species is formed at very low loading of the fulvate is unknown and speculative. On one hand, maybe a limited number of strong sites are responsible for a strong binding of Np(IV). Such sites might be carboxylic groups which are in near vicinity, like oxalic acid, and hence, have low pK_s values. In this case the binding mechanism is governed by a more chelating effect. The shift of the absorption band to longer wavelengths points to such a mechanism. On the other hand, we have seen a kinetic effect for the complexation according to Fig. 5. It is conceivable that a more condensed species is formed due to local high concentrations of Np(IV) or fulvate by adding them to the solution. The re-organization of such a colloid than may be hindered kinetically. Unfortunately, a more detailed evaluation of the data is not possible, because the free Np(IV) species cannot be determined under the given experimental conditions.

Another remarkable observation is made when batch experiments are compared with the titration method at almost same conditions. In **Figure 10** the relative concentrations of total $NpFA(IV)_{aq}$, $NpFA(IV)_{aggr}$ and free Np(IV) for both methods are plotted against the ratios $Np(IV)_t/FA(IV)_t$. and the values are picked out from Table II (appendix). It is cleared out, that the relative concentrations of $Np(IV)FA_{aq}$ and $Np(IV)FA_{aggr}$ are more close and increase parallel for the batch experiment contrary to the titration method. But for the titration method a constant value of $NpFA(IV)_{aggr}$ is reached at $[Np(IV)]_t/[FA(IV)]_t$ ratios >0.08, in contrast to

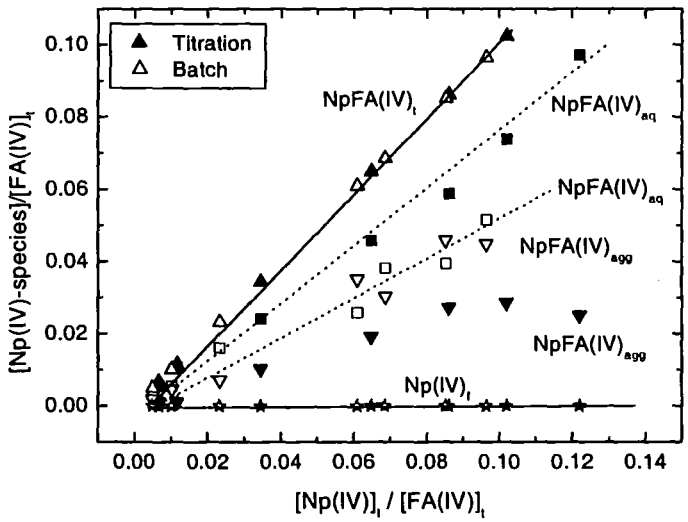

Fig. 10: Relative concentrations of Np(IV) species at pH 1.0 obtained by both batch experiments and titration method.

the batch method. But nevertheless, when the total formed neptunium fulvate ($NpFA(IV)_t$) is compared, they are identical for both methods. The distribution of the two different fulvate species (aggregate and solution species) depends on the history of the preparation, but does not influence the total amount of neptunium fulvate.

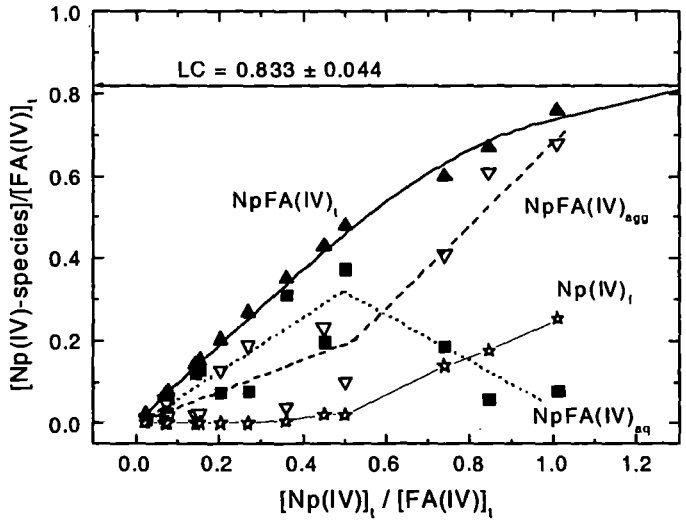

Fig. 11: Relative concentrations of Np(IV) species in fulvic acid solution at pH 1.5. The data of the total Np(IV)-fulvate is fitted according [10] (solid line). The other lines are free-plotted in order to make clear trends of each species.

Fulvate complexation at pH 1.5

It is known from many studies that metal fulvate complexation depends on the pH value. In order to prove the influence of the pH experiments were performed at pH 1.5. The absorption spectra of Np(IV) in fulvic acid solutions at pH 1.5 (Fig. 4) resemble the spectra at pH 1 (see Fig. 1-3). The absorption bands for the free Np(IV) at 960 nm and the two Np(IV)-fulvate species at 967.5 nm and 974.5 nm are observed. The evaluation was made in the same way described for pH 1. In Table III (appendix) the concentrations of the Np(IV) species are listed and in **Figure 11** the mol fractions of each species is shown as a function of the $Np(IV)_t/FA(IV)_t$ ratio. The limit, where no free Np(IV) can be measured is shifted to $Np(IV)_t/FA(IV)_t \sim 0.4$ (pH 1 ~ 0.1), and this shift represents a higher complexation of Np(IV) by fulvic acid. At higher loading more $NpFA(IV)_{agg}$ is observed and consequently, smaller amounts of neptunium fulvate are found in solution. By fitting the data of the total amount of neptunium fulvate a LC of 0.833 ± 0.044 is deduced. This is much higher than at pH 1 and can at the moment not explained. However, a deconvolution of the NpFA(IV) absorption peak in two contributions, one peak at 968 and the other at 975 nm, have yielded no reliable data for the absorbances of $NpFA(IV)_{968}$ and $NpFA(IV)_{975}$, as seen in **Figure 12.** Obviously, no relationship between $[Np(IV)]_t/[FA(IV)]_t$ ratios and the absorbances of the pure NpFA(IV) species can be observed. But if only samples are considered, that show only the absorption band at 974.5 nm a molar absorption coefficient for $Np(IV)FA_{975}$ is estimated to 51 ± 5 L

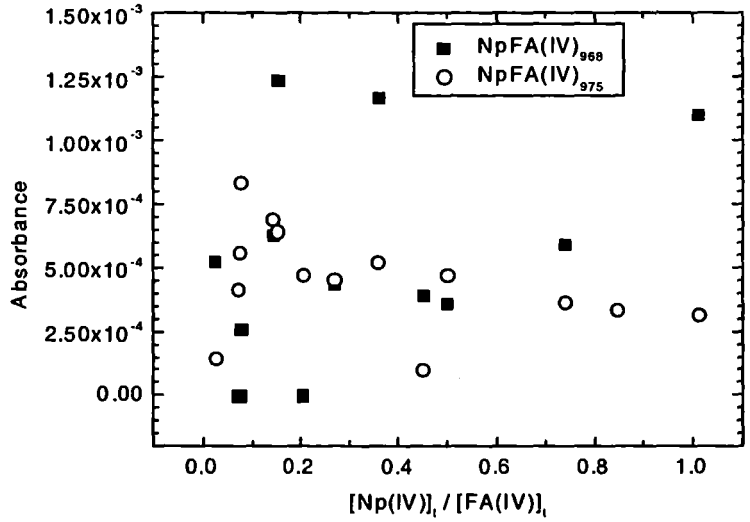

Fig. 12: Absorbance of $NpFA(IV)_{968}$ and $NpFA(IV)_{975}$ obtained by deconvolution of the spectra as a function of $[Np(IV)]_t/[FA(IV)]_t$

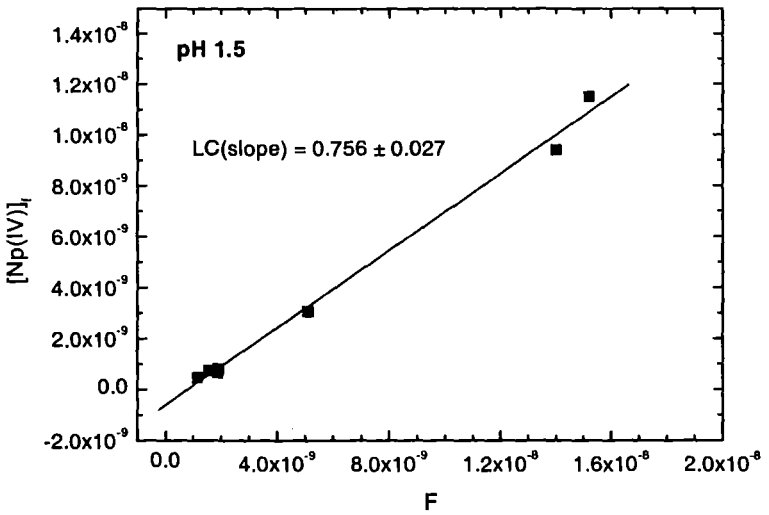

Fig. 13: Evaluation of the loading capacity for the Np-fulvic acid complexation at pH 1.5 according Eq. (9).

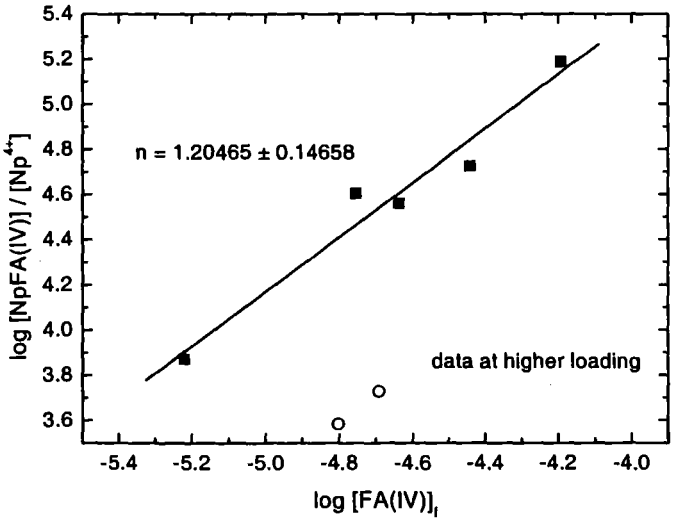

Fig. 14: Verification of the Np(IV) fulvate complexation according the assumed reaction (1) at pH 1.5. The unfilled points are data evaluated at high Np(IV) loading of the fulvic acid.

mol^{-1} cm^{-1} which is similiar with the value estimated at pH 1.0. Seemingly, the spectroscopic properties of the Np-fulvate species are sensitive against the conditions in solution and maybe the state of aggregation .

The loading capacity, which is calculated according to the linear relationship Eq. (9) is 0.76 ± 0.03 (**Figure 13**) and, comparable with the high value deduced from the saturation curve in Fig. 11. Finally, the complexation constant log β is calculated at pH 1.5 by taking

into consideration the LC and the hydrolysis with the same assumptions made at pH 1. A log β of

$$\log \beta = 9.18 \pm 0.17$$

is obtained:

In the same manner as for pH 1 the complexation reaction (1) is verified according to Eq. (10) by plotting log [NpFA(IV)]/[Np^{4+}] against log $[FA(IV)]_f$. The free fulvate complexation is deduced from Eq. (6). The data point, illustrated in **Figure 14,** results by a linear regression in a slope of n = 1.20 ± 0.15, which is a little higher than 1. At high loading of the fulvate data points are calculated which do not fit in the line of unity and confirm again the unknown mechanism of interaction of Np(IV) with fulvic acid.

4. Conclusion

This work reveals a strong interaction of tetravalent neptunium with fulvic acid at pH 1 and 1.5. Three problems arise from the results. First, the degree of deprotonation of fulvic acid is at such acidic conditions very small. Loading with metal and neutralizing the charge of the fulvic acid lead to destabilization of the colloid behaviour and the fulvic acid aggregates to bigger particles. The role of the aggregates in the binding of Np(IV) is up to now unclear. Second, the spectra show two simultaneously existing fulvate species, which can not be characterized in detail up to now. Especially for the species at 974.5 nm the nature is unclear. Third, the hydrolysis of the Np(IV) occurs in the used pH range and two main hydrolysed species, $Np(OH)^{3+}$ and $Np(OH)_2^{2+}$, are proposed by calculations. In the interpretation of the results it is assumed, that the hydrolysed species are not involved in the fulvate complexation. From earlier studies with trivalent actinides mixed complexes can not be ignored and the role of them for the tetravalent actinides has to be elucidated.

These problems are expressed in a very high loading capacity of 75 %, which is much more than expected from the degree of deprotonation, and a higher complexation constant log β at pH 1.5 compared to pH 1.

The understanding of the fulvate complexation of tetravalent actinides is far away and the present contribution is only the beginning of a lot of necessary activities.

5. Acknowledgements

This work has been performed under a collaboration between the Institute für Nukleare Entsorgungstecknik (INE, Forschungzentrum Karlsruhe) and the Belgian Nuclear Center (SCK•CEN). It was funded partially by the European Commission in the frame of a Marie Curie Grant. The co-author, Vera Pirlet, would like to thank particularly Prof. J-I Kim for the welcome to his laboratory in Karlsruhe where the work was mainly done.

6. References

[1] Zeh, P., Kim, J. I., Marquardt, C. M., and Artinger, R.: The Reduction of Np(V) in Groundwater Rich in Humic Substances, Radiochim.Acta, **87**, 23 (1999).

[2] Artinger, R., Marquardt, C. M., Kim, J. I., Seibert, A., Trautmann, N., and Kratz, J. V.: Humic Colloid-Borne Np Migration: Influence of the Oxidation State, Radiochim.Acta, (2000).

[3] Kim, J. I., Rhee, D. S., Buckau, G., and Morgenstern, A.: Americium(III)-Humate Interaction in Natural Groundwater: Influence of Purification on Complexation Properties, Radiochim.Acta, **79**, 173 (1997).

[4] Kim, J. I. and Marquardt, C. M.: Chemical Reaction of Np(V) With Humic Colloids in Groundwater: Influence of Purification on the Complexation Behaviour, Radiochim.Acta, **87**, 105 (1999).

[5] von Maravic, H.: Migration of radionuclides in the geosphere (Mirage project - Third phase), EUR 15914, Brussels, 1993.

[6] Mikhailov, V. A. Analytical chemistry of Neptunium. Slutzkin, D. 1973. Halsted Press. Ref Type: Book, Whole

[7] Marquardt, C. and Kim, J. I.: Complexation of Np(V) With Humic Acid: Intercomparison of Results From Different Laboratories, Radiochim.Acta, **80**, 129 (1998).

[8] Kim, J. I. and Czerwinski, K. R.: Complexation of Metal Ions With Humic Acid: Metal Ion Charge Neutralization Model, Radiochim.Acta, **73**, 5 (1996).

[9] Neck, V.: Thermodynamic Database for Actinides: Hydrolysis Constants and Solubility Constants for Hydroxide, Oxide, and Carbonate Solid Phases, ANDRA-Project: No. 008790 - FZK-INE 014/99, 1999.

[10] Kim, J. I. and Sekine, T.: Complexation of Neptunium(V) With Humic Acid, Radiochim.Acta, **55**, 187 (1991).

Appendix

Table I: Experimental results of the complexation of Np(IV) ion with fulvic acid at pH 1 ([Np(IV)] constant)
- the subscript "t" means the total concentration.
- the subscript "aq" means concentration in solution.
the subscript "agg" means concentration of aggregated NpFA(IV)

[FA(IV)]t (x10-4eq/l)	[Np(IV)]t (x10-4M)	[Np(IV)] (x10-5M)	[NpFA(IV)]aq (x10-5M)	[NpFA(IV)]agg (x10-5M)
1.62	0.79	6.17	1.50	0.18
4.23	1.03	3.15	4.08	3.07
6.35	1.23	3.58	5.52	3.20
7.41	1.18	2.4	5.80	3.61
8.47	1.11	0.99	6.14	3.97
9.53	1.15	0.89	5.52	5.09
10.6	1.02	~0	3.93	6.27
12.7	1.13	~0	6.13	5.17
2.12	1.17	~0	5.52	6.50

Table II: Experimental results of the complexation of Np(IV) ion with fulvic acid at pH 1 ([FA(IV)] constant) by a titration method for the first set of data and by a batch experiment for the second set of data.

	[FA(IV)]t (x10-4eq/l)	[Np(IV)]t (x10-5M)	[Np(IV)] (M)	[NpFA(IV)]aq (x10-5M)	[NpFA(IV)]agg (x10-5M)
Titration	7.15	0.47	~0	0.397	0.075
	7.12	0.82	~0	0.746	0.074
	7.08	2.43	~0	1.70	0.727
	7.05	4.53	~0	3.20	1.33
	7	5.99	~0	4.10	1.90
	6.97	7.10	~0	5.12	1.98
	6.94	8.43	~0	6.70	1.73
Batch	7.125	0.35	~0	0.218	0.13
	7.125	0.72	~0	0.388	0.33
	7.125	1.65	~0	1.14	0.51
	7.125	4.34	~0	1.84	2.50
	7.125	4.88	~0	2.72	2.16
	7.125	6.06	~0	2.80	3.26
	7.125	6.87	~0	3.67	3.20

Table III: Experimental results of the complexation of Np(IV) ion with fulvic acid at pH 1.5 ([Np(IV)] constant at 2 different values)

[FA(IV)]t (x10-4eq/l)	[Np(IV)]t (x10-5M)	[Np(IV)] (x10-5M)	[NpFA(IV)]aq (x10-5M)	[NpFA(IV)]agg (x10-5M)
0.79	8.03	2.01	2.23	3.79
0.93	7.88	1.64	1.79	4.45
2.2	7.89	0.12	4.39	3.38
5.00	7.59	~0	2.41	5.18
5.69	8.12	~0	2.53	5.59
9.75	7.49	~0	2.37	5.12
0.38	2.81	0.53	0.72	1.56
0.63	3.15	0.13	2.37	0.65
0.70	3.15	0.14	1.39	1.62
0.81	3.36	0.083	1.96	1.32
1.19	3.19	~0	1.12	2.07
1.25	2.54	~0	2.90	2.25
4.75	3.49	~0	1.89	1.60
5.5	3.85	~0	1.55	2.30

Annex 4

Modeling of Humic Colloid Borne Americium(III) Migration using the Transport/Speciation Code K1D

(W. Schüßler, R. Artinger, J.I. Kim, N.D. Bryan and D. Griffin
(FZK/INE, Uni-Manchester and RMC-E))

3rd Technical Progress Report

EC Project:

"Effects of Humic Substances on the Migration of Radionuclides: Complexation and Transport of Actinides"

Project No.: FI4W-CT96-0027

Modeling of Humic Colloid Borne Americium(III) Migration Using the Transport/Speciation Code K1D

W. Schüßler, R. Artinger, J.I. Kim, N.D. Bryan* and D. Griffin**

Forschungszentrum Karlsruhe, Institut für Nukleare Entsorgung, Karlsruhe, Germany

*University of Manchester, Department of Chemistry, Manchester, UK

**RMC-E, Abingdon, UK

Modeling of humic colloid borne Americium (III) migration using the transport/speciation code K1D

W. Schüßler*, R. Artinger, and J.I. Kim, Institut für Nukleare Entsorgungstechnik
Forschungszentrum Karlsruhe, Postfach 3640, D-76021 Karlsruhe, Germany
N.D. Bryan, University of Manchester, Department of Chemistry, Oxford Road,
GB-M13 9PL Manchester, United Kingdom
D. Griffin, RMC Environmental Ltd, Suite 7, Hitching Court, Abingdon Business Park,
Abingdon, Oxfordshire OX14 1RA
*Corresponding author. Tel.: +49-7247-6024; fax: +49-7247-3927;
e-mail: wolfram@ine.fzk.de

Abstract
The humic colloid borne Am(III) transport was investigated in column experiments for Gorleben groundwater/sand systems. It was found that the interaction of Am with humic colloids is kinetically controlled, which strongly influences the migration behavior of Am(III). These kinetic effects have to be taken into account for transport/speciation modeling.

The KICAM (KInatically Controlled Availability Model) was developed to describe actinide sorption and transport in laboratory batch and column experiments. It is an approach based on association/dissociation kinetics of actinides onto or from humic colloids and mineral surfaces. The application of the KICAM requires a chemical transport/speciation code, which simultaneously models both; kinetically controlled processes and equilibrium reactions. Therefore, the code K1D was developed as a flexible research code that allows the inclusion of kinetic data in addition to transport features and chemical equilibrium.

The application of the KICAM concept is presented using the K1D code for column experiments which show the unretarded breakthrough of humic colloid borne Am as well as retarded Am migration. The model parameters were determined for a Gorleben groundwater system of high humic colloid concentration. A single set of parameters was used to model a series of column experiments. Model results correspond well to experimental data for the unretarded humic borne Am breakthrough. Modeling of the distribution of Am sorbed onto sediment in a column was less successful because the interaction between Am and the humic coated sediment surface could not be characterized in detail from experimental data.

1. Introduction

The colloid borne transport of contaminants is widely recognized (Honeyman, 1999; Kim, 1994; Kim et al., 1984; McCarthy and Zachara, 1989; Ouyang et al., 1996). There is evidence for the potential impact of colloid facilitated mobilization of actinides (Artinger et al., 1998; Buddemeier and Hunt, 1988; Kaplan et al., 1994; Kersting et al., 1999; Kim et al., 1994; Marley et al., 1993; McCarthy et al., 1998; Nagasaki et al., 1997; Randall et al., 1994; Saltelli et al., 1984). Therefore, this process has to be quantified for the safety assessment in high level radioactive waste disposal.

Laboratory investigations on humic colloid facilitated actinide transport has been conducted by both, column and batch experiments. Some of the important chemical processes

controlling the behavior of actinides in such experiments were found to be kinetically controlled (Artinger et al., 1998; Artinger et al., 1999a; Artinger et al., 1999b). To describe these experiments the KICAM model (**KI**netically **C**ontrolled **A**vailability **M**odel (Schüßler et al., 1999)) was developed. The KICAM is an approach based on the kinetics of association/dissociation reactions of metals with humic colloids and mineral surfaces.

To implement the KICAM for reactive transport modeling, adequate numerical tools (computer codes) have to be developed. Although some of the chemical processes controlling the actinide migration in column experiments were found to be kinetically controlled (Artinger et al., 1998; Artinger et al., 1999b; Davies et al., 1999; Geckeis et al., 1999; Pompe et al., 1999), others can be assumed to be in local equilibrium. It is possible to simulate equilibrium reactions using rate constants. However, this is very inefficient in terms of computing time. For this reason, the K1D code (Bryan et al., 1999) was developed for this work instead of using existing codes (e.g. (Bo and Carlsen, unpublished)).

The aim of this paper is to verify and test the applicability of both the KICAM model and the K1D code, in order to establish a reliable tool for quantifying colloid facilitated radionuclide migration.

2. Description of the Kinetically Controlled Availability Model (KICAM)

The reasons for the special structure and a detailed description of the KICAM development is given in Schüßler et al. (1999). The reaction scheme adopted in the KICAM model (Fig. 1) considers the following Am(III) species: dissolved inorganic Am(III) (Am^{io}); Am(III) sorbed onto the sediment (AmSurf); and humic colloid bound Am(III); two binding modes: *"fast"* ($Am(HA^{fast})$) and *"slow"* ($Am(HA^{slow})$).

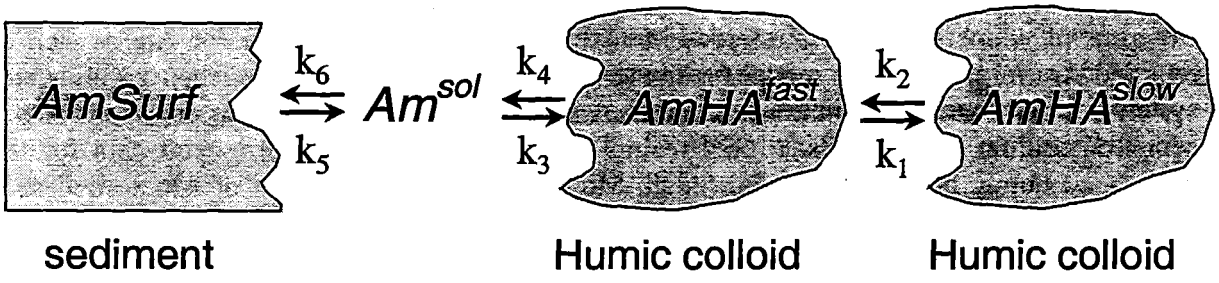

Fig. 1 Concept of the Kinetically Controlled Availability Model (KICAM) (for details see text).

Taking into account the experimental data the KICAM consists of three chemical reactions (Table 1) resulting in four coupled differential equations (Table 2). The rate constants k_1-k_6 controlling the interaction of Am(III) with humic colloids and mineral surfaces are determined from batch and column experiments using equations (1-4). The set of rate and corresponding equilibrium constants derived is shown in (Table 3).

Table 1 Chemical reactions considered in the KICAM.

$Am(HA^{fast}) + HA \underset{k_2}{\overset{k_1}{\rightleftharpoons}} Am(HA^{slow})$	K^{I}	I
$Am^{io} + HA \underset{k_4}{\overset{k_3}{\rightleftharpoons}} Am(HA^{fast})$	K^{II}	II
$AmSurf \underset{k_6}{\overset{k_5}{\rightleftharpoons}} Am^{io} + Surf$	K^{III}	III

Table 2 Differential equations for the Am species considered in the KICAM.

$$\frac{d[Am(HA^{slow})]}{dt} = k_1 \cdot [HA] \cdot [Am(HA^{fast})] - k_2 \cdot [Am(HA^{slow})] \quad (1)$$

$$\frac{d[Am(HA^{fast})]}{dt} = k_2 \cdot [Am(HA^{slow})] + k_3 \cdot [HA] \cdot [Am^{io}] - (k_1 \cdot [HA] + k_4) \cdot [Am(HA^{fast})] \quad (2)$$

$$\frac{d[Am^{io}]}{dt} = k_4 \cdot [Am(HA^{fast})] + k_5 \cdot [AmSurf] - (k_3 \cdot [HA(I)] + k_6 \cdot [Surf]) \cdot [Am^{io}] \quad (3)$$

$$\frac{d[AmSurf]}{dt} = k_6 \cdot [Surf] \cdot [Am^{io}] - k_5 \cdot [AmSurf] \quad (4)$$

Table 3 Equilibrium and rate constants for Am(III) association/dissociation reactions determined from the GoHy-2227 system using the KICAM.

rate constants		equilibrium constants	
$\log(k_1 \cdot sec \cdot mol \cdot l^{-1})$	-3.2	$\log(K^{I} \cdot mol \cdot l^{-1})$	2.8 ± 0.1
$\log(k_2 \cdot sec)$	-6.0	$\log(K^{II} \cdot mol \cdot l^{-1})$	5.6 ± 0.5
$\log(k_3 \cdot sec \cdot mol \cdot l^{-1})$	1.5	$\log(K^{III} \cdot mol \cdot l^{-1})$	6.2 ± 0.5
$\log(k_4 \cdot sec)$	-4.1		
$\log(k_5 \cdot sec)$	-3.9		
$\log(k_6 \cdot sec \cdot mol \cdot l^{-1})$	2.3		

3. Description of the K1D

The K1D code was developed to be used as tool for modeling humic colloid borne radionuclide migration. It is able to use equilibrium and rate constants to describe the association/dissociation reactions of radionuclides with humic colloids and mineral surfaces. The code uses three different sets of equations to solve for the chemistry of the system: mass balance equations, equilibrium equations, and kinetic or rate equations. The transport of the chemical species is described by a simple 1-dimensional advection/dispersion model (for details see Bryan et al. (1999)). The K1D source code is written in FORTRAN and was compiled for different systems (Windows, Unix, Linux). Numerical calculations are based on equidistant space increments and time steps. The numerical tool K1D allows the implementation of the KICAM for reactive transport modeling

4. Verification of the K1D

The KICAM model was applied to the Am batch and column experiments of Artinger et al. (1998). A set of these experiments was used to determine the KICAM rate constants for Am (Schüßler et al., 1999). The Am breakthrough in the column experiments was calculated using this parameter set and the K1D code. The experimentally determined and calculated Am breakthrough curves for three column experiments are shown in Fig. 2. The K1D code allows the implementation of the KICAM to model the humic colloid mediated Am migration. Real recoveries (Artinger et al. 1998) were found to agree with those predicted using the K1D code. Hence, the code has been verified by comparison with experimental data.

5. Application of the KICAM using the code K1D

The KICAM now is applied to a column experiment investigating the unimpeded and retarded Am migration. Due to the high distribution coefficient of Am onto the sediment surface (up to R_S = 100-1000 $ml \cdot g^{-1}$ (Artinger et al., 1998)) only the breakthrough of the unimpeded Am migration could be observed in the effluent. The retarded Am migration could only be quantified by examining the spatial distribution of the Am sorbed in the column. The Am distribution in the column was modeled using the data set determined from the GoHy-2227 batch and column experiments (Table 3). From the modeling results of Schüßler et al. (1999) it is expected, that the direct application of these parameter set to the GoHy-412 system will

qualitatively describe the experimental results. However, comparing the absolute values of the experimental data to the calculated data, a discrepancy of about a factor of 3 is expected (Am recovery calculated for the Gohy-412 system by Schüßler et al. (1999) R_{calc} = 2 %, experimental determined recovery R_{exp} = 6 %).

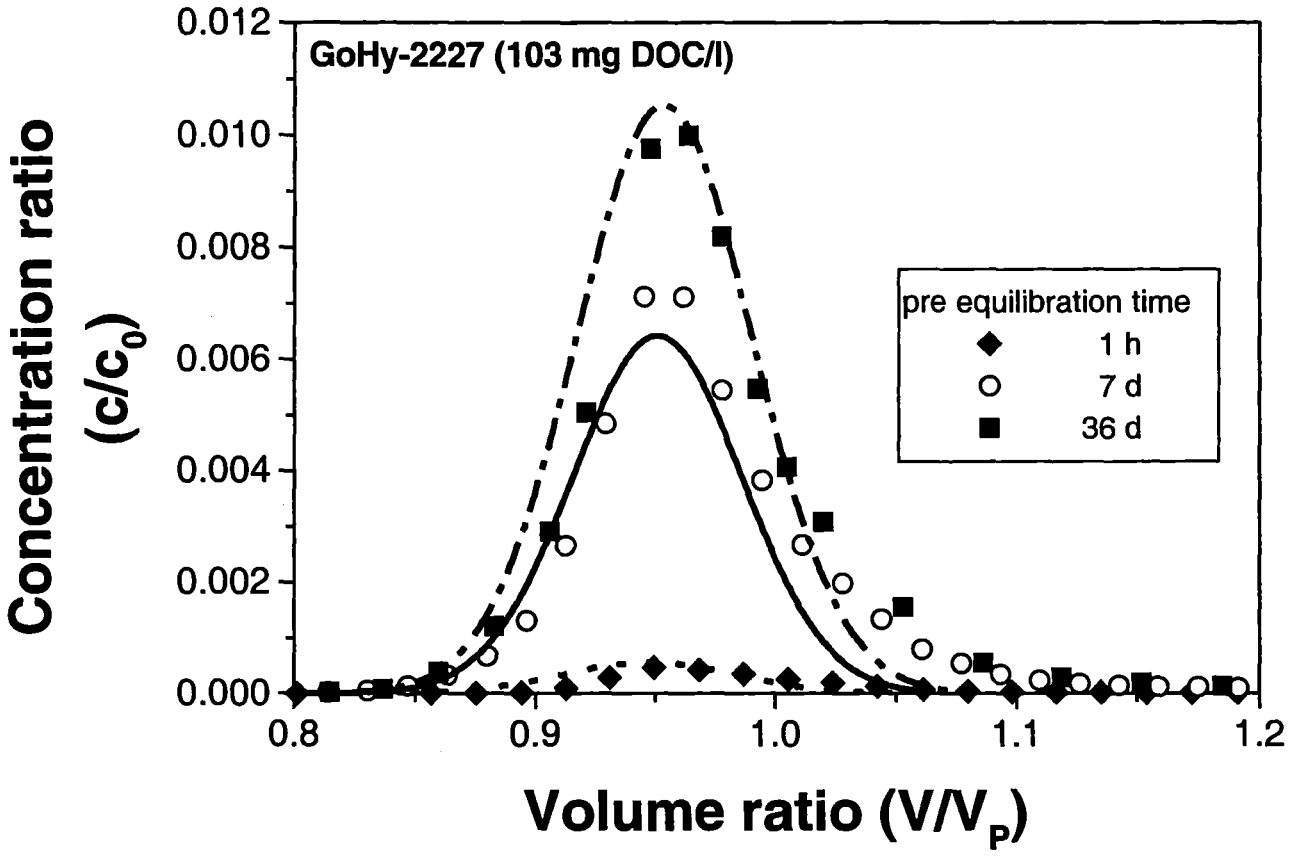

Fig. 2 Experimental determined (symbols) and calculated (lines) Am breakthrough curves for GoHy-2227 column experiments varying the Am groundwater equilibration time. The Am breakthrough was calculated by means of the KICAM/K1D tool.

Two model approaches, local chemical equilibrium and kinetically controlled Am association/dissociation (KICAM), were tested. Fig. 3 shows that both approaches are not able to describe the Am distribution in the column satisfactorily. For the equilibrium approach this reflects the fact, that the principle processes controlling the humic colloid facilitated Am migration in the column are not in local chemical equilibrium.

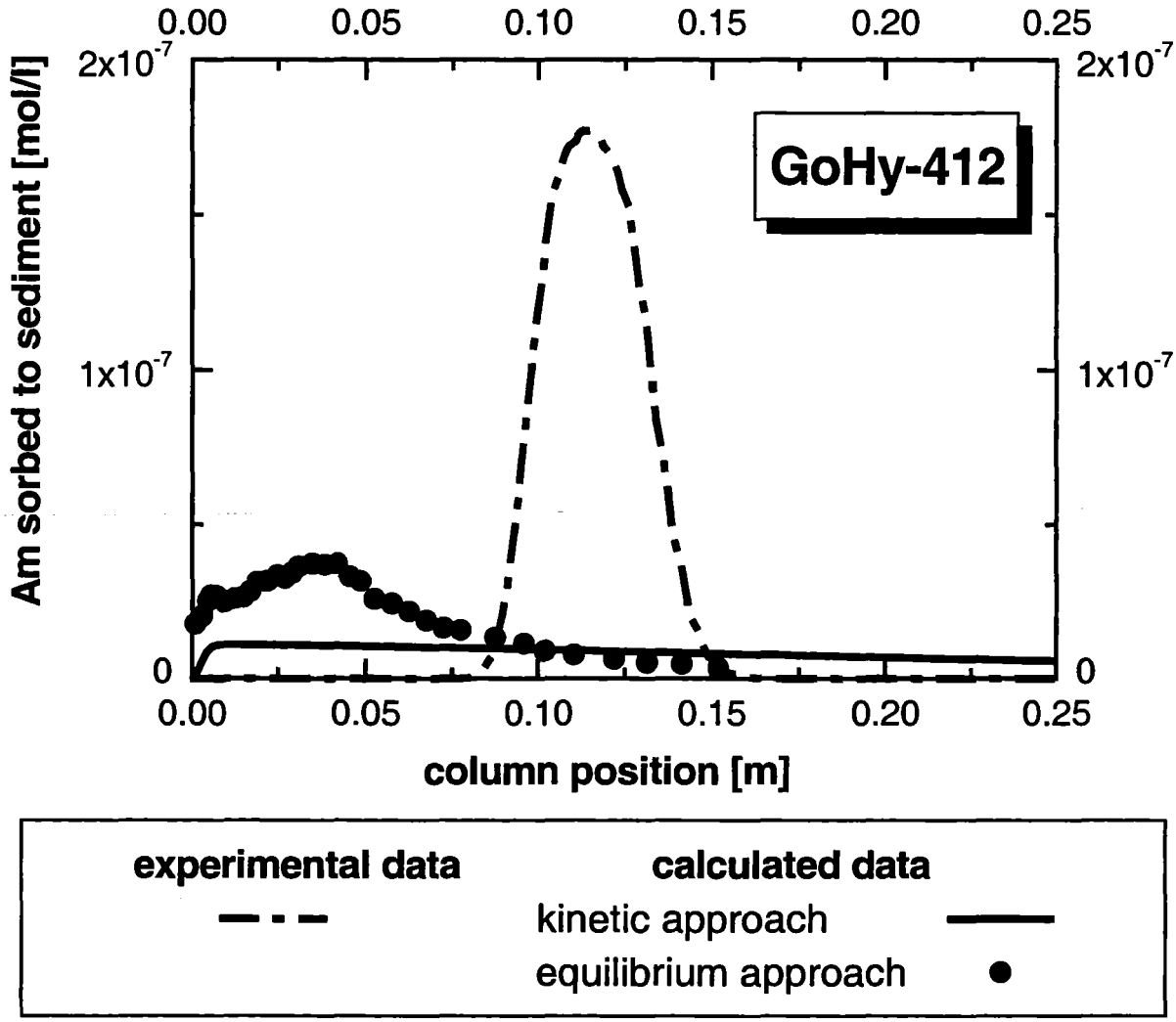

Fig. 3 Experimental determined and calculated spatial distribution of Am sorbed onto the sediment in a GoHy-412 column experiments after 400 days.

The KICAM approach describes qualitatively the experimental data but, as expected from the modeling results, problems exist with quantification. Compared to the experimental data, the model result for the GoHy-412 system shows a broader Am distribution within the column of a lower concentration level and a higher Am recovery. The recovery calculated by means of the KICAM/K1D approach corresponds to the values given by Schüßler et al. (1999). The calculated distribution and the calculated recovery for the GoHy-412 system do not fit to the experimental data, but they are consistent: If the dissociation of Am from the humic colloid becomes slower, the recovery increases. Also, the mass transfer of Am from the humic colloid onto the mineral surface becomes slower. Thus a higher Am recovery corresponds to a broader Am distribution and a lower concentration level in the column. The consistency of the modeling results show, that the KICAM in principle is able to describe the experimental findings. However, the reaction scheme used in the KICAM approach seems to be to simple to allow a direct application of the GoHy-2227 KICAM rate constants to the GoHy-412

system. This is due to the system differences, i.e. solution speciation, which are neglected in the KICAM model. In addition, the systems also differ in humic colloid composition. To produce a better model with parameter transferability, system diversity has to be taken into account.

5. Discussion

The KICAM approach using the K1D code is an appropriate tool to access the humic colloid mediated actinide migration. The tool is able to describe and predict laboratory experiments. However, the kinetically controlled association/dissociation processes of Am with humic colloids and sediment surfaces must be described on a more sophisticated level, to allow a better quantification of the Am migration behavior and a better transferability of rate constants. To reach this goal, the reactions and species have to be verified by independent methods (e.g. EXAFS or TRLFS). Also, the influence of relevant system parameters (e.g. pH, carbonate, and composition of the humic colloids) must be described and quantified.

The tool (KICAM/K1D) can be used in performance assessment studies. The impact of humic colloids on the actinide migration may be quantified and scenarios relevant to PA can be identified.

The computing time required to calculate the 400 day column experiment presented in this paper, was about 3 weeks CPU time on a PC Pentium III 550 MHz. This long computing time is due to the fact, that the kinetic reactions of the KICAM could not be approximated by equilibrium equations. The columns were discretisised by 200 equidistant space increments and $3 \cdot 10^7$ time steps (corresponding to a spatial increment of about 1 mm and a time step of about 1 second). In order to reduce the computing time, the K1D code will be improved further.

References

Artinger, R., Kienzler, B., Schüßler, W. and Kim, J.I., 1998. Effects of humic substances on the ^{241}Am migration in a sandy aquifer: column experiments with Gorleben groundwater/sediment systems. J. Contam. Hydrol., 35(1-3): 261-275.

Artinger, R. et al., 1999a. Humic colloid-mediated transport of uranium in column experiments. Adv. Environ. Res., Submitted for publication.

Artinger, R. et al., 1999b. Humic colloid-borne Np migration: Significance of the oxidation state. submitted to Migration'99.

Bo, P. and Carlsen, L., unpublished. COLUMN3: A computer code for modelling transport and distribution of complex mixtures. .

Bryan, N.D. et al., 1999. Combined Mechanistic and Transport Modelling of Metal Humate Complexes. In: G. Buckau (Editor), Effects of humic substances on the migration of radionuclides: complexation and transport of actinides. Second technical progress report., Karlsruhe, pp. 303-338.

Buckau, G., Bryan, N.D., Schüßler, W., Artinger, R. and Kim, J.I., 1999. Actinide Migration Case Study in the Gorleben Aquifer System. submitted to Migration'99.

Buddemeier, R.W. and Hunt, J.R., 1988. Transport of colloidal contaminants in groundwater: radionuclide migration at the Nevada Test Site. Appl. Geochem., 3: 535-548.

Davies, J., Higgo, J., More, Y. and Milne, C., 1999. The Characterizaqtion of a Fulvic Acid and its Interaction with Uranium and Thorium. In: G. Buckau (Editor), Effects of humic substances on the migration of radionuclides: complexation and transport of actinides. Second technical progress report., Karlsruhe, pp. 59-80.

Geckeis, H., Rabung, T. and Kim, J.I., 1999. Kinetic Aspects of the Metal Ion Binding to Humic Substances. In: G. Buckau (Editor), Effects of humic substances on the migration of radionuclides: complexation and transport of actinides. Second technical progress report., Karlsruhe, pp. 47-58.

Honeyman, B.D., 1999. Colloidal culprits in contamination. Nature, 397: 23-24.

Kaplan, D.I., Bertsch, P.M., Adriano, D.C. and Orlandini, K.A., 1994. Actinide association with groundwaters colloids in a coastal plain aquifer. Radiochim. Acta, 66/67: 181-187.

Kersting, A.B. et al., 1999. Migration of plutonium in groundwater at the Nevada Test Site. Nature, 397: 56-59.

Kim, J.I., 1994. Actinide colloids in natural aquifer systems. Mat. Res. Soc. Bull., 19(12): 47-53.

Kim, J.I., Buckau, G., Baumgärtner, F., Moon, H.C. and Lux, D., 1984. Colloid generation and the actinide migration in Gorleben groundwaters. Mat. Res. Soc. Symp. Proc., 26: 31-40.

Kim, J.I., Delakowitz, B., Zeh, P., Klotz, D. and Lazik, D., 1994. A column experiment for the study of colloidal radionuclide migration in Gorleben aquifer systems. Radiochim. Acta, 66/67: 165-171.

Marley, N.A., Gaffney, J.S., Orlandini, K.A. and Cunningham, M.M., 1993. Evidence for radionuclide transport and mobilization in a shallow, sandy aquifer. Environ. Sci. Technol., 27: 2456-2461.

McCarthy, J.F., Czerwinski, K.R., Sanford, W.E., Jardine, P.M. and Marsh, J.D., 1998. Mobilization of transuranic radionuclides from disposal trenches by natural organic matter. J. Contam. Hydrol., 30: 49-77.

McCarthy, J.F. and Zachara, J., M., 1989. Subsurface transports of contaminants. Environ. Sci. Technol., 23(5): 496-502.

Nagasaki, S., Tanaka, S. and Suzuki, A., 1997. Interfacial behavior of actinides with colloids in the geosphere. J. Nucl. Mat., 248: 323-327.

Ouyang, Y., Shinde, D., Mansell, R.S. and Harris, W., 1996. Colloid-Enhanced Transport of Chemicals in Subsurface Environments: A Review. Environ. Sci. Technol., 26(2): 189-204.

Pompe, S. et al., 1999. Investigation of the Migration Behavior of Uranium in an Aquifer System Rich in Humic Substances: Laboratory Column Experiments. In: G. Buckau (Editor), Effects of humic substances on the migration of radionuclides: complexation and transport of actinides. Second technical progress report., Karlsruhe, pp. 59-80.

Randall, A., Warwick, P., Lassen, P., Carlsen, L. and Grindrod, P., 1994. Transport of Europium and Iodine through Sand Columns in the Presence of Humic Acids. Radiochim. Acta, 66/67: 363-368.

Saltelli, A., Avogadro, A. and Bidoglio, G., 1984. Americium filtration in glauconitic sand columns. Nucl. Technol., 67: 245-254.

Schüßler, W., Artinger, R., Kienzler, B. and Kim, J.I., 1999. Modeling of humic colloid borne Americium Migration by a kinetic approach. submitted to Environ. Sci.Technol.

Annex 5

Complexation Studies of Uranium and Thorium with Natural Fulvic Acid

(J. Davis, J. Higgo, D. Noy and P. Hooker (BGS))

3rd Technical Progress Report

EC Project:

"Effects of Humic Substances on the Migration of Radionuclides: Complexation and Transport of Actinides"

Project No.: FI4W-CT96-0027

BGS Contribution to Task 2 (Complexation)

Complexation Studies of Uranium and Thorium with a Natural Fulvic Acid

J.R. Davis, J.J.W. Higgo, D.J. Noy and P.J. Hooker

British Geological Survey, Keyworth, Nottingham, NG12 5GG, United Kingdom

ABSTRACT

The BGS investigations under Task 2 focussed on laboratory experiments to elucidate the complexation behaviour of aqueous U(VI) and Th(IV) with a well-characterised natural fulvic acid, DE72 FA, collected from the Derwent Reservoir, Derbyshire, UK. This paper summarises the previous BGS work on U and Th complexation and describes some new results for Th dissociation.

Three laboratory batch methods, involving ion-exchange, solvent extraction and kinetics experiments, were used to study the complexation behaviour of U and Th with DE72FA covering a range of ionic strengths and pH. The ion exchange and solvent extraction experiments gave similar conditional stability constant results for U, and the log beta values were of the same order as those obtained previously for other U-natural fulvic acid systems.

Batch kinetics experiments were used to measure the rates of dissociation of U and Th from their complexes with DE72 FA. The calculated rate constants were reciprocated to give the average-lives or time-constants ($\tau 1$, $\tau 2$ and $\tau 3$) of the metals in the three binding modes. The $\tau 3$ times for Th undergoing slow dissociation ranged from 470 to 1913 hours and were much less sensitive to metal-fulvic acid equilibration time and ionic strength than the $\tau 3$ values for U. The slow dissociation rates for U were comparable to the Th rates after the longest period of U-fulvic acid equilibration, but the fraction of U remaining in the hindered sites was much smaller (~7% compared to ~55% for Th). Although it was not possible to determine the irreversibly-bound proportions of these fractions of U and Th in the hindered sites, these new data serve as important constraints when modelling the far-field transport of actinide-fulvate complexes under *in-situ* conditions.

1. INTRODUCTION

It is important to derive new data for the complexation of actinide ions with humic substances under oxidation states and geochemical conditions relevant to the performance assessment of radioactive waste repositories. The potential for actinides to be transported from a radioactive waste repository via colloids is an important process to consider in a performance assessment e.g. Kersting et al. (1999). Organic colloids in the form of aqueous humic substances could carry complexed actinides away from a repository to the biosphere. The greater the stability of such actinide complexes, the longer the potential migration pathways and greater the radiological risk. In this context, the BGS investigations under Task 2 focussed on laboratory experiments to elucidate the complexation behaviour of aqueous U(VI) and Th(IV) with a well-characterised natural fulvic acid.

2. LABORATORY METHODS

Three laboratory batch methods, involving ion-exchange, solvent extraction and kinetics experiments, were used to study the complexation behaviour of U and Th with the Derwent Reservoir fulvic acid (DE72 FA). This natural fulvic acid was fully characterised and described by Higgo *et al*, (1998a; 1998b). A pH range of 4 to 8 and an ionic strength range from 0.01 to 0.1 M were used in the experiments. The speciation of U and Th within these ranges is well documented. As the pH increases, the uranyl ion increasingly speciates with carbonates, but over the series of batch experiments this did not appear to interfere significantly with U-fulvate binding.

2.1 Stability constant experiments

Conditional stability constants were determined using two versions of Schubert's competition method. One, an ion-exchange method, has been described in detail elsewhere (Higgo *et al*, 1992; 1993). The other, a solvent extraction method, was similar to that used by Nash & Choppin (1979), as detailed in Davis *et al*, (1999). Uranium data were obtained by both methods. Thorium stability constants were measured only by solvent extraction but with higher concentrations of HDEHP, [bis(2-ethylhexyl) hydrogen phosphate], in the toluene solvent. This was needed to attain workable distribution coefficients (in the absence of fulvic acid) with increasing pH. Silanised vessels were used to minimise the sorption of uranium and thorium to vessel walls at high pH (Caceci & Choppin 1983). Buffers were not added to control pH.

The conditional stability constants (log β) were calculated from the data obtained with the Schubert-type methods using the following equation:

$$\log\left(\frac{D_0}{D} - 1\right) = \log \beta + i \log [L]$$

where Do is the distribution ratio in the absence of complexing ligand

D is the distribution ratio in the presence of complexing ligand

i is the mole ratio of ligand to metal (assumed to be 1)

[L] is the concentration of ligand, DE72 FA.

The conditional stability constants were calculated in terms of total unbound metal in solution (mol/L) with the fulvic acid concentrations in g/L and in mol/L, using a weight-average molecular weight of 4000 Dalton (Higgo *et al*, 1998b).

2.2 Kinetics experiments

Batch kinetics experiments were used to measure the rates of dissociation of U and Th from their complexes with DE72 fulvic acid. The method was detailed in Davis *et al.* (1999). The solutions were pre-conditioned from 1 to 262 days, simulating a range of metal-fulvic acid equilibration times. Following the pre-conditioning step, resin (Cellphos or Hyphan) was added to the system to induce dissociation by removing the U and Th from the binding sites in the fulvate complexes. Cellphos and Hyphan resins work by chelation, and they were found to be more efficient than cation-exchange resins for quickly mopping up free Th and U in the metal-fulvate solutions. This dissociation stage was monitored with time, typically up to 42 days, to produce the kinetic data. The possible effects of equilibration time, pH and ionic strength on the rates of dissociation were investigated. It should be noted that a suitable resin could not be found for measuring the kinetics of thorium-fulvate dissociation below pH 6. Typical plots of some Th kinetics data are shown in Figures 1 and 2.

The kinetics data were parameterised using a function that is a sum of decaying exponentials terms:

$$f(t)=\sum_{i=1}^{n} a_i e^{-k_i t}$$

with n=3 in most cases. The fitting process was outlined in (Davis *et al*, 1999). The graphical procedure involved plotting the data as log (count rate) against time and making least-squares straight-line fits to the data points. The intercept and slope of each line provided estimates of a_n and k_n respectively. The three calculated first-order rate-constants k1, k2 and k3 (min^{-1}) were calculated for the initially fast, then medium and finally slow dissociation processes respectively. The k1, k2 and k3 values were reciprocated to give the average-lives or time-constants τ1, τ2 and τ3 (h) of the metals in the three binding modes.

Figure 1. **Typical Th-DE72 FA dissociation plots.**

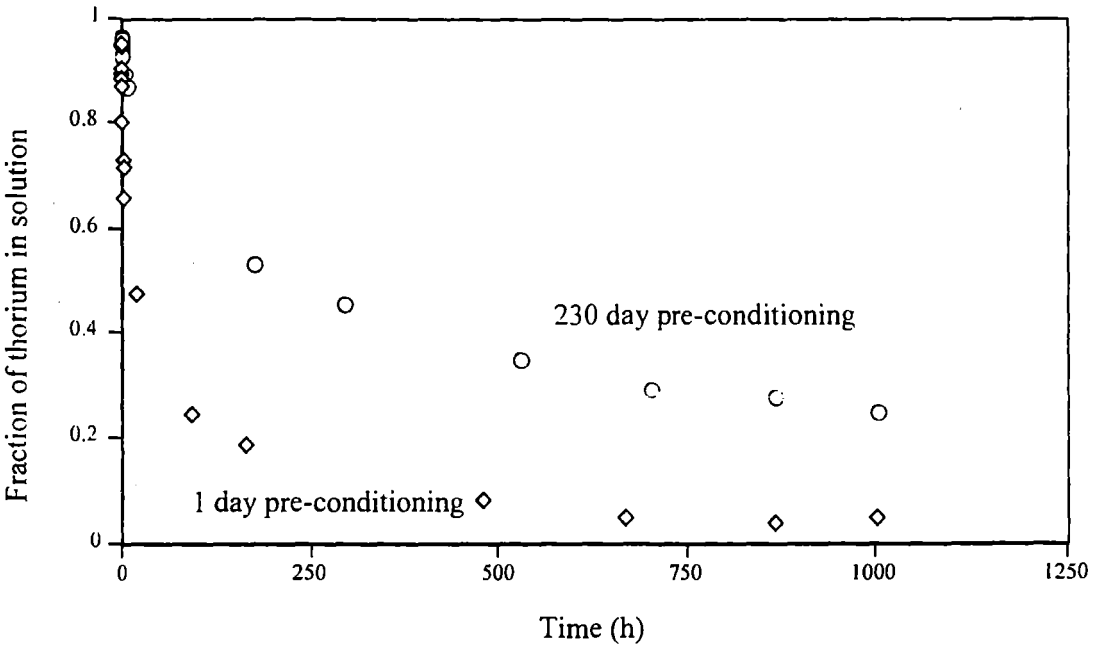

Figure 2. **A typical regression plot.**

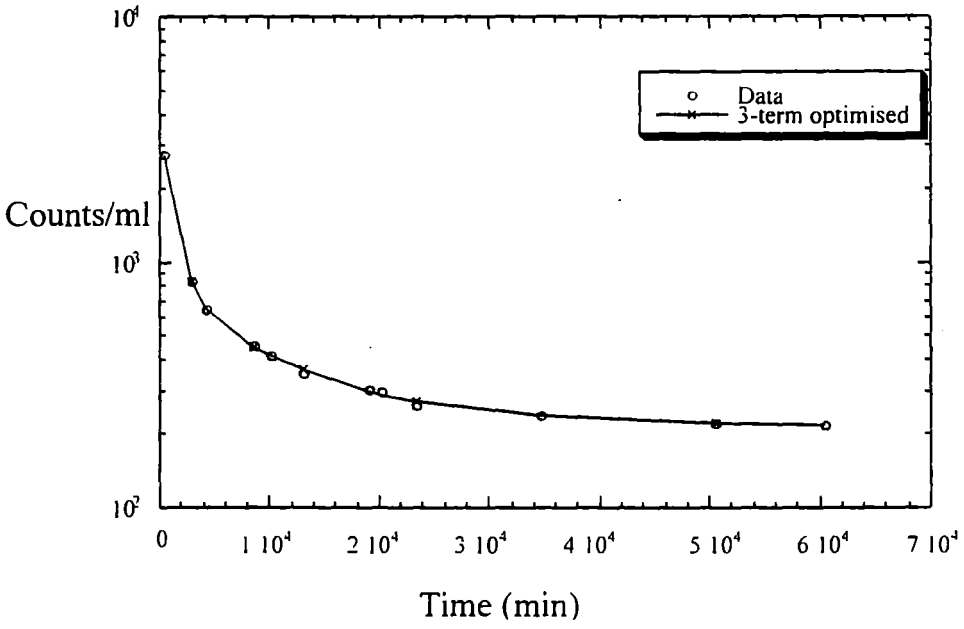

The value of $\tau 3$, the average-life of the metal resident in slow or kinetically hindered sites, was calculated first in the parameterisation process, and therefore $\tau 3$ had smaller errors than the $\tau 2$ and $\tau 1$ values.

The slope data after ~20 days of resin contact gave the best indication of the slow rates of dissociation of the Th from the kinetically hindered sites in the fulvate complexes. For the U case, the dissociation rates were usually much faster, and a one day resin contact time was often sufficient to dissociate most of the U from the complexes with DE72 FA, especially after relatively short pre-conditioning times.

3. RESULTS

3.1 Stability constants

The ion exchange and solvent extraction experiments gave similar conditional stability constant results for U. The log beta values (Table 1) were of the same order as those obtained previously for uranium with fulvic acids extracted from Drigg and Broubster groundwaters (Higgo *et al*, 1992 & 1993), and were similar to other values reported in the literature (Czerwinski *et al.*, 1994).

Table 1. U(VI) and Th(IV) fulvate stability constants by the solvent extraction method.

Ion	pH	Ionic Strength I M (NaCl)	log β (L/g)	log β (L/mol)
U (VI)	3.9	0.1	2.9	6.5
	4.1	0.03	2.7	6.3
	5.9	0.1	3.2	6.8
	7.2	0.1	3.9	7.5
Th (IV)	5.3	0.01	2.0	5.6
	5.5	0.01	1.5	5.1
	6.5	0.1	2.6	6.2

The solvent extraction method worked well for Th at low pH values but at higher values a third layer appeared and more Th appeared to be extracted by the solvent in the presence rather than absence of DE72 FA. It is difficult to compare these thorium

log β values with those in the literature without the aid of a model because of the differences in experimental techniques and reporting methods (see discussion in Davis *et al*, 1999). Log beta values given in Table 1 have been calculated in terms of total unbound thorium in solution and therefore appear low compared with the values in Nash and Choppin (1979), which were calculated on the basis of Th^{4+} only.

3.2 Kinetics results

Tables 2 and 3 summarise the kinetics results for the dissociation of the uranium and thorium-fulvic acid complexes. The data in Table 2 and 3 supersede and correct some data previously reported.

Concentrating first on the fast and medium dissociation rates represented by the τ1 and τ2 time-values, it is apparent that the ranges for U and Th are different. The τ1 range for U (0.06 - 2.1 h) was found to be ten times lower than the τ1 range for Th (0.5 - 23 h). Initially, U dissociated from the labile or loosely binding sites much quicker than Th. The τ2 range for U (0.23 - 93 h) is much wider than the range found for Th (37 - 85 h). The medium rates of dissociation for U were therefore more variable than those for Th, probably as a result of the dissociation being more dependent on the experimental variables of ionic strength and pre-conditioning time.

Table 2. Summary of uranium kinetics data.

[U] M	FA ppm	Equili-bration time (d)	Total resin contact time (d)	I (M)	pH at start of resin contact	pH at end of resin contact	τ 1 (h)	τ2 (h)	τ 3 (h)	%U in hindered sites
E-08	54	1	1	0.01	3.0	3.4	-	0.23	8	8.4
E-08	54	13	1	0.01	3.0	3.2	0.25	1.7	65	3.6
E-08	54	20	1	0.01	3.0	3.5	0.23	1.7	146	3.0
E-08	54	1	1	0.10	3.3	3.6	0.07	0.33	7	3.6
E-08	54	20	1	0.10	3.2	3.5	0.06	0.33	14	4.9
E-07	21	1	42	0.10	6.6	7.0	0.26	1.4	22	13
E-07	20	1	42	0.10	6.6	7.2	0.26	1.6	22	15
E-08	44	162	37	0.010	6.8	7.5	1.8	69	1049	8.1
E-08	48	162	37	0.010	6.4	7.4	2.1	93	950	6.5

From Table 2 it appears that the τ3 values for U undergoing slow dissociation increased with increasing equilibration time and decreasing ionic strength. The effect of pH on τ3 was confounded by the effects of the other variables.

Experiments with lengthy pre-conditioning times seemed to have the most effect on the slow dissociation rates of U from the kinetically hindered sites in the fulvic acid. It is this slow dissociation step that is the focus of interest, as it is the relatively stable metal-fulvate complexes that are more likely to be mobile in the field. The proportion of U that had entered into the kinetically hindered sites was relatively small and variable, but this process could be significant in natural systems where long equilibration times are available for more U to populate the hindered sites.

Table 3. Summary of thorium kinetics data.

[Th] M *	FA ppm	Equili-bration time (d)	Resin contact time (d)	I (M)	pH at start of resin contact	pH at end of resin contact	τ1 (h)	τ2 (h)	τ3 (h)	%Th in hindered sites
E-14	18.8	4	45	0.09	7.3	7.8	1.8	37	470	24
E-14	19.2	4	45	0.09	7.5	7.8	2.6	66	1367	10
E-14	19.8	1	42	0.09	6.6	6.9	3.3	71	530	19
E-14	20.1	1	42	0.09	6.6	7.3	2.9	85	722	17
E-08	53.5	262	42	0.09	7.5	7.0	23	45	1387	55
E-08	53.4	244	42	0.02	7.2	7.0	1.9	42	1250	53
E-08	51.1	242	42	0.03	7.6	7.0	0.53	48	1215	58
E-07	11.8	140	42	0.01	6.3	6.4	nd	nd	1112	1.5
E-07	11.6	140	42	0.01	6.3	6.4	nd	nd	1200	1.5
E-07	11.9	4	42	0.01	6.5	6.4	nd	nd	1207	0.66
E-07	11.8	4	42	0.01	6.5	6.5	nd	nd	991	0.68
E-07	12.7	1	42	0.11	6.4	6.5	nd	nd	883	0.41
E-07	13.0	1	24	0.11	6.4	6.5	nd	nd	1913	0.44

*Thorium was either as Th^{234} (at E-14 M) or Th^{230} (at E-07 and E-08 M). nd means not determined.

The τ3 times for Th ranged from 470 to 1913 hours (Table 3) and appeared less sensitive to metal-fulvic acid equilibration time and ionic strength than the τ3 values for U. The thorium slow dissociation rates were less affected by changes in the experimental parameters than the U rates.

4. DISCUSSION

Analytically, the most precise data for $\tau 3$ for both U and Th were obtained from the experiments with the longest equilibration and resin contact times. Table 4 displays these $\tau 3$ data with the smallest errors (typically +/- 4% between replicates). The $\tau 3$ times for thorium (mean 1284 h) were slightly greater than those for U (mean 1000 h).

Table 4. Slow dissociation rate data for U and Th.

Expt *	Equilibration time (d)	Resin contact time (d)	I (M)	$\tau 3$ (h)	% metal still bound after resin contact time
U	162	37	0.01	1049	8.1
U	162	37	0.01	950	6.5
Th	242	42	0.03	1215	58
Th	244	42	0.02	1250	53
Th	262	42	0.09	1387	55

*All experiments at ~50 ppm DE72 FA, pH ~7 and E-08 M of metal.

There were also significant differences in the proportions of U and Th that were complexed in the kinetically hindered sites (Table 4). Thorium was much more extensively bound than uranium in the hindered sites. At the slow dissociation rate, a significant fraction of the Th (up to 0.58) was bound in the kinetically hindered sites. Geckeis *et al*, (1999) found that significant fractions of the trace elements Th, Eu and U, which are naturally present in Gorleben groundwater humic colloids, were remaining in solution after dissociation treatment with Chelex resin.

Although the average-life values for U in the hindered sites were comparable to the average-life values for Th after these longest periods of metal-fulvic acid pre-conditioning, the fraction of U remaining in the hindered sites was considerably smaller (~0.07). This implies that Th is more populous in these sites than U because of thorium's greater thermodynamic stability in these sites. How much of this Th becomes irreversibly bound and fixed is open to question (see also Geckeis *et al*, 1999). Quantifying this proportion would be important for placing limits, by analogy, on other actinide (IV) species.

The laboratory conditions represented in Table 4 were the closest approximation to those found in the field. Nevertheless, the laboratory times used for metal-fulvic acid complexation and dissociation were limited in scale, and it was not possible, therefore, to determine the proportions of these fractions of U and Th in the hindered sites that were irreversibly bound. However, these new data can be used as important constraints when modelling the far-field transport of actinide-fulvate complexes under *in-situ* conditions (see e.g. Bryan *et al*, 1999a and b).

5. CONCLUSIONS

Batch experiments, involving ion-exchange, solvent extraction and kinetics, were used to study the complexation behaviour of U and Th with the well-characterised Derwent Reservoir fulvic acid DE72 FA. Experiments were conducted over a range of pH (4 to 8) and ionic strengths (0.01 to 0.1 M), and at different fulvic acid and metal concentrations. The conditional stability constant log beta values obtained for U by a Schubert-type solvent extraction method were of the same order as those obtained previously for U complexed with natural fulvic acids.

Batch kinetics experiments were used to measure the rates of dissociation of U and Th from their complexes with DE72 FA. The dissociation data were described by three kinetic terms for the initially fast, then medium and finally slow rates. The calculated rate constants were reciprocated to give time-constants or the average-lives of the metals in the three binding modes ($\tau 1$, $\tau 2$ and $\tau 3$). The $\tau 3$ times for Th undergoing slow dissociation ranged from 470 to 1913 hours and were much less sensitive to metal-fulvic acid equilibration time and ionic strength than the $\tau 3$ values for U. After the longest periods of metal-fulvic acid pre-conditioning, the average-life values for U in the hindered sites (mean 1000 h) was comparable to the average-life values for Th (mean 1284 h). However, the fraction of U remaining in the hindered sites was much smaller, ~0.07 compared to ~0.55 for Th. Although it was not possible to determine the proportions of these fractions that had U and Th irreversibly fixed, these new data serve as important constraints for modelling the far-field transport of actinide-fulvate complexes under *in-situ* conditions.

6. ACKNOWLEDGEMENTS

This work was funded by the European Commission and the UK Environment Agency. The results will be used in the formulation of Government policy but do not necessarily represent that policy. This paper is published by the permission of the Director of the British Geological Survey (NERC).

7. REFERENCES

Bryan, N.D., Jones, D., Griffin, D., Regan, L., King, S., Warwick, P., Carlsen, L. and Bo, P. (1999a). Combined mechanistic and transport modelling of metal humate complexes. In *Second Technical Progress Report of the EC project 'Effects of Humic Substances on the Migration of Radionuclides: Complexation and Transport of Actinides'* (ed. G. Buckau). Forschungszentrum Karlsruhe Report FZKA 6324, pp. 301-337.

Bryan, N.D., Griffin, D. and Regan, L. (1999b). Implications of humic chemical kinetics for radiological performance assessment. In *Second Technical Progress Report of the EC project 'Effects of Humic Substances on the Migration of Radionuclides: Complexation and Transport of Actinides'* (ed. G. Buckau). Forschungszentrum Karlsruhe Report FZKA 6324, pp. 339-356.

Caceci, M.S. and Choppin, G.R. (1983). An improved technique to minimize cation adsorption in neutral solutions. *Radiochimica Acta*, **33**, 113-114.

Czerwinski, K., Buckau,G., Scherbaum, F. and Kim, J.I. (1994). Complexation of the uranyl ion with aquatic humic acid. *Radiochimica Acta,* **65**, 111-119.

Davis, J., Higgo, J., Moore, Y. and Milne, C. (1999). The characterisation of a fulvic acid and its interactions with uranium and thorium. In *Second Technical Progress Report of the EC project 'Effects of Humic Substances on the Migration of Radionuclides: Complexation and Transport of Actinides'* (ed. G. Buckau). Forschungszentrum Karlsruhe Report FZKA 6324, pp. 61-80.

Geckeis, H., Rabung, Th. And Kim, J.I. (1999). Kinetic aspects of the metal ion binding to humic substances. In *Second Technical Progress Report of the EC project 'Effects of Humic Substances on the Migration of Radionuclides: Complexation and Transport of Actinides'* (ed. G. Buckau). Forschungszentrum Karlsruhe Report FZKA 6324, pp. 45-58.

Higgo, J.J.W., Davis, J., Smith, B., Din, S., Crawford, M.B., Tipping, E., Falck, W.E., Wilkinson, A.E., Jones, M.N. and Kinniburgh, D. (1992). Comparative study of humic and fulvic substances in groundwaters: 3. Metal complexation with humic substances. *British Geological Survey Technical Report* no. WE/92/12.

Higgo, J.J.W., Kinniburgh, D., Smith, B. and Tipping, E. (1993). Complexation of Co^{2+}, Ni^{2+}, UO_2^{2+} and Ca^{2+} by humic substances in groundwaters. *Radiochimica Acta*, **61**, 91-103.

Higgo, J.J.W., Davis, J., Smith, B. and Milne C. (1998a). Extraction, purification and characterisation of fulvic acid. *British Geological Survey Technical Report* no. WE/98/22.

Higgo, J.J.W., Davis, J.R., Smith, B. and Milne, C. (1998b). Extraction, purification and characterization of fulvic acid. In *First Technical Progress Report of the EC project 'Effects of Humic Substances on the Migration of Radionuclides: Complexation and Transport of Actinides'* (ed. G. Buckau). Forschungszentrum Karlsruhe Report FZKA 6124, pp. 103-128.

Kersting, A.B., Efurd, D.W., Finnegan, D.L., Rokop, D.J., Smith, D.K. and Thompson, J.L. (1999). Migration of plutonium in groundwater at the Nevada test site. *Nature*, **397**, 56-59.

Nash, K.L. and Choppin, G.R. (1979). Interaction of humic and fulvic acids with Th(IV). *Journal of Organic Nuclear Chemistry*, **42**, 1045-1050.

Annex 6

Complexation of Eu(III) by Humic Substances: Eu speciation determined by Time-Resolved Laser-Induced Fluorescence

(G. Plancque, C. Moulin, V. Moulin, P. Toulhoat (CEA))

3rd Technical Progress Report
EC Project:

"Effects of Humic Substances on the Migration of Radionuclides: Complexation and Transport of Actinides"

Project No.: FI4W-CT96-0027

CEA Contribution to Task 2 (Complexation)

Complexation of Eu (III) by Humic Substances : Eu Speciation determined by Time-Resolved Laser-Induced Fluorescence

Gabriel Plancque*, Christophe Moulin*, Valérie Moulin, Pierre Toulhoat

Commissariat à l'Energie Atomique, Centre d'Etudes de Saclay, Fuel Cycle Division,
DESD/SESD/LMGS *DPE/SPCP/LASO
91191 Gif-sur-Yvette, France

1. INTRODUCTION

The understanding of radioelement behaviour in natural systems in relation with nuclear waste disposals in geological formations necessitates the knowledge of their speciation in these systems. In particular, this implies to determine the influence of *humic substances* (humic and fulvic acids, HA/FA) as natural organic substances present at different concentrations in groundwaters on the migration of radionuclides, particularly actinide elements. This induces in particular to study the complexation of actinides with humic substances as complexing agents. Hence, our objective is to obtain data (interaction constants, complexing capacities) on the interactions between humic/fulvic acids and actinides under relevant geochemical conditions (pH, ionic strength, presence of competing cations). Moreover, it is also important to focus on the possible existence of *mixed complexes (or ternary)*, namely M-OH/CO_3-HA/FA, which will then completely modify the actinide speciation compared to the absence of such complexes.

The technique retained to study such complexes is *Time-Resolved Laser-Induced Fluorescence*, which has been used, up to now, by both CEA laboratories for the study of trivalent actinides and lanthanides for pH<7, and for the study of mixed complexes in the case of uranium (Moulin et al., 1999a)

The approach developed for U(VI) for the investigation of mixed complexes is applied in the case of europium, which has been chosen as a chemical analogue of trivalent actinides and which can be analysed at low level by TRLIF (Bador et al., 1989, Decambox et al., 1989). Its hypersensitive transition is a relevant indicator of the complexation phenomena (Horrocks et al., 1979, Dobbs et al., 1989, Moulin et al., 1999 b). Firstly, a spectrum data base concerning the different complexes (hydroxide, carbonate and humate) is obtained on model systems with all spectroscopic characteristics (lifetimes, fluorescence wavelengths). And, secondly, from these data, titrations of europium solutions by humic substances are carried out at fixed pH and ionic strength and at atmospheric pressure.

2. EXPERIMENTAL

2.1 APPARATUS

Time-resolved laser-induced fluorescence : A Nd-YAG laser (Model minilite, Continuum) operating at 266 nm (quadrupled) or 355 nm (tripled) and delivering about 2.5 mJ of energy in a 4 ns pulse with a repetition rate of 15 Hz is used as the excitation source. The laser output energy is monitored by a laser power meter (Scientech). The laser beam is directed into the cell of the

spectrofluorometer "FLUO 2001" (Dilor, France) by a quartz lens. The radiation coming from the cell is focused on the entrance slit of the polychromator. Taking into account dispersion of the holographic grating used in the polychromator, measurement range extends to approximately 200 nm into the visible spectrum with a resolution of 1 nm. The detection is performed by an intensified photodiodes (1024) array cooled by Peltier effect (-20°C) and positioned at the polychromator exit. Recording of spectra is performed by integration of the pulsed light signal given by the intensifier. The integration time adjustable from 1 to 99 s allows for variation in detection sensitivity. Logic circuits, synchronised with the laser shot, allow the intensifier to be active with determined time delay (from 0.1 to 999 μs) and during a determined aperture time (from 0.5 to 999 μs). The whole system is controlled by a microcomputer.

2.2 FLUORESCENCE MEASUREMENT PROCEDURE

All fluorescence measurements are performed at 20°C. The pH of the solution in the cell is measured with a conventional pH meter (Model LPH 430T, Tacussel) equipped with a subminiature combined electrode (Model PHC 3359-9).

For each identification, europium concentration, pH, ionic strength were perfectly fixed and controlled. From a spectroscopic point of view, various gate delay and duration were used to certify the presence of only one complex by the measurement of a single fluorescence lifetime and spectrum.

Fluorescence spectra were analysed using the deconvolution software GRAMS 386®. All peaks were described using mixed Gaussien-Lorentzian profile (the apparatus function was previously recorded using a mercury lamp). Fluorescence lifetime measurements were made by varying the temporal delay with fixed gatewidth.

2.3 MATERIALS

Standard solutions of europium (III) in sodium perchlorate ($NaClO_4$ 0.1 M) or in potassium carbonate (K_2CO_3 0.01M, 0.1 M or 1 M) are obtained from suitable dilution of a solution prepared by dissolution of high purity europium oxide powder (Alfa) with concentrated perchloric acid (Merck).

Purified Aldrich humic acids (HA) are used in a protonated form. Their main characteristics are detailed in Kim et *al.* (1991), as part of an EC Mirage project (Kim, 1990). Their proton capacities are 5.4 meq/g for HA-Aldrich (determined by potentiometric titrations). Their apparent acidity constants (determined as the pH at mid-equivalence) are: $pK_a^{HA} = 4.3$. Stock solutions of 1

g/l for Aldrich HA in 0.1 M $NaClO_4$ have been prepared after dissolution in NaOH medium (pH~10; ratio 1/10) in the case of HA.

Perchloric acid and sodium hydroxide (Merck) are used for pH adjustment. The ionic strength is fixed by the sodium perchlorate concentration at 0.1 M for most of the experiments excepted those realised in potassium carbonate (K_2CO_3 0.1 M or 1 M). All chemicals used are reagent grade and Millipore water is used throughout the procedure.

3. INORGANIC SPECIATION

The characterisation of the inorganic complexes (with hydroxides and carbonates ligands) of europium implies to identify them temporally, *i.e.* by the determination of the lifetime and spectrally *i.e.* by the determination of the fluorescence spectrum. These different species under study are the hydroxide and carbonate complexes, in addition to free europium.

With the interaction constants (log β) listed in the literature (Dierckx et *al.*, 1994, Wolery et *al.*, 1992) (table I), the Eu speciation diagram at atmospheric pressure in which the hydroxide and carbonate complexes are only taken into account, can be built (figure 1). No mixed Eu complexes (Eu-OH-HCO_3/CO_3) are considered. It is also possible to work under a controlled atmosphere (without air) and then to only consider the hydroxide complexes as seen on figure 2.

Table I : Interaction constants of inorganic complexes of europium at I=0.1 M

Species	$EuOH^{2+}$	$Eu(OH)_2^+$	$Eu(OH)_3$(aq.)	$Eu(OH)_4^-$	$Eu(CO_3)^+$	$Eu(CO_3)_2^-$	$Eu(CO_3)_3^{3-}$
log β	5.55	10.72	15.71	17.71	6.96	12.45	14.1

These diagrams allow us to determine the best chemical conditions to identify one particular species, as previously done for uranium (Moulin et al, 1998, 1999 a). In our case, the following conditions were chosen :

- atmospheric pressure and acidic pH to study free europium Eu^{3+}.
- carbonate medium and alkaline pH to study the carbonato complexes.
- controlled atmosphere ($pCO_2 = 0$) and alkaline pH to study the hydroxo complexes.

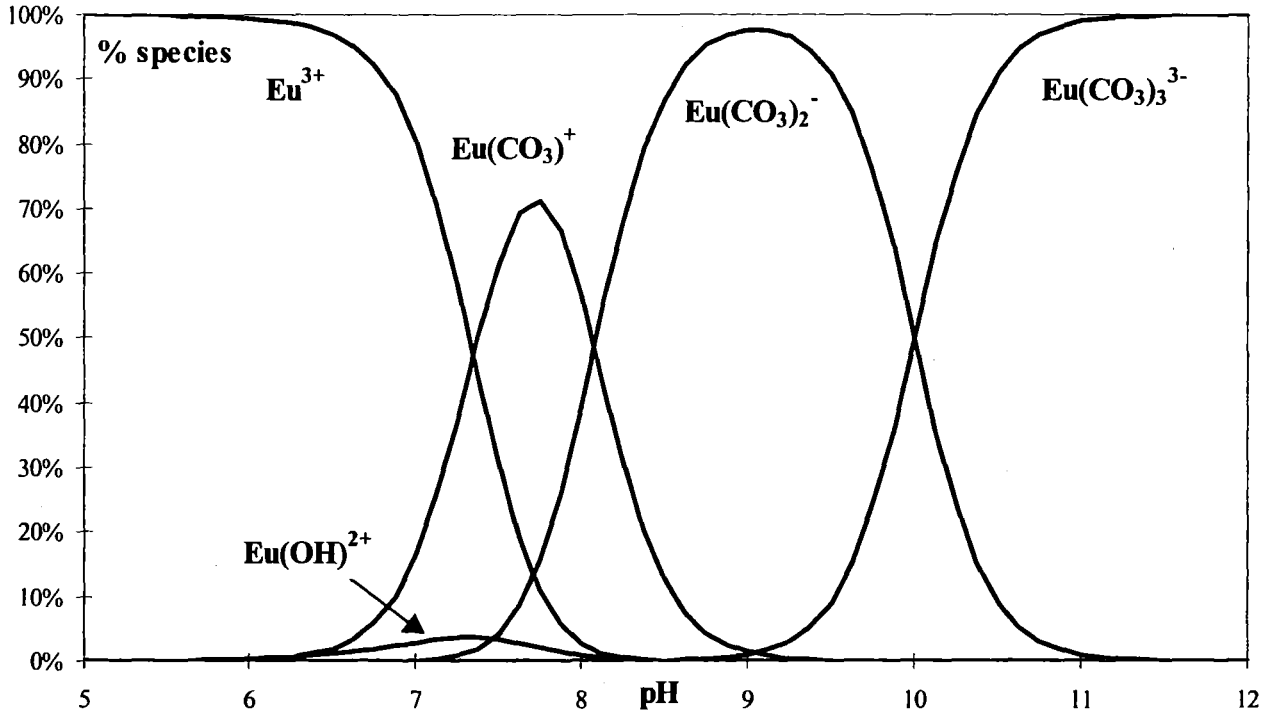

Figure 1 : Speciation diagram of europium at atmospheric pressure (I = 0.1 M)

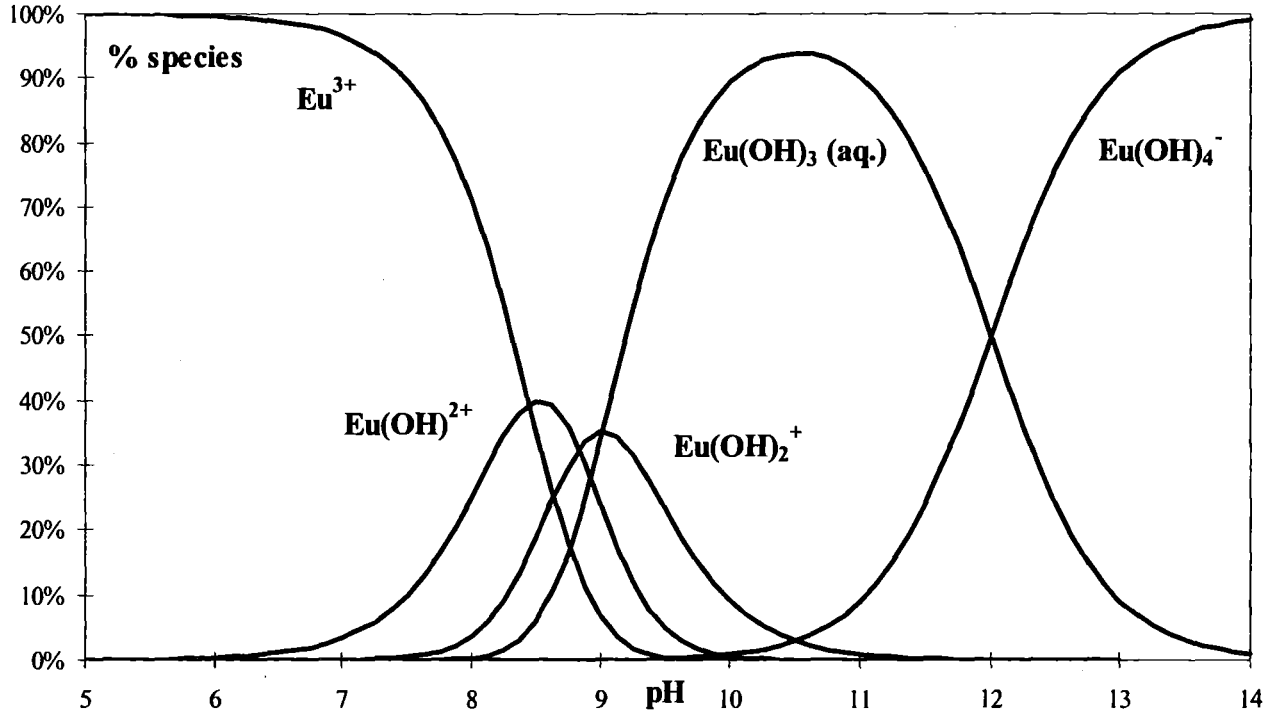

Figure 2 : Speciation diagram of europium at $pCO_2 = 0$ (I = 0.1 M)

3.1 CARBONATE SYSTEM

The experimental conditions are the following :

- for Eu^{3+} : [Eu] = 1 mg/l, I = 0.1 M ($NaClO_4$), pH = 2 and atmospheric pressure,
- for mono-carbonate : [Eu] = 1 mg/l, I = 0.1 M ($NaClO_4$), [K_2CO_3] = 0.01 M,
- for di-carbonate : [Eu] = 1 mg/l, [K_2CO_3] = 0.1 M,
- for tri-carbonate : [Eu] = 1 mg/l, [K_2CO_3] = 1 M.

Figure 3 presents fluorescence spectra of the carbonato species together with free europium.

The spectrum of **free europium** presents two peaks : 593 nm with a full width at mid height (FWMH) equals to 6.5 nm and 618 nm with a FWMH equals to 9.5 nm. The peak ratio 593 / 618 is equal to 4 to 1. This is characteristic of europium which presents a fluorescence spectrum in the red with strongest lines around 580, 593, 618, 650 and 700 nm ($^5D_0 \rightarrow {}^7F_J$, J = 0-4)), the transition at 618 nm ($^5D_0 \rightarrow {}^7F_2$) being hypersensitive. This feature is very important in complexation studies since its intensity is enhanced in the case of complexation with a ligand, relative to its intensity in aqueous medium (no complexation). The lifetime of free europium is found to be equal to 110 µs.

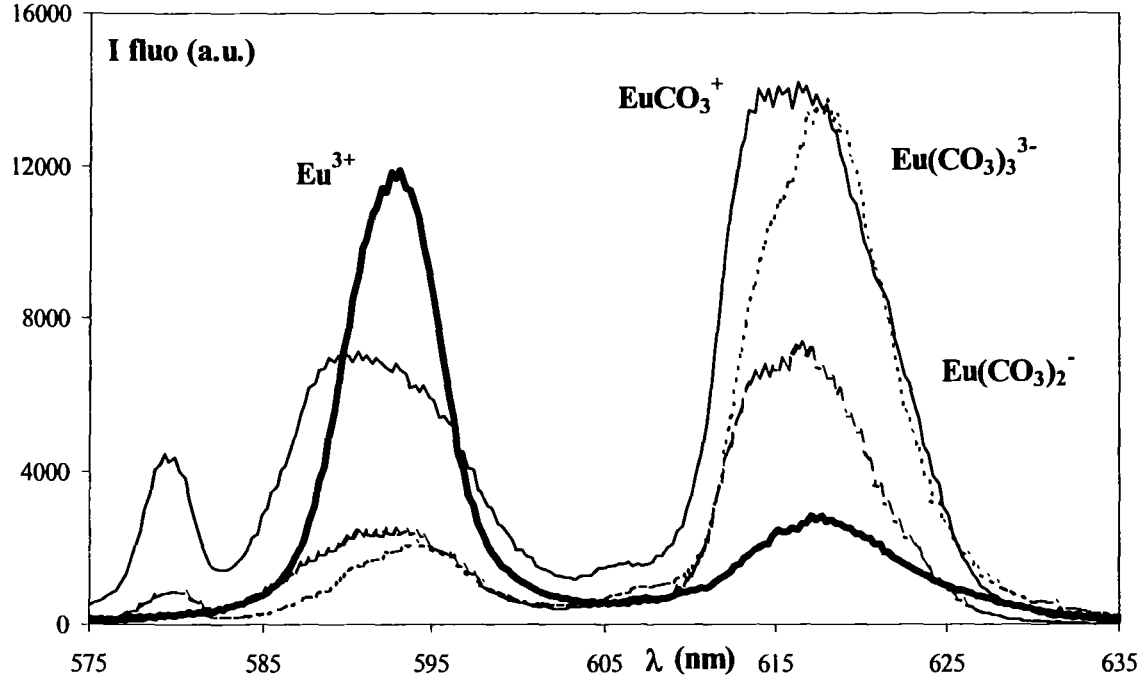

Figure 3 : Spectra of the carbonato complexes of europium

For the mono carbonate complex $\mathbf{Eu(CO_3)^+}$, two peaks are present : 592 nm with a FWMH equals to 11.0 nm, and 616 nm with a FWMH equals to 10.0 nm. Under these conditions, due to complexation with carbonate ions, the peak ratio 592 / 616 is equal to 1 to 2. The lifetime of the mono-carbonate is found to be equal to 180 µs.

For the di carbonate complex $\mathbf{Eu(CO_3)_2^-}$, two peaks are present : 592 nm with a FWMH equals to 10.0 nm, and 616 nm with a FWMH equals to 9.0 nm. Under these conditions, due to complexation with carbonate ions, the peak ratio 592 / 616 is equal to 1 to 3. The lifetime of the di-carbonate is found to be equal to 290 µs.

For the tri carbonate complex $\mathbf{Eu(CO_3)_3^{3-}}$, two peaks are present : 594 nm with a FWMH equals to 8.0 nm, and 618 nm with a FWMH equals to 9.5 nm. A little shoulder is observed on the 618 nm peak. Under these conditions, due to complexation with carbonate ions, the peak ratio 594 / 618 is equal to 1 to 6. The lifetime of the tri-carbonate is found to be equal to 440 µs.

All the results are summarised in table 2 : for each species, the spectral data (main fluorescence wavelengths and full width at mid height) and the lifetimes are presented. Results obtained for the lifetimes and for the spectrum of the tri-carbonate complex are in good agreement with literature data (Kim et *al.*, 1994).

3.2 HYDROXIDE SYSTEM

The experimental conditions are the following :

- for Eu^{3+} : [Eu] = 1 mg/l, I = 0.1 M ($NaClO_4$), pH = 2 and atmospheric pressure,
- for hydroxide complexes : [Eu] = 1 mg/l, I = 0.1 M ($NaClO_4$), pCO_2 = 0 and different pH.

Figure 4 presents the evolution of the spectra of the hydroxo complexes with the pH.

There is no great differences between all spectra. For all hydroxo complexes $\mathbf{Eu(OH)_n^{(3-n)+}}$, two peaks are observed : one at 593 nm with a FWMH larger than for free europium (12.0 nm instead of 6.5 nm) and one at 615 nm with a shoulder at 623 nm. The peak ratio is equal to 1 to 1. Spectral deconvolution is in progress and results obtained will be published in 2000. As the same way, the lifetime of all species is equal to 50 µs. Results are also summarised in table II.

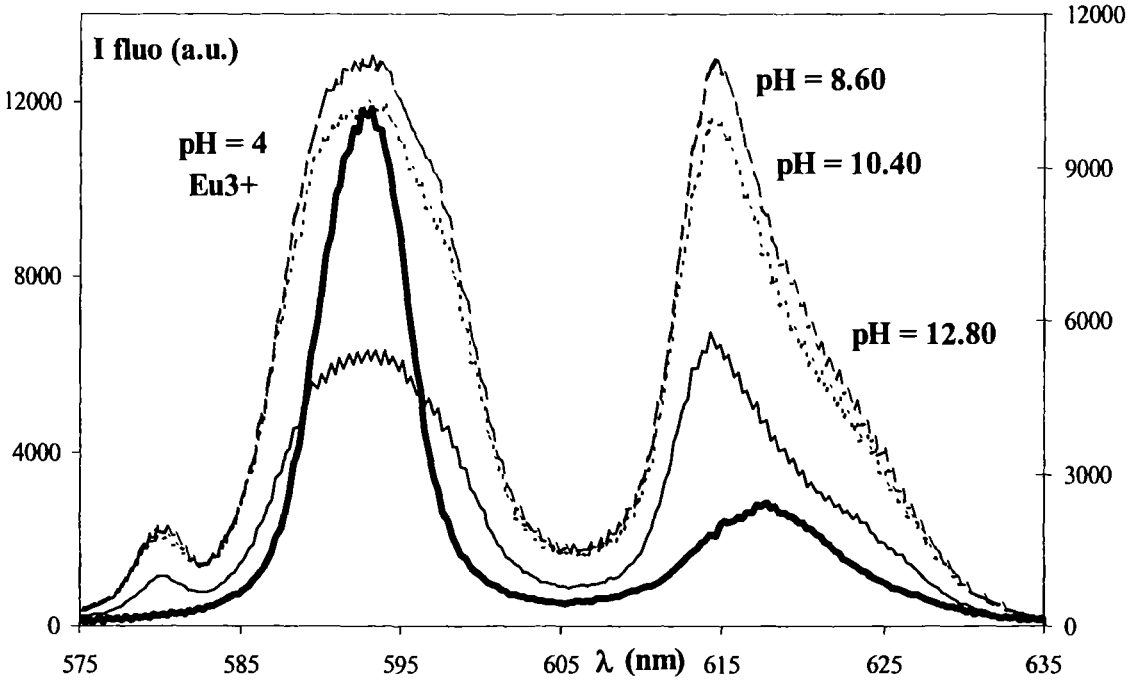

Figure 4 : Evolution of the spectra of the hydroxo complexes of europium with pH.

Table II : Spectral data and lifetimes for inorganic complexes of europium.

Species	Fluorescence wavelength (nm) and peak ratio [ ]	FWMH (nm)	Lifetime (μs)
Eu^{3+}	593 / 618 [4/1]	6.5 / 9.5	110 ± 10
$Eu(OH)^{2+}$	593 / 615 [1/1]	12.0 / -	50 ± 5
$Eu(OH)_2^{+}$	593 / 615 [1/1]	12.0 / -	50 ± 5
$Eu(OH)_3$ (aq.)	593 / 615 [1/1]	12.0 / -	50 ± 5
$Eu(OH)_4^{-}$	593 / 615 [1/1]	12.0 / -	50 ± 5
$Eu(CO_3)^{+}$	592 / 616 [1/2]	11.0 / 10.0	180 ± 10
$Eu(CO_3)_2^{-}$	592 / 616 [1/3]	10.0 / 9.0	290 ± 15
$Eu(CO_3)_3^{3-}$	594 / 618 [1/6]	8.0 / 9.5	440 ± 30

4. COMPLEXATION OF Eu (III) WITH HUMIC SUBSTANCES STUDIED BY TRLIF

4.1 EXPERIMENTAL SECTION

The interaction of humic acids with Eu^{3+} has been studied by using TRLIF as technique of investigation of organic complexes as performed in other studies (Moulin et al., 1992, 1996, 1999 b). Titration experiments have been performed in order to obtain characteristic data, namely the complexing capacity W and interaction constants β. The experimental approach is the following : a Eu^{3+} solution is titrated by a humic acid solution at controlled pH and controlled ionic strength. At the beginning and at the end of the titration, the lifetime τ is measured, the fluorescence spectra are monitored and the pH is checked. The fluorescence intensities are measured at each point and these intensities are corrected with humic acid absorbance and laser energy variation.

The experimental conditions are the following :

- [Eu] = 1 mg/l (6.6 µmol/l)
- I = 0.1 M ($NaClO_4$)
- two pH have been studied : pH = 5.0 and pH = 6.5 in order to determine the effect on the interaction constant and the complexing capacity
- humic acids from Aldrich (purified form used as reference in the project)

Figure 5 presents the titrations obtained at pH = 5.0. There is a good agreement between the three experiments.

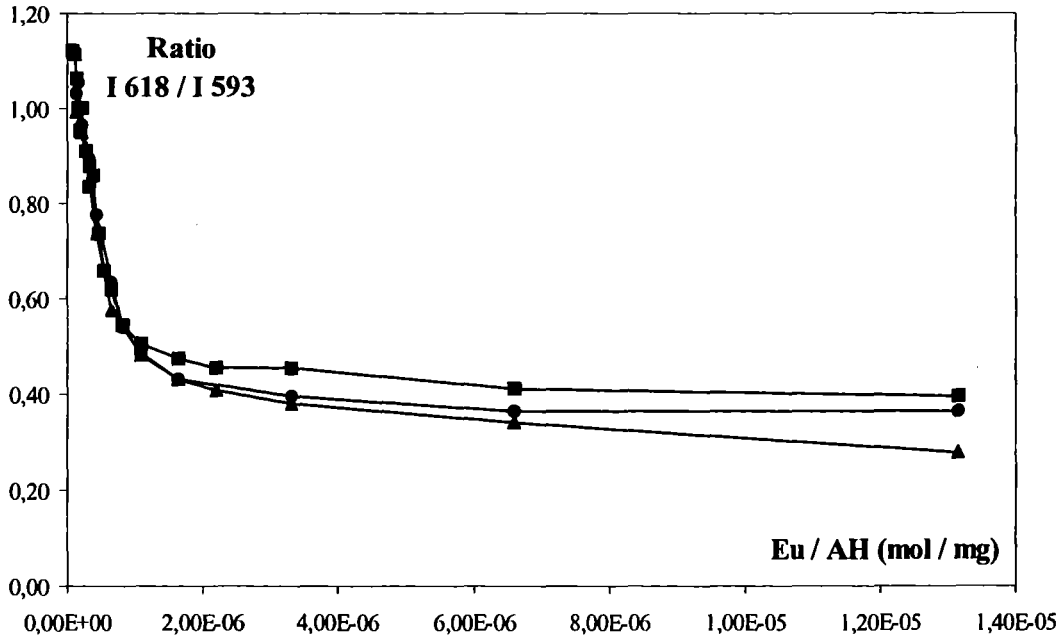

Figure 5 : Titrations of Eu (1 mg/l) by HA (100 mg/l), pH = 5.0

Figure 6 presents the titrations obtained at pH = 6.5.

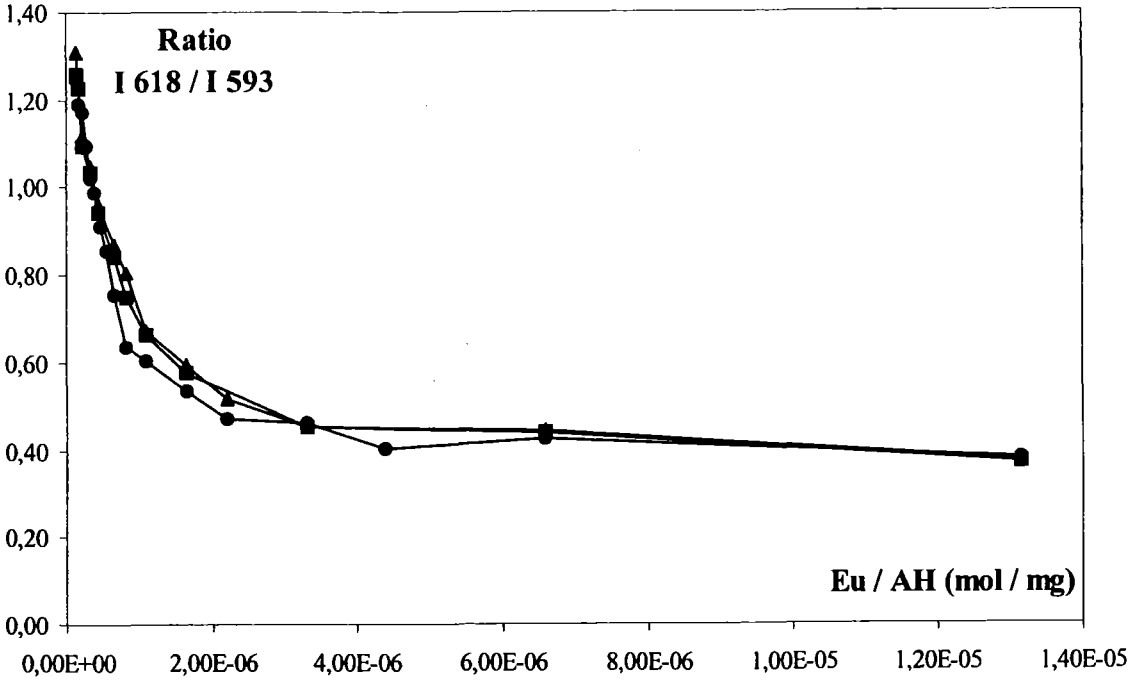

Figure 6 : Titrations of Eu (1 mg/l) by HA (100 mg/l), pH = 6.5

Figure 7 presents the evolution of the spectra of the europium during the titration.

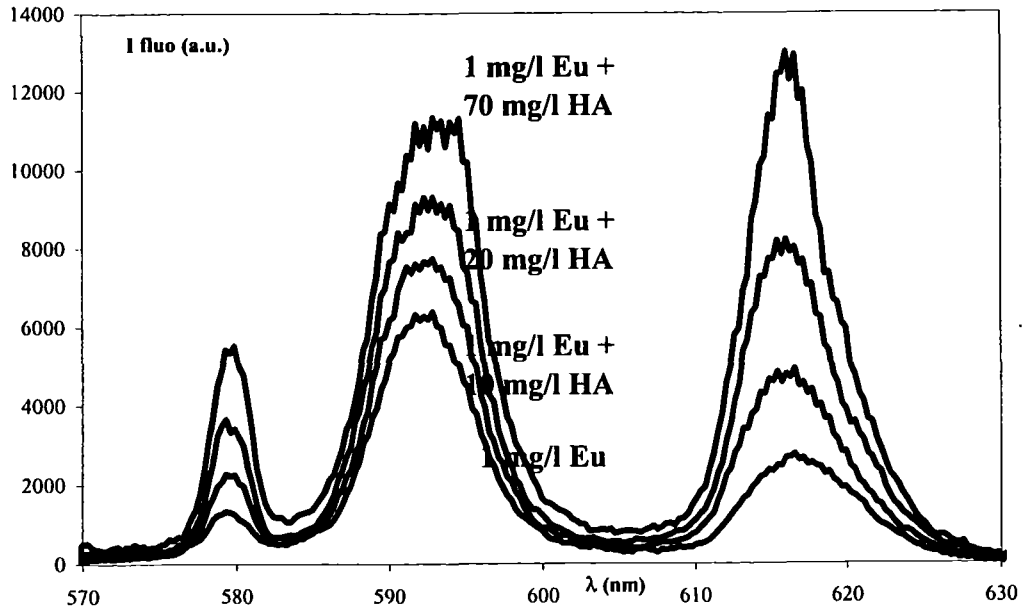

Figure 7 : Evolution of the spectra during the titration of Eu by HA (pH = 5.0)

During the titration, the fluorescence intensity increases in the presence of humic acid and the Eu spectrum changes (evolution of the ratio I_{618} / I_{593}). It is a proof of the complexation of Eu by humic acid (hypersensitive transition at 618 nm). Moreover, the lifetime has not changed between the beginning and the end of the titration (110 µs) so that the complex is an outer sphere complex.

Experiments have been done to check the absence of photodegradation of the humic substances during the titration. As the pulse laser has a very low energy (Nd-YAG, 2.5 mJ per pulse), photodegradation can not occur or occurs very weakly.

4.2 CALCULATION SECTION

The interaction constants and the complexing capacities have been calculated by using the ***"single site model"***. The goal is to determine the interaction constant relative to the concentration and the complexing capacity of humic acids towards europium.

Since the humic substances are heterogeneous and complex molecules, the ligand is defined as a monodentate site (L) with no particular assumption on its chemical structure. Complexes of 1:1 (metal : ligand) stoechiometry are assumed to be formed according to the following equilibrium :

$$Eu^{3+} + L^{-} \Leftrightarrow EuL^{2+}$$

where :

$$[L]_{total} = W \times [HA] = [L]_{free} + [EuL]$$

$$[Eu]_{total} = [Eu]_{free} + [EuL]$$

W = complexing capacity expressed in mmol/g (number of millimoles of cations bound per gram of organic ligand).

Moreover, the hypersensitive transition at 618 nm of the europium is a very good indicator of the complexation phenomena so that the interaction data can be obtained by using the ratio of the fluorescence intensities at 593 nm and 618 nm. Indeed, the fluorescence at 593 nm is considered to be the contribution of free europium and complexed europium whereas the fluorescence at 618 nm is considered to be the contribution of free europium and complexed europium affected by a coefficient due to the hypersensitivity of this transition (Dobbs et al., 1989, Moulin et al., 1999 b).

This can be summarised as follows :

- $I_{593\,nm} = x\,([Eu]_{free} + [EuL])$
- $I_{618\,nm} = y\,([Eu]_{free} + k\,.\,[EuL])$,

where k is the hypersensitive contribution factor.

By plotting the ratio of the fluorescence intensities ($R = I_{618}/I_{593}$) as a function of the ratio of the concentrations ([Eu]/[AH]) (see figure 8), the complexing capacity W is obtained, graphically, by intersection of the two slopes and the interaction constant β is obtained from a non-linear regression giving β as a function of W, k, R, [HA], [Eu].

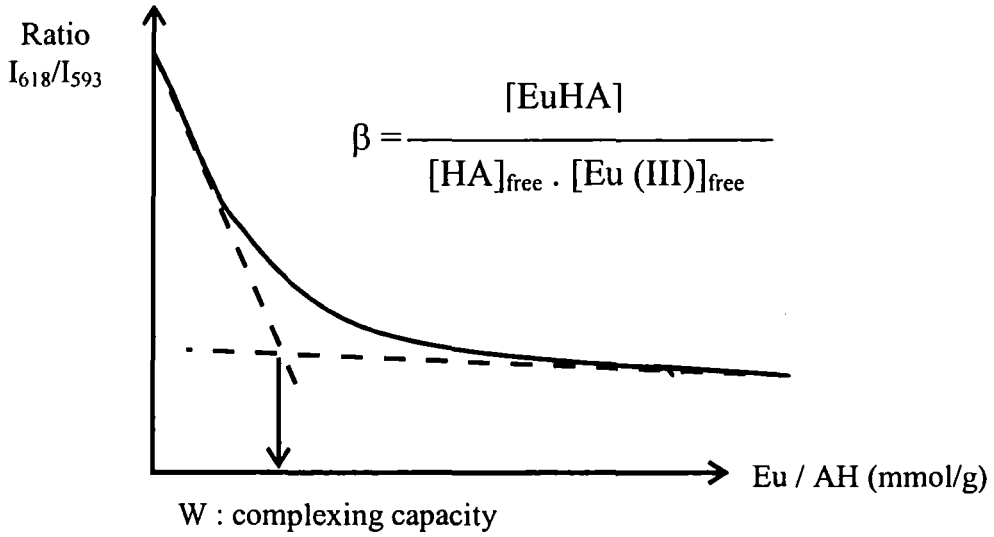

Figure 8 : Titration of europium by humic acid.

The values obtained are presented in table III.

Table III : Interaction constants and complexing capacities for the Eu-HA system.

[Eu], I, pH	Log β	W (mmol/g AH)
1 mg/l, 0.1 M, 5.0	5.2 ± 0.4	0.9 ± 0.1
1 mg/l, 0.1 M, 6.5	5.3 ± 0.4	0.9 ± 0.1

In these experiments, the interaction constants and the complexing capacities are not affected by the pH in the range 5 to 6 and are in good agreement with literature data (Bidoglio et al., 1991).

5. EXISTENCE OF MIXED COMPLEXES

A solution, representative of Mol site (interstitial clay water) and containing carbonate ions and humic acids, has been studied by time-resolved laser-induced fluorescence (Moulin et al., 1999 c). The exact composition of this solution is given in table 4. This solution has been characterised by its spectrum (figure 9) and its lifetime (equal to 170 μs). By comparing this spectrum with our

spectrum data base, it seems that there is a new species. It is impossible to obtain this new spectrum by convolution of humate complex spectrum with carbonato complex spectrum and the lifetime is longer than the other possible simple complex. These two results are in favour of the existence of a mixed complex.

	Synthetic water containing Eu, CO_3, AH
pH	9.3
$MgSO_4$ (mg/l)	12.0
KCl (mg/l)	20.0
Na_2SO_4 (mg/l)	1.5
NaF (mg/l)	8.0
NaCl (mg/l)	44.0
$NaHCO_3$ (mg/l)	1250
$CaCO_3$ (mg/l)	Saturated
HA (mg/l)	150.0
Eu (mol/l)	8×10^{-6}

Table 4 : Composition of the "Mol water"

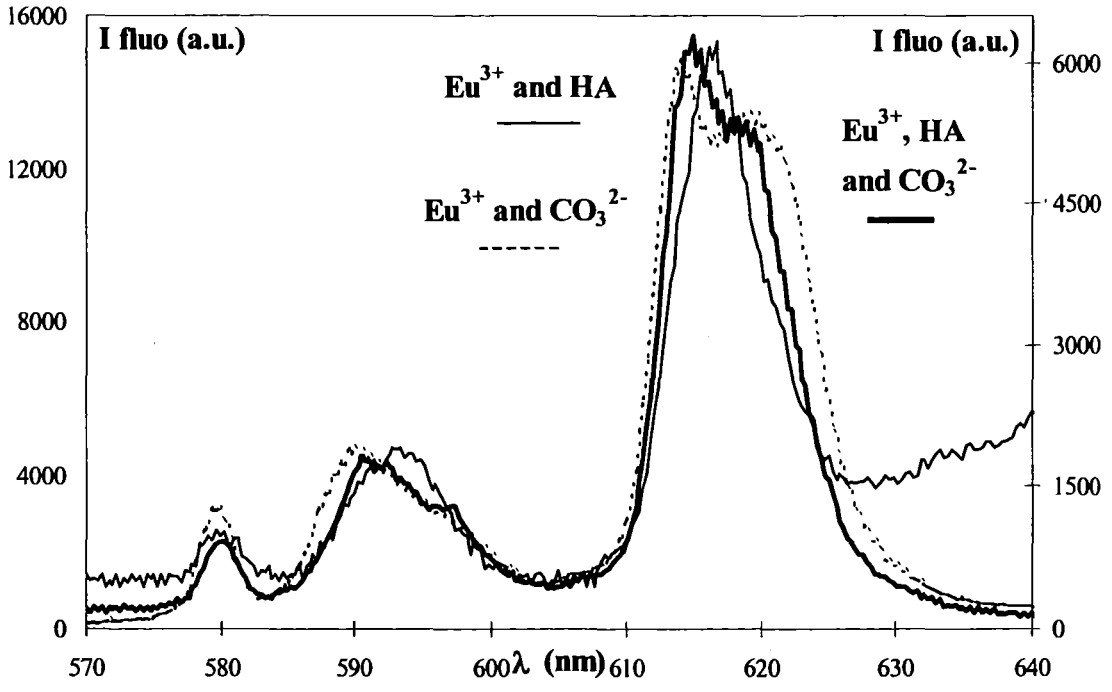

Figure 9 : Spectra of the "Mol water".

6. CONCLUSIONS AND PERSPECTIVES

Three model systems have then been studied with europium :

- the carbonato system
- the hydroxo system
- the humate system.

The data obtained on these systems (from a spectroscopic and chemical point of view) are of prime importance to investigate the formation of ternary complexes and to determine interaction constants relative to such complexes. The impact of such complexes on Eu speciation can be then estimated. This will be the next step of this work. Nevertheless, these data here obtained have allowed to understand the behaviour of europium in complex environment, namely a synthetic natural water : in fact, europium is present as a ternary complex with humate and carbonate ligands under physico-chemical conditions representative of interstitial clay waters.

7. REFERENCES

Bador R., Morin M., Dechaud H. (1989) Detection of Eu and Sm by chelation and laser excited time-resolved fluorimetry. *Analytica Chimica Acta* **219**, 66

Bidoglio G., Grenthe I., Qi P., Robouch P., Omenetto N. (1991) Complexation of Eu and Tb with fulvic acids as studied by time-resolved laser-induced fluorescence. *Talanta* **38**, 999.

Decambox P., Berthoud T., Kirsch B., Mauchien P. and Moulin C. (1989) Direct determination of traces of lanthanide ions in aqueous solutions by laser-induced time-resolved spectrofluorimetry. *Analytica Chimica Acta* **220**, 235.

Dierckx, A. Maes A. and Vancluysen J. (1994) Mixed complex formation of europium with humic acid and competing ligand. *Radiochimica Acta* **66/67**, 149.

Dobbs J.C., Susetyo W., Knight F.E., Castles M. A., Carreira L.A., Azaraga L.V. (1989) Characterisation of metal binding sites in fulvic acids by lanthanide ion probe spectroscopy. *Analytical Chemistry* **61**, 483.

Horrocks W. de W., Sudnick D. R. (1979) Lanthanide ion probes of structure in biology. Laser induced luminescence decay constant provide a direct measure of the number of metal coordinated water molecules. *Journal of the American Chemical Society* **101**, 334.

Kim, J.I., Buckau, G., Klenze R., Rhee D.S., Wimmer H. (1991) Characterisation and complexation of humic acids. CEC Report EUR 13181.

Kim, J.I. (1990) Geochemistry of actinides and fission products in natural aquifer systems. In « *CEC Project Mirage-Second Phase on Migration of Radionuclides in the Geosphere* » (B. Côme, Ed.), EUR Report 12858.

Kim J.I., Klenze R., Wimmer H., Runde W. and Hauser W. (1994) A study of the carbonate complexation of Cm and Eu by Time-Resolved Laser-Induced Fluorescence. *Journal of Alloys and Compounds* **213/214**, 333.

Moulin V., Tits J., Moulin C., Decambox P., Mauchien P. and De Ruty O. (1992) Complexation behaviour of humic substances towards actinides and lanthanides studied by Time-Resolved Laser-Induced Fluorescence. *Radiochimica Acta* **58/59**, 121.

Moulin V., Moulin C and Dran J.C. (1996) Role of humic substances and colloids on the behaviour of radiotoxic elements in relation with nuclear waste disposals: confinement or enhancement of migration? In ACS Volume on *"Humic and Fulvic Acids and organic colloidal materials in the environment"*, pp 259-272.

Moulin C., Laszak I. , Moulin V. and Tondre C. (1998) Time-resolved laser-induced fluorescence as a unique tool for uranium speciation at low level. *Applied Spectroscopy* **52**, 528.

Moulin V., Reiller P., Dautel C., Plancque G., Laszak I., Moulin C. (1999 a) Complexation of Eu(III), Th(IV) and U(VI) by humic substances. In « *Effects of humic substances on the migration of radionuclides : complexation and transport of actinides*. Second Technical Progress Report (Ed. G. Buckau). Rapport FZKA 6324, pp. 81-118.

Moulin C., Larpent C., Gazeau D. (1999 b) Interaction studies between europium and a surfactant cage TAC8 by Time-Resolved Laser-Induced Fluorescence. *Analytica Chimica Acta* **378**, 47.

Moulin C., Wei J., Van Iseghem P., Laszak I., Plancque G., Moulin V. (1999 c) Europium complexes investigations in natural waters by time-resolved laser-induced fluorescence. *Analytica Chimica Acta* **396**, 253.

Wolery T., Daveler S. A. (1992) EQ6, a computer program for reaction path modelling of aqueous geochemical systems. UCRL-MA-110662, LLNL.

Annex 7

Complexation of Th(IV) with Humic Substances

(P. Reiller, V. Moulin, C. Dautel, F. Casanova (CEA))

3rd Technical Progress Report
EC Project:

"Effects of Humic Substances on the Migration of Radionuclides: Complexation and Transport of Actinides"

Project No.: FI4W-CT96-0027

CEA Contribution to Task 2 (Complexation)

Complexation of Th(IV) by Humic Substances

Pascal Reiller, Valérie Moulin, Christian Dautel, Florence Casanova

Commissariat à l'Energie Atomique, Centre d'Etudes de Saclay, Fuel Cycle Division,
DESD/SESD/LMGS
91191 Gif-sur-Yvette, France

1.INTRODUCTION

The understanding of radionuclides behaviour in natural systems in relation with nuclear waste disposals in geological formations necessitates the knowledge of their speciation in these systems. In particular, this implies to determine the influence of humic substances (humic and fulvic acids, HA/FA) as natural organic substances present in more or less concentrations in ground waters on the migration of radionuclides, particularly actinide elements. Humic substances can influence the migration of cations as a complexing ligand for cations in solution. If the majority of the works upon the complexation of cations by HA has been led with very important mono, di or trivalent cations, there is still a lack of accurate data onto the complexation of tetravalent actinides *i.e.* U(IV), Np(IV), and Pu(IV).

In a previous study (Moulin *et al.*, 1999), the method retained to study the complexation of Th(IV) by humic substances has been developed. This method is an indirect one based on the competition between humic complexation and sorption onto silica colloids. The sorption of thorium(IV) onto silica with or without the presence of humic acids has been investigated. Th(IV) is considered as an analogue of the tetravalent actinides, (Choppin, 1999), whose species are predominant, at least partly in the case of Pu, under reducing natural conditions. HA are known to be very weakly sorbed onto silica in the pH range of ground waters (Labonne, 1993; Labonne-Wall *et al.*, 1997). Thus, the evolution of Th(IV) sorption properties towards SiO_2 in the presence of HA would be the almost direct information of the extent of the humic complexation of Th(IV). Our aim was to examine the influence of the presence of HA onto Th(IV) sorption onto silica, one of the major constituent of soils both as oxide and as part of clays (silanol groups). After having characterised the interactions between Th(IV) and colloidal silica (binary system), extraction of data from the ternary system (Th/HA/Silica) would permit us to characterise the interaction between tetravalent actinides and humic acids.

In a previous paper (Moulin *et al.*, 1999), we did undoubtedly show that the presence of HA drastically influenced the sorption of Th(IV) onto colloidal silica in the pH range of natural ground waters, and a first estimation of interaction constants and mechanisms has been proposed. Unfortunately, the dispersion of the sorption data of the binary system at varying pH has prevented us from presenting accurate surface complexation data that could fully describe this system. Nevertheless, the addition of HA at varying pH, has led to an important decrease of the sorption of Th(IV) for as much as 1 mg HA/L, and to the reach a minimum for 10 mg HA/L figure 1. This fact was confirmed by a study at a constant pH of 6.3 and varying HA concentration (figure 2).

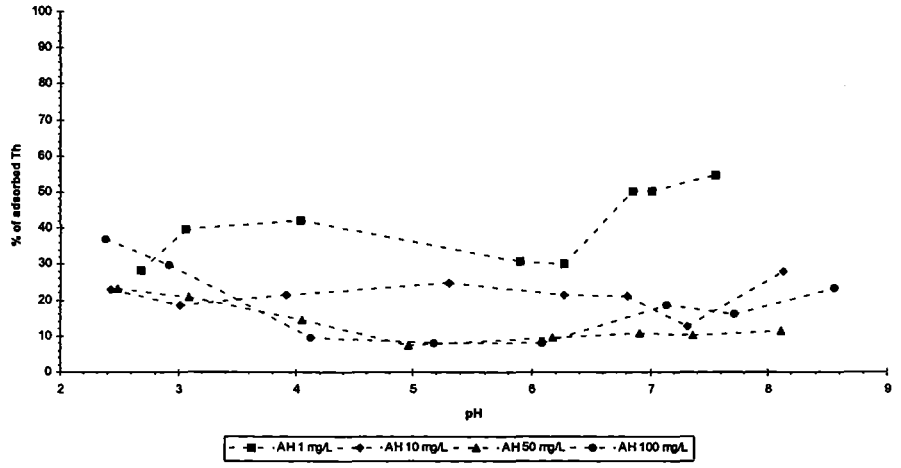

Figure 1: Sorption of thorium onto silica in the presence of humic acid *vs.* pH; [Th] = 1.15 10^{-12} M, [SiO_2] = 50 mg.L^{-1}, I = 0.1 M (Moulin *et al.*, 1999).

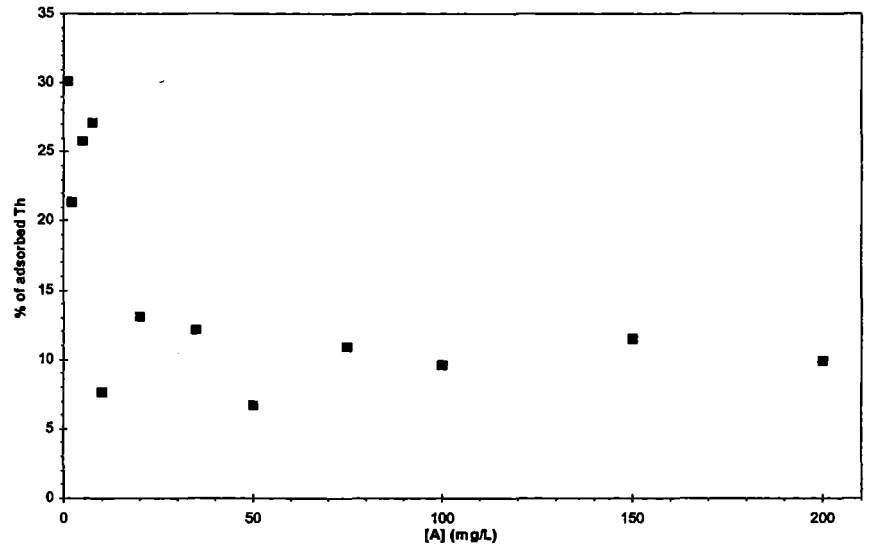

Figure 2: Sorption of Th(IV) onto silica in the presence of Aldrich humic acid pH = 6.3, [Th] = 1.15 10^{-12} M, [SiO_2] = 50 mg.L^{-1}, 1 ≤ [AH] (ppm) ≤ 200, I = 0.1 M ($NaClO_4$) (Moulin *et al.*, 1999).

2. ESTIMATION OF THORIUM-SILICA INTERACTIONS

2.1 RESULTS

Even if the dispersion of the results would prevent us from extracting robust data for the binary system, an estimation of the surface complexation constants can be attempted. The experimental results we obtained can be fitted using Fiteql 3.2 code (Herbelin and Westall, 1996). The results with the non electrostatic surface complexation model and Bäes and Mesmer (1976) hydrolysis constants of Th(IV) gives the estimation of the interaction constants reported in table I. It is to be noted that for $\equiv SiOTh(OH)_4^-$, the value of –18.4 is in agreement with the value obtained with the Kurbatov approach in Moulin *et al.* (1999), *i.e.* $\log \beta = -18.1$.

Table I: Estimation of the non electrostatic surface complexation model for Th(IV)/silica system.

Equilibrium	$\log K_n$
$\equiv SiOH + Th^{4+} \leftrightarrows \equiv SiOHTh^{4+}$	4.6
$\equiv SiOH + Th^{4+} \leftrightarrows \equiv SiOTh^{3+} + H^+$	1.02
$\equiv SiOH + Th^{4+} + H_2O \leftrightarrows \equiv SiOThOH^{2+} + 2H^+$	X
$\equiv SiOH + Th^{4+} + 2H_2O \leftrightarrows \equiv SiOTh(OH)_2^+ + 3H^+$	–7.02
$\equiv SiOH + Th^{4+} + 3H_2O \leftrightarrows \equiv SiOTh(OH)_3 + 4H^+$	– 12.9
$\equiv SiOH + Th^{4+} + 4\,H_2O \leftrightarrows \equiv SiOTh(OH)_4^- + 5H^+$	–18.4

2.2 REDUCTION OF EXPERIMENTAL DISPERSION

The possible factors that could induce the dispersion of the binary system data has been investigated in the period including:

1. The concentration of SiO_2 colloidal suspension was initially of 50 mg/L, resulting in a possible extensive dissolution. Thus, the concentration of SiO_2 in solution was increased to 250 mg/L, but the ratio between Th and SiO_2 was kept constant: no significant improvement was obtained in the dispersion.
2. The efficiency of the ultracentrifugation separation at 40,000 rpm at varying pH was checked by Photon Correlation Spectroscopy: no significant signal indicating remaining suspended colloids was recorded in the different supernatant.

3. The ultracentrifugation speed was increased to 50,000 rpm, and experiments has been done by another operator: the results of the last assay did not seem to improve significantly the dispersion of the data.

Referring to the highly reproducible results we have obtained with another system that we have examined during this project (*i.e.* Th–hematite, Reiller *et al.*, 2000), two hypothesis can be proposed:

- the silica colloidal suspension we used undergoes ageing and the silica is not nominal;
- a complexation reaction occurred between Th(IV) and H_4SiO_4 as it has been postulated in the case of Pu(IV) (Pazukhine *et al.*, 1990).

3. ESTIMATION OF THORIUM(IV) HUMIC COMPLEXATION

We have seen that the data dispersion of the binary system prevented us from extracting accurate surface complexation constants. Nevertheless, an estimation of the extent of humic complexation of Th(IV) in our conditions (figure 1 and 2) can be proposed using the first estimation of the surface complexation constant (table I). We can though propose approximate log β^{HA} values referring to our experimental data considering β^{HA} related to the equation:

$$Th + HA \rightleftarrows ThHA \qquad (I),$$

With β^{HA} written as:

$$\beta^{HA} = \frac{[ThHA]}{[Th]\,[HA]} \qquad (1).$$

The binary system can be described with the following system:

$$\equiv SiOH + Th^{4+} + n\,H_2O \leftrightarrows \equiv SiOTh(OH)_n^{(3-n)+} + n+1\,H^+ \qquad (II)$$

with the apparent stability constant K_n:

$$K_n = \frac{[\equiv SiOTh(OH)_n^{(3-n)+}]\,[H^+]^{n+1}}{[\equiv SiOH]\,[Th^{4+}]} \qquad (2).$$

The proportion P of thorium that is sorbed onto silica surface is calculated through:

$$P = \frac{[Th_{fixed}]}{[Th_{Total}]} \cdot 100 \qquad (3),$$

and the material balance of thorium is written as:

$$[Th_{Total}] = [Th_{hydrol}] + [Th_{Humic}] + [Th_{fixed}] = \alpha\,[Th^{4+}] + \beta^{HA}\,[HA]\,[Th^{4+}] + \sum_{n}\left[\equiv SiOTh(OH)_n^{(3-n)+}\right] \quad (4).$$

Considering equation 2, the complexation of thorium by HA and thorium hydrolysis, the expression of P becomes:

$$P = \frac{\sum_{n} K_n\,[SiOH]\,[Th^{4+}]\,[H^+]^{-(n+1)}}{\alpha\,[Th^{4+}] + \beta^{HA}\,[Th^{4+}]\,[HA] + \sum_{n} K_n\,[SiOH]\,[Th^{4+}]\,[H^+]^{-(n+1)}} \cdot 100 \quad (5),$$

Considering that humic complexation is the main phenomenon in solution when HA $\geq$ 10 mg/L:

$$P \cong \frac{\sum_{n} K_n\,[SiOH]\,[Th^{4+}]\,[H^+]^{-(n+1)}}{\beta^{HA}\,[Th^{4+}]\,[HA]} \cdot 100 \cong \frac{\sum_{n} K_n\,[SiOH]\,[H^+]^{-(n+1)}}{\beta^{HA}\,[HA]} \quad (6),$$

Knowing the ionisation of silanols surface sites:

$$\equiv SiOH \rightleftarrows \equiv SiO^- + H^+ \quad (III),$$

the expression of C_e, the exchange capacity can be expressed as:

$$C_e = [\equiv SiOH] + [\equiv SiO^-] + \sum_{n}\left[\equiv SiOTh(OH)_n^{(3-n)+}\right] \cong [\equiv SiOH] + [\equiv SiO^-] = \alpha_{SiOH}\,[\equiv SiOH] \quad (7).$$

And finally, β^{HA} can be expressed as:

$$\beta^{HA} \cong \frac{C_e \sum_{n}(K_n\,[SiOH]\,[H^+]^{-(n+1)})}{P\,\alpha_{SiOH}\,[HA]} \cdot 100 \cong \frac{C_e \sum_{n}(K_n\,[SiOH]\,10^{(n+1)\,pH})}{P\,(1 + 10^{-6.54+pH})\,[HA]} \quad (8).$$

Using the surface complexation constants that we have estimated earlier, a first estimation of the humic complexation constant of Th(IV) in the pH range 6-8 can be proposed in table II comparing with the data that can be calculated from the values of Nash and Choppin (1980) and Choppin and Allard (1985):

$$\log \beta^{HA} = 7.1\,\alpha^{HA} + 9.2 \quad (9),$$

and using Torres (1982) data for Lac Bradford HA.

The differences obtained in the lower part of the pH range can be attributed to the residual sorption of HA onto silica (Labonne, 1993) leading to an overestimation of Th(IV) sorption onto silica and thus an underestimation of the log β^{HA}. Nevertheless, for pH 7 the estimation of log β^{HA} is in fair agreement with the value that can be calculated through equation 9. The estimation for pH 8 clearly shows that Th(IV) is more sensitive to humic complexation than previously stated, as in the case of the Th(IV)-hematite-HA system studied through the same EC program (Reiller *et al.*, 2000).

Table II: Estimation of log $\beta^{HA}(Th^{4+})$ compared with data of Nash and Choppin (1980) and Choppin and Allard (1985).

	100 mg/L			50 mg/L			Nash and Choppin (1980)	Choppin and Allard (1985)
pH	P	β	log β^{HA}	P	β	log β	log β^{HA}	log β^{HA}
8	18	$5.61\ 10^{18}$	18.7	11	$9.41\ 10^{18}$	19.0		16.2
7	17	$6.97\ 10^{13}$	13.8	11	$1.08\ 10^{14}$	14.0		15.6
6	8	$2.20\ 10^{9}$	9.3	9	$1.96\ 10^{9}$	9.3		14.7
5 (LBHA)							13.2	

4. CONCLUSIONS

The technique retained to investigate the complexation of thorium by humic substances is based on the study of a ternary system involving the metal, humic acids (HA) and a mineral surface (silica colloids) considered as a competitor for HA. Although some problems arose on the binary system consisting of Th-silica (dispersion of experimental data), the studies which have been conducted have shown a great influence of HA onto Th(IV) behaviour. Hence, HA have an important effect upon the sorption of tetravalent actinides onto silanol surface groups of silica, even in the pH range of ground waters: a strong decrease of Th(IV) sorption through the formation of Th-humate complexes in solution.

Overall, these works permit us to verify at laboratory scale the strong influence of HA in natural systems onto the chemistry of tetravalent elements in general, and of tetravalent actinides in particular. In the case of Th(IV) as an analogue, this effect is important even when the concentration of HA is relatively low (1 ppm) in the neutral to slightly alkaline pH range, signifying the importance of humic complexation reaction in almost all natural waters, which could be waters representative of geologic formations for an underground radioactive waste disposal.

5. REFERENCES

Choppin G.R. (1999), Utility of oxidation state analogs in the study of plutonium behavior, *Radiochim Acta*, **85**, 89-96.

Choppin G.R. and Allard B. (1985), Complexes of actinides with naturally occurring organic compounds, *in* "Handbook on the Physics and Chemistry of the Actinides" Chap. 11, Ed. Freeman A.J. & Keller C., Elsevier Sci. Pub.

Herbelin A.L. and Westall J.C. (1996), FITEQL a computer program for determination of chemical equilibrium constants from experimental data, Oregon State Univerty, report 96-01.

Labonne N. (1993), Rôle des matières organiques dans les phénomènes de rétention des actinides sur la silice, Thèse de doctorat de l'université PARIS XI ORSAY, N° 2911, 10 novembre 1993.

Labonne-Wall N., Moulin V. and Vilarem J.P. (1997), Retention properties of humic substances onto amorphous silica: consequences for the sorption of cations, *Radiochim. acta*, **79**, 37-49.

Moulin V., Reiller P., Dautel C., Plancque G., Laszak I. and Moulin C., Complexation of Eu(III), Th(IV) and U(VI) by humic substances, in "Effects of humic substances on the migration of radionuclides: complexation and transport of actinides", " Second progress report, FZK Report, FZKA 6324, June 1999, p. 82.

Nash K.L. and Choppin G.R. (1980), Interaction of humic and fulvic acids with Th(IV), *J. Inorg. Nucl. Chem.*, **42**, 1045-1050.

Pazukhine E. M., Krivokhatskiy A. S., and Kudryavtsev E. G (1990), Possible formation of plutonium (IV) complexes with soluble silicon -oxygen compounds. *Soviet Radiochem.*, **32**, 325-329.

Reiller P., Moulin V. and Dautel C. (2000), Sorption behaviour of humic substances towards hematite: consequences on thorium availability, *in* "Effect of humic substances on the migration of radionuclides: complexation and transport of actinides" Third progress report.

Torres R.A. (1982), Humic acid complexation of europium, americium and plutonium, Ph. D Thesis Florida State University.

Annex 8

Sorption Behavior of Humic Substances Towards Hematite: Consequences on Thorium Availability

(P. Reiller, V. Moulin, C. Dautel (CEA))

3rd Technical Progress Report
EC Project:

"Effects of Humic Substances on the Migration of Radionuclides: Complexation and Transport of Actinides"

Project No.: FI4W-CT96-0027

CEA Contribution to Task 3 (Transport)

Sorption Behavior of Humic Substances towards Hematite: Consequences on Thorium Availability

Pascal Reiller, Valérie Moulin, Christian Dautel

Commissariat à l'Energie Atomique, Centre d'Etudes de Saclay, Fuel Cycle Division,
DESD/SESD/LMGS
91191 Gif-sur-Yvette, France

1. GENERAL INTRODUCTION

The understanding of radionuclides behaviour in natural systems in relation with nuclear waste disposals in geological formations necessitates the knowledge of their speciation in these systems including their distribution between the solution and the mineral phases. In particular, this implies to determine the influence of humic substances (humic and fulvic acids, HA/FA) as natural organic substances present in more or less concentrations in ground waters on the migration of radionuclides, particularly actinide elements. Humic substances can influence the sorption of cations onto mineral surface firstly as a complexing ligand for cations in solution, and secondly as an adsorbent by modifying the properties of the mineral surface.

The sorption of metal ions onto mineral surfaces as clays or iron oxides has been extensively studied (Lieser *et al.*, 1990; Degueldre, 1997). So does is the influence of humic substances onto these retention properties. It has been thoroughly studied and led to numerous models and interpretations. The majority of the works conducted onto this subject has been performed onto highly important mono, di or trivalent radionuclides such as Cs(I), Np(V) (Tanaka and Senoo, 1995), Zn Ni Cu (II), Young and Harvey, 1992) Co(II) (Zachara *et al.*, 1994), Cd(II) (Davis and Bhatnagar, 1995; Vermeer, 1996), U(VI) (Payne *et al.*, 1996) or Am(III) (Labonne-Wall *et al.*, 1997). A little has been done on tetravalent cations due to their very low solubility (Ryan and Rai, 1987; Adair *et al.*, 1997). Thorium is usually regarded as an analogue for the other tetravalent actinides (Choppin, 1999). The available data about the complexation of Th(IV) with humic substances have been obtained by Nash and Choppin (1980) revised by Choppin and Allard (1985). Unfortunately, these data have been obtained in an acidic pH range ($3.5 \leq pH \leq 5$), and the question which arises is the extrapolation at other pH values representative of the conditions of natural waters. This fact has been clearly shown by Moulin *et al.* (1999), as humic acids have been shown to desorb Th(IV) from silica up to pH = 8, whereas speciation calculation predicts the contrary. Otherwise, Zeh *et al.* (1995) noted that in groundwaters, thorium is associated with particulate matter at somewhat higher pH values.

The aim of this study is to determine for which conditions humic substances modify the migration, and in particular the **retention** of actinides onto mineral surfaces and under relevant geochemical conditions (pH, ionic strength, presence of competing cations). For this purpose, the behaviour of humic substances towards mineral phases is important to know, and particularly the formation of an organic film. The objective of the present work is to study the retention of humic acids onto hematite as a function of physico-chemical parameters (pH, ionic strength, humic concentration) and to appreciate the effect of this phenomenon onto the actinides retention onto mineral surfaces.

In the framework of this study we choose a system consisting of hematite (α-Fe_2O_3), one of the major component of the colloidal matter contained in natural waters (Degueldre, 1994), Aldrich humic acids and thorium(IV). Cromières *et al.* (1998) already quantified the interaction of Th(IV) with hematite colloids using non electrostatic and diffuse double layer surface complexation models, and the hydrolysis

constants recommended by Bäes and Mesmer (1976). The objectives of this work are to study the influence of humic acids upon the sorption of a tetravalent actinide upon hematite.

2. EXPERIMENTAL

2.1. MATERIALS

The hematite suspension used was obtained from AEA Harwell though an EC project (Moulin *et al.*, 1996; Cromières, 1996). The characterisation has been performed by Cromières (1996). The colloids are of spherical morphology. The size distribution is monomodal centred on a diameter of 55 nm. The specific surface was measured, using the BET/N_2 method, to be 19 $m^2.g^{-1}$. The proton exchange capacity is C_e = 3.8 10^{-5} $eq.g^{-1}$, and the estimated pK_a's determined with the diffuse double layer model (Dzomback and Morel, 1990) are :

- $\equiv SOH + H^+ \rightleftarrows \equiv SOH_2^+$ $\qquad pK_{a1} = -7.32$
- $\equiv SOH \rightleftarrows \equiv SO^- + H^+$ $\qquad pK_{a2} = 8.06$
- $pH_{pzc} = 7.69$

A distribution diagram of the surface sites can proposed using the diffuse double layer model (figure 1).

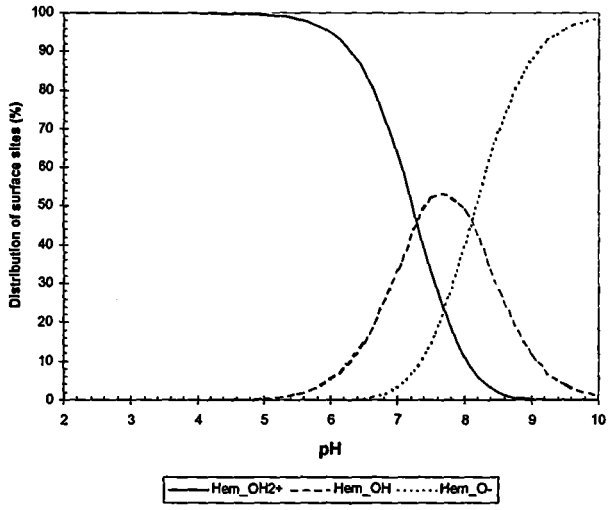

Figure 1: Distribution of surface sites of hematite; [α-Fe_2O_3] = 500 mg/L, I = 0.1 M

Purified Aldrich humic acids (HA) are used in a protonated form. The main characteristics are detailed in Kim *et al.* (1991), as part of an EC MIRAGE project (Kim, 1990). The proton capacity is W_{HA} = 5.4 $meq.g^{-1}$ for HA-Aldrich (determined by potentiometric titrations). The apparent acidity constant (determined as the pH at mid-equivalence) are: $pK_a^{HA} = 4.52$.

The initial solution of thorium – ^{228}Th in 2 N HNO_3 – was obtained from Amersham. This solution was diluted in order to obtain a 1.09 10^{-9} M stock solution in 0.9 M $NaClO_4$ and HNO_3 0.2 M.

All other chemicals were reagent grade, and Millipore water was used.

2.2. SORPTION PROCEDURE

The sorption experiments are conducted in batch procedure at room temperature in polycarbonate vials sealed with screwcaps. The concentration of the hematite suspension is fixed at the desired concentration by diluting the stock solution in the background electrolyte, aliquots of humic acids are added and the pH is adjusted at the desired value with a TACUSSEL pHmetre (PHM 220 MeterLab) equipped with a combined TACUSSEL electrode (Radiometer type XC 161, modified $NaClO_4$ 0.1 M, NaCl 10^{-2} M), using $HClO_4$ or freshly prepared NaOH. The ionic strength is kept constant – $NaClO_4$ – through all of the experiments. Humic acids concentration is measured spectrophotometrically at 254 nm (Shimadzu UV-2100). The obtained suspension is shaked for 24 hours to allow equilibration of the adsorbent. The radionuclide is added to obtain a final concentration of 1.15 10^{-12} M; the pH is adjusted. The solution is shaked again for 24 hours, and 2 aliquots of 1 mL of the suspension are sampled for thorium activity measurement (A_1), in order to get rid of Th(IV) adsorption upon the vial walls as described by Cromières (1996) and Cromières *et al.* (1998). The colloids are separated from the liquid phase by ultracentrifugation (90 min, 50 000 rpm), the pH of the supernatant is measured, then two other aliquots of 1 mL are sampled from the supernatant for thorium activity measurement (A_2).

The activities of ^{228}Th are measured by liquid scintillation counting. The previous aliquots are added to 4 mL of liquid scintillator (Ultima Gold AB). The activity measurements are performed after one month in order to attain the seculary equilibrium of ^{228}Th with its daughters. The initial thorium activity (A_o) was determined by direct addition into the liquid scintillator.

Sorption percentage is calculated form the activities of the suspension (A_1) and of the supernatant (A_2) according to the following equation:

$$R\,(\%) = \frac{A_1 - A_2}{A_1} \times 100$$

The distribution coefficient, K_d, is given by:

$$K_D\,(mL.g^{-1}) = \frac{[Th]_{sorbed}}{[Th]_{solution}} = \frac{R}{100 - R} \times \frac{10^6}{[Fe_2O_3](mg.L^{-1})}$$

2.3. THORIUM CHEMISTRY

Regarding to the low Th concentration, and the isolation of the system from atmospheric CO_2, only the monomers induced by the hydrolysis are taken into account. There is a discrepancy in the various published data on Th(IV) hydrolysis. The most accepted values are those determined by Bäes and Mesmer (1976) and confirmed by Grenthe and Lagerman (1991). The cumulative constants of thorium(IV), corrected for 0.1 M ionic strength using SIT, are reported in table I – $\varepsilon_{Th(IV)}$ were taken as equal to $\varepsilon_{U(IV)}$ in Grenthe *et al.* (1992) –. The total carbonate concentration in this closed system has been estimated by Labonne (1993) and Cromières (1996) to be 5.10^{-5} M. The trihydroxo carbonato and pentacarbonato thorium(IV) complexes evidenced by Östhols *et al.* (1994) have been taken into account. A speciation diagram corresponding to our experimental conditions can be seen on figure 2.

Table I: Complexation cumulative constants of Th(IV), corrected for 0.1 M ionic strength using SIT method (Grenthe et al. (1992)).

Equilibrium	log $*\beta_i$ Bäes and Mesmer (1976) I = 0.1 M	log $*\beta_i$ Grenthe and Lagerman (1991) Östhols *et al.* (1994) I = 0.1 M
$Th^{4+} + H_2O \rightleftarrows Th(OH)^{3+} + H^+$	–3.86	–3.79
$Th^{4+} + 2\ H_2O \rightleftarrows Th(OH)_2^{2+} + 2\ H^+$	–8.01	
$Th^{4+} + 3\ H_2O \rightleftarrows Th(OH)_3^+ + 3\ H^+$	–12.99	–9.08
$Th^{4+} + 4\ H_2O \rightleftarrows Th(OH)_4 + 4\ H^+$	–17.16	–13.87
$Th^{4+} + CO_3^{2-} + 3\ H_2O \rightleftarrows ThCO_3(OH)_3^- + H^+$		–1.69

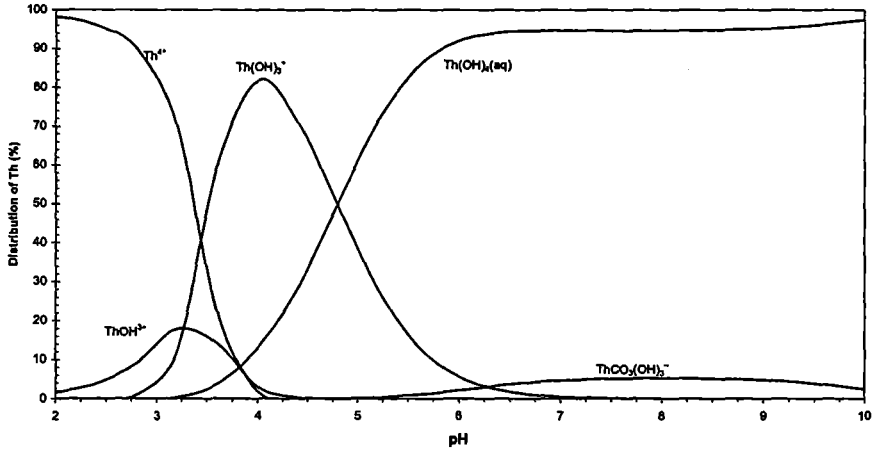

Figure 2: Speciation of Th(IV) referring to Grenthe and Lagerman (1991) and Östhols *et al.* (1994); [Th] = 1.10^{-12} M, total carbonate 5.10^{-5} M, I = 0.1 M.

3. RESULTS AND DISCUSSIONS

3.1. SORPTION OF HUMIC ACIDS ONTO HEMATITE

In this first part of the study, the sorption of HA onto a colloidal suspension of hematite is characterised, and the effect of the concentration of HA, pH and ionic strength on this sorption phenomenon is investigated. In the following, the experimental conditions are as follows: the concentration of hematite is 500 mg/L, leading to surface sites concentration C_{SOH} of 1.9 10^{-5} eq/L (3.8 10^{-5} eq/g × 0.5 g/L), and the concentration of humic acids is 11.1 mg/L, leading to humic sites concentration C_{HA} of 6 10^{-5} eq site/L (5.4 meq/g × 11.1 mg/L).

3.1.1. EFFECT OF HA CONCENTRATION

The sorption experiments have been conducted at constant pH and ionic strength – pH = 5.08 ± 0.03; I = 0.1 M –. The retention profile of HA onto hematite is reported on figure 3. As expected, the proportion of HA fixed to the surface is decreased when increasing the HA concentration. The theoretical HA concentration needed to attain the saturation can be calculated through:

$$C_{HA} = \frac{[\alpha\text{-}Fe_2O_3]\, C_e}{W_{HA}} = \frac{0.5\ g/L \times 3.8\ 10^{-5}\ eq/g}{5.4\ 10^{-3}\ eq/g} \cong 3.5\ mg\ HA/L$$

Referring to figure 3, the actual concentration can be estimated to 4-5 mg HA/L leading to a saturation capacity of:

$$C_e = (4.8 \pm 1)\ 10^{-5}\ eq/g$$

Considering the uncertainty of the determination of the actual C_e, the actual saturation concentration is in fair agreement with the theoretical one. The fact that an *oversaturation* can occur is not surprising when taking into account the description of *loops and tails*, where part of the humic acids molecule is extended into the solution and part is attached to the mineral surface (Fleer *et al.*, 1993).

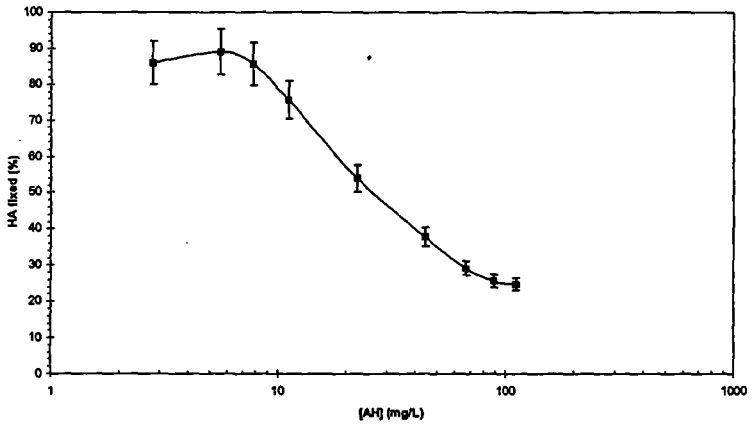

Figure 3: Retention of HA onto hematite at pH = , [α-Fe_2O_3] = 500 mg/L, I = 0.1 M($NaClO_4$).

3.1.2. *EFFECT OF pH*

The purpose of this part of the study is to appreciate the effect of pH on the sorption of HA onto hematite. Using the same experimental conditions as in the previous chapter, except the pH value, the results obtained in the case of the retention of HA onto hematite *vs.* pH are reported in figure 4.

A strong sorption of HA onto the surface of colloidal hematite is observed in the acidic to neutral pH range and is decreasing when increasing pH. The retention of HA is clearly decreasing with the ionisation of HA, and as the hematite surface becomes less positive with increasing pH (figure 1), as it has been generally observed, from more than 97% at pH 3 to nearly 25% at pH 10.4.

Plotting the logarithm of the distribution coefficient K_D *vs.* pH permits to notice a clear step in the retention profile when pH exceeds the pK_a^{HA} of humic acids. Below pH 7, figure 1 shows that the surface charge of hematite is highly positive ($pH < pH_{pzc}$) . In the first part of the retention profile, up to pH 4, protonated HA sites and positive sites of hematite are the dominant species. The retention mechanism is supposed to be mainly of hydrogen bound type (Liu and Gonzalez, 1999). At this low pH value, the humic acids are from almost neutral to weakly negatively charged and the repulsion of charge is minimised. The conformation of the polyelectrolyte is folded and a high amount of sorbed humic acids is observed.

After the step observed on figure 4b at $pH \geq 4.5$, the dominant species are the deprotonated form of humic sites (A^-), whereas the surface of hematite is still highly positive, the decreasing of the humic acids retention is then stopped by the electrostatic interaction between negative humic acids and positive hematite surface. The subsequent decrease of the retention of HA is produced by the progressive repulsion between A^- and the surface of hematite at it becomes negative.

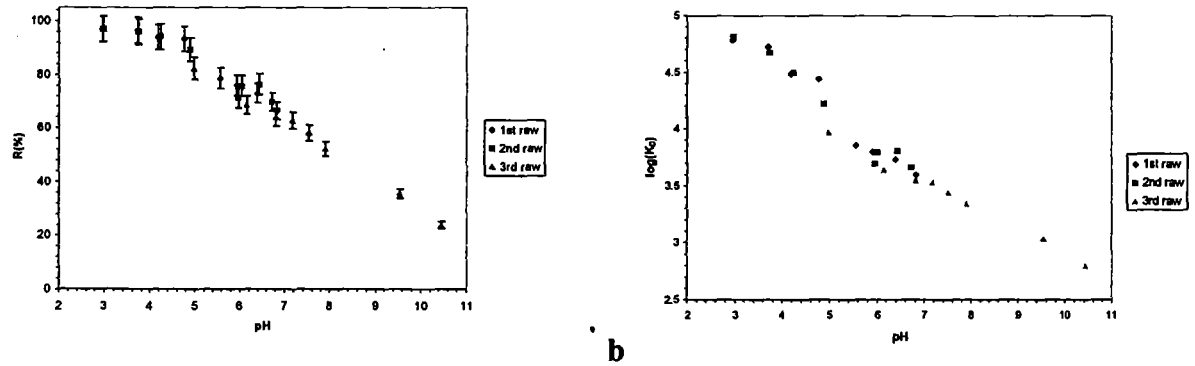

A b

Figure 4: Retention of HA onto hematite vs. pH;
[HA] = 10 mg/L, [α-Fe_2O_3] = 500 mg/L, I = 0.1 M (NaClO4).

3.1.3. *EFFECT OF IONIC STRENGTH*

The influence of the ionic strength on the retention of HA onto hematite colloids can be seen on figure 5. For $I \geq 0.01$ M, the effect of ionic strength on HA retention seems to be very week. This effect can only be taken into account when $I = 10^{-3}$ M and for HA concentration less than 10 mg/L. In a previous study with gœthite (Reiller *et al.*, 1999), we observed a similar, but slightly more pronounced

effect of this parameter. As the salt concentration increases, two phenomena can occur. The first one is in relation with the fact that when decreasing ionic strength, the conformation of humic/fulvic molecules goes from a folded structure to an opened and unfolded structure (Buffle, 1988). Then at high ionic strength the molecules are smaller than at low ionic strength, which explains the higher sorption capacity at higher ionic strength. The second phenomenon is related with the screening of the lateral repulsion of the HA segments due to the higher salt concentration (Van der Steeg, 1992) leading to more HA entities on the surface.

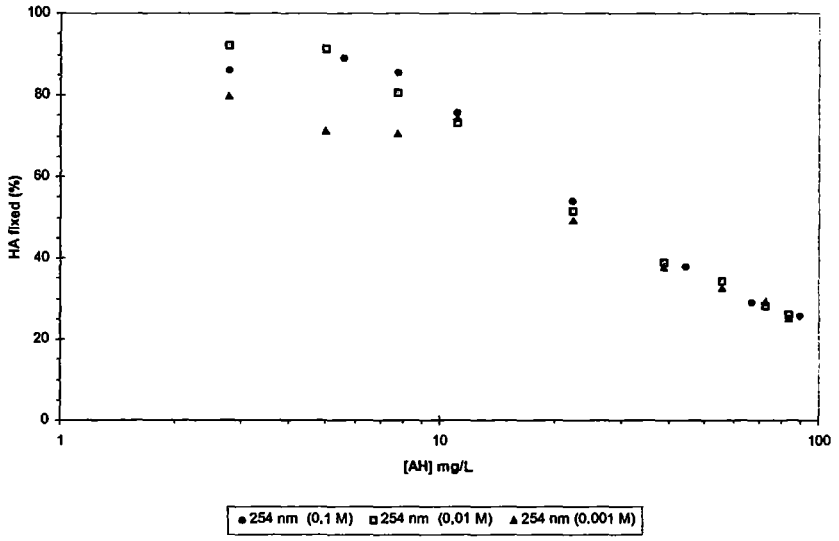

Figure 5: Influence of ionic strenght upon HA sorption onto hematite; [α-Fe_2O_3] = 500 mg/L, [HA] = 11.1 mg/L.

3.2. INFLUENCE OF HUMIC ACIDS UPON SORPTION OF THORIUM ONTO HEMATITE.

The aim of this second part of the study is to appreciate the effect of the presence of humic acids on the Th(IV) sorption onto a colloidal suspension of hematite. The colloidal suspension and HA will be pre-equilibrated, so the tetravalent actinide is considered as a perturbation in the system. Firstly, the sorption will be studied at constant pH varying the HA concentration and, then the effect of pH at constant HA concentration will be considered.

3.2.1. SORPTION ISOTHERM AT CONSTANT PH

The sorption experiments have been conducted at constant pH and ionic strength – pH = 7.14 ± 0.03 and 8.06 ± 0.04; I = 0.1 M –. For these pH values, Th(IV) is in its tetra hydroxo form: $Th(OH)_4(aq)$ (≅ 94.7 % pH 7 and 8). Under these experimental conditions, 60 % of 10 ppm of HA are sorbed onto hematite (figure 4a). We can infer that for a lower concentration of HA, R(HA) would be higher, and that for a higher concentration, R(HA) would be lowered as it can be seen on figure 3 at pH ≅ 5.

The experimental curve on figure 6 can be divided in two distinct regions. In the first region, the retention seems to be constant: Th(IV) is sorbed onto hematite, either in the form of a binary complex with the hematite surface sites, or in the form of a ternary complex with the HA sorbed onto the hematite surface. Since the surface is not saturated, there is not enough HA sites in solution that could affect the mass action law and permit the humic competition to be effective. In the second region, the sorption of Th(IV) onto hematite is strongly decreased with increasing HA concentration ; as the surface of hematite is saturated with HA, the more the concentration of HA, the more free humic complexing sites are available in solution. The concentration of HA sites is high enough to act on the mass action law and compete with Th(IV) sorption onto hematite.

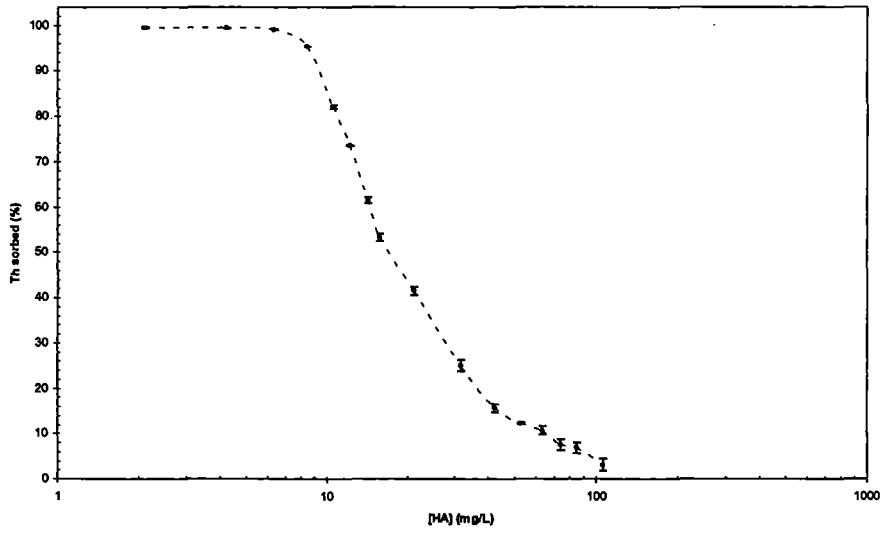

Figure 6: Retention of thorium(IV) onto hematite *vs.* HA concentration at pH 7; [Th] = 1 10^{-12} M, [α-Fe_2O_3] = 500 mg/L, I = 0.1 M ($NaClO_4$).

The sorption experiments conducted at pH 8 reveals a similar behaviour as it can be seen on figure 7. The two different regions that have been evidenced at pH 7 can also be seen at pH 8, and the stronger impact in term of Th(IV) "free" proportion is for HA concentration greater than 10 ppm. Furthermore, the sorption of Th(IV) onto hematite is enhanced at this higher pH compared to pH 7. This enhancement of the Th(IV) sorption can be interpreted as the combination of different but related phenomena for [HA] $\geq$ 10 mg/L.

The first phenomenon is the increased desorption of HA from the hematite surface at pH 8 compared to pH 7 (figure 4). The negative net surface charge of hematite at pH 8 (figure 1) repels the ionised HA sites (carboxylates) and increases the proportion of HA in solution. The second and intensely related phenomenon is the competition between the complexation by HA and the sorption of Th(IV) by hematite. Referring to Cromières *et al.* (1998), Th(IV) is complexed by hematite surface site in its tetrahydroxo form in this pH range following the equilibrium:

$$\equiv FeOH + Th^{4+} + 4\ H_2O \rightleftarrows \equiv FeOTh(OH)_4^- + 5\ H^+$$

A similar behaviour was proposed by Laflamme and Murray (1987) and Hunter *et al.* (1988) to model the sorption of Th(IV) onto gœthite (α-FeOOH). Since more HA sites are in solution at pH 8 compared to pH 7, more "free" hematite surface sites are available and can compete for Th(IV) complexation. A similar behaviour has been evidenced by Takahashi *et al.* (1999) in the case of the Zr(IV) and Hf(IV)-HA-Kaolinite ternary systems.

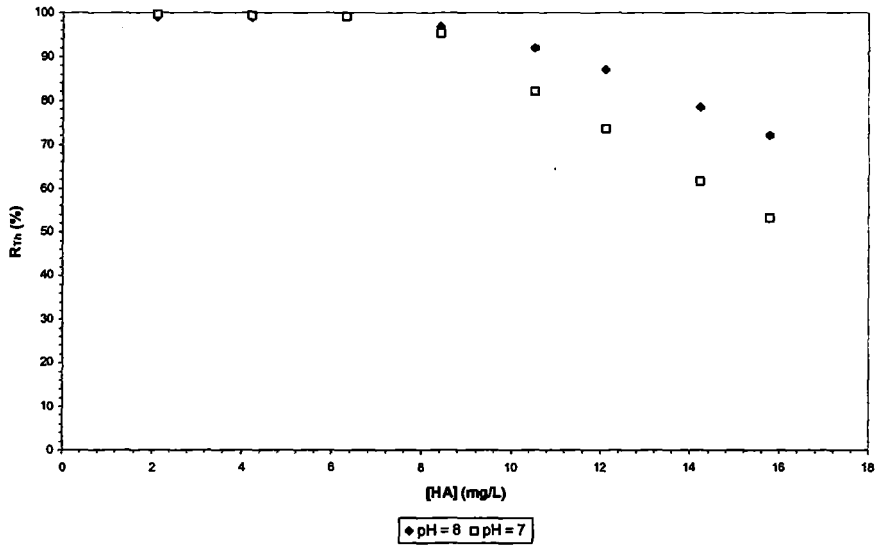

Figure 7: Comparison of thorium(IV) retention onto hematite *vs.* HA concentration at pH 7 and pH 8; [Th] = 1 10^{-12} M, [α-Fe_2O_3] = 500 mg/L, I = 0.1 M ($NaClO_4$), ◆ pH = 8.06 ± 0.04, ■ pH = 7.14 ± 0.03 .

3.2.2. SORPTION VS. PH

The results for the thorium sorption onto hematite in the presence of HA when the pH is varied are shown on figure 8, compared with the data obtained by Cromières *et al.* (1998) for the binary system without HA (*i.e.* Th–α-Fe_2O_3). In order to compare our results with those of Cromières *et al.* (1998), the hematite concentration in solution was lowered to 50 mg/L.

The retention curve of Th(IV) in the ternary system presented on figure 8 can be divided in three different parts. Within the first region – $2 \leq pH \leq 3.5$ –, the sorption of Th(IV) is higher than in the binary system: this enhancement is due to the coating of the mineral surface by HA, leading to the modification of the surface and to the complexation of Th(IV) by HA sorbed onto hematite, as it has been noted in different laboratory or natural systems (Labonne-Wall *et al.*,1997; Payne *et al.*, 1996; Davis and Bhatnagar, 1995;Young and Harvey, 1992; Zachara *et al.*, 1994). The second region lies between pH 3.5 and pH 6.5, where the sorption of Th(IV) is markedly decreased with increasing pH: this is partly due to the progressive desorption of HA from the hematite surface, as it can be seen on figure 4, leading to the complexation of Th(IV) in solution, and partly to the increase in the complexing strength of HA with increasing pH. The last region is when pH exceeds 6.5, where the sorption of Th(IV) is slightly increased

from less that 10 % at pH 6.77 to 15.36 % at pH 7.65: as we have already noticed in the previous paragraph, the cumulative effects of both the desorption of HA and the competition between sorption and humic complexation slightly improve the thorium sorption onto hematite, but the humic complexation is still the dominant phenomenon. As we have noticed earlier, these observations are in agreement with the works of Takahashi *et al.* (1999) on Zr(IV) (and Hf(IV)) reported on figure 9. These works can directly be compared with ours as the ratio between the available sites of hematite and humic acids are almost equal (table II).

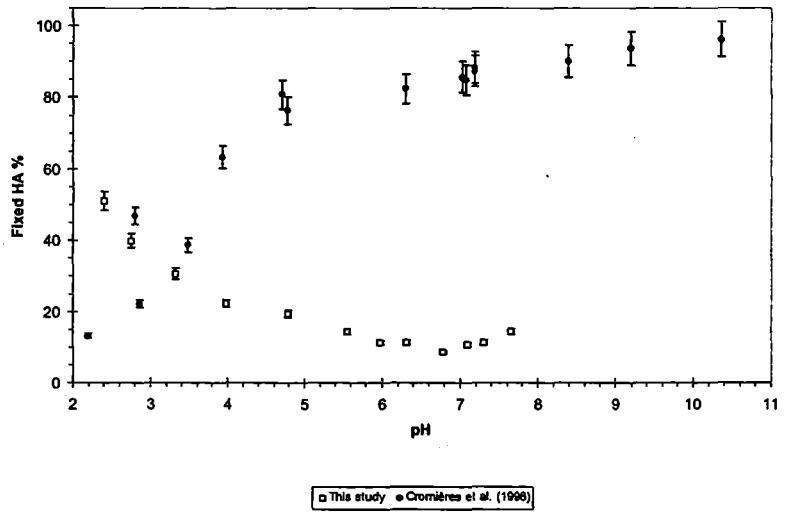

Figure 8: Influence of HA on the sorption of Th(IV) onto hematite *vs.* pH;
[Th] = 1.15 10^{-12} M, [α-Fe_2O_3] = 50 mg.L^{-1}, [HA] = 10 mg/L, I = 0.1 M ($NaClO_4$).

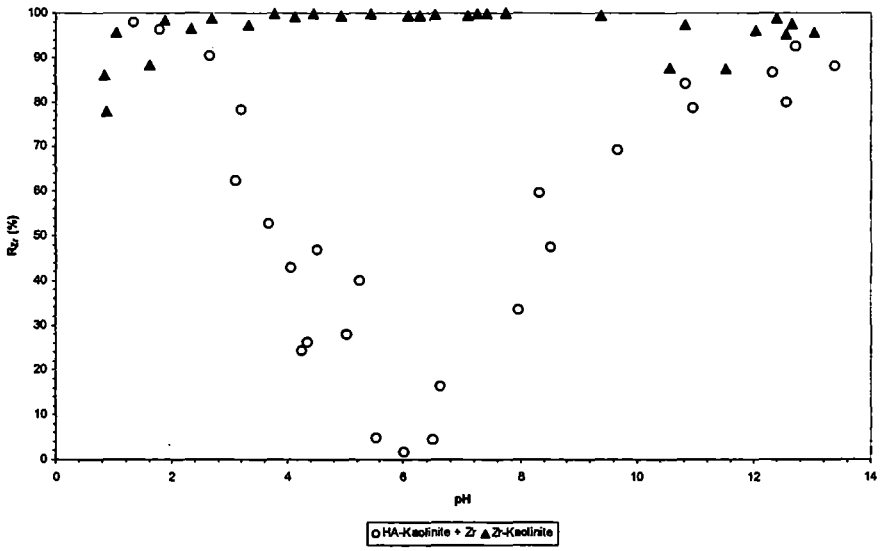

Figure 9: Retention of Zr(IV) onto kaolinite *vs.* pH;
[Zr] < 10^{-13} M, Kaolinite = 2 g/L (5.8 10^{-5} eq/L); [HA] = 30 mg/L (1.8 10^{-4} eq/L), I = 0.02 M.
▲ binary system, O ternary system.
Data from Takahashi *et al.* (1999).

Table II: Comparison between Takahashi *et al.* (1999) and This work.

Takahashi *et al.* (1999)	This work
$[Zr] \leq 10^{-13}$ M	$[Th] = 1\ 10^{-12}$ M
Kaolinite : 2 g/L	Hematite : 50 mg/L
2.9 meq/100g : $5.8\ 10^{-5}$ eq site/L	5.8 meq/100g : $1.9\ 10^{-6}$ eq site/L
[HA] = 30 mg/L $\Rightarrow$ $30\ 10^{-3} . 6.1\ 10^{-3} =$ $1.8\ 10^{-4}$ eq/L (Takahashi *et al.*, 1995)	[HA] = 10 mg/L $\Rightarrow$ $10\ 10^{-3} . 5.4\ 10^{-3} =$ $5.4\ 10^{-5}$ eq/L
[Kaolinite] / [HA] = 0.32	[Hematite] / [HA] = 0.35

4. CONCLUSIONS

The strong influence of humic acids onto the sorption of tetravalent actinides onto hematite has been shown and quantified as a function of HA concentration, pH and ionic strength. It is strongly related to the complexing behaviour of HA towards tetravalent elements.

The sorption of HA onto hematite colloids is important and induces an important modification of the surface. The number of humic sites associated to the mineral surface exceeds the number of available hematite surface sites, exhibiting a loops and tails conformation of the humic acids in our experimental conditions. The interactions between HA and hematite surface is led by two factors: the electrostatic interaction between negatively charged HA sites and the hematite surface at pH relevant of natural media (*i.e.* $6 \leq pH \leq 9$), and a more strong interaction combining H-bond and screening of charge repulsion at low pH due to the folding of the humic structure. Similarly, the modification of HA structure with ionic strength leads to the decrease in sorption, but only when HA concentration approaches saturation of the surface.

The sorption of Th(IV) onto colloidal hematite is indeed strongly influenced by the presence of humic acids and the formation of strong complexes between Th and HA. This influence is also deeply related to the ratio between the number of available surface and humic sites. Nevertheless, for HA concentration and pH values that are relevant of natural media, Th(IV) is clearly in competition between the mineral phase (more or less coated with HA) and free humic acids. This implies that hematite, as constituent of soils or as oxidation product of canister may not be able to efficiently sorb tetravalent actinides in the presence of humic acids.

In these experiments, Th(IV) is considered as an immediate perturbation of a pre-equilibrated system. Works are under progress in order to investigate the influence of the kinetic parameter (Bryan *et al.*, 1999). Thus, comparing the results obtained in this study with the ones obtained by Takahashi *et al.* (1999), it seems obvious that the humic complexation of tetravalent elements is of great importance in all the pH range relevant of the natural ground waters. The study of these complexation reactions is investigated in (Reiller *et al.*, 2000)

5. REFERENCES

Adair J.H., Krarup H.G., Venigalla S. and Tsukada T. (1997), A review of the aqueous chemistry of the zirconium - Water system to 200 °C, *Mat. Res. Symp. Proc.*, **432**, 101-112 .

Bäes and Mesmer (1976), The hydrolysis of cations, Wiley-Interscience Publications, New York.

Bryan N.D., Griffin D. and Regan L. (1999), Implication of humic chemical kinetics for radiological performance assessment, , *in* "Effect of humic substances on the migration of radionuclides: complexation and transport of actinides" Second progress report, FZK Report, FZKA 6324, June 1999, p. 341.

Choppin G.R. and Allard B. (1985), Complexes of actinides with naturally occurring organic compounds, *in* "Handbook on the Physics and Chemistry of the Actinides" Chap. 11, Ed. Freeman A.J. and Keller C., Elsevier Sci. Pub.

Choppin G.R. (1999), Utility of oxidation state analogs in the study of plutonium behavior, *Radiochim Acta*, **85**, 89-96.

Cromières L. (1996), Sorption d'éléments lourds (U(VI), Np(V), Th(IV), Am(III), Co(II), Cs(I), I(-I)) sur des colloïdes d'hématite. Proposition de mécanismes réactionnels, Thèse de doctorat de l'Université PARIS XI ORSAY, N° 4601, 13 décembre 1996.

Cromières L., Moulin V., Fourest B., Guillaumont R. and Giffaut E. (1998), Sorption of thorium onto hematite colloids, *Radiochim. Acta*, **82**, 249-256.

Davis A.P. and Bhatnagar V. (1995), Adsorption of cadmium and humic acid onto hematite, *Chemosphere*, **30**, 243-256.

Degueldre C. (1994), Colloid properties in groundwaters from crystalline formations, NAGRA Report NTB 92-05.

Degueldre C. (1997), Groundwater colloid properties and their potential influence on radionuclide transport, Mat. Res. Soc. Symp. Proc., 465, 835-846 (1997)

Dzomback D.A. and Morel M.M. (1990), *in* "Surface complexation modelling", John Wiley & Sons.

Fleer G.J., Cohen Stuart M.A., Scheutjens J.M.H.M., Cosgrove T. and Vincent B. (1993), *in* "Polymers at interfaces", Chapman & Hall Eds, London.

Grenthe I. and Lagerman B. (1991), Studies on metal carbonate equilibria. 23. Complex formation in the Th(IV)-H_2O-CO_2(g) system, *Acta Chem. Scand.*, **45**, 231-238.

Grenthe I., Fuger L., Konings R.G.M., Lemire R.J., Muller A.B., Nguyen-Trung C. and Wanner H. (1992), Chemical thermodynamics of uranium, NEA-OCDE, Wanner & Forest Eds. Amsterdam.

Kim, J.I., Buckau, G., Klenze R., Rhee D.S., Wimmer H. (1991) Characterisation and complexation of humic acids. CEC Report EUR 13181.

Kim, J.I. (1990) Geochemistry of actinides and fission products in natural aquifer systems. In " *CEC Project Mirage-Second Phase on Migration of Radionuclides in the Geosphere* " (B. Côme, Ed.), EUR Report 12858.

Labonne N. (1993), Rôle des matières organiques dans les phénomènes de rétention des actinides sur la silice, Thèse de doctorat de l'université PARIS XI ORSAY, N° 2911, 10 novembre 1993.

Labonne-Wall N., Moulin V. and Villarem J.P. (1997), Retention properties of humic substances onto amorphous silica: consequences for the sorption of cations, *Radiochim. acta*, **79**, 37-49.

Lieser K.H., Ament A., Hill R., Singh R.N., Stingl U. & Thybusch B. (1990), Colloids in groundwater and their influence on migration of trace elements and radionuclides, *Radiochim. Acta*, **49**, 83-100.

Liu A. and Gonzalez R. (1999), Adsorption/desorption in a system consisting of humic acid, heavy metal, and clay minerals, *J. Colloid Interface Sci.*, **218**, 225-232.

Moulin V., Casanova F., Labonne N., Vilarem J.P., Dran J.C., Pieri J., Milcent M.C., Boulay C., Durand J.P., Goudard F., Della Mea G., Rigato V., La,g H., Turrero M.J., Gomez P., Rivas P., Melon A.M., Adell A., Grindrod P., Crompton S., Balek V. and Malek Z. (1996), The role of colloids in the transport of radionuclides in geological media, Contract No FI2W-CT91-0097, EUR 16880 EN.

Nash K.L. and Choppin G.R. (1980), Interaction of humic and fulvic acids with Th(IV), *J. Inorg. Nucl. Chem.*, **42**, 1045-1050.

Östhols E., Bruno J. and Grenthe I. (1994), On the influence on mineral dissolution: III. The solubility of microcrystalline ThO_2 in CO_2-H_2O media, *Geochim. Cosmochim. Acta*, **58**, 613-623.

Payne T.E., Davis J.A. and Waite T.D. (1996), Uranium adsorption on ferrihydrite - effects of phosphate and humic acid, *Radiochim. Acta*, **74**, 239-243.

Ryan J.L. and Rai D. (1987), Thorium(IV) hydrous oxide solubility, *Inorg. Chem.*, **26**, 4140-4142.

Reiller P., Moulin V. and Casanova F. (1999), Sorption behaviour of humic substances towards iron oxides, *in* "Effect of humic substances on the migration of radionuclides: complexation and transport of actinides" Second progress report, FZK Report, FZKA 6324, June 1999, p. 119.

Reiller P., Moulin V. Dautel C. and Casanova F. (2000), Complexation of Th(IV) by humic substances, , *in* "Effect of humic substances on the migration of radionuclides: complexation and transport of actinides" Third progress report.

Takahashi Y., Minai Y., Kimura T., Meguro Y. and Tominaga T. (1995), Formation of actinides(III)-humate and its influence on adsorption on kaolinite, *Mat. Res. Soc. Symp. Proc.*, **353**, 189-196.

Takahashi Y, Minai Y., Ambe S., Makide Y. and Ambe F. (1999), Comparison of adsorption behavior of multiple inorganic ions on kaolinite and silica in the presence of humic acid using the multitracer technique - A comparison with dissolved aluminum, *Geochim. Cosmochim. Acta*, **63**, 815-836.

Tanaka T. and Senoo M (1995), Sorption of ^{60}Co, ^{85}Sr, ^{237}Np and ^{241}Am on soil under coexistence of humic acid , effects of molecular size if humic acid, *Mat. Res. Soc. Symp. Proc.*, **353**, 1013-1019.

Young L. B. and Harvey H.H. (1992), The relative importance of manganese and iron oxides and organic matter in the sorption of trace metals by surficial lake sediments, *Geochim. Cosmochim. Acta*, **56**, 1175-1186.

Van der Steeg, H.G.M., Cohen Stuart M.A., De Keizer A. and Bijsterbosch B.H. (1992), Polyelectrolyte adsorption: a subtle balance of forces, *Langmuir*, **8**, 2538-2546.

Vermeer R. (1996), Interactions between humic acid and hematite and their effects on metal speciation, pH.D Thesis, Landbouwuniversiteit Wageningen, The Netherlands.

Zachara J.M., Resch C.T. and Smith S.C. (1994), Influence of humic substances on Co^{2+} sorption by a subsurface mineral separate and its mineralogic components, *Geochim. Cosmochim. Acta*, **58**, 553-566 .

Zeh P., Kim J.I. and Buckau G. (1995), Aquatic colloids composed of humic substances, Binding models concerning natural organics in performance assessment, Proceedings, OECD NEA, pg. 81.

Annex 9

Kinetic Studies of the Uranium(VI) and Humic Acid Sorption onto Phyllite, Ferrihydrite and Muscovite

(K. Schmeide, V. Brendler, S. Pompe,
M. Bubner, K.H. Heise and G. Bernhard (FZR/IfR))

Third Technical Progress Report

EC Project:

"Effects of Humic Substances on the Migration of Radionuclides: Complexation and Transport of Actinides"

Project No.: FI4W-CT96-0027

FZR/IFR Contribution to Task 3 (Actinide Transport)

Kinetic Studies of the Uranium(VI) and Humic Acid Sorption onto Phyllite, Ferrihydrite and Muscovite

Reporting period 1999

K. Schmeide, V. Brendler, S. Pompe, M. Bubner, K.H. Heise, G. Bernhard

Forschungszentrum Rossendorf e.V.
Institute of Radiochemistry
P.O. Box 510119
01314 Dresden
Germany

Abstract

We studied the kinetics of uranium(VI) and humic acid adsorption by the rock material phyllite and by the minerals ferrihydrite and muscovite at pH 6.5 under aerobic conditions. The sequence in which uranium and humic acid were added to the solid containing solutions was varied in order to obtain more detailed information on the sorption mechanisms. The results showed that sorption of uranium and humic acid onto phyllite and ferrihydrite is rapid, that onto muscovite is slower. The initial uranium sorption rates were found to depend on the sequence of addition of uranium and humic acid. For ferrihydrite the initial uranium sorption rate decreased with increasing amounts of uranyl humate complexes in solution. In contrast, addition of humic acid to muscovite resulted in a faster uranium sorption, since the amount of easily accessible surface sites for uranyl ions is enhanced largely by sorbed humic acid. Phyllite showed an overlapping of different processes which is attributed to the complex nature of the phyllite rock. The total uranium uptake decreased in the following order: ferrihydrite ≥ phyllite > muscovite. The results have shown that the amount of uranium sorbed on minerals in equilibrium is determined by the total number of surface sites as well as their affinity and accessibility to solutes. For ferrihydrite indications to mineral dissolution in the presence of humic acid were found. The results of the kinetic experiments confirm that the sorption behavior of phyllite to uranium and humic acid is dominated by minor amounts of ferrihydrite, that is formed as secondary mineral phase due to weathering of phyllite. The contribution of minerals, naturally present in the rock material phyllite, to the total sorption behavior of phyllite could also be shown.

Furthermore, we compared the sorption behavior of two different humic acids, a natural humic acid Kranichsee HA and a ^{14}C-labeled synthetic humic acid type M1, onto phyllite in the pH range 3.5 to 9.5 by batch experiments. Their influence on uranium(VI) sorption onto phyllite was also studied and compared to uranium sorption in the absence of humic acid. Results revealed that sorption of humic acids and their effect on uranium sorption is influenced by the total content of humic acid functional groups and its fractions that are actually involved in sorption reactions or are available for binding of uranyl ions, together with the molecular size and the amount of aromatic structural elements of humic acids. The results also confirmed that the synthetic humic acid ^{14}C-M1 is suitable for experiments studying the kinetics and reversibility of uranium and humic acid sorption onto minerals in the pH range 3.5 to 7.5 since its sorption behavior and its influence on uranium sorption is comparable to that of natural humic acids.

1 Introduction

We are investigating the sorption and leaching behavior of phyllite because this rock material is closely associated with uranium deposits in the former uranium mining areas in East Germany. Phyllite is one of the main components of the resulting waste rock piles. Consequently, its sorption and leaching behavior contributes largely to the overall sorption and leaching behavior of the waste rock resulting either in retention or release of radioactive contaminants present in the rock piles.

Previous batch experiments investigating the uranium sorption onto the rock material phyllite and onto its main mineralogical constituents in the absence (Arnold et al., 1998) and presence (Schmeide et al., 2000) of humic material have shown that the sorption behavior of phyllite is dominated by small amounts of ferrihydrite. This ferrihydrite is formed as secondary mineral phase due to weathering of phyllite. It is known to form coatings on the surface of other minerals or rock materials and it has a high sorption potential for inorganic and organic contaminants.

In this paper, experimental results are shown with regard to the kinetics of uranium(VI) and humic acid adsorption by phyllite, ferrihydrite and muscovite at pH 6.5. For the kinetic experiments various experimental modes were applied to obtain indications to the sorption mechanisms. That means, uranium and humic acid were added in different sequences to the solid containing solutions. As humic acid, we applied a ^{14}C-labeled synthetic humic acid (^{14}C-M1). Its concentration in solution can be easily determined by ^{14}C liquid scintillation counting (LSC). Furthermore, it is possible to determine directly the uptake of the ^{14}C-labeled humic acid onto rock materials by LSC measurements after combustion of the samples. UV/Vis spectrophotometry that is usually used for determination of humic acid concentration in solution is less suitable for kinetic experiments because the samples that can be taken in the course of the experiments are relatively small (2 mL).

Since previous batch sorption experiments in the presence of humic acid (Schmeide et al., 2000) were performed with a site-specific natural humic acid (Kranichsee HA), a further series of steady-state sorption experiments was carried out with the synthetic humic acid ^{14}C-M1 in the pH range 3.5 to 9.5 to compare the sorption of the two humic acids onto phyllite and to identify structural elements and functional properties of humic acids that affect their sorption. The results are also shown in this paper.

2 Experimental

2.1 Substances and concentrations

The concentrations of solids and solutes applied to steady-state and kinetic experiments are compiled in Tab. 1. The total volume was 40 mL for steady-state and 400 mL for kinetic experiments. The ionic strength was 0.1 M ($NaClO_4$).

Table 1: Concentrations of solids and solutes applied to steady-state and kinetic experiments.

Solids	Concentration	Surface site density [sites/nm^2]	Specific surface area [m^2/g]	Content in 400 mL solution [g/400 mL]
Ferrihydrite	26.7 mg/L (=3·10^{-4} M Fe [a])	0.054 strong sites 2.258 weak sites	600 [b]	0.0107
Phyllite	12.5 g/L 31.8 mg/L [c]	3.35 [d]	4.0 [e]	5 0.0127
Muscovite	12.5 g/L	2.61 [e]	1.4 [e]	5
Solutes	**Concentration**	**Functional group content [meq/g]**		**Content in 400 mL solution [µeq/400 mL]**
^{14}C-M1	5 mg/L	COOH: 1.34 ± 0.05 Phenolic OH: 2.4 ± 0.1		2.68 4.8
Kranichsee HA	5 mg/L	COOH: 3.88 ± 0.41 Phenolic OH: 3.87 ± 0.52		7.76 7.74
Uranium(VI)	1·10^{-6} mol/L			0.8

[a] Assuming the formula $Fe_2O_3 \cdot H_2O$ following Dzombak and Morel (1990).
[b] Dzombak and Morel (1990)
[c] Ferrihydrite formed in phyllite.
[d] Calculated from surface site densities of mineral components of phyllite (quartz, chlorite, muscovite, and albite).
[e] Arnold et al. (2000)

A detailed characterization of phyllite and muscovite is given elsewhere (Arnold et al., 1998). Ferrihydrite was precipitated from 1·10^{-3} M iron(III) nitrate solution by slowly raising the pH to 7 (Cornell and Schwertmann, 1996). This suspension was aged for 60 min before the pH was lowered to 5 and the ionic strength was adjusted to 0.1 M $NaClO_4$. Then, the aging of the ferrihydrite proceeded by continuously stirring at room temperature for further 9 days.

The natural humic acid (Kranichsee HA) was isolated from surface water of the mountain bog 'Kleiner Kranichsee' that is located in the vicinity of uranium mining sites at Johanngeorgenstadt (Saxony, Germany) (Schmeide et al., 1998). The ^{14}C-labeled synthetic humic acid (^{14}C-M1) was synthesized from xylose, phenylalanine, and [2-^{14}C]glycine (Bubner et al., 1998) and had a specific activity of 59 MBq/g.

2.2 Steady-state sorption experiments

The steady-state sorption experiments for the comparison of the sorption of the two humic acids (Kranichsee HA and ^{14}C-M1) onto phyllite and their influence on the uranium sorption in the pH range 3.5 to 9.5 were carried out as described in Schmeide et al. (2000). Briefly, phyllite was suspended in 0.1 M $NaClO_4$ solution. After adjusting the desired pH, a humic acid stock solution was added to achieve a concentration of 5 mg/L. The experiment was started by adding a uranyl perchlorate stock solution to obtain a uranium concentration of $1 \cdot 10^{-6}$ M. The samples were rotated end-over-end at room temperature for about 60 h. Then, the solutions were centrifuged (10000 rpm, 20 min), filtered (450 nm, Minisart N, Sartorius) and analyzed for the final uranium and humic acid concentrations. Uranium was determined by ICP-MS (Mod. ELAN 5000, Perkin Elmer). The concentration of Kranichsee HA was determined by UV/Vis spectrophotometry (Mod. 8452A, Hewlett Packard) at 254 nm. The concentration of ^{14}C-M1 in solution and the amount of this humic acid sorbed onto phyllite was determined by LSC (Series LS 6000 LL, Beckman Instruments) after combustion of the samples with a sample oxidizer (Mod. P 307, Canberra-Packard). For comparison, the ^{14}C-M1 concentration in solution was additionally determined by UV/Vis spectrophotometry. The results of both methods agree well (relative standard deviation: 5 % (2σ)). The uranium and humic acid sorption onto phyllite was corrected for the corresponding sorption onto the vial walls.

2.3 Kinetic sorption experiments

The ^{14}C-labeled synthetic humic acid ^{14}C-M1 was used. For each kinetic experiment, 400 mL of the solid containing solutions were prepared. The pH of the suspensions was adjusted to pH 6.50 ± 0.03 using dilute $HClO_4$ or NaOH. The pH was considered to be stable when the pH of the continuously stirred suspensions had changed less than 0.05 pH units after additional 24 h. Then, appropriate amounts of stock solutions were added to achieve initial total uranium and humic acid concentrations of $1 \cdot 10^{-6}$ M and 5 mg/L, respectively. The pH of the humic acid stock solution and of the preconditioned uranyl humate stock solution was also adjusted to pH 6.5 prior to their addition to the solid containing solutions.

We applied five experimental modes for the addition of the reactants:

1. addition of uranium to the solid containing solution, without humic acid,
2. addition of humic acid to the solid containing solution, without uranium,
3. the solid containing solution was preconditioned with humic acid, then addition of uranium,
4. uranium and humic acid were added simultaneously to the solid containing solution,
5. uranium and humic acid were preconditioned for 48 h, then addition to the solid containing solution.

The humic acid and uranyl sorption onto the solids was determined by monitoring the corresponding concentrations in solution over time. Samples were taken after different time intervals between about 20 sec and 55 h (phyllite, ferrihydrite) or between 20 sec and 300 h (muscovite) after addition of all components. The pH of the suspensions was checked several times. While stirring, at each sampling time a 2-mL aliquot of the suspension was taken from each bottle and filtered using Minisart N membranes (Sartorius) with a pore size of 450 nm. The concentrations of ^{14}C-M1 and uranium in solution were determined by LSC after combustion of the samples with a sample oxidizer and by ICP-MS, respectively. In contrast to the steady-state sorption experiments, the uranium and humic acid sorption onto the bottle walls (PP, Nalgene) could not be determined during the kinetic experiments.

3 Results and discussion

3.1 Steady-state sorption experiments on phyllite

The natural humic acid Kranichsee HA and the synthetic humic acid ^{14}C-M1 were compared with regard to their sorption behavior on phyllite and their influence on the uranium sorption onto phyllite in the pH range 3.5 to 9.5.

3.1.1 Humic acid sorption

In Fig. 1a the humic acid uptake by phyllite is shown for Kranichsee HA and for ^{14}C-M1 as a function of pH. Both humic acids are strongly taken up over the entire pH range studied. From pH 3.5 to 7.7 between 86 and 94 % of the Kranichsee HA are adsorbed. Above pH 8, the humic acid sorption decreases to 78 % at pH 9.4. The sorption of ^{14}C-M1 between pH 3.5 to pH 7.7 is somewhat lower (4 to 6 %) and above pH 8 higher (2 to 5 %) than that of Kranichsee HA.

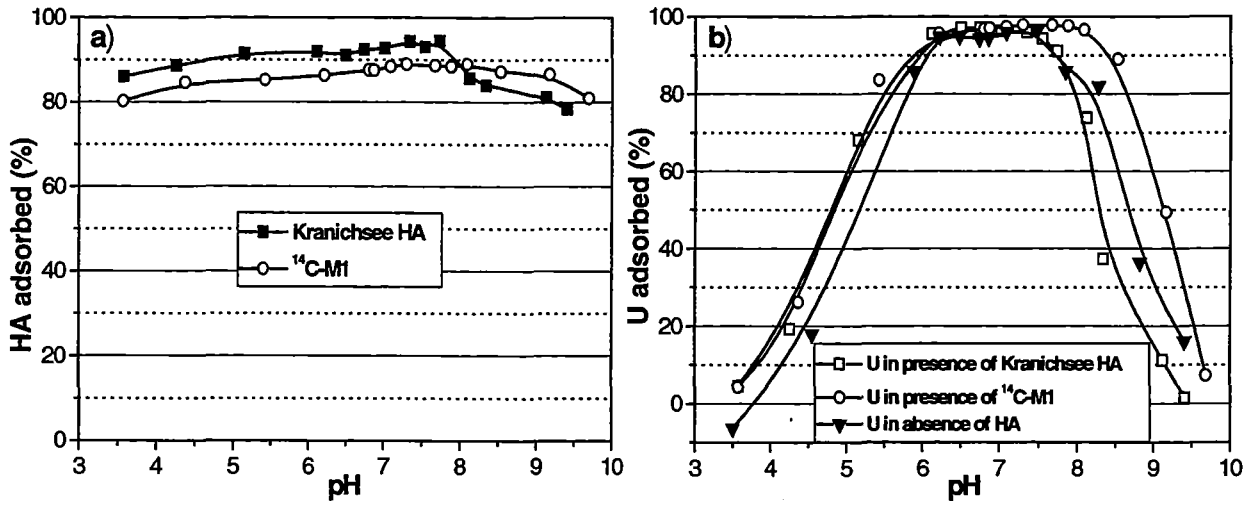

Figure 1: Humic acid (a) and uranium (b) uptake by phyllite in experiments conducted with $1 \cdot 10^{-6}$ M uranium and 5 mg HA/L.
(Kranichsee HA: determined by UV/Vis spectrophotometry; ^{14}C-M1: determined by LSC)
Data for uranium uptake in the absence of humic acid (Arnold et al., 1998) are also shown.

The adsorption of humic acids onto minerals is primarily determined by their functional group content. Thus, it is generally accepted that mainly carboxylic groups and also hydroxyl groups (ortho-positioned with respect to carboxylic groups) bind to oxide surface sites via surface complexation and ligand exchange (Tipping, 1981; Davis, 1982; Gu et al., 1994, 1995).

For Kranichsee HA the content of carboxylic and phenolic OH groups was determined with 3.88 ± 0.41 meq/g and 3.87 ± 0.52 meq/g, respectively (Schmeide et al., 1998). The content of carboxylic and phenolic OH groups determined for ^{14}C-M1 (Pompe et al., 1999) is with 1.34 ± 0.05 meq/g and 2.4 ± 0.1 meq/g lower. This should result in a considerably lower sorption of ^{14}C-M1. However, the differences in the sorption of the two humic acids are relatively small compared to the differences in the functional group contents.

Furthermore, from the literature follows that the sorption affinity and capacity of humic substances and other organic polymers on mineral surfaces increase with their molecular size, their content of aromatic moieties, and amino acid groups (Davis, 1982; Ramachandran and Somasundaran, 1987; McKnight et al., 1992; Murphy et al., 1992; Gu et al., 1994). Capillary electrophoresis, IR and NMR spectroscopy applied to Kranichsee HA and ^{14}C-M1 show that ^{14}C-M1 has both a larger molecular size and a higher amount of aromatic structural elements than Kranichsee HA (Schmeide et al., 1999; Pompe et al., 1999). ^{14}C-M1 could also contain amino acid groups since phenylalanine and glycine were used as precursors. This explains the high adsorption of ^{14}C-M1 despite its low functional group content.

3.1.2 Uranium sorption

Fig. 1b shows the uranium sorption onto phyllite in the absence and presence of humic acid. The concurrent presence of humic acid and uranium in solution means competition between humic acid and uranyl ions for available surface sites. Therefore, a reduced direct sorption of uranium onto phyllite surface groups should be expected. But compared to the uranium sorption onto phyllite in the absence of humic material, the uranium sorption is increased by both humic acids in the pH range from 3.5 to 6. Obviously, the number of mineral binding sites blocked by humic acids is overcompensated by additional binding sites for uranyl ions stemming from the humic acid itself. Thus, the net effect is a promotion of uranyl binding on phyllite through the presence of humic acid.

This effect is observed for both types of humic acids, despite their above discussed differences in structure and sorption affinity to phyllite. A possible explanation is, that ^{14}C-M1 has comparatively less carboxylic groups involved in adsorption reactions, since functional groups on the larger molecules should be more sterically hindered for reaction with surface sites than those of the smaller Kranichsee HA molecules. Therefore, comparatively more unreacted functional groups of ^{14}C-M1 are available for binding of uranium.

Above pH 7.5, both humic acids have a relatively strong but contrary influence on the uranium sorption onto phyllite (Fig. 1b). The apparent enhancement of the uranium sorption in the presence of ^{14}C-M1 together with the high sorption of ^{14}C-M1 above pH 7.5 is caused most likely by a low solubility of uranyl humate complexes formed by ^{14}C-M1 due to a low content of free carboxylic groups. In contrast, Kranichsee HA decreases uranium sorption onto phyllite due to formation of better soluble uranyl humate complexes.

3.2 Kinetic sorption experiments

Results of kinetic experiments investigating the uranium and humic acid (^{14}C-M1) sorption onto ferrihydrite, phyllite and muscovite at pH 6.5 are shown in Figs. 2 to 5. The pH value 6.5 corresponds to the maximum of uranium and humic acid sorption onto phyllite and ferrihydrite. The sorption over time as well as the sorption capacity after reaching equilibrium is studied in dependence on the sequence in which components are added.

3.2.1 Ferrihydrite

To ease the interpretation of the kinetic data some calculations with the Generalized Two-Layer Model for surface complexation (Dzombak and Morel, 1990) were performed using the geochemical speciation software MINTEQA2 (Allison et al., 1991). Therefore, uranyl sorption data from Dicke and Smith (1996) were applied. Data for uranium speciation in solution were taken from the NEA data base (Grenthe et al., 1992).

As shown in Tab. 2, approximately 93 % of total uranium are bound onto ferrihydrite which is consistent with our experimental findings. On the other hand, about 65 % of the strong and nearly all weak binding sites are still available for other solutes, such as humic acid.

Table 2: Distribution of uranium species in a ferrihydrite suspension and distribution of strong (s) and weak (w) surface sites of ferrihydrite under experimental conditions applied in this study.

UO_2^{2+} species distribution (%)		Distribution of strong surface sites (%) (total : $5.8 \cdot 10^{-7}$ mol/400 mL)		Distribution of weak surface sites (%) (total : $2.4 \cdot 10^{-5}$ mol/400 mL)	
$UO_2(OH)_{2\,(aq)}$	6.5	$=(Fe_SO)UO_2OH$	35.0	$=(Fe_WO)UO_2OH$	0.7
$=(Fe_SO)UO_2OH$	50.5	$=(Fe_SOH)$	45.9	$=(Fe_WOH)$	70.1
$=(Fe_WO)UO_2OH$	42.4	$=(Fe_SOH_2)^+$	16.1	$=(Fe_WOH_2)^+$	24.6
		$=(Fe_SO)^-$	3.0	$=(Fe_WO)^-$	4.6

In Fig. 2 the kinetics of uranium and humic acid sorption onto ferrihydrite is shown. It is obvious that sorption in all cases is rapid since uranium and humic acid concentrations in solution decreased significantly within 10 min. This can be attributed to the high specific surface area of ferrihydrite, which is 600 m^2/g (Dzombak and Morel, 1990), combined with a strong sorption affinity.

In general, the amounts of uranium sorbed in equilibrium do not show any difference (Fig. 2) as already discussed in detail for the steady-state experiments. The differences in the uranium sorption kinetics in dependence on the sequence in which components were added will be discussed below.

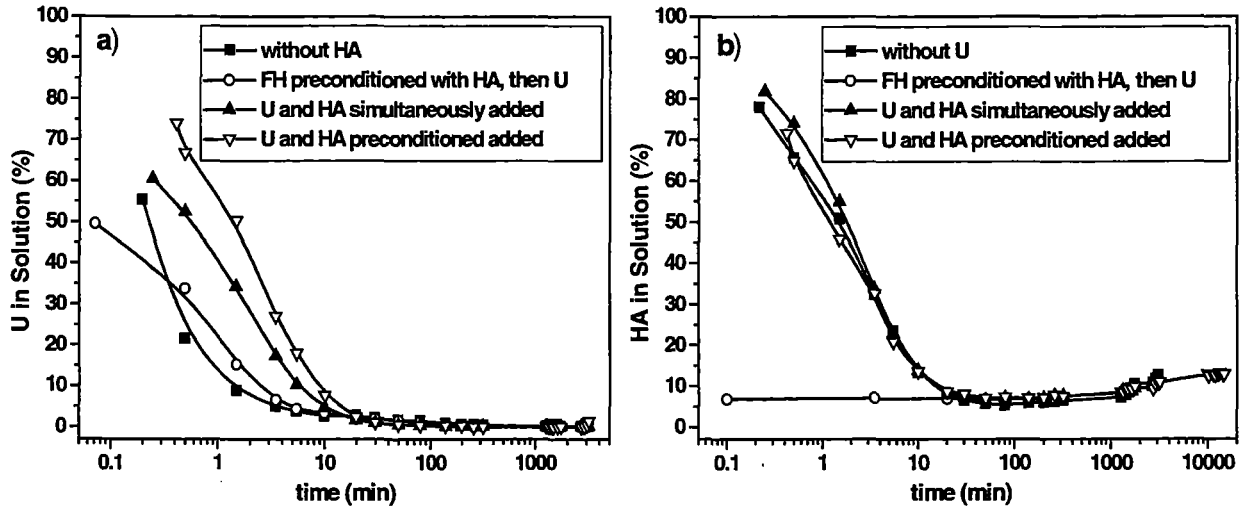

Figure 2: Kinetics of uranium (a) and humic acid (b) sorption onto ferrihydrite (FH) in dependence on the order in which components were added.

Ferrihydrite is a poorly ordered mineral, that has both external and internal surface sites. Particle diameters reported for the 2-line ferrihydrite (Zhao et al., 1993) and for the 6-line ferrihydrite (Russell, 1979) are 2-3 nm and 4-6 nm, respectively. For the sorption of small uranyl ions, with an estimated size of 5 Å, a great variety of surface sites is accessible, both external and internal. In contrast, humic acid molecules with typical molecule diameters between 10 to 100 Å (Zänker et al., 1999) will sorb preferentially onto the outermost surface sites of ferrihydrite that are accessible for them.

For the different experimental modes the following results were obtained:

- In the absence of humic acid, uranium has the highest sorption rate.
- When ferrihydrite is first coated (preconditioned) with humic acid, strong sorption sites of ferrihydrite are partly blocked by sorbed humic acid. This will mostly concern external surface sites. Thus, uranyl ions either have to diffuse to internal sorption sites of the porous ferrihydrite particles or must replace humic acid molecules or must bind to available functional groups of sorbed humic acid. All these processes lead to the observed slightly slower uranium sorption.
- When uranium and humic acid are added simultaneously to the ferrihydrite containing solution, the uranium sorption is further retarded. In a quick first step, humic acid binds considerably amounts of uranium. The actual sorption of these uranyl humate complexes onto ferrihydrite is a second slower step. It may be accompanied by partly redistribution of uranyl ions onto ferrihydrite binding sites.

- When aliquots of preformed uranyl humate complexes are added to start the experiment, the uranium sorption takes place at the 'lowest' rate compared with the other experimental modes. The responsible processes will be the same as discussed for the preceding experimental mode, but even more pronounced because after 48 h preconditioning the complex formation process is more advanced. Furthermore, uranyl ions may have reached thermodynamically more stable binding sites inside the humic acid molecules which again will retard any reverse redistribution process.

The results show, that with increasing amounts of dissolved uranyl humate complexes the uranium sorption rate approaches the humic acid sorption rate. Then, the uranium sorption rate onto ferrihydrite is determined by the humic acid sorption rate.

Whereas humic acid significantly influences uranium sorption rates, the opposite effect is not detectable. This can be attributed to the excess of humic acid functional groups (COOH: 2.68 µeq/400 mL, phenolic OH: 4.8 µeq/400 mL) compared to uranium (0.8 µeq/400 mL).

3.2.2 Phyllite

The uranium and humic acid sorption onto phyllite is shown in Fig. 3. After a rapid uranium sorption in the first seconds, the uranium concentration continued to decrease for about 300 min when finally the steady state is reached.

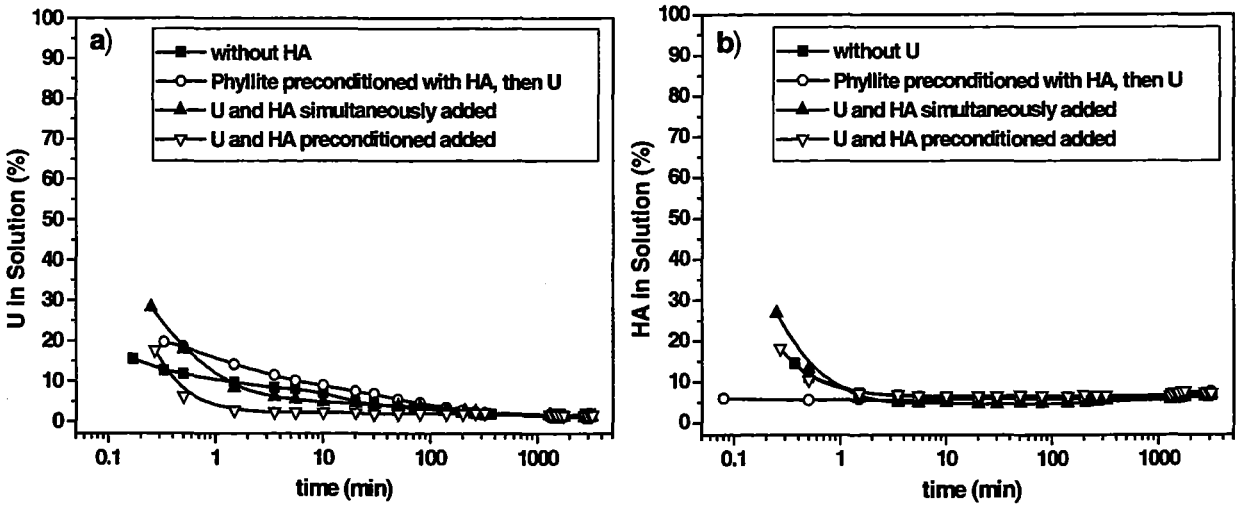

Figure 3: Kinetics of uranium (a) and humic acid (b) sorption onto phyllite in dependence on the order in which components were added.

Before discussing kinetic aspects the focus will be on the sorption capacity. For phyllite, it is somewhat lower than for ferrihydrite under these experimental conditions. This is shown in Fig. 4a for experiments, where uranium and humic acid were added as a stock solution that was pre-conditioned for 48 h. The uranium and humic acid sorption related to one gram of the solids is depicted. The sorption coefficient R_S was calculated by

$$R_S = \frac{c_0 - c}{c} \frac{V}{m} \quad (mL/g)$$

where c_0 is the initial uranium and humic acid concentration in mol/L and Bq/mL, respectively; c is the uranium or humic acid concentration after a given reaction period, V the solution volume (mL) and m the mass of solids (g).

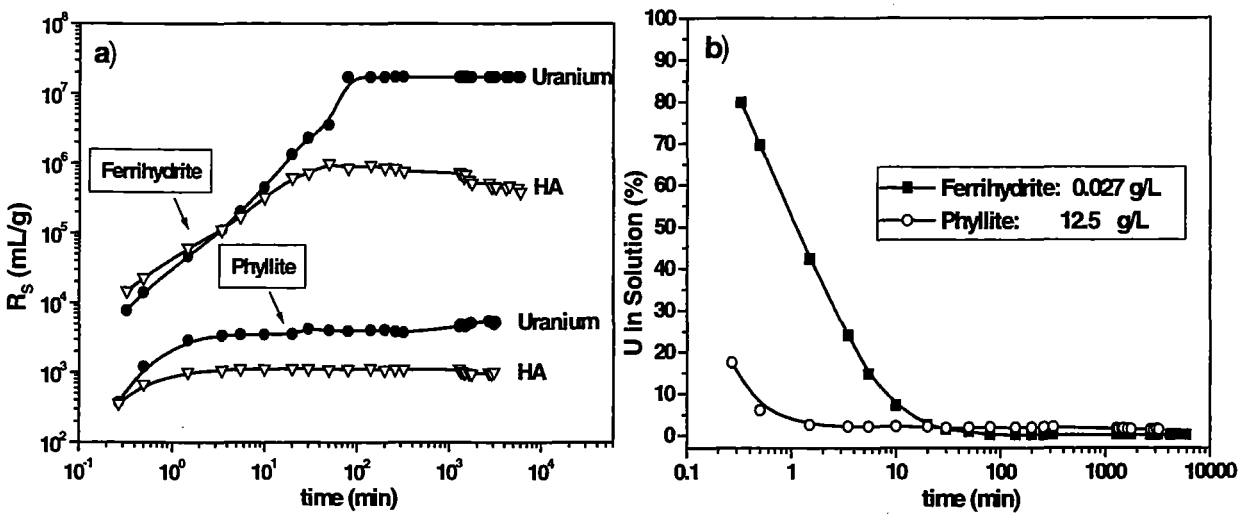

Figure 4: Comparison of the sorption capacity (a) and kinetics (b) of uranium sorption onto ferrihydrite (0.027 g/L) and phyllite (12.5 g/L); Uranium and humic acid were added as preconditioned solution (48 h).

One possible explanation is the heterogeneity of surface sites of phyllite, contrary to ferrihydrite:

- Phyllite has about 3.4 sites/nm^2 due to its major mineralogical constituents (quartz, chlorite, muscovite, and albite). These are primarily Si- and Al-, and also Fe-, and Mg-surface sites. Altogether these sites have a lower sorption affinity than the Fe-surface sites of ferrihydrite.
- In addition, ferrihydrite is formed due to weathering of phyllite thereby strongly increasing the number of highly reactive surface sites in the system. Based on Mössbauer spectroscopic measurements by Arnold et al. (2000) it is calculated that 12.7 mg ferrihydrite are formed from 5 g phyllite powder in 400 mL solution. This amount of ferrihydrite is 1.2 times the ferrihydrite concentration which was applied in our kinetic studies with pure ferrihydrite (10.7

mg/400 mL). However, ferrihydrite particles formed from phyllite are most likely larger than those of the pure mineral used in the kinetic studies. Thus, in a suspension of ground phyllite, iron hydroxide particles with diameters between 6 to 25 nm were detected by Zänker et al. (2000). Evidence was also found that iron hydroxide particles below 6 nm exist. Such nanoparticles of ferrihydrite agglomerate and tend to form larger units of ferrihydrite particles. This would mean, that the ferrihydrite formed from phyllite is less reactive since it has comparatively more internal sorption sites that are less accessible for solutes.

In combination, these effects lead to the observed lower specific sorption capacity of phyllite.

Looking at the initial uranium sorption rates, those for phyllite are higher compared to ferrihydrite for all experimental modes. As shown for a selected experimental mode in Fig. 4b, the differences in the sorption kinetics during the first 20 min also indicate a contribution of more weakly sorbing surface sites belonging to quartz, chlorite, muscovite, and albite. Such sites may indeed be accessible. Although ferrihydrite as a weathering product will mainly occur on the outside of the phyllite grains it cannot be expected to completely cover the phyllite grain surfaces.

In contrast to ferrihydrite, the dependence of the uranium sorption rate on the sequence of addition of reactants for phyllite (Fig. 3a) does not exhibit a clear pattern. Effects are weak and ambiguous. This can be attributed to the complex nature of the phyllite rock.

The very fast humic acid sorption onto phyllite is apparently independent of uranium addition.

3.2.3 Muscovite

Fig. 5 shows results of comparable experiments with muscovite, one of the main mineral constituents of phyllite.

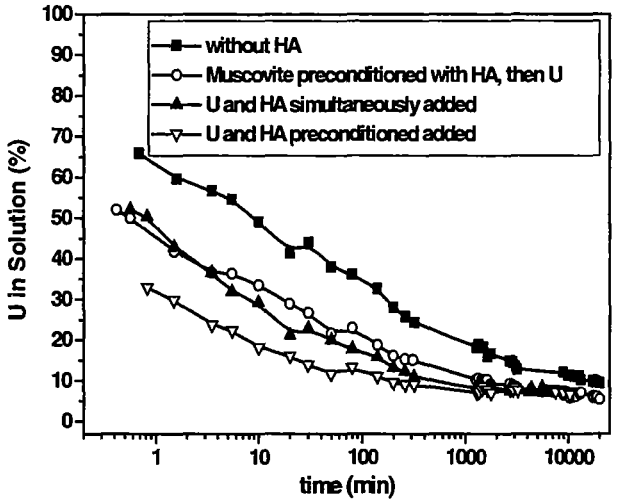

Figure 5: Kinetics of uranium sorption onto muscovite depending on the order in which components were added.

The total uranium uptake by muscovite is lower compared to phyllite although an absolute equilibrium was apparently not reached even after 13 days. This relatively low uranium sorption onto muscovite results from its lower specific surface area (1.4 m^2/g), together with a lower sorption affinity of its surface sites (mainly Si- and Al-, and also Mg- and Fe-sites). The uranium sorption onto muscovite at pH 6.5 is enhanced by humic acid which corresponds to results of previous steady-state sorption experiments (Schmeide et al., 2000).

With regard to the uranium sorption rate the following results were obtained:

- The uranium sorption rates of muscovite observed for all experimental modes are lower than those of phyllite (see Fig. 3a). Here, it must be considered, that micas, such as muscovite, have multiple sorption sites including planar, edge, and interlayer sites, with some of the latter sites being partially to totally collapsed (Sumner, 2000) resulting in slow sorption reactions. Thus, sorption onto mica can involve two to three different reaction rates: high rates on external sites, intermediate rates on edge sites, and low rates on interlayer sites (Comans and Hockley, 1992).
- The uranium sorption in the presence of humic acid is faster than in the absence of humic acid. The reason could be that the amount of surface sites is enhanced largely by humic acid. The uranium will prefer these easily accessible surface sites (mostly unreacted carboxylic groups), and thus, it is not forced to diffuse to interlayer sites. That means, slow sorption reactions are replaced by faster sorption reactions leading to higher total uranium sorption rates.

3.2.4 Indications for dissolution of ferrihydrite

Fig. 2b and also Fig. 4a show that a part of the humic acid sorbed onto ferrihydrite apparently desorbs after a certain time (about 200 min after starting the experiments) since the humic acid concentration in solution increases again after the adsorption phase. However, a desorption of sorbed humic acid without previous changes of experimental conditions, such as pH or ionic strength, is very unlikely. This would require detachment of all functional groups of the humic acid molecules in question approximately at the same time. But desorption of humic material from iron oxide surfaces was found to be very slow by Gu et al. (1994). Instead, we assume that the increasing humic acid concentration in solution is caused by formation of soluble complexes between humic acid and the iron of ferrihydrite leading to dissolution of a small amount of ferrihydrite.

This interpretation is supported by results of a dissolution experiment (data not shown). After sorption of humic acid onto ferrihydrite, its concentration in solution again increased from 5 % to 11.9 % within 28 days. The extent of iron dissolution could not be determined by conventional flame AAS technique due to very low iron concentrations.

Our assumption is also supported by results of Liu and Millero (1999) who found that organic matter increases the solubility of iron in NaCl medium over a wide range of pH (pH 4 to 12). The impact of humic acid on iron solubility was found to be biggest in the neutral pH range where the $Fe(OH)_3$ species predominates. This solubility enhancement was explained by solution complexation and/or stabilization of colloidal form of iron by organic ligands. Furthermore, Cornell and Schwertmann (1996) reported that the dissolution rate of iron oxides can be substantially increased by complexes of both organic and inorganic ligands with the surface functional groups. For the dissolution of an M^{III} oxide by an organic ligand three consecutive reactions are proposed by Stumm and Furrer (1987), namely, ligand adsorption, metal detachment and proton adsorption/surface restoration. Kuma et al. (1996) reported that the iron(III) solubility in surface coastal waters (1-10 nM at pH 8) is much higher than in open-ocean waters (0.6 nM at pH 8) which was attributed to higher concentrations of organic ligands in the coastal waters.

Also for phyllite, a slight dissolution enhancement due to humic acid was observed in steady-state sorption experiments. However, the amount of humic acid released from phyllite after previous sorption observed in these kinetic experiments is small compared to ferrihydrite. Since the amounts of ferrihydrite were comparable in the kinetic sorption experiments with phyllite and

ferrihydrite, the lower desorption of humic acid from phyllite again point to the fact that surface sites of phyllite's mineralogical constituents (quartz, chlorite, muscovite, and albite) also contribute to sorption of uranium and humic acid. But these sites (e.g., =SiOH, =AlOH) are less susceptible to dissolution by humic acid.

4 Conclusions

The results of the steady-state sorption experiments on phyllite have shown that sorption of humic acids and their effect on uranium sorption is influenced by several factors, such as the total content of humic acid functional groups and its fractions that are actually involved in sorption reactions or are available for binding of uranyl ions, together with the molecular size and the amount of aromatic structural elements of humic acids.
It could be shown that the ^{14}C-labeled synthetic humic acid (^{14}C-M1) is suitable for experiments studying the kinetics and reversibility of uranium and humic acid sorption onto minerals in the pH range 3.5 to 7.5 since its sorption behavior is comparable to that of natural humic acids.

The results of the kinetic experiments studying the uranium and humic acid sorption on ferrihydrite, phyllite and muscovite at pH 6.5 can be summarized as follows:
The total uranium uptake onto solids decreases in the following order: ferrihydrite ≥ phyllite > muscovite. Whereas, the uranium uptake onto ferrihydrite and phyllite is not changed by humic acid, the uranium uptake onto muscovite is enhanced.
These results have shown that the amount of uranium sorbed on minerals in equilibrium is determined both by the total number of surface sites and by their affinity and accessibility to solutes which are differently charged and have various molecule sizes, such as uranium and humic acid. The number of mineral surface sites accessible for uranium is decreased by sorbed humic acid. But simultaneously, free humic acid functional groups that are not involved in sorption reactions can bind additional uranyl ions. Which effect dominates, is determined by the mineral.
Sorption of uranium and humic acid onto phyllite and ferrihydrite is rapid, that onto muscovite is slower. This again points to a different affinity and accessibility of surface sites.
The dependence of the initial uranium sorption rates on the order of addition of uranium and humic acid to the solid containing solutions was found to be different for the three solids. For

ferrihydrite the initial uranium sorption rate decreased with increasing amounts of uranyl humate complexes in solution. In contrast, addition of humic acid and especially addition of uranyl humate complexes to muscovite resulted in a faster uranium sorption. In the latter case, the amount of easily accessible surface sites for uranyl ions is enhanced largely by sorbed humic acid. The rock material phyllite showed an overlapping of different processes which is attributed to its complex nature.

It was confirmed that the sorption capacity of phyllite for uranium and humic acid is dominated by minor amounts of ferrihydrite, that is formed as secondary mineral phase due to weathering of phyllite. The contribution of minerals, naturally present in phyllite (quartz, chlorite, muscovite, albite), to the total sorption behavior of phyllite could also be shown.

Acknowledgements

The authors would like to thank R. Jander and S. Wallner for their help in performing the batch experiments and W. Wiesener and A. Schäfer for ICP-MS and AAS analyses.

References

Allison, J.D., Brown, D.S., and Novo-Gradac, K.J. (1991) MINTEQA2/PRODEFA2, a Geochemical Assessment Model for Environmental Systems: Version 3.0 User's Manual. U.S. Environmental Protection Agency, Environmental Research Laboratory, EPA/600/3-91/021.

Arnold, T., Zorn, T., Bernhard, G., and Nitsche, H. (1998) Sorption of Uranium(VI) onto Phyllite. *Chemical Geology* **151**, 129.

Arnold, T., Zorn, T., Zänker, H., Bernhard, G., and Nitsche, H. (2000) Sorption Behavior of U(VI) on Phyllite: Experiments and Modeling. Submitted to J. of Contaminant Hydrology.

Bubner, M., Pompe, S., Meyer, M., Heise, K.H., and Nitsche, H. (1998) Isotopically Labelled Humic Acids for Heavy Metal Complexation. *J. Labelled Compounds and Radiopharmaceuticals* **XLI**, 1017.

Comans, R.N.J. and Hockley, D.E. (1992) Kinetics of Cesium Sorption on Illite. *Geochim. Cosmochim. Acta* **56**, 1157.

Cornell, R.M. and Schwertmann, U. (1996) *The Iron Oxides*. VCH, Weinheim.

Davis, J.A. (1982) Adsorption of Natural Dissolved Organic Matter at the Oxide/Water interface. *Geochim. Cosmochim. Acta* **46**, 2381.

Dicke, C. and Smith, R.W. (1996) Surface Complexation Modeling of Uranium Adsorption on Naturally Occurring Iron Coated Sediments. Presentation given at the American Chemical Society Annual Meeting in New Orleans on March 28, 1996.

Dzombak, D.A. and Morel, F.M.M. (1990) *Surface Complexation Modeling – Hydrous Ferric Oxide*. John Wiley & Sons, New York.

Grenthe, I., Fuger, J., Lemire, R.J., Muller, A.B., Nguyen-Trung, C., and Wanner, H. (1992) *Chemical Thermodynamics of Uranium*, 1st ed., Elsevier Science Publishers, Amsterdam.

Gu, B., Schmitt, J., Chen, Z., Liang, L., and McCarthy, J.F. (1994) Adsorption and Desorption of Natural Organic Matter on Iron Oxide: Mechanisms and Models. *Environ. Sci. Technol.* **28**, 38.

Gu, B., Schmitt, J., Chen, Z., Liang, L., and McCarthy, J.F. (1995) Adsorption and Desorption of Different Organic Matter Fractions on Iron Oxide. *Geochim. Cosmochim. Acta* **59**, 219.

Kuma, K., Nishioka, J., and Matsunaga, K. (1996) Controls on Iron(III) Hydroxide Solubility in Seawater: The Influence of pH and Natural Organic Chelators. *Limnol. Oceanogr.* **41**, 396.

Liu, X. and Millero, F.J. (1999) The Solubility of Iron Hydroxide in Sodium Chloride Solutions. *Geochim. Cosmochim. Acta* **63**, 3487.

McKnight, D.M., Bencala, K.E., Zellweger, G.W., Aiken, G.R., Feder, G.L., and Thorn, K.A. (1992) Sorption of Dissolved Organic Carbon by Hydrous Aluminum and Iron Oxides Occurring at the Confluence of Deer Creek with the Snake River, Summit County, Colorado. *Environ. Sci. Technol.* **26**, 1388.

Murphy, E.M., Zachara, J.M., Smith, S.C., and Phillips, J.L. (1992) The Sorption of Humic Acids to Mineral Surfaces and Their Role in Contaminant Binding. *Sci. Total Env.* **117/118**, 413.

Pompe, S., Bubner, M., Schmeide, K., Heise, K.H., Bernhard, G., and Nitsche, H. (1999) Influence of Humic Acids on the Migration Behavior of Radioactive and Non-Radioactive Substances under Conditions Close to Nature. Synthesis, Radiometric Determination of Functional Groups, Complexation. *Final Report*, BMBF Project No. 02 E 8815 0.

Ramachandran, R. and Somasundaran, P. (1987) Competitive Adsorption of Polyelectrolytes: A Size Exclusion Chromatographic Study. *J. Coll. Interf. Sci.* **120**, 184.

Russell, J.D. (1979) Infrared Spectroscopy of Ferrihydrite: Evidence for the Presence of Structural Hydroxyl Groups. *Clay Miner.* **14**, 109.

Schmeide, K., Zänker, H., Heise, K.H., and Nitsche, H. (1998) Isolation and Characterization of Aquatic Humic Substances from the Bog 'Kleiner Kranichsee'. In: *FZKA 6124, Wissenschaftliche Berichte*, (G. Buckau, ed.). Forschungszentrum Karlsruhe, 161.

Schmeide, K., Zänker, H., Hüttig, G., Heise, K.H., and Bernhard, G. (1999) Complexation of Aquatic Humic Substances from the Bog 'Kleiner Kranichsee' with Uranium (VI). In: *FZKA 6324, Wissenschaftliche Berichte*, (G. Buckau, ed.). Forschungszentrum Karlsruhe, 177.

Schmeide, K., Pompe, S., Bubner, M., Heise, K.H., Bernhard, G., and Nitsche, H. (2000) Uranium(VI) Sorption onto Phyllite and Selected Minerals in the Presence of Humic Acid. Submitted to Radiochim. Acta.

Stumm, W. and Furrer, G. (1987) The Dissolution of Oxides and Aluminum Silicates: Examples of Surface-coordination-controlled Kinetics. In: *Aquatic Surface Chemistry*, (W. Stumm, ed.). J. Wiley and Sons, New York, 197.

Sumner, M.E. (2000) *Handbook of Soil Science*. CRC Press LLC, Boca Raton.

Tipping, E. (1981) The Adsorption of Aquatic Humic Substances by Iron Oxides. *Geochim. Cosmochim. Acta* **45**, 191.

Zänker, H., Mertig, M., Böttger, M., and Hüttig, G. (1999) The Colloidal States of Humic Acid. In: *FZKA 6324, Wissenschaftliche Berichte*, (G. Buckau, ed.). Forschungszentrum Karlsruhe, 155.

Zänker, H., Hüttig, G., Arnold, T., Zorn, T., and Nitsche, H. (2000) Detection of Iron and Aluminum Hydroxide Colloids in a Suspension of Ground Phyllite. Submitted to Aquatic Geochemistry.

Zhao, J., Huggins, F.E., Feng, Z., Lu, F., Shah, N., and Huffman, G.P. (1993) Structure of Nanophase Iron Oxide Catalyst. *J. Catalysis* **143**, 499.

Annex 10

Influence of Sulfate on the Kinetics of Uranium(VI) Sorption onto Ferrihydrite/Humic Acid Systems

(K. Schmeide, V. Brendler, S. Pompe,
M. Bubner, K.H. Heise and G. Bernhard (FZR/IfR))

Third Technical Progress Report

EC Project:

"Effects of Humic Substances on the Migration of Radionuclides: Complexation and Transport of Actinides"

Project No.: FI4W-CT96-0027

FZR/IFR Contribution to Task 3 (Actinide Transport)

Influence of Sulfate on the Kinetics of Uranium(VI) Sorption onto Ferrihydrite/Humic Acid Systems

Reporting period 1999

K. Schmeide, V. Brendler, S. Pompe, M. Bubner, K.H. Heise, G. Bernhard

Forschungszentrum Rossendorf e.V.
Institute of Radiochemistry
P.O. Box 510119
01314 Dresden
Germany

Abstract

Since seepage and flood waters of abandoned uranium mines in Saxony and Thuringia (Germany) contain relatively high amounts of sulfate, we studied the influence of sulfate on the kinetics of uranium(VI) adsorption onto ferrihydrite both in the absence and presence of humic acid at pH 6.5 under aerobic conditions. The sequence in which sulfate, uranium and humic acid were added to the ferrihydrite containing solutions was varied in order to obtain indications to sorption mechanisms. Two different sulfate concentrations were applied (0.005 and 0.02 M Na_2SO_4). The ionic strength was held constant at 0.1 M as sum of $NaClO_4$ and Na_2SO_4. The uranium(VI) concentration was $1 \cdot 10^{-6}$ M and the humic acid concentration was 5 mg/L.

In the absence of humic acid, the uranium sorption rate and the total uranium sorption in equilibrium decreased with increasing sulfate concentration due to blocking of strong ferrihydrite surface sites by sorbed sulfate. This leads to an increased availability of uranium. Variations of the order of addition of uranium and sulfate primarily affected the initial uranium sorption rate but not its sorption capacity. Direct competition of uranium and sulfate for strong ferrihydrite surface sites predominates electrostatic effects due to changes in net surface charge of ferrihydrite upon sulfate sorption.

In experiments with humic acid, the competitive effect of sulfate on humic acid sorption at pH 6.5 is small. This is attributed to a higher sorption affinity of humic acid for ferrihydrite surface sites compared to that of sulfate. The initial humic acid sorption rate was not affected by sulfate, only the total humic acid sorption was somewhat reduced by sorbed sulfate. Since the total number of potential binding sites for uranyl ions is increased by sorbed humic acid, more uranium is sorbed in the presence than in absence of humic acid. Thus, the influence of sulfate on uranium sorption is smaller when humic acid is present in solution. This effect becomes even more pronounced with increasing amounts of uranyl humate complexes in solution.

1 Introduction

The influence of humic substances on the sorption of actinides onto various rock materials or minerals has been described widely in the literature (Beneš et al., 1998; Labonne-Wall et al., 1997; Lenhart and Honeyman, 1999; Payne et al., 1996; Ticknor et al., 1996; Zuyi et al., 2000). However, also the effect of further competing ions, being of environmental interest, has to be studied. For instance, sulfate has to be taken into account beside phosphate, arsenate, selenate, or molybdate. Acidic sulfate waters are produced by the aerobic leaching of sulfide-bearing rocks, sediments and soils, and thus, sulfate containing waters are usually associated with anthropogenic activities such as mining or soil drainage (Bigham et al., 1996). For example, seepage waters from mine tailing piles of the Saxonian uranium mining area in Germany contain relatively high concentrations of both uranium (10^{-5} M) and sulfate ($3 \cdot 10^{-2}$ M) (Geipel et al., 1996). Depending on natural conditions such as pH, ionic strength and composition of the waters this sulfate can occur in the aqueous phase or as structural constituent in solid mineral phases such as jarosite and schwertmannite (Bigham et al., 1996) or it can be sorbed on the surface of rock materials or minerals present in the environment. Sulfate sorbed onto amorphous iron oxyhydroxides can be released again by increasing the solution pH which is primarily a result of desorption, rather than by the structural breakdown of the Fe phases (Rose and Elliott, 2000).

Batch sorption experiments investigating the influence of sulfate on the uranium sorption onto phyllite in the absence and presence of humic acid in the pH range 3.5 to 9.5 (data not presented) have shown that the uranium sorption is decreased by sulfate both in the absence and in the presence of humic acid. The humic acid sorption is also decreased upon sulfate sorption.

Furthermore, binary- and ternary-sorbate experiments with cupper, sulfate and low molecular model organic acids (phthalic acid and chelidamic acid) showed that sulfate effectively competes with organic acids for surface sites on goethite. The authors concluded that the extent of the influence of organic acids such as humic substances on the sorption of metal ions may be strongly dependent on the presence of other sorbing anions, such as sulfate (Ali and Dzombak, 1996a; 1996b). The sorption of natural organic matter on iron oxide was shown to be substantially reduced by specifically adsorbed anions such as phosphate and sulfate, with the effect of phosphate being greater than sulfate (Gu et al., 1994; 1995). Sibanda and Young (1986) showed that humic substances and phosphate compete strongly with each other for oxide surface sites.

Previous batch experiments investigating the influence of humic acid on the uranium sorption onto the rock material phyllite have shown that the relatively high uranium and humic acid sorption over the entire pH range can be attributed to ferrihydrite, which is formed as secondary mineral in the course of the sorption experiments (Schmeide et al., 2000a). The reason for the dominating sorption behavior of ferrihydrite, compared to the other mineralogical constituents of the phyllite, is the high specific surface area of ferrihydrite (600 m^2/g (Dzombak and Morel, 1990)), together with a strong sorption affinity both to uranium and to humic acid. Therefore, we used ferrihydrite as a representative of phyllite in the following kinetic experiments studying the influence of sulfate on the uranium(VI) adsorption onto ferrihydrite at pH 6.5 in the absence and presence of humic acid.

2 Experimental

As humic acid, we used the ^{14}C-labeled synthetic humic acid type M1 (Bubner et al., 1998).
A ferrihydrite stock solution ($1 \cdot 10^{-3}$ M Fe, 0.04 M $NaClO_4$) was freshly prepared as described in Schmeide et al. (2000b). From this solution, 400 mL ferrihydrite solutions ($3 \cdot 10^{-4}$ M Fe) were prepared for each kinetic experiment that contained 0, 0.005 or 0.02 M Na_2SO_4. Appropriate amounts of Na_2SO_4 and $NaClO_4$ stock solutions were added to adjust the total ionic strength to 0.1 M. During the following 7 days the aging of the ferrihydrite proceeded and the pH of the continuously stirred suspensions was adjusted to pH 6.50 ± 0.03 using dilute $HClO_4$ or NaOH. Then, to start the kinetic experiments appropriate amounts of uranium and humic acid stock solutions were added to give initial total concentrations of $1 \cdot 10^{-6}$ M and 5 mg/L, respectively. The pH of the humic acid stock solution and of the preconditioned uranyl humate stock solution was also adjusted to pH 6.5 prior to their addition to the ferrihydrite suspensions.
The reactants were added in different sequences to the ferrihydrite suspensions:

Experiments without humic acid:

1. addition of uranium to the ferrihydrite suspension, without sulfate,
2. the ferrihydrite suspension was preconditioned with sulfate, then addition of uranium,
3. uranium and sulfate were added simultaneously to the ferrihydrite suspension.

Experiments with humic acid:

1. uranium and humic acid were added simultaneously to the ferrihydrite suspension that did not contain sulfate,
2. uranium and humic acid were added simultaneously to the ferrihydrite suspension which was preconditioned with sulfate,
3. uranium and humic acid were preconditioned for 48 h, then addition to the ferrihydrite suspension that did not contain sulfate,
4. uranium and humic acid were preconditioned for 48 h, then addition to the ferrihydrite suspension which was preconditioned with sulfate.

Uranyl and humic acid concentrations in solution were monitored over time to determine their sorption onto ferrihydrite. Samples were taken after different time intervals between about 20 sec and 240 h after addition of the components. The pH of the suspensions was checked several times. Usually no readjustments were necessary. At each sampling time, a 2-mL aliquot of the continuously stirred suspension was taken from each bottle and filtered (450 nm, Minisart N, Sartorius). The concentration of uranium was determined by ICP-MS (Mod. ELAN 5000, Perkin Elmer). That of ^{14}C-M1 was determined by liquid scintillation counting (Series LS 6000 LL, Beckman Instruments) after combustion of the samples with a sample oxidizer (Mod. P 307, Canberra-Packard). The uranium and humic acid sorption onto the bottle walls (PP, Nalgene) could not be determined during the kinetic experiments.

3 Results and discussion

Kinetic experiments were carried out at pH 6.5 which corresponds to the maximum of the uranium and humic acid (HA) sorption onto ferrihydrite (FH). Since the sulfate sorption is dependent on ionic strength (Geelhoed et al., 1997; Persson et al., 1996), the ionic strength of the solutions, as sum of Na_2SO_4 and $NaClO_4$, was held constant at 0.1 M.

3.1 Influence of sulfate on uranium sorption in the absence of humic acid

3.1.1 Steady-state speciation

In order to describe the sorption processes that occur in the ternary system ferrihydrite/uranium/sulfate, the Generalized Two-Layer Model for surface complexation (Dzombak and Morel, 1990) was used for first calculations with the geochemical speciation software

MINTEQA2 (Allison et al., 1991). Therefore, uranyl sorption data taken from Dicke and Smith (1996) and sulfate sorption data taken from Dzombak and Morel (1990) were applied. Data for uranium speciation in solution were taken from the NEA data base (Grenthe et al., 1992).

As shown in Fig. 1, the total amount of uranium sorbed onto strong (s) and weak (w) surface binding sites of ferrihydrite decreases from about 93 % in the absence of sulfate to about 84 % in the presence of 0.02 M sulfate. The uranium in solution occurs as $UO_2(OH)_2$ (aq), no uranyl sulfate complexes are formed at pH 6.5.

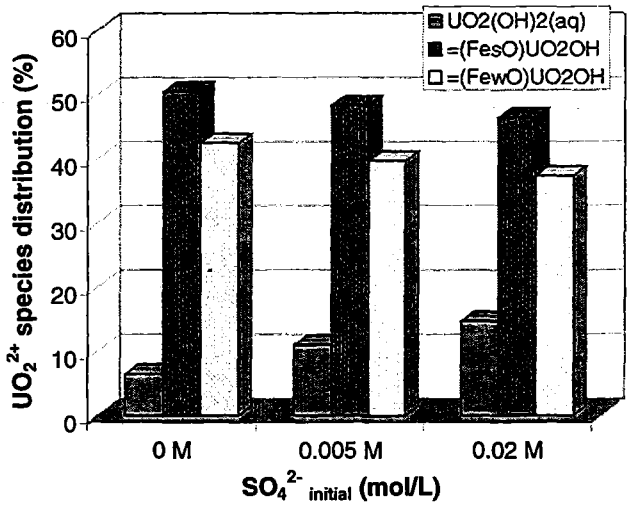

Figure 1: Distribution of uranium species in ferrihydrite suspensions with different sulfate concentrations (0 M, 0.005 M, and 0.02 M SO_4^{2-}).

From Fig. 2, showing the distribution of strong and weak surface sites, follows that the total sulfate sorption onto strong and weak surface sites increases with increasing initial sulfate concentration. Simultaneously, the amount of unreacted strong and weak surface sites (=(Fe_SOH) and (=(Fe_WOH)) decreases largely and an increasing amount of ferrihydrite surface sites becomes protonated (=$(Fe_SOH_2)^+$ and =$(Fe_WOH_2)^+$).

The sulfate sorbs predominantly onto weak surface sites: $1.1 \cdot 10^{-5}$ M and $1.5 \cdot 10^{-5}$ M of the weak surface sites but only $1.8 \cdot 10^{-7}$ M or $2.4 \cdot 10^{-7}$ M of the strong surface sites are occupied by sulfate at 0.005 and 0.02 M sulfate, respectively. Because the surface complexation model does not discriminate between strong and weak surface sites for anions, this behavior was expected.

Compared to sulfate, a higher quantity of strong surface sites is occupied by uranium: $5 \cdot 10^{-7}$ M in the absence of sulfate and $4.6 \cdot 10^{-7}$ M when sulfate is present at 0.02 M. That means, sulfate sorption causes only a 2.8 % decrease in the uranium sorption capacity. This leads to the conclu-

sion, that only a part of strong ferrihydrite surface sites are blocked by sulfate. The percentage of weak surface sites that are occupied by uranium is negligible.

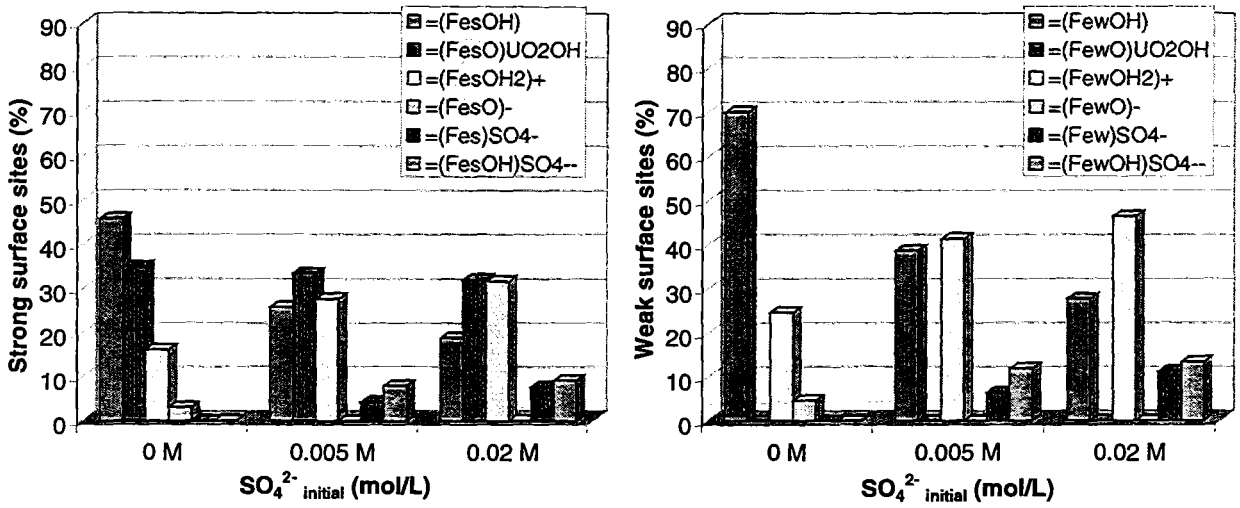

Figure 2: Distribution of strong and weak surface sites of ferrihydrite under experimental conditions applied in this study.

3.1.2 Kinetic sorption experiments

Figs. 3a and 3b show the kinetics of uranium sorption onto ferrihydrite in dependence on the initial sulfate concentration and on the order in which uranium and sulfate were added.

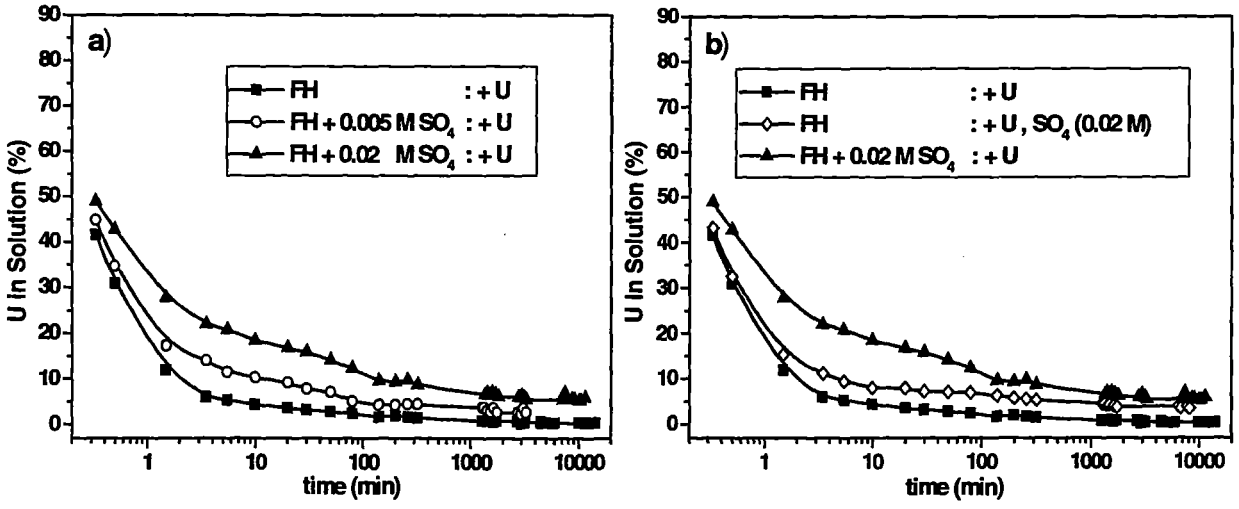

Figure 3: Uranium sorption onto ferrihydrite in dependence on the initial sulfate concentration (a) and on the order in which components were added (b).

Fig. 3a shows experiments where sulfate was added to ferrihydrite containing solutions about 7 days prior to addition of uranium, allowing for sorption equilibrium between all partners.
With increasing total sulfate concentration and thus, with increasing sulfate sorption onto ferrihydrite, the initial rate of uranium sorption decreases. Following the results of the previous calculations, a part of strong ferrihydrite surface sites is blocked by presorbed sulfate. This has two effects on the uranium sorption:

- First, uranyl ions have to diffuse to internal ferrihydrite sorption sites.
- Second, uranyl ions displace sorbed sulfate ions since they have a higher sorption affinity to ferrihydrite surface sites compared to sulfate.

Both effects lead to the observed lower uranium sorption rates in the presence of sulfate.
In contrast, the supply of unreacted weak surface sites for uranium sorption is sufficient even after sulfate sorption. This explains why the effect of sulfate on uranium sorption is relatively small despite the large excess of sulfate (4 and 16 meq/400 mL) compared to uranium (0.8 μeq/400 mL).
As shown in Fig. 3a, in the presence of sulfate, the uranium sorption rate is increasingly slowed down with progressing uranium sorption (between 1 and 100 min). This is attributed to a decreasing number of surface sites that are easily accessible for uranyl ions.
The total uranium sorption onto ferrihydrite decreases with increasing sulfate concentration, which again shows the blocking of surface sites by sorbed sulfate. The percentages of total uranium sorption are generally consistent with our calculation results, although the sorption in the experiments is apparently slightly higher since the vial wall sorption of uranium could not be taken into account.

When uranium and sulfate are added simultaneously to the ferrihydrite suspension, as shown for the experiment with 0.02 M sulfate in Fig. 3b, then uranium and sulfate compete for ferrihydrite surface sites. The initial rate of uranium sorption is as high as in the absence of sulfate, since at the beginning of both experiments a sufficient quantity of external strong sorption sites is available for the uranium sorption. However, with progressing uranium and sulfate sorption, a part of strong surface sites becomes occupied by sulfate. Thus, uranyl ions have to diffuse to internal sorption sites. Consequently, the uranium sorption rate decreases (curve no. 2 in Fig. 3b). Finally, the amount of uranium sorbed onto ferrihydrite seems to approach the uranium distribution found in the experiment where sulfate could sorb onto ferrihydrite prior to the addition of ura-

nium. This means, that uranium is able to replace to a certain extent presorbed sulfate due to its higher sorption affinity.

These results show, that although the sorption of sulfate onto the positively charged ferrihydrite surface (point of zero charge is 8.0 (Dzombak and Morel, 1990)) causes net surface charge to become less positive, the uranium sorption onto ferrihydrite is not promoted as one could expect. This result is consistent with previous experiments (Arnold et al., 1998; Schmeide et al., 2000a) where the uranium sorption onto strongly sorbing solids, such as phyllite and ferrihydrite, was found to be independent of the net surface charge.
The formation of iron oxide-sulfate-uranium ternary surface complexes is not discussed here, since there is no spectroscopic evidence for them so far.

3.2 Influence of sulfate on uranium sorption in the presence of humic acid

Uranium and humic acid were added either simultaneously or as a preconditioned solution (48 h) to ferrihydrite suspensions that contained different amounts of sulfate.

As was observed for experiments in the absence of humic acid, the amounts of uranium sorbed in equilibrium decrease with increasing total sulfate concentration. However, differences in the initial uranium sorption rate and in the extent of the reduction of uranium sorption are observed:

- When uranium and humic acid are added simultaneously to the ferrihydrite suspensions (Fig. 4a), the initial uranium sorption rate and the total uranium sorption decrease with increasing sulfate concentration.
- When aliquots of preformed uranyl humate complexes are added (Fig. 4b), the initial uranium sorption rates are almost unchanged by presorbed sulfate. The decrease of the total uranium sorption onto ferrihydrite with increasing sulfate concentrations is slightly smaller than that of the preceding experimental mode.

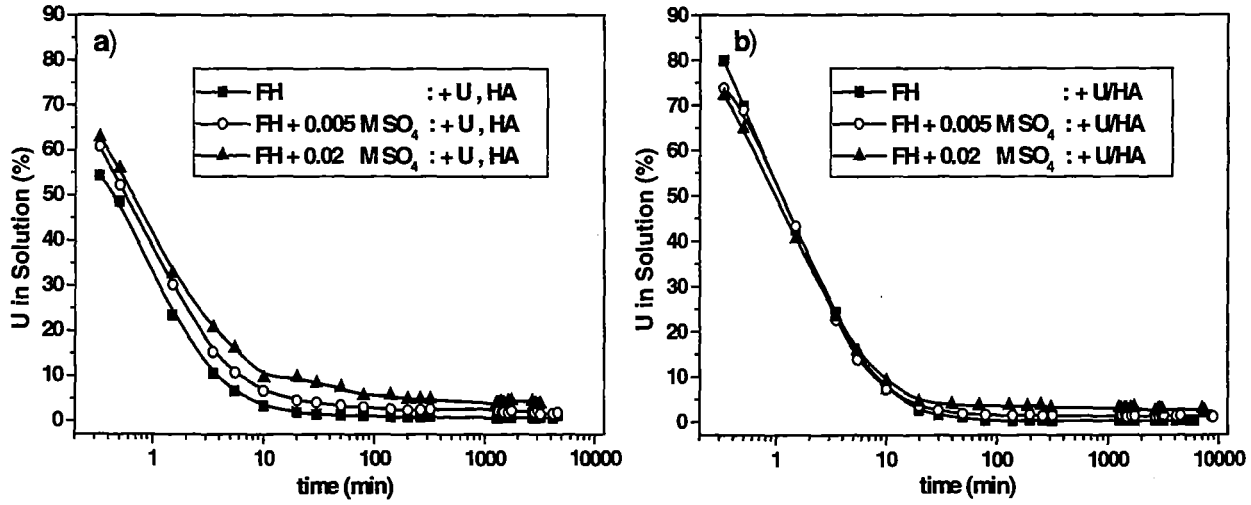

Figure 4: Influence of sulfate on uranium adsorption onto ferrihydrite in the presence of humic acid. Uranium and humic acid were added simultaneously (a) or as a preconditioned solution (b).

With regard to humic acid sorption (Fig. 5), an effect of the sequence of uranium and humic acid addition to the ferrihydrite suspension was not detectable since the uranium concentration (0.8 µeq/400 mL) is small compared to humic acid (2.68 µeq/400 mL). Furthermore, the initial humic acid sorption rate within the first 10 min is hardly influenced by presorbed sulfate. However, the total humic acid sorption decreases somewhat with increasing amount of sorbed sulfate.

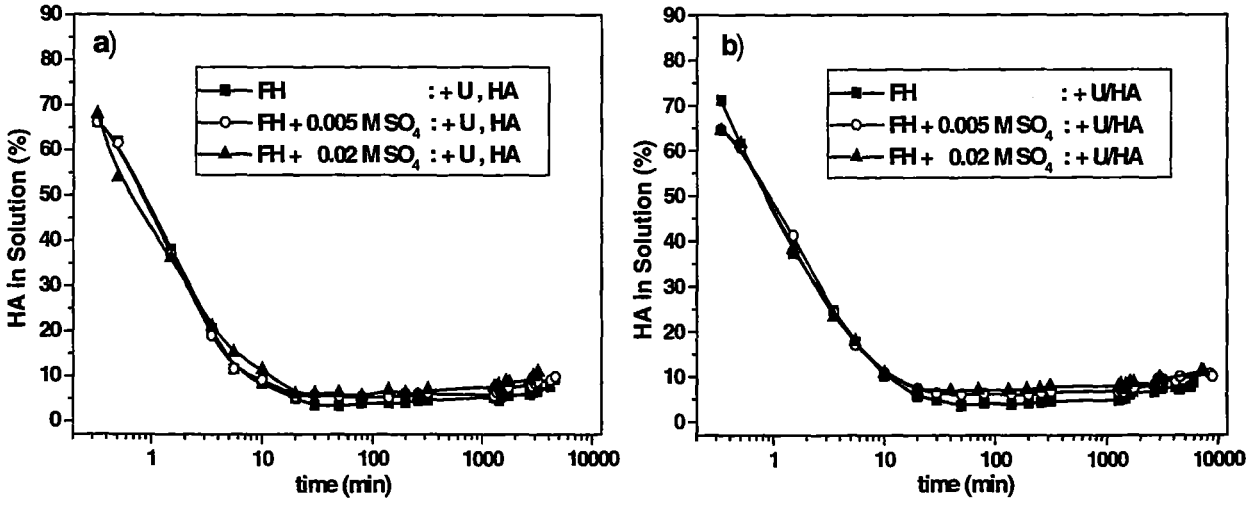

Figure 5: Influence of sulfate on humic acid adsorption onto ferrihydrite in the presence of uranium. Uranium and humic acid were added simultaneously (a) or as preconditioned solution (b).

Since the large humic acid molecules most likely can only sorb onto the outermost ferrihydrite surface sites (Schmeide et al., 2000b) the decreasing humic acid sorption observed in these ex-

periments implies that some of the external surface sites are blocked by presorbed sulfate. Furthermore, the surface charge of ferrihydrite at a given pH becomes less positively charged upon sulfate sorption. This should also lead to a reduced humic acid sorption. However, despite the large excess of sulfate (4 and 16 meq/400 mL) compared to humic acid functional groups (COOH: 2.68 µeq/400 mL, phenolic OH: 4.8 µeq/400 mL) the effect of sulfate on total humic acid sorption is small.

There can be two reasons for this:

- First, after presorption of sulfate, there is still a sufficient quantity of external surface sites accessible for the large humic acid molecules. Primarily =(FeOH) and $=(FeOH_2)^+$ surface sites come into question, since humic acid molecules bind to surface sites via surface complexation and ligand exchange.
- Second, humic acid with a higher adsorption affinity displaces sulfate with a lower affinity that had been previously adsorbed.

The changes of surface charge by sorbed sulfate are too small to have a significant effect on the strongly sorbing humic acid.

As was observed in previous experiments (Schmeide et al., 2000b), a part of the sorbed humic acid is released again from ferrihydrite since the humic acid concentration in solution increases slightly. This is attributed to a formation of soluble iron humate complexes leading to an increased solubility of ferrihydrite in the presence of humic acid.

3.3 Comparison of the influence of sulfate on uranium sorption onto ferrihydrite in the absence and presence of humic acid

The uranium sorption onto ferrihydrite in the absence and presence of humic acid is compared in Fig. 6 for experiments with different initial sulfate concentrations: a) 0 M Na_2SO_4, b) 0.005 M Na_2SO_4 and c) 0.02 M Na_2SO_4.

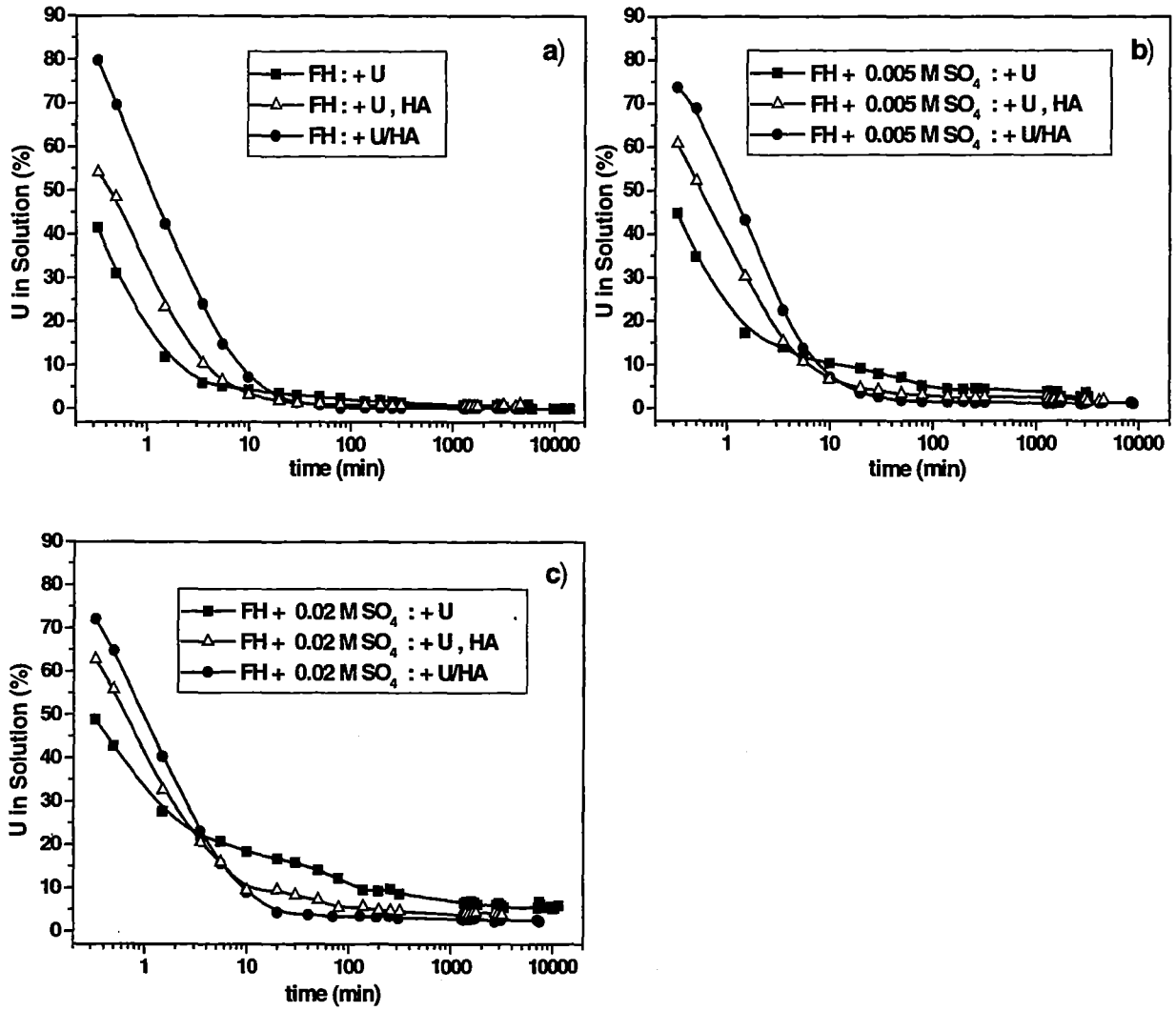

Figure 6: Comparison of the uranium sorption onto ferrihydrite in the absence and presence of humic acid for experiments with different initial sulfate concentrations: a) 0 M Na_2SO_4, b) 0.005 M Na_2SO_4 and c) 0.02 M Na_2SO_4.

The sequence of the initial uranium sorption rates in dependence on the uranium and humic acid addition is the same for all sulfate concentrations (0 M, 0.005 M and 0.02 M Na_2SO_4):

- In the absence of humic acid, uranium sorb with the highest initial rate.
- In the presence of humic acid, the initial uranium sorption is increasingly retarded with increasing amounts of uranyl humate complexes in solution until it approaches the humic acid sorption rate.

This is consistent with results of previous experiments (Schmeide et al., 2000b).

The influence of sulfate on uranium sorption can be summarized as follows:

- In the absence of humic acid, the initial uranium sorption rates are high, but after occupation of the first surface sites the uranium sorption slows down since strong ferrihydrite surface sites are blocked by presorbed sulfate. The uranium is forced to diffuse to internal sorption sites or to replace sorbed sulfate. These effects become stronger with increasing total sulfate concentration.
- In the presence of humic acid, the initial uranium sorption rate is lower than in the absence of humic acid. However, it is less slowed down with progressing sorption compared to the uranium sorption in the absence of humic acid. This leads to an intersection of the curves about 6 min and about 3 min after the start of the experiments with 0.005 M and 0.02 M sulfate, respectively. The total uranium sorption onto ferrihydrite in the presence of humic acid is higher, particularly in the presence of higher amounts of uranyl humate complexes. There are two reasons for this: First, uranium is bound to dissolved humic acid molecules and sorbs as uranyl humate complex onto ferrihydrite. Second, unreacted carboxylate groups of sorbed humic acid molecules can complex uranyl ions thereby increasing uranium sorption.

The differences in the total uranium sorption in dependence on the experimental modes (solely addition of uranium; addition of uranium and humic acid simultaneously or as a preconditioned solution) increase with increasing sulfate sorption (Fig. 6a to Fig. 6c).

4 Conclusions

Influence of sulfate on the uranium sorption in the absence of humic acid at pH 6.5:

Sulfate, present at naturally relevant concentrations (0.005 M or 0.02 M), reduces both the uranium sorption rate and the total uranium sorption, since the number of strong surface sites, accessible for uranium, is reduced upon adsorption of sulfate. This leads to an increased availability of uranium.

Variations of the sequence of addition of sulfate and uranium mainly affected the initial uranium sorption rate showing the competition of uranium and sulfate for ferrihydrite sorption sites. However, the total uranium sorption was not affected, which implies that uranium is able to replace to a certain extent presorbed sulfate because it has a higher sorption affinity.

We conclude, that direct competition of uranium and sulfate for sorption sites of ferrihydrite predominates electrostatic effects due to the change in net surface charge of the ferrihydrite upon sulfate sorption.

Influence of sulfate on the uranium sorption in the presence of humic acid at pH 6.5:

The competitive effect of sulfate on humic acid sorption is small despite the large excess of sulfate compared to humic acid. This reflects a high affinity of humic acid for ferrihydrite surface sites. Furthermore, in contrast to sorbed sulfate, sorbed humic acid molecules have a number of functional groups that are not involved in sorption reactions. Thus, the total number of potential binding sites for uranyl ions is higher in the presence of humic acid which leads to a higher uranium sorption. Consequently, the influence of sulfate on uranium sorption is smaller when humic acid is present in solution. Especially in the presence of higher amounts of uranyl humate complexes, the reducing effect of sulfate on the total uranium sorption is almost counterbalanced by humic acid.

Acknowledgements

The authors thank R. Jander and S. Wallner for their help during the batch experiments and W. Wiesener and A. Schäfer for ICP-MS analyses.

References

Ali, M.A. and Dzombak, D.A. (1996a) Competitive Sorption of Simple Organic Acids and Sulfate on Goethite. *Environ. Sci. Technol.* **30**, 1061.

Ali, M.A. and Dzombak, D.A. (1996b) Interactions of Copper, Organic Acids, and Sulfate in Goethite Suspensions. *Geochim. Cosmochim. Acta* **60**, 5045.

Allison, J.D., Brown, D.S., and Novo-Gradac, K.J. (1991) MINTEQA2/PRODEFA2, a Geochemical Assessment Model for Environmental Systems: Version 3.0 User's Manual. U.S. Environmental Protection Agency, Environmental Research Laboratory, EPA/600/3-91/021.

Arnold, T., Zorn, T., Bernhard, G., and Nitsche, H. (1998) Sorption of Uranium(VI) onto Phyllite. *Chemical Geology* **151**, 129.

Beneš, P., Kratzer, K., Vlcková, Š., and Šebestová, E. (1998) Adsorption of Uranium on Clay and the Effect of Humic Substances. *Radiochim. Acta* **82**, 367.

Bigham, J.M., Schwertmann, U., Traina, S.J., Winland, R.L., and Wolf, M. (1996) Schwertmannite and the Chemical Modeling of Iron in Acid Sulfate Waters. *Geochim. Cosmochim. Acta* **60**, 2111.

Bubner, M., Pompe, S., Meyer, M., Heise, K.H., and Nitsche, H. (1998) Isotopically Labelled Humic Acids for Heavy Metal Complexation. *J. Labelled Compounds and Radiopharmaceuticals* **XLI**, 1017.

Davis, J.A. and Leckie, J.O. (1980) Surface Ionization and Complexation at the Oxide/Water Interface 3. Adsorption of Anions. *J. Colloid Interf. Sci.* **74**, 32.

Dicke, C. and Smith, R.W. (1996) Surface Complexation Modeling of Uranium Adsorption on Naturally Occurring Iron Coated Sediments. Presentation given at the American Chemical Society Annual Meeting in New Orleans on March 28, 1996.

Dzombak, D.A. and Morel, F.M.M. (1990) *Surface Complexation Modeling – Hydrous Ferric Oxide.* John Wiley & Sons, New York.

Geelhoed, J.S., Hiemstra, T., and Van Riemsdijk, W.H. (1997) Phosphate and Sulfate Adsorption on Goethite: Single Anion and Competitive Adsorption. *Geochim. Cosmochim. Acta* **61**, 2389.

Geipel, G., Brachmann, A., Brendler, V., Bernhard, G., and Nitsche, H. (1996) Uranium(VI) Sulfate Complexation Studied by Time-Resolved Laser-Induced Fluorescence Spectroscopy. *Radiochim. Acta* **75**, 199.

Grenthe, I., Fuger, J., Lemire, R.J., Muller, A.B., Nguyen-Trung, C., and Wanner, H. (1992) *Chemical Thermodynamics of Uranium*, 1st ed., Elsevier Science Publishers, Amsterdam.

Gu, B., Schmitt, J., Chen, Z., Liang, L., and McCarthy, J.F. (1994) Adsorption and Desorption of Natural Organic Matter on Iron Oxide: Mechanisms and Models. *Environ. Sci. Technol.* **28**, 38.

Gu, B., Schmitt, J., Chen, Z., Liang, L., and McCarthy, J.F. (1995) Adsorption and Desorption of Different Organic Matter Fractions on Iron Oxide. *Geochim. Cosmochim. Acta* **59**, 219.

Labonne-Wall, N., Moulin, V., and Vilarem, J.-P. (1997) Retention Properties of Humic Substances onto Amorphous Silica: Consequences for the Sorption of Cations. *Radiochim. Acta* **79**, 37.

Lenhart, J.J. and Honeyman B.D. (1999) Uranium(VI) Sorption to Hematite in the Presence of Humic Acid. *Geochim. Cosmochim. Acta* **63**, 2891.

Payne, T.E., Davis, J.A., and Waite, T.D. (1996) Uranium Adsorption on Ferrihydrite - Effects of Phosphate and Humic Acid. *Radiochim. Acta* **74**, 239.

Persson, P. and Lövgren, L. (1996) Potentiometric and Spectroscopic Studies of Sulfate Complexation at the Goethite-Water Interface. *Geochim. Cosmochim. Acta* **60**, 2789.

Rose, S. and Elliott, W.C. (2000) The Effects of pH Regulation Upon the Release of Sulfate From Ferric Precipitates Formed in Acid Mine Drainage. *Applied Geochemistry* **15**, 27.

Schmeide, K., Pompe, S., Bubner, M., Heise, K.H., Bernhard, G., and Nitsche, H. (2000a) Uranium(VI) Sorption onto Phyllite and Selected Minerals in the Presence of Humic Acid. Submitted to Radiochim. Acta.

Schmeide, K., Brendler, V., Pompe, S., Bubner, M., Heise, K.H., and Bernhard, G. (2000b) Kinetic Studies of the Uranium(VI) and Humic Acid Sorption onto Phyllite, Ferrihydrite and Muscovite. This Third Technical Progress Report.

Sibanda, H.M. and Young, S.D. (1986) Competitive Adsorption of Humus Acids and Phosphate on Goethite, Gibbsite and Two Tropical Soils. *J. Soil Sci.* **37**, 197.

Ticknor, K.V., Vilks, P., and Vandergraaf, T.T. (1996) The Effect of Fulvic Acid on the Sorption of Actinides and Fission Products on Granite and Selected Minerals. *Applied Geochemistry* **11**, 555.

Zuyi, T., Taiwei, C., Jinzhou, D., XiongXin, D., and Yingjie, G. (2000) Effect of Fulvic Acids on Sorption of U(VI), Zn, Yb, I and Se(IV) onto Oxides of Aluminum, Iron and Silicon. *Applied Geochemistry* **15**, 133.

Annex 11

Structural Investigation of the Interaction of Uranium(VI) with Modified and Unmodified Humic Substances by EXAFS and FTIR Spectroscopy

(K. Schmeide, S. Pompe, M. Bubner, T. Reich
K.H. Heise and G. Bernhard (FZR/IfR))

Third Technical Progress Report

EC Project:

"Effects of Humic Substances on the Migration of Radionuclides: Complexation and Transport of Actinides"

Project No.: FI4W-CT96-0027

FZR/IFR Contribution to Task 2 (Complexation)

Structural Investigation of the Interaction of Uranium(VI) with Modified and Unmodified Humic Substances by EXAFS and FTIR Spectroscopy

Reporting period 1999

K. Schmeide, S. Pompe, M. Bubner, T. Reich, K.H. Heise, G. Bernhard

Forschungszentrum Rossendorf e.V.
Institute of Radiochemistry
P.O. Box 510119
01314 Dresden
Germany

Abstract

We studied the interaction of uranium(VI) with humic and fulvic acids to obtain information on the binding of uranium(VI) onto functional groups of humic substances. Therefore, various natural and synthetic humic acids (HAs) were chemically modified resulting in HAs with blocked phenolic OH groups. From the original and modified HAs, solid uranyl humate complexes were prepared at pH 2. FTIR spectroscopy and U L_{III}-edge extended X-ray absorption fine structure (EXAFS) analysis were applied to study the derivatization process of HAs, to study the structure of the uranyl humates and to evaluate the effect of HA functional groups (carboxylic and phenolic OH groups) on the uranyl complexation.

By FTIR spectroscopy it could be shown that the synthesis of modified HAs with blocked phenolic OH groups was successful. These modified HAs are suitable model substances to study the complexation of actinides by humic substances, especially to study the role of phenolic OH groups of HAs in dependence on pH.

By EXAFS, identical structural parameters were determined for all uranyl humates. Axial U-O bond distances of 1.78 Å were determined. In the equatorial plane approximately five oxygen atoms were found at a mean distance of 2.39 Å. The blocking of phenolic OH groups of HAs did not change the near-neighbor surrounding of uranium(VI).

The comparison of results obtained by FTIR spectroscopy and EXAFS analyses for uranyl humates, prepared from original and modified HAs, confirmed that predominantly HA carboxylate groups are responsible for binding of uranyl ions at pH 2. These carboxylate groups are monodentate coordinated to uranyl ions. The influence of phenolic OH groups is insignificant.

1 Introduction

Humic substances are known to influence the speciation and thus, the mobility of radionuclides in the environment due to their high complexing ability. Therefore, risk-assessments, related to the migration behavior of radionuclides in the environment, require basic knowledge about the interaction of humic substances with metal ions. Numerous studies of the complexation of radionuclides, such as uranium, by humic substances have been performed. However, due to the chemical and structural heterogeneity of humic substances, the

nature of metal complexation sites in humic substances is still uncertain (Korshin et al., 1998).

Carboxylic groups are often considered the only functional groups of HAs involved in the complexation of metal ions at pH values below 9 (e.g., Choppin and Allard, 1985). Other authors suggest that further HA functional groups, such as phenolic, enolic, and alcoholic OH groups (Stevenson, 1994; Sarret et al., 1997; Korshin et al., 1998; Pompe et al., 2000) as well as amino groups (Ephraim and Marinsky, 1986; Luster et al., 1996; Heise et al., 2000), can also contribute to the complexation of metal ions. For instance, these groups can form chelate rings together with carboxylate groups.

A recent study (Pompe et al., 2000), investigating the uranyl complexation by HAs by time-resolved laser-induced fluorescence spectroscopy at pH 4, has shown that, already at pH 4, phenolic OH groups contribute to the interaction between HA and uranyl ions.

This shows that the nature of HA functional groups, responsible for binding of metal ions, should be studied systematically in dependence on pH.

In the present paper, we studied the complexation of uranium(VI) by humic substances at pH 2. In addition to unmodified natural and synthetic HAs, we employed chemically modified HAs with blocked phenolic OH groups as model substances. The comparison of the complexation behavior of the original and modified HAs enables evaluation of the effects of different functional groups such as carboxylic and phenolic OH groups. FTIR spectroscopy and EXAFS analysis were applied for this study. FTIR spectroscopy was applied to verify the blocking of phenolic OH groups in the modified HAs and to study the binding of uranyl ions onto HA functional groups. EXAFS was used to determine structural parameters of the near-neighbor surrounding of uranium(VI) complexed by humic substances.

2 Experimental

2.1 Humic substances

Three natural and two synthetic humic substances were applied. The natural humic substances were Kranichsee humic acid (KHA) and Kranichsee fulvic acid (KFA) that were isolated from surface water of the mountain bog 'Kleiner Kranichsee' (Saxony, Germany) (Schmeide et al., 1998) as well as the commercial Aldrich HA (AHA, charge A2/97) (Aldrich, Steinheim,

Germany). AHA was purified prior to use according to a method described by Kim and Buckau (1988). The synthetic products were the HAs type M1 (Pompe et al., 1996) and type M42 (Pompe et al., 1998).

Modified HAs with blocked phenolic OH groups were synthesized starting from the original HAs type KHA, AHA, M1 and M42. In a first step, HA functional groups (carboxylic and acidic (phenolic) OH groups) were permethylated. Therefore, methanolic suspensions of original HAs were stirred with diazomethane, which was previously prepared from Diazald® (Sigma-Aldrich, Steinheim, Germany), at –5 to 5 °C for 3 hours. Then, the solvent was distilled off. The permethylation procedure was repeated several times until no further diazomethane was incorporated into the HA. The solvent, that was distilled from the reaction mixture, was then yellow colored due to unreacted diazomethane. The resulting permethylated HAs were lyophilized. They are termed HA-B. In a second step, the ester groups were hydrolyzed by reacting the permethylated HAs with 2 M NaOH (Merck, Darmstadt, Germany) under inert gas at room temperature for 8 hours. The alkali-insoluble residue was separated by centrifugation. The modified HAs were precipitated with 2 M HCl (Merck) and separated by centrifugation. The washed, dialyzed (Thomapor®, MWCO < 1000, Reichelt Chemietechnik, Heidelberg, Germany) and lyophilized products were applied for this study. The HAs with blocked phenolic OH groups are termed HA-PB.

All HAs (HA, HA-B, HA-PB) were characterized for their functional group content.

2.2 Preparation of uranyl humate complexes

Uranyl humate complexes were prepared from natural and synthetic unmodified humic substances (KHA, KFA, AHA, M1, M42) and from the corresponding modified HAs with blocked phenolic OH groups (KHA-PB, AHA-PB, M1-PB, M42-PB).

Solid uranyl humate complexes were prepared by reacting aqueous HA suspensions, that were previously deaerated, with 0.1 M uranyl perchlorate solutions at pH 2. The low pH value of 2 of the HA suspension was achieved by adjusting the pH in the supernatant repeatedly with 0.1 M $HClO_4$ or 0.1 M NaOH. For these pH adjustments, the supernatant was separated from the humic material each time. The reaction products were isolated by centrifugation, washed with ultrapure water, dialyzed (Thomapor®, MWCO < 1000), and lyophilized. The uranium

content of the uranyl humates was determined by ICP-MS (Mod. ELAN 5000, Perkin Elmer) after digestion of the samples with HNO_3 in a microwave oven.

2.3 FTIR spectroscopy

The samples were dispersed in KBr (Uvasol®, Merck, Darmstadt, Germany) and pressed as 13 mm diameter pellets. The FTIR spectra were recorded using a FTIR spectrometer (Mod. 2000, Perkin Elmer Ltd., Beaconsfield, Buckshire, UK) in the middle infrared region (4000 to 400 cm^{-1}) at room temperature.

2.4 EXAFS analysis

The samples were dispersed in Teflon and pressed as 13 mm diameter pellets. The uranium content of the resulting pellets was 11 to 22 mg uranium. The EXAFS measurements were carried out at the Rossendorf Beamline (ROBL) at the European Synchrotron Radiation Facility (ESRF) in Grenoble. Uranium L_{III}-edge X-ray absorption spectra were collected in transmission mode at room temperature. The Si(111) water cooled double-crystal monochromator was used in the channel-cut mode.

Data analysis was performed according to standard procedures (Koningsberger and Prins, 1988) using the EXAFSPAK software developed by George and Pickering (1995). The program FEFF6 (Rehr et al., 1992) was used to calculate theoretical scattering amplitudes and phase-shift functions.

The EXAFS oscillations were fitted using a two-shell fit with oxygen atoms as backscatterers. The multiple scattering along the uranyl unit at 3.6 Å was also included into the fit. The coordination number of the axial oxygen atoms (N_{ax}) in the uranyl group and the shift in threshold energy (ΔE_0) were held constant at 2 and -13.6 eV, respectively. The *k*-range of the fits was between 2.8 and 16.7 $Å^{-1}$.

3 Results and discussion

3.1 Characterization of humic substances and uranyl humates

The functional group contents of the various humic substances are compiled in Tab. 1. Due to permethylation of HAs methyl ester and methyl ether groups are formed from carboxylic groups and acidic (phenolic) OH groups, respectively. The carboxylic and phenolic OH groups of the permethylated HAs (HA-B) are almost completely blocked. Due to saponification of the permethylated HAs the methyl ester groups are hydrolyzed whereas the phenolic OH groups remain blocked. However, Tab. 1 shows that the number of phenolic OH groups increased somewhat during the saponification step. This may be attributed to an unfolding of HA molecules thereby uncovering functional groups that were previously sterically hindered. This leads to modified HAs (HA-PB) whose phenolic OH group contents are 59-74 % lower than those of the unmodified HAs. That means that the phenolic OH groups are only partially blocked due to the modification. The carboxylic group contents of the modified HAs (HA-PB) are also somewhat lower than those of the unmodified HAs. Possible reasons are a partial decomposition of HA molecules in acid-soluble components and/or leaching of smaller HA molecules with a higher carboxylic group content from the HA mixture (Pompe et al., 2000) or an incomplete hydrolysis of the ester groups that were previously formed during permethylation.
Nevertheless, Tab. 1 shows that the molar ratio of phenolic OH to carboxylic groups becomes always smaller due to the modification process.

The loading of HAs with uranyl ions in the uranyl humates was between 15 to 22 % of the carboxylic group capacity of the humic substances (Tab. 1). The uranyl loading of HAs, expressed in (mg U/g HA) or related to the carboxylic group content (% COOH), is always lower for the HAs with blocked phenolic OH groups (HA-PB) than for unmodified HAs. The uranyl loading mainly correlates with the carboxylic group content of the HAs, and to a small extent with their phenolic OH group content.

Table 1: Functionality of humic substances and uranyl loading of humic substances in uranyl humates

Humic Substance	Functionality			Uranyl Humate	Uranyl Loading	
	Phenolic OH[a] (meq/g)	COOH[b] (meq/g)	Phenolic OH / COOH		(mg U/g HA)	(% COOH)[c]
KHA	3.9 ± 0.5	4.20 ± 0.17	0.93	UO_2-KHA	110.2	22
KHA-B	0.3	<0.1[a]	-			
KHA-PB	1.6 ± 0.4	2.83 ± 0.05	0.57	UO_2-KHA-PB	50.2	15
AHA	3.4 ± 0.5	4.41 ± 0.11	0.77	UO_2-AHA	99.8	19
AHA-B	0.6 ± 0.3	<0.1[a]	-			
AHA-PB	1.1 ± 0.4	3.25 ± 0.05	0.34	UO_2-AHA-PB	70.4	18
M1	2.4 ± 0.1	1.34 ± 0.05	1.79	UO_2-M1	28.9	18
M1-B	0.3	<0.1[a]	-			
M1-PB	0.9 ± 0.3	1.16 ± 0.03	0.78	UO_2-M1-PB	24.1	17.5
M42	2.3 ± 0.4	4.10 ± 0.10	0.56	UO_2-M42	89.3	18
M42-B	0.6 ± 0.1	<0.1[a]	-			
M42-PB	0.6 ± 0.3	3.21 ± 0.08	0.19	UO_2-M42-PB	60.6	16
KFA	4.8 ± 0.7	6.05 ± 0.31	0.79	UO_2-KFA	118.5	16.5

[a] Radiometrically determined (Bubner and Heise, 1994).
[b] Determined by calcium acetate exchange (Schnitzer and Khan, 1972).
[c] Calculated on the assumption that one uranyl ion occupies two proton exchanging sites of the HA molecule.

3.2 FTIR spectroscopy

Exemplary for all natural and synthetic HAs the FTIR spectra of the original and modified HAs type KHA are shown in Fig. 1.

The spectrum of the original KHA is discussed in detail in Schmeide et al. (1998, 1999). Thus, in the following only the IR absorption bands pointing to the formation of methyl ester and/or methyl ether groups in the spectra of the modified HAs are discussed as well as absorption bands confirming the complexation of uranium.

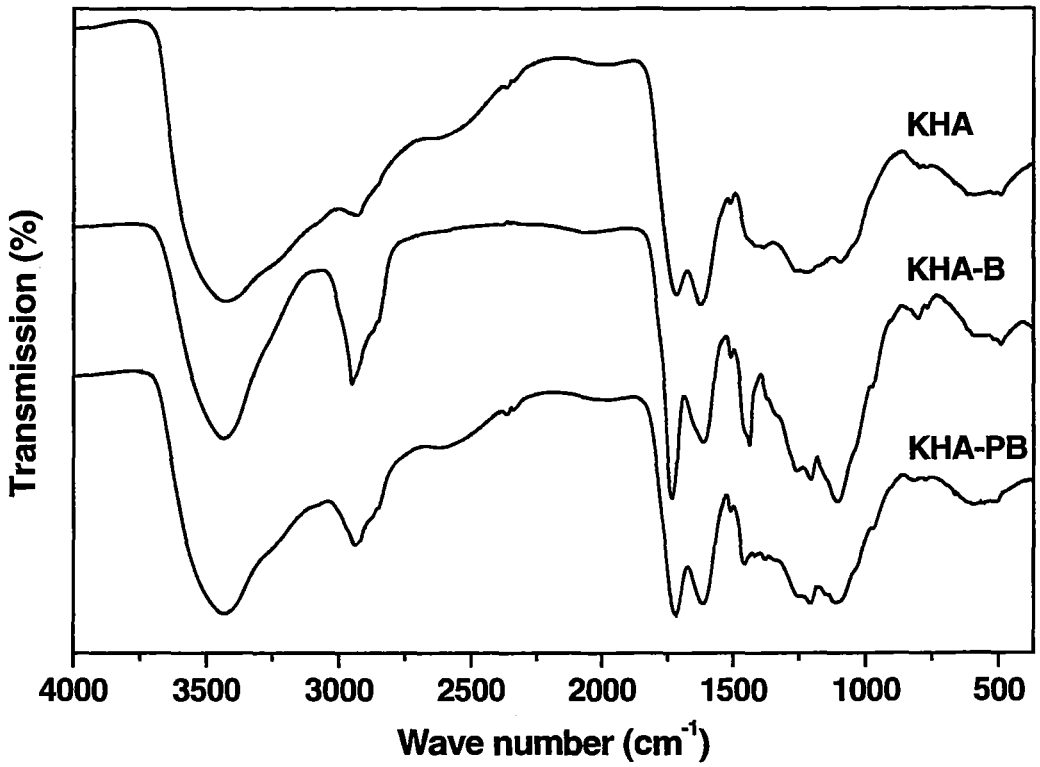

Figure 1: FTIR spectra of the HAs type KHA (original HA), KHA-B (permethylated HA) and KHA-PB (HA with blocked phenolic OH groups).

Compared to the spectrum of KHA the intensity of the absorption bands at 2950 cm^{-1} and 2852 cm^{-1} (aliphatic C-H stretching) as well as 1457 cm^{-1} and 1439 cm^{-1} (C-H deformation of CH_3 groups) is increased in the spectrum of KHA-B. This is attributed to the formation of methyl ether and ester groups upon permethylation of KHA with diazomethane (cf. paragraph 2.1). In addition, the broad band centered at about 3424 cm^{-1} (O-H stretching vibrations) is smaller and its intensity is somewhat decreased. The band near 2630 cm^{-1} (OH stretching of COOH), present in the spectrum of KHA, is absent in the spectrum of KHA-B. The absorption band at 1720 cm^{-1} (C=O stretching of carboxylic groups), observed in the spectrum of KHA, is shifted to 1735 cm^{-1} and its intensity is significantly increased. This indicates the formation of ester groups that absorb at higher wave numbers than carboxylic groups (Schnitzer and Khan, 1972). The intensity of the absorption band caused by C-O stretch at 1205 cm^{-1} is also increased. Furthermore, the intensity of the bands and shoulders at 1106, 1153 and 1260 cm^{-1} is enhanced which is attributed to the formation of ether groups.

The hydrolysis of the permethylated HA (KHA-B) leads to KHA-PB. The band near 2630 cm^{-1} (OH stretching of COOH) is again present in the spectrum. Furthermore, the absorption band at 1735 cm^{-1} (C=O stretching of ester groups), observed in the spectrum of KHA-B, is shifted back to 1721 cm^{-1} (C=O stretch vibration of carboxylic groups) and its intensity is decreased in the spectrum of KHA-PB. This shows that the ester groups present in KHA-B are hydrolyzed by reacting the permethylated HAs with NaOH. However, compared to KHA, the intensity of the absorption band at 1721 cm^{-1} relative to the intensity of the band at 1617 cm^{-1} as well as the intensity of the band at 1207 cm^{-1} is somewhat higher in the spectrum of KHA-PB. This could mean that the ester groups formed during the permethylation are not completely hydrolyzed. This is supported by the somewhat lower COOH content of KHA-PB compared to KHA (cf. Tab. 1).

The intensity of the bands at 2938, 2852, and 1457 cm^{-1} is lower in the spectrum of KHA-PB compared to the spectrum of KHA-B, but higher than in the spectrum of KHA. Furthermore, the bands and shoulders at 1110, 1153 and 1260 cm^{-1} are somewhat enhanced in the spectrum of KHA-PB compared to those in the spectrum of KHA. This verifies that phenolic OH groups remained blocked during the hydrolysis.

The FTIR spectra of the uranyl humate complexes of KHA and KHA-PB are shown in Fig. 2. The following changes are observed for the uranyl humates compared to the corresponding HAs (cf. Fig. 1): A new absorption band occurs at 933.5 cm^{-1} which is attributed to the asymmetric stretching vibration of UO_2^{2+}. The absorption band at about 1720 cm^{-1} (C=O stretch vibrations of COOH) is decreased since a part of the COOH groups is converted to the COO^- form during the complexation process. Simultaneously, the intensity of the band between 1580 and 1510 cm^{-1} (COO^- asymmetric stretching) and that of the band at 1384 cm^{-1} (COO^- symmetric stretching) is increased.

The lower uranyl loading of the HA with blocked phenolic OH groups (cf. Tab. 1) is visible in the lower intensity of the band at 933.5 cm^{-1} in the spectrum of UO_2-KHA-PB. Furthermore, the intensity decrease of the band at about 1720 cm^{-1} relative to the band at about 1620 cm^{-1} is smaller for UO_2-KHA-PB than for UO_2-KHA. This implies that in case of KHA-PB less carboxylic groups are involved in the complexation of uranyl ions than in case of KHA.

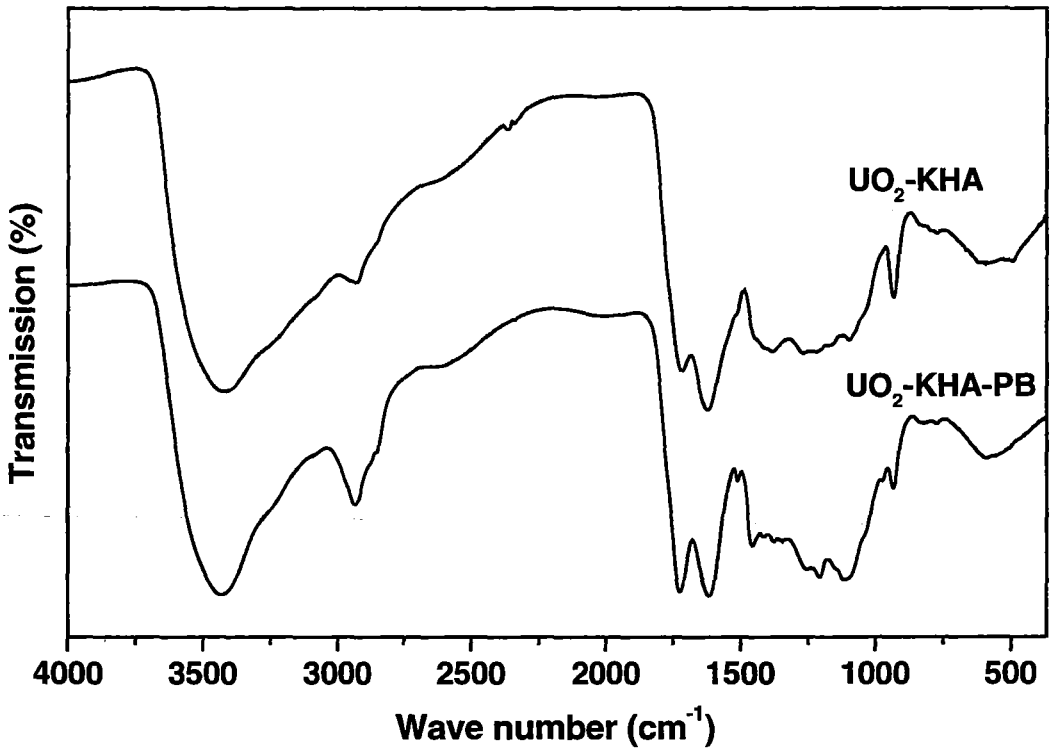

Figure 2: FTIR spectra of the uranyl humates UO_2-KHA and UO_2-KHA-PB.

The difference between the asymmetric and the symmetric stretching frequency of COO^-, which is about 150 cm^{-1} for both uranyl humate complexes, is comparable to that generally observed for monodentate carboxylate coordination (Kakihana et al., 1987).

The intensity of the bands and shoulders in the region between 1280 and 1070 cm^{-1}, that were previously assigned to phenolic OH groups (mainly at 1260 and 1092 cm^{-1}), is lower in the spectrum of UO_2-KHA compared to that of KHA. In case of the HA with blocked phenolic OH groups (KHA-PB), the intensity of the bands between 1280 and 1070 cm^{-1} is not changed due to uranyl complexation. This could be an indication that phenolic OH groups contribute to the complexation of uranyl ions, although a definite assignment of the bands of this region is especially difficult because of an overlapping of bands caused by different functional groups.

A contribution of phenolic OH groups to the interaction between original HAs and uranyl ions at the low pH value of 2, used for complex preparation, is relatively unlikely. The only conceivable way for such a contribution is that six- or five-membered chelate rings of high stability are formed by phenolic OH groups that are ortho-positioned to carboxylate groups or by neighboring phenolic OH groups. Due to the structural requirements and the high pK_a

values of phenolic OH groups a contribution of these groups to the uranyl complexation at pH 2 must be small compared to that of carboxylic groups.

The results obtained from the FTIR spectra of original and modified HAs type AHA, M1 and M42 and of their corresponding uranyl humates are comparable to those obtained for KHA.

3.3 EXAFS analysis

Representative for all uranyl humates, the U L_{III}-edge k^3-weighted EXAFS spectra and the corresponding Fourier transforms, FTs, of the uranyl humates of HA type KHA, KHA-PB, M1 and M1-PB are shown in Fig. 3 and Fig. 4, respectively. In both figures, the solid lines represent the experimental data, whereas the dotted lines show the theoretical fit of the data. Both the EXAFS oscillations and the Fourier transforms of all uranyl humate complexes are similar. In Tab. 2 the EXAFS structural parameters of the uranyl humates are compiled such as coordination numbers (N), bond distances (R) and Debye-Waller factors (σ^2) obtained from fits to the EXAFS equation.

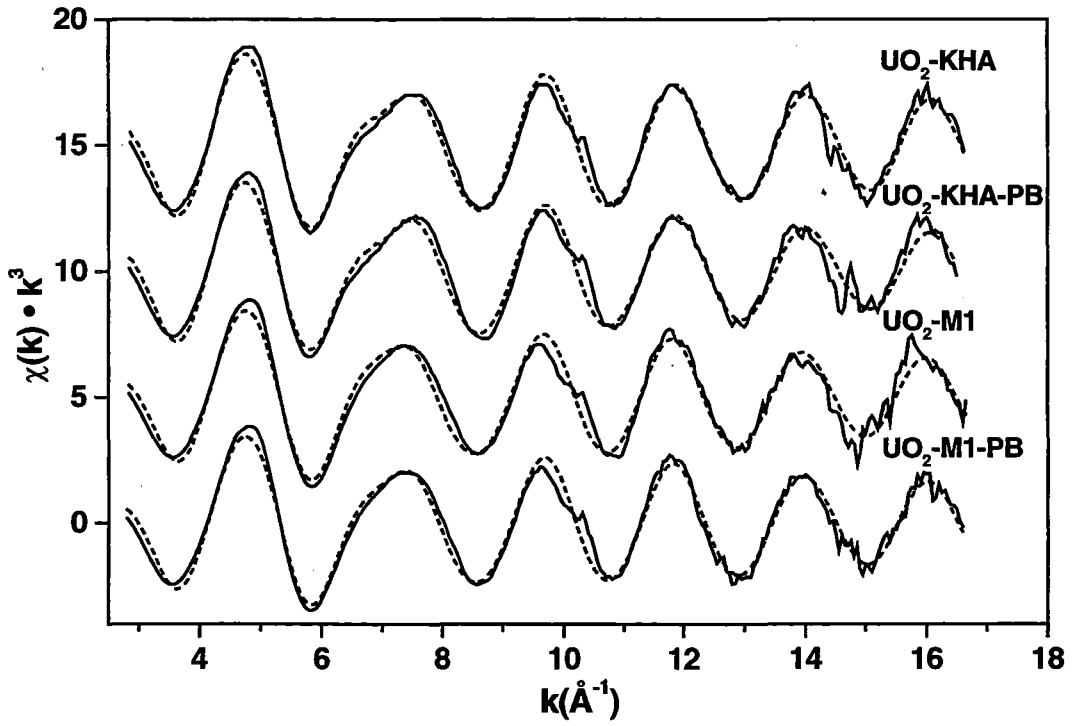

Figure 3: U L_{III}-edge k^3-weighted EXAFS spectra of solid uranyl complexes with KHA, KHA-PB, M1 and M1-PB.

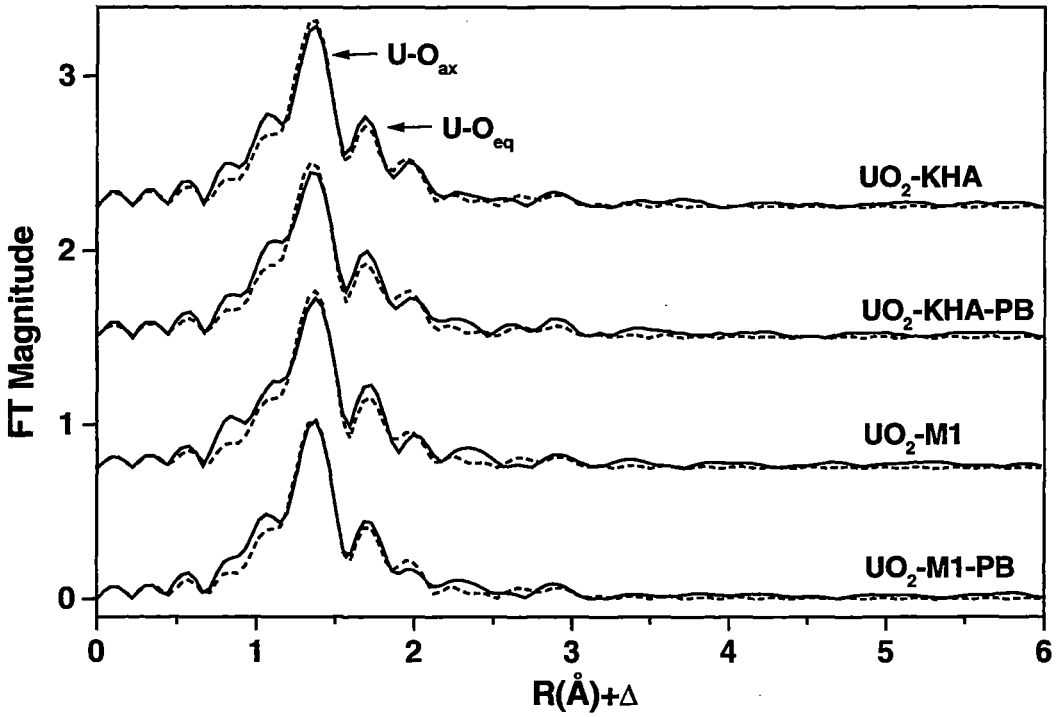

Figure 4: Fourier transforms of the EXAFS spectra of uranyl complexes with KHA, KHA-PB, M1 and M1-PB.

Table 2: Structural parameters of uranyl humates studied by EXAFS analysis

Sample	U - O_{ax}			U - O_{eq}		
	N_{ax}	R (Å)	σ^2 (Å^2)	N_{eq}	R (Å)	σ^2 (Å^2)
UO_2-KHA	2	1.78	0.001	5.2	2.39	0.012
UO_2-KHA-PB	2	1.78	0.002	5.4	2.40	0.013
UO_2-AHA	2	1.78	0.001	5.3	2.40	0.012
UO_2-AHA-PB	2	1.77	0.001	5.1	2.40	0.011
UO_2-M1	2	1.78	0.002	5.2	2.38	0.014
UO_2-M1-PB	2	1.78	0.001	5.0	2.38	0.014
UO_2-M42	2	1.78	0.001	5.4	2.40	0.014
UO_2-M42-PB	2	1.78	0.001	5.4	2.40	0.013
UO_2-KFA	2	1.78	0.002	5.3	2.39	0.012

Errors: N ± 10 %, R ± 0.02 Å

Within the experimental error, for all investigated uranyl humates identical structural parameters are determined (Tab. 2). Axial U-O bond distances amount to 1.78 Å. In the equatorial plane approximately five oxygen atoms are found at a mean distance of 2.39 Å.

For the synthetic, unmodified HAs (M1, M42) and for the natural, unmodified HAs (KHA, AHA) the EXAFS structural parameters are identical although the HAs differ somewhat in their proportion of functional groups (cf. Tab. 1) and in the content of aromatic structural elements. This shows that the synthetic HAs model the complexation behavior of natural HAs very well. Of course, also for KHA and KFA, isolated from the same source, the same structural parameters are determined.

The results, obtained for uranyl humates prepared from unmodified HAs at pH 2, are in good agreement with results of previous EXAFS studies (Denecke et al., 1997, 1998a) on uranyl humates prepared at pH <1 to 4.

Almost identical structural parameters are determined for solid uranyl humates prepared from modified HAs (HA-PB). In case of these modified HAs the phenolic OH groups are predominantly blocked and thus, primarily carboxylic groups are available for complexation of uranyl ions (cf. Tab. 1). The identical structural parameters, determined for modified and unmodified HAs, imply that the short-range order surrounding of the uranyl ion in all humates is comparable although the HAs differ in their phenolic OH/COOH-group ratio. This shows that predominantly the HA carboxylate groups are responsible for binding of uranyl ions under the experimental conditions applied in this study. Thus, the results from Reich et al. (1997) and Denecke et al. (1997), obtained for uranyl complexes with original HAs under comparable experimental conditions, are confirmed. A monodentate coordination of the HA carboxylic groups to uranyl ions follows both from the relatively short bond distances between uranium and equatorial oxygen atoms ($R_{U\text{-}Oeq}$) and from the fact that no carbonyl carbon atoms could be detected. This confirms the results of FTIR spectroscopy.

Furthermore, the EXAFS results show that, compared to carboxylic groups, the phenolic OH groups have only a minor or no influence on the complexation of uranyl ions at pH 2. This is supported by the analytical results of the uranyl humates (cf. Tab. 1), which show that the uranyl loading of the unmodified and of the corresponding modified HAs is correlated stronger with the carboxylic group content of the HAs than with the phenolic OH group content.

Similar results were found by Denecke et al. (1999) who studied the interaction of hafnium(IV) and thorium(IV) both with HA and with Bio-Rex70 at pH 1.6 by EXAFS. Bio-Rex70, a cation exchange resin having solely carboxylate groups, can serve as model

substance for HAs and is comparable with our modified HAs with blocked phenolic OH groups. The authors found similar structural parameters for metal complexes of HA and of Bio-Rex70. From this it was concluded that carboxylate groups are responsible for cation binding in HA and that phenolic OH groups play a subordinate role.

Contrary to the results obtained for the uranyl humate complexes where no influence of the blocking of the phenolic OH groups is detectable, an influence was found for low-molecular weight model compounds by Denecke et al. (1998b). EXAFS structural parameters were determined for two crystalline uranyl carboxylate compounds: first, disalicylatodioxo-uranium(VI), $UO_2[C_6H_4(COO)(OH)]_2$, which contains both carboxylate and phenolic OH groups and second, di-*o*-methoxybenzoatodioxouranium(VI), $UO_2[C_6H_4(COO)(OCH_3)]_2$, in which the phenolic OH group is blocked. Thus, having the same primary functional groups as HAs, these substances in principle could serve as model compounds for our unmodified and modified HAs. The authors found that in $UO_2[C_6H_4(COO)(OH)]_2$ only one to two bidentate coordinated carboxylate groups of the salicylate ligands are bound to uranium and that uranyl units must be linked since the equatorial uranium shell consists of five to six O_{eq} atoms at a distance of 2.42 Å. In $UO_2[C_6H_4(COO)(OCH_3)]_2$ the carboxylate groups were found to be monodentate coordinated ($R_{U\text{-}Oeq}$ = 2.29 Å). That means the blocking of the phenolic OH group by a methyl group changed the mode of coordination of the carboxylic group from bidentate to monodentate. This example shows that it is not always possible to use simple organic substances as structural models for HAs since they do not approach the complexity of HAs.

The influence of phenolic OH groups on the complexation behavior of HAs compared to carboxylic groups should increase with pH as it was shown, for instance, by an EXAFS study of the uranium(VI) complexation with protocatechuic acid (3,4-dihydroxybenzoic acid) as a function of pH (Roßberg et al., 2000a). It was found that at pH 4.3 the carboxylic group in the 1:1 complex is bidentate coordinated to the uranyl cation ($R_{U\text{-}Oeq}$ = 2.45 Å, $R_{U\text{-}Ceq}$ = 2.88 Å). With increasing pH value, the bond distance of the equatorial oxygen decreased. At pH values higher than 5, the ligands coordinate in an *o*-diphenolic bonding fashion to the uranyl cation, the carboxylic group is not longer involved in complexation ($R_{U\text{-}Oeq}$ = 2.36-2.38 Å).

This example shows also that bond distances determined for phenolic OH groups, that are coordinated to uranyl ions, can be similar to our $R_{U\text{-}Oeq}$ of the humates. Further EXAFS analyses of uranium(VI) complexes formed by compounds having solely neighboring phenolic OH but no carboxylic groups such as catechol (1,2-dihydroxybenzene) and pyrogallol (1,2,3-trihydroxybenzene) at pH 5 (Roßberg et al., 2000b) have shown that phenolic OH groups complex to the uranyl ion at a distance of 2.39-2.40 Å. Such a bond distance cannot be distinguished from $R_{U\text{-}Oeq}$ = 2.39 Å that was determined for the uranyl humates.

For the solid uranyl humates that were prepared at pH 2, we conclude that the complexation of uranyl ions is dominated by carboxylic groups of HAs. Phenolic OH groups seem to play a minor role although a contribution of HA phenolic OH groups to the complexation of uranyl ions cannot completely be excluded by EXAFS analysis. The reason is that structural parameters, determined by EXAFS analysis, always represent an average over all interactions between uranyl ions and HA molecules that have a complex and heterogeneous structure. The resulting broad distribution of $U\text{-}O_{eq}$ bond distances is evident in the large Debye-Waller factors (σ^2 = 0.013 Å^2) determined for $R_{U\text{-}Oeq}$ (cf. Tab. 2).
Thus, it is necessary to combine EXAFS with other structure-sensitive methods. This is supported by Korshin et al. (1998) who concluded from the lack of prominent and easily distinguishable features in the FT magnitudes of Cu^{2+}-HA complexes at R > 2.5 Å, that the EXAFS method alone cannot unambiguously determine the nature and structural properties of the atoms lying beyond the first complexation shell of metal-HA complexes.

4 Summary

Chemically modified HAs with blocked phenolic OH groups (HA-PB) were synthesized from various natural and synthetic HAs. Their phenolic OH group contents were 59-74 % lower than those of the corresponding unmodified HAs. The partial blocking of phenolic OH groups in the modified HAs was confirmed by FTIR spectroscopy. The uranyl complexation of the modified HAs at pH 2 was compared to that of the corresponding original, unmodified HAs.
The results of EXAFS analyses showed that the uranium-oxygen (U-O) bond distances are the same, within the experimental error, for uranyl humates prepared from unmodified and modi-

fied HAs. The uranium atom in the uranyl humates is surrounded by two O_{ax} and approximately five O_{eq} atoms at a distance of 1.78 and 2.39 Å, respectively.

Both by FTIR spectroscopy and by EXAFS analyses it could be confirmed that predominantly HA carboxylate groups are responsible for complexation of uranyl ions at pH 2. These carboxylate groups are monodentate coordinated to uranyl ions. The influence of phenolic OH groups is insignificant.

Since the influence of phenolic OH groups should increase with pH, further EXAFS studies on uranyl humate complexation should be performed at higher pH values, preferentially with a HA having a high phenolic OH/COOH-group ratio (e.g., HA type M1). However, then the hydrolysis of uranium has to be taken into account.

The present work has shown that the chemically modified HAs are useful model substances for studies of the complexation of actinides by humic substances. They can be applied to further improve the understanding of the nature of metal complexation sites in humic substances and particularly to clarify the role of phenolic OH versus COOH groups.

Acknowledgements

The authors thank M. Meyer and R. Ruske for their help in modification and characterization of HAs. Furthermore, the authors thank A. Roßberg, C. Hennig and H. Funke for their support during the EXAFS measurements, R. Nicolai for the FTIR measurements and W. Wiesener for ICP-MS analyses.

References

Bubner, M. and Heise, K.H. (1994) Characterization of Humic Acids. II. Characterization by Radioreagent-Derivatization with [^{14}C]Diazomethane. In: *FZR 43, Annual Report 1993*, Forschungszentrum Rossendorf, Institute of Radiochemistry, 22.

Choppin, G.R. and Allard, B. (1985) Complexes of Actinides with Naturally Occurring Organic Compounds. In: *Handbook on the Physics and Chemistry of the Actinides* (A.J. Freeman and C. Keller, eds.). Elsevier Science Publ., Amsterdam, 407.

Denecke, M.A., Pompe, S., Reich, T., Moll, H., Bubner, M., Heise, K.H., Nicolai, R., and Nitsche, H. (1997) Measurements of the Structural Parameters for the Interaction of Uranium(VI) with Natural and Synthetic Humic Acids using EXAFS. *Radiochim. Acta* **79**, 151.

Denecke, M.A., Reich, T., Pompe, S., Bubner, M., Heise, K.H., Nitsche, H., Allen, P.G., Bucher, J.J., Edelstein, N.M., Shuh, D.K., and Czerwinski, K.R. (1998a) EXAFS Investigations on the

Interaction of Humic Acids and Model Compounds with Uranyl Cations in Solid Complexes. *Radiochim. Acta* **82**, 103.

Denecke, M.A., Reich, T., Bubner, M., Pompe, S., Heise, K.H., Nitsche, H., Allen, P.G., Bucher, J.J., Edelstein, N.M., and Shuh, D.K. (1998b) Determination of Structural Parameters of Uranyl Ions Complexed with Organic Acids using EXAFS. *J. of Alloys and Compounds* **271-273**, 123.

Denecke, M.A., Bublitz, D., Kim, J.I., Moll, H., and Farkes, I. (1999) EXAFS Investigations of the Interaction of Hafnium and Thorium with Humic Acid and Bio-Rex70. *J. Synchrotron Rad.* **6**, 394.

Ephraim, J.H. and Marinsky, J.A. (1990) Ultrafiltration as a Technique for Studying Metal-Humate Interactions: Studies with Iron and Copper. *Anal. Chim. Acta* **232**, 171.

George, G.N. and Pickering, I.J. (1995) *EXAFSPAK: A Suite of Computer Programs for Analysis of X-ray Absorption Spectra.* Stanford Synchrotron Radiation Laboratory, Stanford, CA, USA.

Heise, K.H., Nicolai, R., Schmeide, K., Pompe, S., Bubner, M., Klöcking, R., Bernhard, G., and Nitsche, H. (2000) Infrared Study of Uranium(VI) Complexation with Natural and Synthetic Humic Acids. In preparation.

Kakihana, M., Nagumo, T., Okamoto, M., and Kakihana, H. (1987) Coordination Structures for Uranyl Carboxylate Complexes in Aqueous Solution Studied by IR and ^{13}C NMR Spectra. *J. Phys. Chem.* **91**, 6128.

Kim, J.I. and Buckau, G. (1988) Characterization of Reference and Site Specific Humic Acids. In: *RCM-Report 02188*, TU München, Institute of Radiochemistry.

Koningsberger, D.C. and Prins, R. (1988) *X-ray Absorption: Principles, Applications, Techniques of EXAFS, SEXAFS and XANES.* Wiley, New York.

Korshin, G.V., Frenkel, A.I., and Stern, E.A. (1998) EXAFS Study of the Inner Shell Structure in Copper(II) Complexes with Humic Substances. *Environ. Sci. Technol.* **32**, 2699.

Luster, J., Lloyd, T., and Sposito, G. (1996) Multi-Wavelength Molecular Fluorescence Spectrometry for Quantitative Characterization of Copper(II) and Aluminum(III) Complexation by Dissolved Organic Matter. *Environ. Sci. Technol.* **30**, 1565.

Pompe, S., Bubner, M., Denecke, M.A., Reich, T., Brachmann, A., Geipel, G., Nicolai, R., Heise, K.H., and Nitsche, H. (1996) A Comparison of Natural Humic Acids with Synthetic Humic Acid Model Substances: Characterization and Interaction with Uranium(VI). *Radiochim. Acta* **74**, 135.

Pompe, S., Brachmann, A., Bubner, M., Geipel, G., Heise, K.H., Bernhard, G. and Nitsche, H. (1998) Determination and Comparison of Uranyl Complexation Constants with Natural and Model Humic Acids. *Radiochim. Acta* **82**, 89.

Pompe, S., Schmeide, K., Bubner, M., Geipel, G., Heise, K.H., Bernhard, G. and Nitsche, H. (2000) Investigation of Humic Acid Complexation Behavior with Uranyl Ions Using Modified Synthetic and Natural Humic Acids. Radiochim. Acta, accepted.

Rehr, J.J., Albers, R.C., and Zabinsky, S.I. (1992) High-Order Multiple-Scattering Calculations of X-Ray Absorption Fine Structure. *Phys. Rev. Lett.* **69**, 3397.

Reich, T., Hudson, E.A., Denecke, M.A., Allen, P.G. and Nitsche, H. (1997) Structural Analysis of Uranium(VI) Complexes by X-ray Absorption Spectroscopy. *Poverkhnost* **4-5**, 149.

Roßberg, A., Reich, T., Hennig, C., Funke, H., Baraniak, L., Bernhard, G., and Nitsche, H. (2000a) Investigation to Determine the Main Complex Species in the Aqueous System of UO_2^{2+} with Protocatechuic Acid by EXAFS Spectroscopy. In: *FZR-285, Annual Report 1999*, Forschungszentrum Rossendorf, Institute of Radiochemistry, 63.

Roßberg, A., Baraniak, L., Reich, T., Hennig, C., Bernhard, G., and Nitsche, H. (2000b) EXAFS Structural Analysis of Aqueous Uranium(VI) Complexes with Wood Degradation Products. Radiochim. Acta, accepted.

Sarret, G., Manceau, A., Hazemann, J.L., Gomez, A., and Mench, M. (1997) EXAFS Study of the Nature of Zinc Complexation Sites in Humic Substances as a Function of Zn Concentration. *J. Phys. IV France 7*, (C2, X-Ray Absorption Fine Structure, Vol. 2), 799.

Schmeide, K., Zänker, H., Heise, K.H., and Nitsche, H. (1998) Isolation and Characterization of Aquatic Humic Substances from the Bog 'Kleiner Kranichsee'. In: *FZKA 6124, Wissenschaftliche Berichte*, (G. Buckau, ed.). Forschungszentrum Karlsruhe, 161.

Schmeide, K., Zänker, H., Hüttig, G., Heise, K.H., and Bernhard, G. (1999) Complexation of Aquatic Humic Substances from the Bog 'Kleiner Kranichsee' with Uranium(VI). In: *FZKA 6324, Wissenschaftliche Berichte*, (G. Buckau, ed.). Forschungszentrum Karlsruhe, 177.

Schnitzer, M. and Khan, S.U. (1972) *Humic Substances in the Environment* (A.D. McLaren, ed.). Marcel Dekker, Inc., New York.

Stevenson, F.J. (1994) *Humus Chemistry, Genesis, Composition, Reactions*. John Wiley & Sons, Inc., New York, ch. 16.

Annex 12

Reaction Parameters for the Reduction of Tc(VII) and for the Formation of Tc-Humic Substance Complexes with Natural Gorleben Water

(K. Geraedts, A. Maes and J. Vancluysen and (KUL))

3rd Technical Progress report

EC project

K.U.Leuven contribution to task 2 (complexation)

Effects of humic substances on the migration of radionuclides: complexation and transport of actinides

Reaction Parameters for the Reduction of Tc(VII) and for the formation of Tc-Humic Substance Complexes with Natural Gorleben Water

K. Geraedts, A. Maes, J. Vancluysen

K.U.Leuven

Departement Interfasechemie
Laboratorium voor Colloïdchemie
Kardinaal Mercierlaan 92, B-3001 Heverlee

1. Introduction

Under oxidising conditions, Technetium-99 will exist as pertechnetate (TcO_4^-), a highly soluble species, which does not interact with minerals or sediments [1]. However under reducing conditions and when suitable electron donors (eg. Fe(II)-containing minerals) are present, Tc(VII) will be reduced to Tc(IV) [2]. Depending on the total concentration, the reduced Tc(IV) will precipitate to $TcO_2.nH_2O$. When complexing agents are present, such as humic substances, the soluble Tc(IV) species can be associated with these humic substances and this process will result in an enhanced Tc solubility.

The reduction of Tc(VII) to Tc(IV) was previously demonstrated to be catalysed by Fe^{2+} present in reducing surfaces. The association between reduced Tc and humic substances was investigated [3] in presence of pyrite as the reducing surface, and was explained by a complexation reaction mechanism given by the following equation: $Tc_{(IV)}O^{2+}$ + HS $\Leftrightarrow$ $Tc_{(IV)}O^{2+}$-HS. K^{HS}-values of the order of 10^{18}-10^{20} were obtained.

In this contribution we further elaborate
(1) on the influence of the nature of the reducing surface, the nature of organic matter and the distribution of Tc between humic and fulvic acids.
(2) on the correctness of the aforementioned complexation reaction mechanism, by changing parameters such as pH, amount of humic substances and initial Tc concentration. For this purpose mainly Fe_3O_4 was used to exclude eventual interferences from S originating from surfaces such as FeS_2 and FeS.

2. Experimental set-up

All experiments were carried out at ambient temperature (22°C) in a controlled atmosphere glovebox flushed with a mixture of N_2 (95%) and H_2(5%) to minimise the intrusion of oxygen into the reaction vessels. The box atmosphere was circulated over a catalytic converter (Pt) in order to remove excessive oxygen. The mean concentration of O_2 in the glovebox throughout the experiments was below 2 ppm.

All chemicals used were of analytical grade and the water used was deionized, filtered by a Water Purification System (Milli-Q) and finally boiled out to obtain oxygen-free water. ^{99}Tc was purchased from Amersham in 0.1 M NH_4OH aqueous solution. TcO^-_4 solutions in $NaHCO_3$ (10^{-2} M) were prepared by diluting aliquots of a stock solution.

Unpurified organic matter from potential disposal sites was used. The first organic matter sample was Gorleben humic substance containing groundwater (Gohy 2227), which was used as supplied by FZK (Karlsruhe, Germany). The second organic matter sample was extracted from a Boom Clay sample supplied by SCK/CEN (Mol, Belgium) in the frame of the TRANCOM project. As a reference material also purified Na-salt Aldrich humic substances were used.

Magnetite (Fe_3O_4), siderite ($FeCO_3$) and pyrite (FeS_2) were purchased from a mineral shop. Small sized fractions (<125 µm) of the minerals were obtained by sieving after crushing the

solids in the glovebox using an Agate mortar and pestle. Synthetic pyrrhotite ($Fe^{II}S$) was purchased from the Aldrich Chemical Corporation.

The Tc-humate complexation was studied by measuring the enhanced Tc-solubility of a TcO_2 precipitate due to Tc-humate formation

a) in synthetic reducing systems containing a solid (FeS_2, $FeCO_3$, Fe_3O_4 and FeS) suspended in Gorleben Water, and
b) in labscale natural systems containing Gorleben sand and Gorleben groundwater (GoHy 2227).

The reaction is followed as a function of time and at different pH values. Different polypropylene vials were prepared, containing 50 (± 1) mg of the minerals (or between 5 and 20 (± 0.1) g Gorleben Sand) and 20 ml volumes of a prepared solution. These solutions contained 19 ml Gorleben Water and 1 ml of a pertechnetate solution in 10^{-2} M $NaHCO_3$. As a reference for the synthetic systems, also experiments without organic matter were conducted in Synthetic Gorleben Water, a slightly alkaline solution composed of $8x10^{-3}$ M $NaHCO_3$ and $4x10^{-2}$ M NaCl. By diluting the original Gorleben Water with Synthetic Gorleben Water, experiments with different amounts of organic matter could be conducted. The initial TcO_4^- concentration was varied between $1x10^{-7}$ M and $5x10^{-5}$ M. The vials were turned slowly head over head to ensure good mixing. After certain periods of time the minerals and solutions were separated by centrifugation (30 min, 18000 tpm for the synthetic systems and 15 min, 7000 tpm for the natural systems) before being analysed.

The centrifuged samples were analysed for ^{99}Tc in a Packard Liquid Scintillation Analyser using Ultima Gold Liquid Scintillation Cocktail (Packard). The pH measurements were made by a Portatest 655 and a WTW SenTix 50 glass electrode, and the redox potentials were monitored by a combined redox Toledo Mettler P14805-DXK-S8/120 electrode connected to the Portatest 655. The speciation of Tc in the supernatant solution was determined from Gel Permeation Chromatography and/or from a newly developed method as described hereafter.

Tc speciation in solution from gel permeation chromatography

Separation of the TcO_4^-/Tc-humic fraction was determined by gel permeation chromatography. This was carried out by eluting a 1 ml sample over a glass column (30x1 cm), filled with Superdex 30 Prep Grade gel (Pharmacia Biotech). The eluent was a saline NaCl solution (0.15 M containing 0.002% NaN_3). The U.V.-absorbance (at 254 nm) was measured continuously and the collected fractions were β-monitored radiometrically for their Tc-levels.

Previous investigations [3,4] always used Gel Permeation Chromatography to investigate whether the Tc remaining in solution was associated with organic matter or was present as free Tc(IV) species (TcO^{2+}, $TcO(OH)^+$, $TcO(OH)_2$, ...) or a combination of not reduced pertechnetate and free Tc(IV) species. This method is time consuming and unfortunately not very useful in the case of Gorleben organic matter because only 5% of these humic substances eluted from the column. Therefore it was necessary to develop another method.

La-organic matter precipitation method

This new method is based on the assumption that trivalent ions such as La^{3+}, Eu^{3+} and Al^{3+} are able to precipitate organic matter. The following procedure was used: after centrifugation, an aliquot of the supernatant was analysed for total Tc concentration. To another aliquot of the supernatant 1 N $LaCl_3$ was added to precipitate the organic matter. After centrifugation (20 min, 6000 rpm), the supernatant was assayed for ^{99}Tc. The countrate in the supernatant is entirely due to the presence of free Tc species. Hence, the concentration of the Tc-HS complexes is obtained as the difference between the total concentration and the concentration in the humic substance free supernatant.

Tc distribution between humic and fulvic acids

To investigate the distribution of Tc between humic and fulvic acids, the pH of an aliquot (3 ml) of the supernatant was brought below pH 2. This induces a precipitation of the humic acids only. After centrifugation, the Tc content of the supernatant is due to Tc associated with fulvic acids and free Tc species. The distribution between the humic and the fulvic acids can be calculated from the knowledge of the total concentration of Tc in solution and the concentration of the Tc-humic fraction and the Tc associated with total humic substances (humic and fulvic acids) from La-organic matter precipitation.

3. Results

3.1.Alternative speciation method for Tc in solution

The use of La^{3+} to precipitate all humic substances and thus also the Tc associated with humic substances was verified for organic matter from Boom Clay, from Gorleben and from a Podzol. Only one GPC was made for experiments with Gorleben humic substances, because as mentioned before, only 5% of the humic substances eluted from the column.

	%Tc - HS GPC	%Tc - HS La^{3+}
Boom Clay	5.33	6.88
Boom Clay	23.81	24.95
Boom Clay	71.69	68.63
Boom Clay	79.84	62.83
Boom Clay	83.33	86.13
Gorleben	98	93
Podzol	84	84.7
Podzol	91.5	92.6

Table 1: Comparison of the fraction of Tc associated with HS as determined from GPC and La^{3+} precipitation.

The fraction of Tc in solution associated with humic substances is calculated using the two methods (GPC and La^{3+} precipitation). Table 1 summarises the obtained results, and

demonstrates that La^{3+}-organic matter precipitation is a good and quick alternative for Gel Permeation Chromatography.

3.2.The association of Tc(IV) with humic substances: possible interfering parameters

Previous investigations [3, 4] have shown the reduction of pertechnetate to Tc(IV) when suitable conditions are present (such as a reducing surface and the presence of co-ordinatively bound Fe^{2+}). Depending on the concentration, Tc(IV) will precipitate as TcO_2. The resulting Tc concentration in solution was in agreement with the formation of a TcO_2 precipitate.

Reduction in presence of humic substances also resulted in the formation of a TcO_2 precipitate but with an enhanced Tc solubility due to an association between humic substances and soluble Tc(IV) species (presumably, TcO^{2+}).

In this section, different parameters interfering in the redox reaction and Tc-HS are further investigated.

3.2.1. Influence of the nature of the reducing surface

a) Synthetic systems

Only pyrite was previously [4] used as reducing surface to investigate the association between Tc(IV) and humic substances from Gorleben and Boom Clay. The influence of the nature of the surface was further investigated by studying magnetite (Fe_3O_4), pyrrhotite (FeS) and siderite ($FeCO_3$) in presence of Gorleben Water. In all experiments, an initial Tc concentration of $5x10^{-6}$ M was used. Figure 1 shows the large differences in the reduction kinetics and extent of reduction of TcO_4^- dissolved in Gorleben water and in presence of the 4 studied surfaces.

In absence of humic substances a quick (less than 3 hours) and complete reduction of TcO_4^- was observed for the different surfaces. This is demonstrated in figure 2 for the case of magnetite. The reduction kinetics slows down in presence of humic substances, but equilibrium seems to be reached in all cases. The speciation of Tc at equilibrium was measured by the La^{3+}-organic matter precipitation method and is given in table 2 as the free Tc and Tc-HS concentration together with the reaction parameters pH, Eh and humate concentration. The humic substances concentration was calculated from Absorbance measurements (rendering g HS/l) and a value of 3 mEq/l was taken for the proton exchange capacity.

	pH	Eh	[HS] eq/l	Free [Tc] M	[Tc-HS] M
Pyrite	9.5	-270	$4.8x10^{-4}$	$2x10^{-8}$	$2x10^{-6}$
Magnetite	8 - 10	-200	$4.5x10^{-4}$	$3x10^{-8}$	$1 - 2.2 x10^{-6}$
Siderite	9.4	-200	$4.7x10^{-4}$	$4x10^{-8}$	$2.5x10^{-6}$
Pyrrhotite	8.8	-235	$4.5x10^{-4}$	$4x10^{-9}$	$1.9x10^{-8}$

Table 2: Results of equilibrium Tc speciation in batch experiments with pyrite, magnetite, siderite and pyrrhotite as reducing surfaces and Gorleben Water.

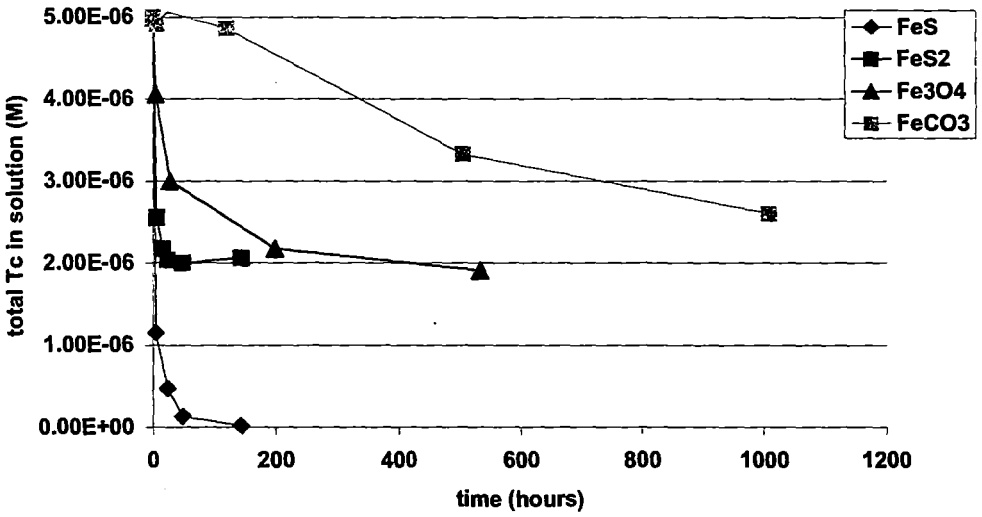

Figure 1: Total Tc in solution versus time for 4 different batch experiments: FeS, FeS_2, Fe3O4 and $FeCO_3$ and Gorleben Water with $[Tc]_{initial} = 5x10^{-6}$ M.

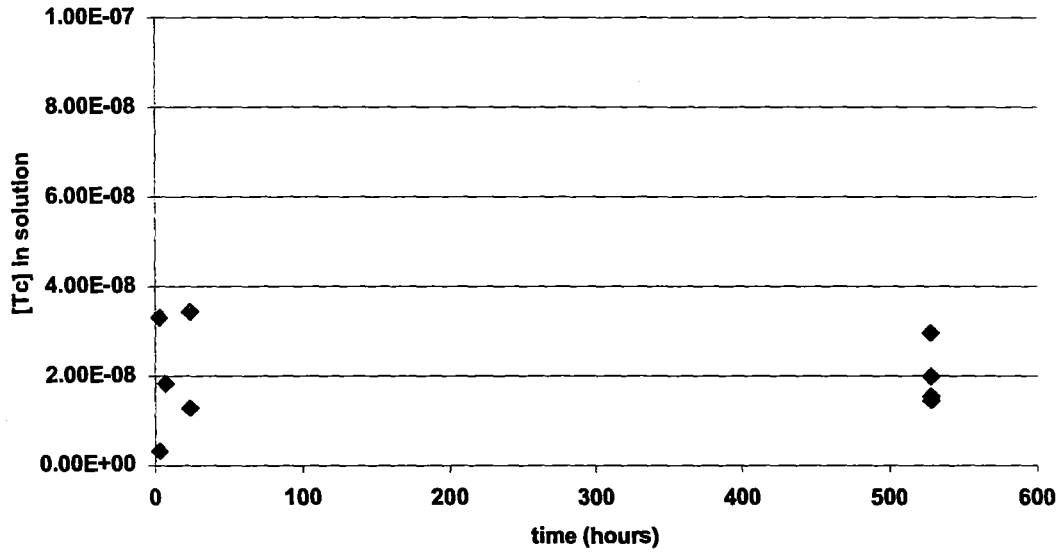

Figure 2: Total Tc in solution versus time for batch experiments with magnetite and synthetic Gorleben Water. $[TcO_4^-]_{initial} = 5x10^{-6}$ M.

Table 2 shows that in the cases of pyrite, magnetite and siderite the free Tc concentration ranged from 2 to 4x10-8 M, hence was of the order of the solubility level of Tc species in equilibrium with a TcO_2 precipitate. Similarly the equilibrium Tc-HS concentrations are of the same magnitude in the cases of pyrite, siderite and magnetite. The small differences that are noticeable are due to different pH conditions (see also 3.2.3: Variation with pH).

The above results indicate that the three surfaces - pyrite, siderite and magnetite - behave similarly with respect to the reduction of pertechnetate and with respect to the complexation of Tc(IV) with humic substances. These surfaces are only acting as electron donors in the overall redox and complexation reaction. They do not seem to have any specific influence on the complexation between Tc(IV) and humic substances.

As seen in table 2, the results in presence of pyrrhotite deviate from those obtained in presence of the 3 other surfaces. In the case of pyrrhotite (FeS) a lower free Tc level and a significantly lower amount of Tc-HS was observed. Probably an amorphous Tc-Sulphide is formed with a lower solubility than $TcO_2.nH_2O$.

b) Labscale natural systems

It was previously shown [3,4] that TcO_4^- reduction and Tc-HS association only occurred in presence of a reducing surface. The aim of the following experiments was therefore to verify whether these findings also apply for the case of Gorleben Sand in presence of Gorleben Water. This system becomes gradually reducing with time and was able to reduce Np(V) to Np(IV) [5].

Batch experiments were conducted in which the time of pre-equilibration of the Gorleben Sand with Gorleben groundwater was varied before the addition of TcO_4^-.

Systems with a long pre-equilibrium period (47 days) (see figure 3) show immediate reduction to

1) a constant free Tc level in solution of $3x10^{-8}$ M in agreement with the solubility level in presence of a TcO_2 precipitate

and to

2) a constant Tc-HS concentration of $3x10^{-6}$ M.

The Tc behaviour in the labscale natural systems is consequently comparable to - and in agreement with observations made in the synthetic systems.

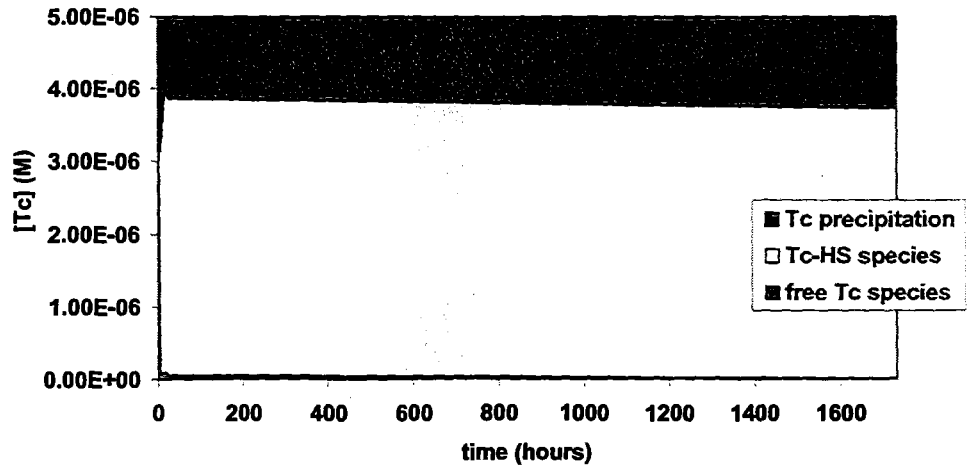

Figure 3: Tc speciation versus time in batch experiments with Gorleben Sand and Gorleben organic matter. Systems with long pre-equilibrium time (47 days). pH = 7.8.

Systems with a short pre-equilibrium time (4 days), see figure 4, do not lead to the equilibrium expected on the basis of the results with long pre-equilibrium times, despite the fact that the total time span of the experiment (1500 hours) exceeded the long pre-equilibrium period (336 hours). Indeed, the free Tc concentration (TcO_4^- + dissolved Tc(IV) species) gradually decreased with time but did not reach the solubility level ($3x10^{-8}$ M) observed in systems with long pre-equilibrium time. Unexpectedly and for unknown reasons the Tc-HS fraction remains constant while the reduction proceeds. Apparently the formation of a Tc-precipitate is favoured.

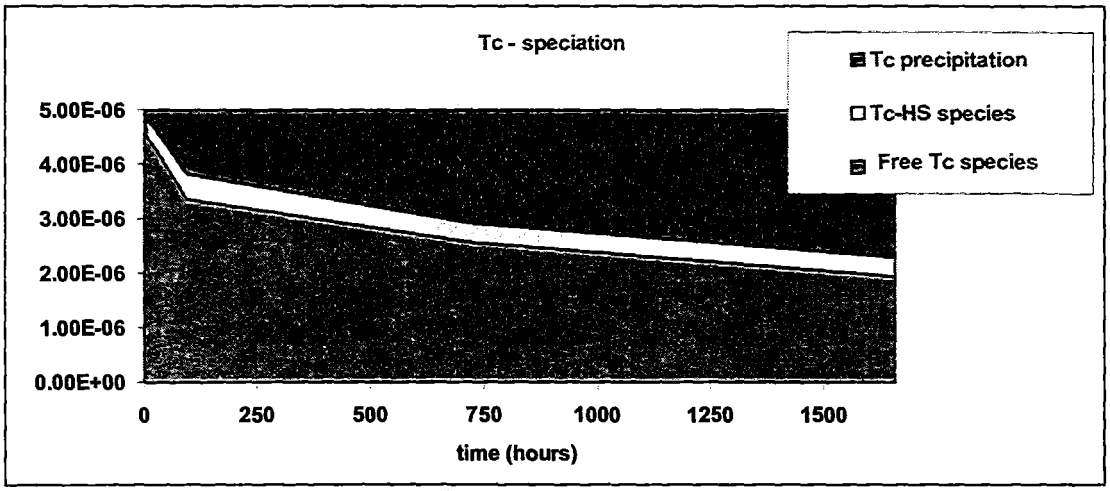

Figure 4: Tc speciation versus time in batch experiments with Gorleben Sand and Gorleben organic matter. Systems with a short pre-equilibrium time (4 days) of Gorleben Sand and Gorleben Water. pH = 8.

3.2.2. Influence of organic matter nature

Experiments with purified Aldrich humic substances in Synthetic Gorleben Water (hence absence of Gorleben organic matter) were conducted at an initial Tc concentration of $5x10^{-6}$ M. 200 and 400 ppm Aldrich humic substances were added. In a second series of experiments, also $5x10^{-6}$ M $Fe^{2+}$was added as a trial to induce redox properties in the Aldrich humic substances.

As can be observed from figure 5, TcO_4^- is completely reduced to TcO_2 in presence of magnetite suspended in Synthetic Gorleben Water (absence of organic matter).

The presence of 200 or 400 ppm purified humic substances from Aldrich prohibits the TcO4-reduction. Indeed all Tc remains in solution and speciation of the supernatant solutions with La^{3+}-precipiation revealed the complete absence of association of Tc and the humic substances.

However, if Fe^{2+} ($5x10^{-6}$ M) was added to the previous system with 200 ppm Aldrich humic acids a slow reduction was observed as is obvious in figure 6. Notice for comparison that the reduction was complete after 200 hours contact time when magnetite was contacted with natural Gorleben Water.

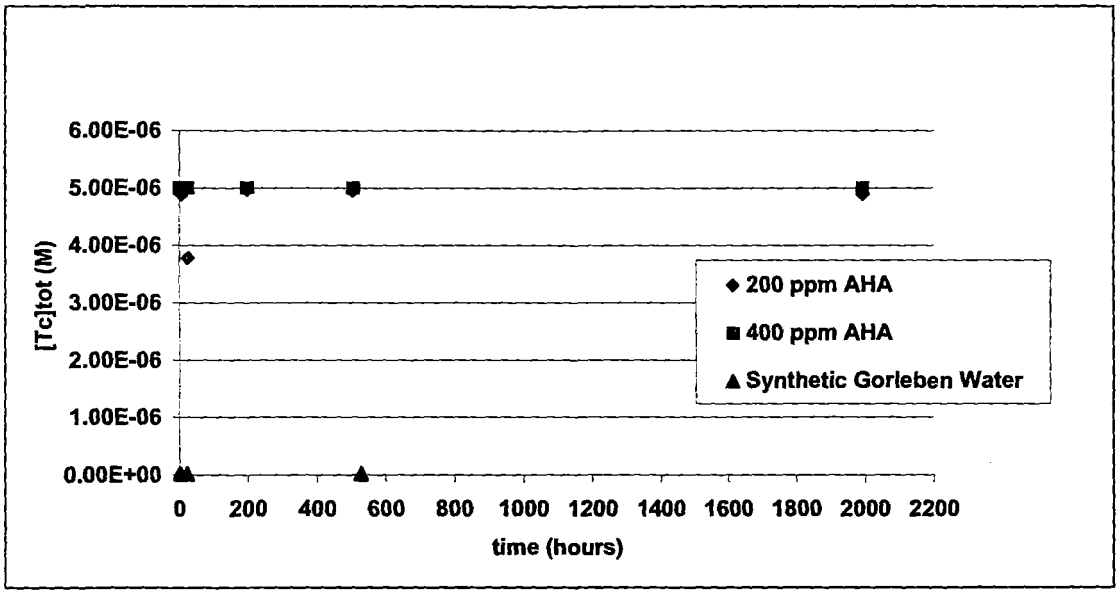

Figure 5: Influence of Aldrich humic acid (0, 200, 400 ppm) dissolved in synthetic Gorleben Water on the reduction of $5x10^{-6}$ M pertechnetate in presence of magnetite.

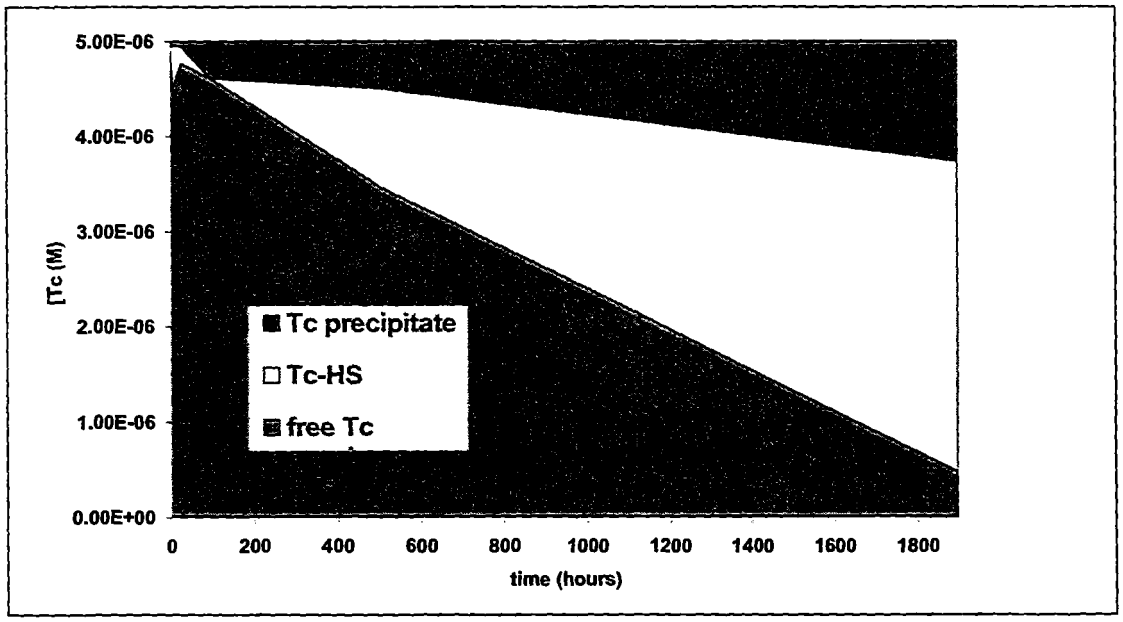

Figure 6. Tc species followed as a function of time for magnetite in presence of 200 ppm Aldrich humic acid and $5x10^{-6}$ M Fe^{2+}. $[TcO_4^-]_{initial}$ = $5x10^{-6}$ M and pH = 9.5.

The foregoing results illustrate that purified humic acids have lost their reducing power and in addition "de-activate" the redox active magnetite surface to reduce TcO_4^-. The detailed processes involved are speculative at present. The reducing activity of the system may however be partly restored by the addition of Fe^{2+}. The results thus again demonstrate the involvement of Fe^{2+} in the reduction process.

3.2.3. *Influence of micro-organisms*

The previous experiments were all conducted with Gorleben Water which was used as obtained from FZK. In a next series of experiments, the contribution of micro-organisms to the reduction process is minimised by filtering the water through a 0.45 µm filter. Under these conditions the micro-organisms are assumed to be removed. Batch experiments with magnetite as the reducing solid phase and the filtered Gorleben water were conducted and can be compared with similar previous experiments in which unfiltered Gorleben Water was used. The initial TcO_4^- concentration was $5x10^{-6}$ M.

The variation of the total Tc concentration in the filtered solution with time is represented in figure 7. As a reference, also the results from an experiment with magnetite and unfiltered Gorleben water are shown. The Tc speciation versus time measured in the previous systems, in which filtered Gorleben water was used, is shown in figure 8a. For comparison figure 8b shows the speciation in the case of using unfiltered water. Filtering of the water over 0.45µm has only a slight influence on the Tc concentration associated with HS (Tc-HS): $3x10^{-6}$ M Tc-HS (filtered) compared to $2x10^{-6}$ M (unfiltered). However a large difference in the free Tc concentration is observed between filtered ($4x10^{-7}$ M Tc) and unfiltered ($3x10^{-8}$ M Tc) systems. This result suggests that the reduction was incomplete because the free Tc concentration ($4x10^{-7}$ M Tc) exceeds the concentration o $3x10^{-8}$ M Tc in theoretical equilibrium with TcO_2 precipitate. Thus the difference in concentration between $4x10^{-7}$ M and $3x10^{-8}$ M is probably present as TcO_4^-. Speciation calculation by CHESS however points out that no TcO_4^- is expected under the conditions of the experiments.

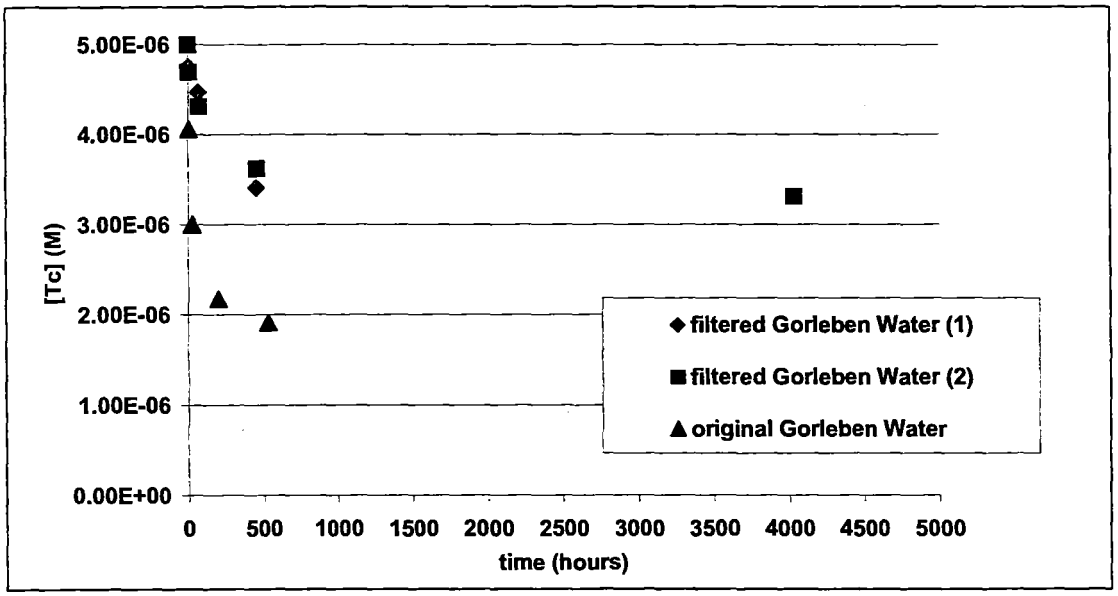

Figure 7: Total Tc in solution versus time in batch experiments with magnetite as reducing phase and filtered (two independent experiments) and unfiltered Gorleben Water.

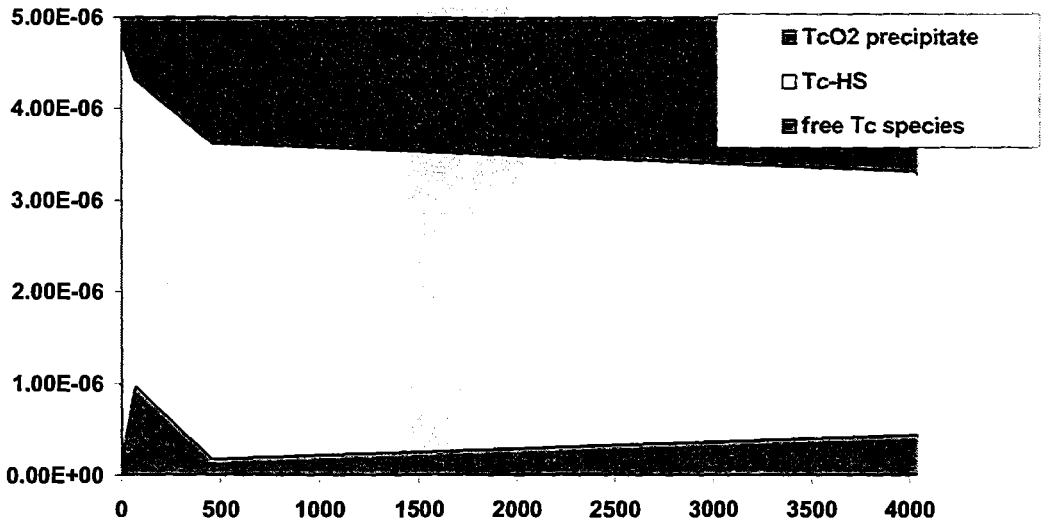

Figure 8a: Speciation of Tc versus time in batch experiments with magnetite and filtered Gorleben Water. Total TcO_4^- added = $5x10^{-6}$ M

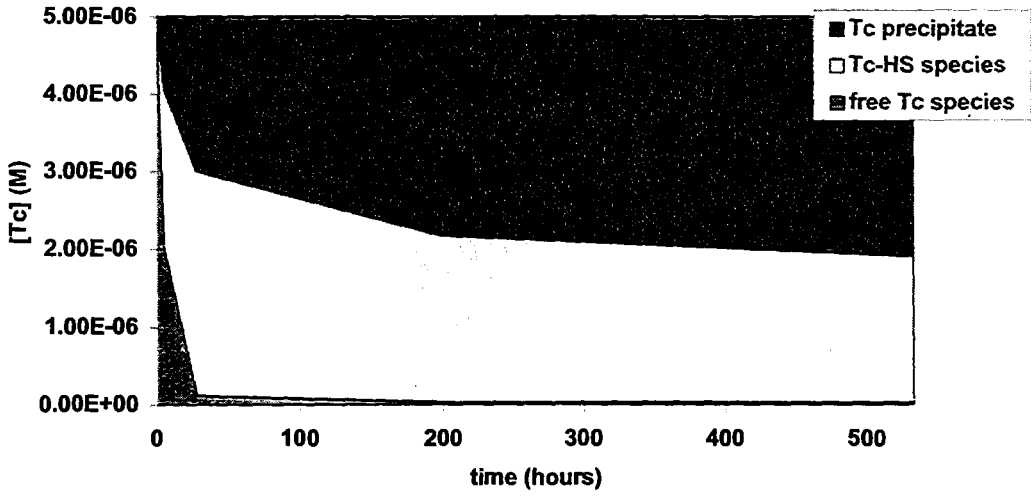

Figure 8b: Speciation of Tc versus time in batch experiments with magnetite and unfiltered Gorleben Water. Total TcO_4^- added = $5x10^{-6}$ M

Since no measurable reduction of TcO_4^- was observed in absence of Fe_3O_4 [4] it is tempting to neglect the contribution of micro-organisms to the reduction process.

An important observation in the experiments with filtered water is that after more than 4000 hours of equilibration, the pH of the supernatant was still equal to the starting pH of the experiment (pH=9.6). In the experiments with unfiltered water, the pH raised slowly from 9.6

to 10.2. This observation at least points to an interference of either 'particulate' matter larger than 0.45µm or 'micro-organisms' resulting in a pH increase.

3.2.4. Conclusions

Investigations were made on the influences of the reducing surfaces, the nature of organic matter and the involvement of micro-organisms.

1) Pyrite, siderite, magnetite and natural Gorleben Sand behave similar with respect to the reduction of Tc(VII) to Tc(IV) and the complexation of Tc(IV) with humic substances present in natural Gorleben Water. Only pyrrhotite showed a different behaviour.
2) Purified Aldrich humic acids are unable to reduce Tc(VII) and prohibit the reduction in presence of Fe_3O_4. Fe^{2+} added to the purified Aldrich HA (partially) restored the reduction potential of Fe_3O_4, demonstrating the involvement of Fe^{2+} in the reduction process.
3) Micro-organisms have no direct effect on the reduction of TcO4- and the subsequent complexation of Tc(IV) with humic substances.

3.3. Reverse equilibrium approach

An alternative approach to investigate the interaction of Tc(IV) with humic substances is to start from a TcO_2 precipitate and to study the Tc-HS interaction by measuring the Tc solubilisation in presence of humic substances.

A TcO_2 precipitate was first prepared by contacting TcO_4^- with magnetite. Subsequently humic substances were added as natural Gorleben groundwater. Tc, HS, pH and Eh were followed during about 300 days.

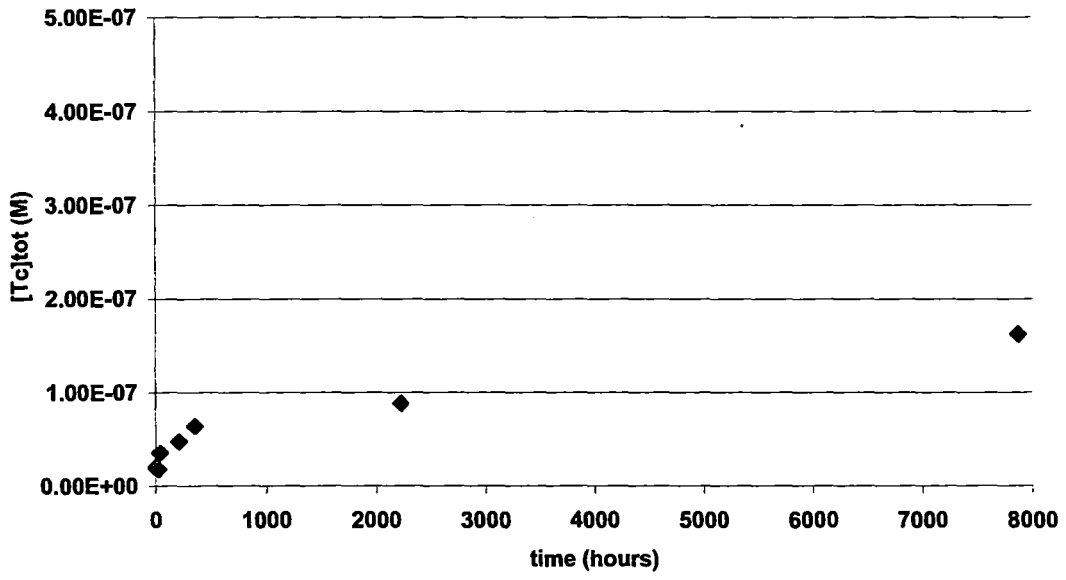

Figure 9: Total Tc concentration in solution versus time upon contacting natural Gorleben Water with a previously prepared TcO_2 precipitate.

Figure 9 shows a slowly increasing solubility of Tc with time. Speciation of the solution reveals that most of the Tc is associated with the organic matter. The amount of Tc, not associated with the humic substances was equal to $3x10^{-8}$ M and therefore in agreement with the Tc(IV) solubility in presence of a $TcO_2.nH_2O$ precipitate.

Comparison of the Tc-HS concentration observed in previous systems (starting from TcO4-) with the present systems (starting from TcO_2 precipitate) reveals that the former lead to Tc-HS concentrations of the order of $2x10^{-6}$ M, which largely exceeds the present Tc-HS concentration of $2x10^{-7}$ M. It seems therefore that resolubilisation is a very slow process.

3.4. Distribution of Tc between humic and fulvic acids.

The distribution of Tc(IV) between the humic and fulvic acids present in Gorleben Water has been measured in both synthetic (eg. magnetite surface) and natural systems (Gorleben Sand). The purpose was to detect eventual differences in the strength of Tc - association with each of these components.

Figure 10 shows the average of the Tc(IV) distribution between humic and fulvic acids on a total of 40 different experimental systems. The result is 20 (±10) % of Tc in solution is associated with fulvic acids and 80 (±10)% is associated with the humic acids. The humics in Gorleben Water have a composition of about 90% humic acids and 10% fulvic acids [6]. The present findings point to a slight preference for the formation of Tc(IV) fulvic acid complexes.

However, the standard deviation on the foregoing results was 10% and was due to a large variability in the systems with magnetite as reducing phase. In these cases, fractions of Tc associated with the fulvic acids varied between 5 and 60%.

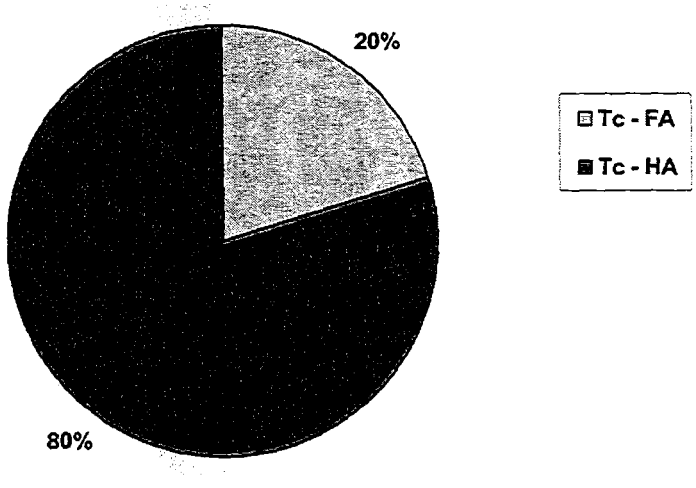

Figure 10. Mean association of Tc(IV) with fulvic and humic acids observed for 40 experimental points.

If only the observations for the natural systems are considered, a distribution of respectively 9 (±2)% and 91 (±2)% for fulvic and humic acids is obtained. In this case, Tc (IV) shows no preference for fulvic or humic acids.

3.5. Quantitative determination of the interaction constant of Tc with HS.

The observed association between Tc and humics was previously [3] interpreted and described by a complexation reaction mechanism between TcO^{2+} and humic substances. Alternatively all soluble Tc(IV) species (TcO^{2+}, $TcO(OH)^{+}$, ...) were also assumed to interact with humics. Interaction constants K^{HS} were calculated for both assumptions: K^{HS}- values of the order of 10^{21} for the association of TcO^{2+} and HS and of the order 10^{5} in the second case (K^{HS}_{TOT}) were obtained for Gorleben humic substances in presence of pyrite as reducing surface. Hereafter we apply the same reaction mechanism for results obtained with different reducing surfaces

3.5.1. Theoretical background

The solubility of Tc(IV) at sufficiently low redox potentials (~ -200 mV) and in equilibrium with $TcO_2.nH_2O$ precipitate can be calculated from the following hydrolysis equilibria:

$$Tc_{IV}O^{2+} + H_2O \overset{10^{-1.14}}{\Leftrightarrow} TcO(OH)^{+} + H^{+}$$

$$Tc_{IV}O^{2+} + 3\,H_2O \overset{10^{-3.3}}{\Leftrightarrow} TcO(OH)_2 + 2\,H^{+}$$

$$2\,Tc_{IV}O^{2+} + 4\,H_2O \overset{10^{-0.13}}{\Leftrightarrow} (TcO(OH)_2)_2 + 2\,H^{+}$$

$$Tc_{IV}O^{2+} + 3\,H_2O \overset{10^{4.23}}{\Leftrightarrow} TcO_2.2H_2O(am) + 2\,H^{+}$$

The K values refer to zero ionic strength.

The total solubility of Tc in absence of humic substances is predicted to be:

$$Tc_{TOT} = [TcO^{2+}] + [TcO(OH)] + [TcO(OH)_2] + [(TcO(OH)_2)_2]$$

$$= [TcO^{2+}](1 + 10^{-1.14}/(H^{+}) + 10^{-3.3}/(H^{+})^2 + 10^{-0.13}[TcO^{2+}]/(H^{+})^4)$$

$$= 10^{-4.23}\,(H^{+})^2(1 + 10^{-1.14}/(H^{+}) + 10^{-3.3}/(H^{+})^2 + 10^{-4.36}/(H^{+})^2)$$

(H^{+}) stands for the proton activity.

In presence of humic substances we assume the following complexation reaction:

$$TcO^{2+} + HS \overset{K^{HS}}{\Leftrightarrow} TcO^{2+} - HS$$

The equilibrium constant K^{HS} for this reaction is $K^{HS} = \frac{[TcO2+-HS]}{[TcO2+][HS]}$, in which the Tc species are given in mol/l and [HS] is expressed in Eq/l. The proton charge estimated from the end point (around pH 7) of an acid base titration is used.

In presence of humic substances the Tc solubility is enhanced by the formation of TcO^{2+}- HS. Tc_{TOT} extends to:

$$Tc_{tot}^{HS} = [TcO^{2+}] + [TcO(OH)^{+}] + [TcO(OH)_2] + [(TcO(OH)_2)_2] + [TcO^{2+} - HS]$$

$$= 10^{-4.23} (H^{+})^2(1 + 10^{-1.14}/(H^{+}) + 10^{-3.3}/(H^{+})^2 + 10^{-4.36}/(H^{+})^2 + K^{HS} [HS])$$

The correctness of the aforementioned complexation reaction is unverified at present. We do not know which Tc(IV) species interacts with the available humic substances.

3.5.2. Calculation of K values for the different experiments

In all previously described experiments, an initial Tc concentration of $5x10^{-6}$ M was used. In table 3, an overview is given of reaction parameters and the K^{HS} and K^{HS}_{TOT}-values calculated for (near) equilibrium conditions and relating to the interaction of Gorleben HS (natural Gorleben Water) with Tc(IV) as catalysed by various reducing surfaces.

Reducing medium	**pH**	**Eh**	**K^{HS}**
Pyrite	9.5	-270	$7x10^{20}$
Magnetite	8 - 10	-200	$10^{19} - 10^{21}$
Siderite	9.4	-200	$4.6x10^{20}$
Pyrrhotite	8.8	-235	$(2.3x10^{17})$
Gorleben Sand	7 - 10	-250	$5x10^{16} - 10^{21}$

Table 3: Range of values observed for the interaction of Tc(IV) with HS form Gorleben after reduction of $5x10^{-6}$ M TcO_4^- in presence of different reducing surfaces.

In the case of pyrite, magnetite, siderite and Gorleben Sand similar K^{HS}-values of the order of $10^{20} - 10^{21}$ are obtained. The differences in K^{HS}-values are due to differences in pH (see also 3.6.1, variation of pH).

Only in the case of pyrrhotite, a significantly lower K^{HS}-value was obtained. This observation is probably due to the formation of a Tc-sulphide precipitate induced by the presence of FeS. Therefore the calculated K values (given in brackets in tables 3) largely deviate from the others, which were based on the assumption of a TcO_2 precipitate. Although pyrite is also a

sulphur bearing surface the observed K values agree with those of non sulphur bearing reducing surfaces (magnetite and siderite). A possible explanation is that the solubility is FeS_2 is orders of magnitude lower than the solubility of FeS and thus may kinetically limit the formation of TcS_2.

3.6. Verification of proposed reaction mechanism.

In this section, we try to validate the proposed complexation reaction mechanism by investigating the influence of parameters such as pH, concentration of humic substances and initial concentration of TcO_4^- on the value of K^{HS}.

3.6.1. Variation with pH.

Additional experiments were conducted in a pH range from 8 till 10.5 for synthetic systems (magnetite and Natural Gorleben Water) and from 7 till 10.5 for natural systems (Gorleben Sand and Natural Gorleben Water). Lower pH values were obtained by adding known volumes of HCl ($1.5x10^{-2}$ M). The systems initially contained $5x10^{-6}$ M TcO_4^- and were allowed to equilibrate during 14 days. Previous kinetic experiments showed that equilibrium was reached during this time period.

The amount of Tc remaining in the solution after La^{3+}-orgnaic matter precipitation, in each case, proved to correspond to the expected solubility ($3x10^{-8}$ M).

Figure 11 shows the pH dependency of the K^{HS}. Previously obtained results are also incorporated in the figure. The K^{HS} varies linearly between $10^{15.5}$ at pH 7.2 to 10^{22} at pH 10.2. The regression line has the following equation: log K^{HS} = 2.145*pH + 0.335 with R^2 = 0.9937.

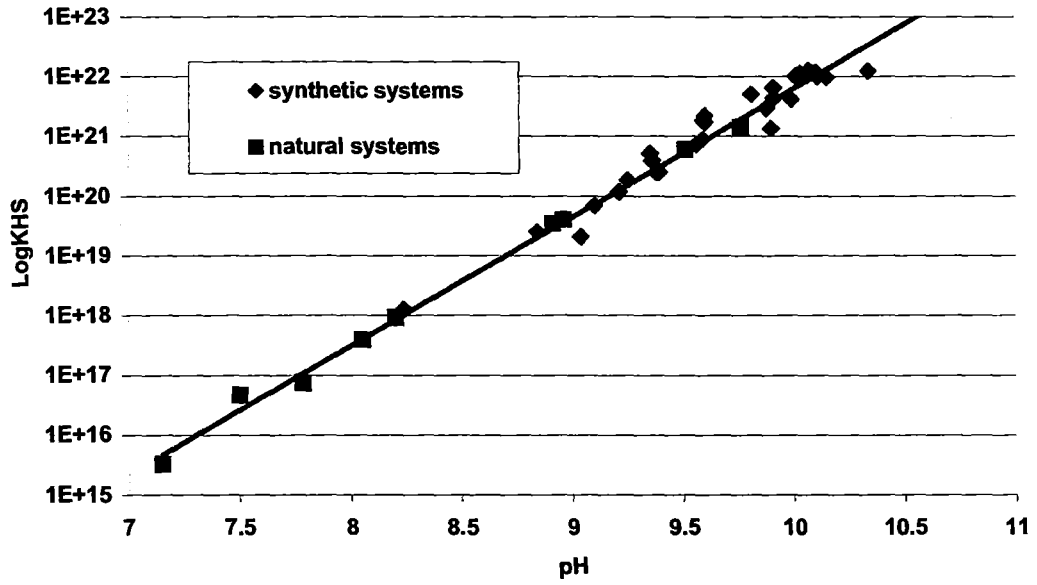

Figure 11: Log K^{HS} versus pH in synthetic systems (magnetite and Natural Gorleben Water) and natural systems (Gorleben Sand and Natural Gorleben Water).

The observation that the K value linear increases with pH is not a surprise since this behaviour is frequently observed for humic substances metal complexation [7].

Since all results refer to the same humic substances concentration, the LogKHS versus pH plot is similar to a Kurbatov plot. Therefore the slope of 2 indicates that 2 H^+ are liberated in the reaction.

Rewriting the reaction equilibrium equation as:

$$TcO^{2+} + HS \overset{K_H}{\Leftrightarrow} TcO^{2+}\text{-}HS + 2\,H^+$$

and recalculation of the data leads to the variation of $LogK_H$ with pH shown in figure 12.

A rather constant Log K_H = 1.7 is obtained. Since we do not know the exact nature of the functional groups involved in the complexation reaction, nor their H^+ dissociation constant, we did not make corrections for the dissociation of the complexing ligands at present. It seems however plausible that TcO^{2+} reacts with surface OH groups.

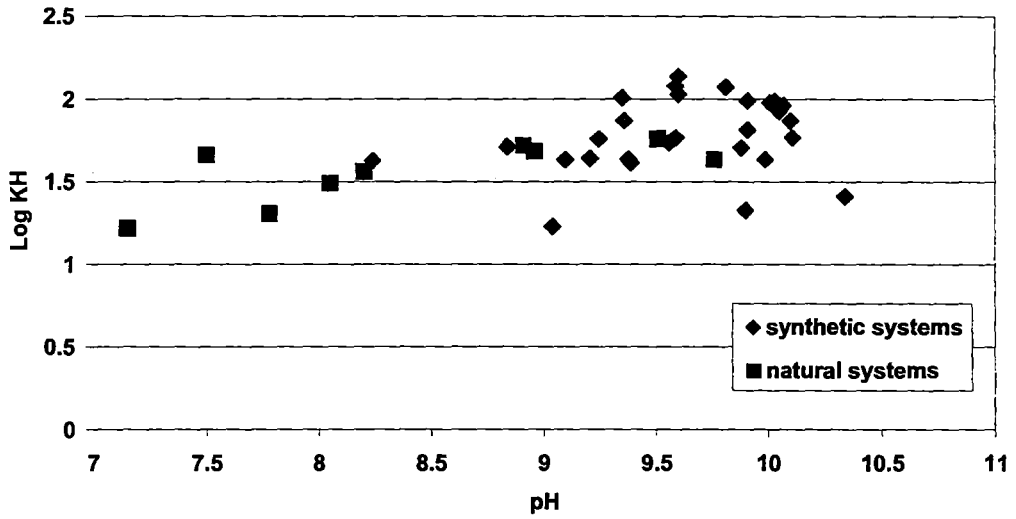

Figure 12: Log KH versus pH in synthetic systems (magnetite and Natural Gorleben Water) and natural systems (Gorleben Sand and Natural Gorleben Water).

3.6.2. Variation with HS concentration

In theory, K^{HS} values should be independent of the concentration of the humic substances.

Varying HS concentrations were obtained by diluting natural Gorleben groundwater with Synthetic Gorleben Water to respectively 75, 50, 25 and 10% of the initial HS concentration. All experiments were conducted in presence of pyrite.

The K^{HS} values, calculated at equilibrium, are given in table 4 together with similar previously published values (marked with $^{(*)}$).

% of initial HS concentration	pH	Eh	K^{HS}
100%	10.19	-306	10^{22}
100% (*)	9.4	-300	$3.8x10^{20}$
75%	9.84	-285	$1.5x10^{21}$
50%	9.45	-273	$7.3x10^{20}$
50 % (*)	9.2	-280	$2.7x10^{20}$
25%	9.33	-200	$2x10^{20}$
10%	8.4	-162	$9x10^{18}$
10% (*)	9.0	-200	$3x10^{20}$

Table 4: K^{HS} values observed for batch experiments with pyrite and different concentrations of Gorleben humic substances.

From table 4, differences are noticeable between the observed K^{HS} values, however as demonstrated in the previous section, these differences are due to the experimental pH differences. The obtained K^{HS} values are compared in figure 13 with the previously obtained results in natural Gorleben Water represented by the regression line. This figure proves that the K^{HS} values are independent of the humic substance concentration.

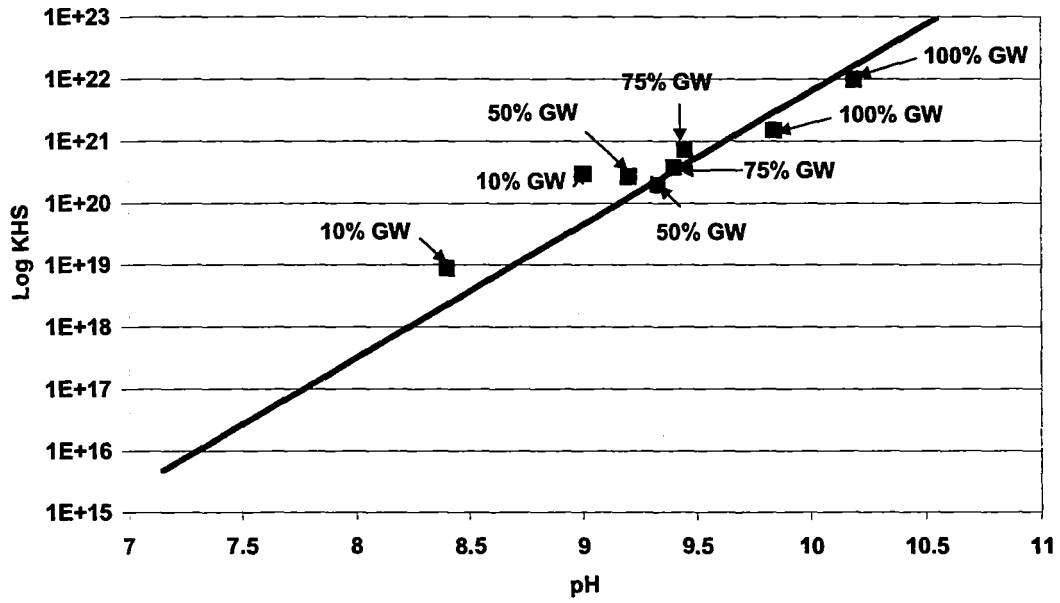

Figure 13: Comparison of $LogK^{HS}$ values obtained at different dilutions of the Natural Gorleben Water, with previous results represented by the regression line:
Log K^{HS} = 2.145* pH+0.335.

3.6.3. *Variation of initial Tc concentration*

The previous experiments were all conducted with a constant initial Tc concentration of $5x10^{-6}$ M. In a new series of experiments with natural Gorleben groundwater different Tc concentrations were added. The concentrations varied between $5x10^{-6}$ M and $5x10^{-5}$ M in experiments with Gorleben sand and between $5x10^{-7}$ M and 10^{-5} M in experiments with magnetite as reducing surfaces.

Figure 14abc and figure 15abcd show the speciation of Tc added in various concentrations to Natural Gorleben groundwater in presence of respectively Gorleben sand and magnetite.

Independent of the Tc concentration added, all experimental systems displayed the same pattern: a fraction of Tc was found precipitated, a fraction was associated with the humic substances and a fraction was free dissolved in solution.

The free Tc concentration was in agreement with the TcO_2 solubility ($3x10^{-8}$ M) when $5x10^{-7}$, 10^{-7} and $5x10^{-6}$ TcO_4^- was initially added. However, higher free Tc concentrations were observed at the highest TcO_4^- doses of 10^{-5} M (Gorleben Sand) and $5x10^{-5}$ M (Gorleben Sand and magnetite): respectively $6x10^{-8}$ M and $4x10^{-7}$ M total free Tc were measured. Probably the redox capacity of the surfaces was limited.

Upon reduction of TcO_4^- in presence of magnetite or Gorleben sand a TcO_2 precipitate was formed. At all concentrations a TcO_2 precipitate was formed even at the smallest TcO_4^- gift of $5x10^{-7}$ M. In presence of humic substances also a Tc - Hs complex is formed.

If the mechanism of interaction of Tc with HS is truly a complexation between Tc(IV) and humic substances, always identical ratios of Tc-HS/HS should be obtained at all pH values. Indeed, in presence of a TcO_2 precipitate the concentration of TcO^{2+} is governed by the solubility constant of TcO_2 and is equal to $10^{-4.23}x(H^+)^2$. Incorporation into the previous constant K_H leads to:

$$K_H = \frac{[Tc-HS][H^+]}{10^{-4.23}[H^+][HS]} = \frac{[Tc-HS]}{10^{-4.23}[HS]}$$

Thus, the latter equation predicts that the ratio [Tc-HS]/[HS] should remain constant.

Unexpectedly, the Tc-Hs/HS ratio depends on the total Tc concentration, as seen in figure 16. Indeed increasing Tc-Hs levels correspond to increasing tot TcO_4^- gifts.

Figure 16 demonstrates also that the calculated K_H values versus pH remain constant for each initial Tc concentration but increase with increasing total Tc concentration in the system. The reason for this behaviour is presently unknown.

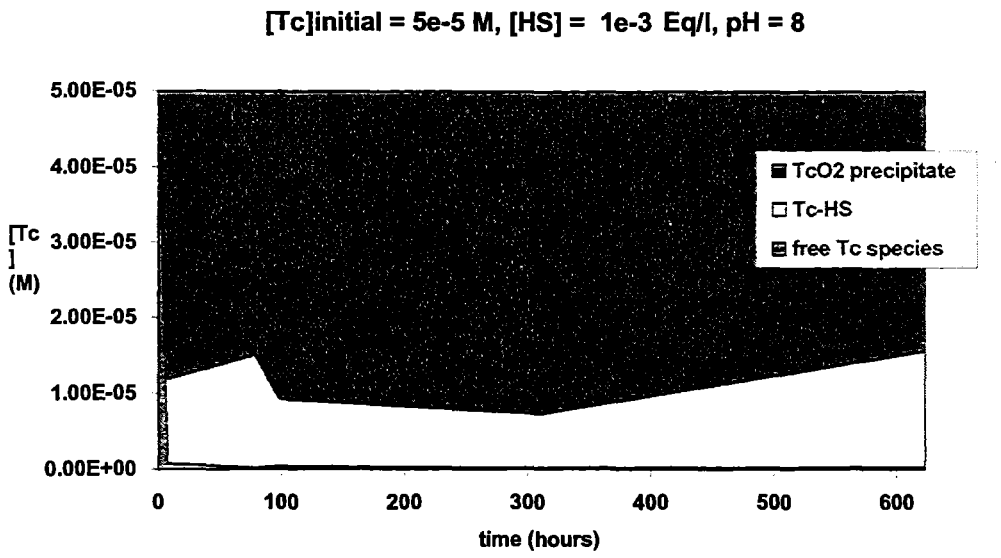

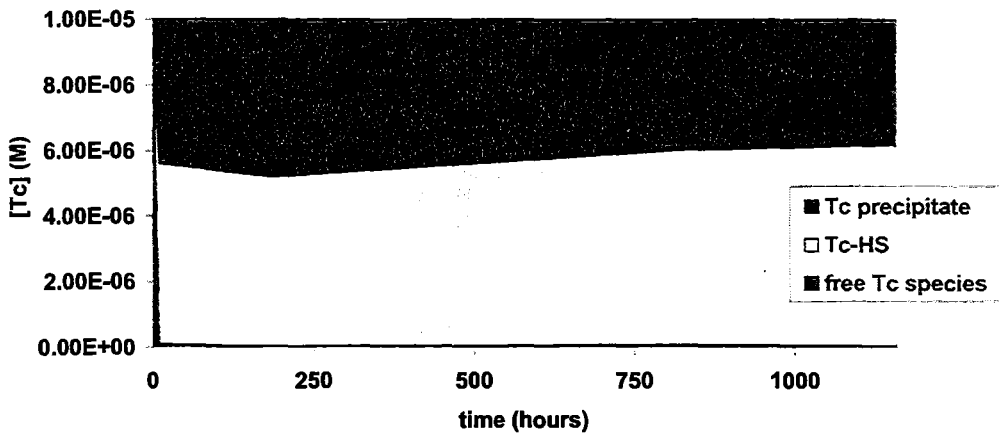

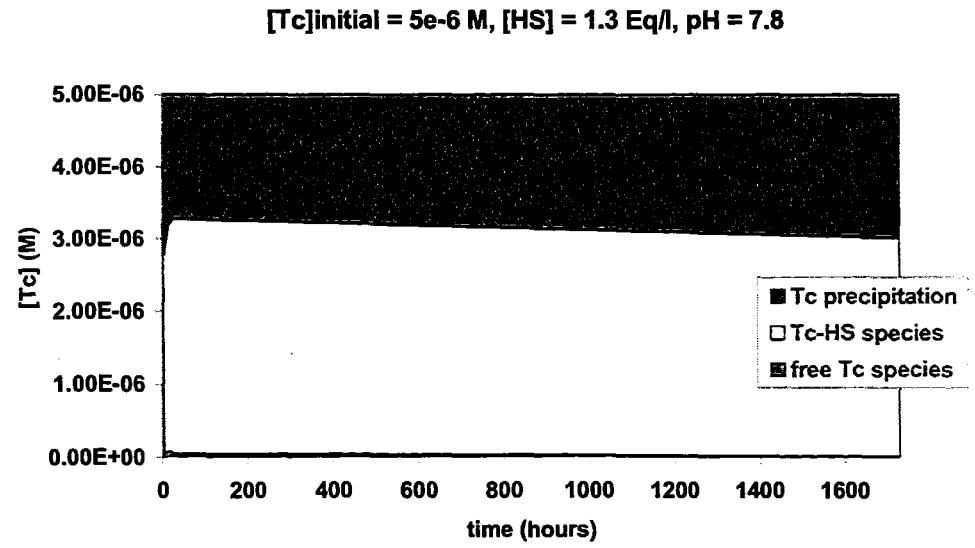

Figures 14abc: Tc-speciation versus time in experiments with Gorleben Sand and Gorleben groundwater and for different initial TcO_4^- concentrations.

[Tc]initial = 5e-5 M, [HS] = 5e-4 Eq/l, pH = 9.8

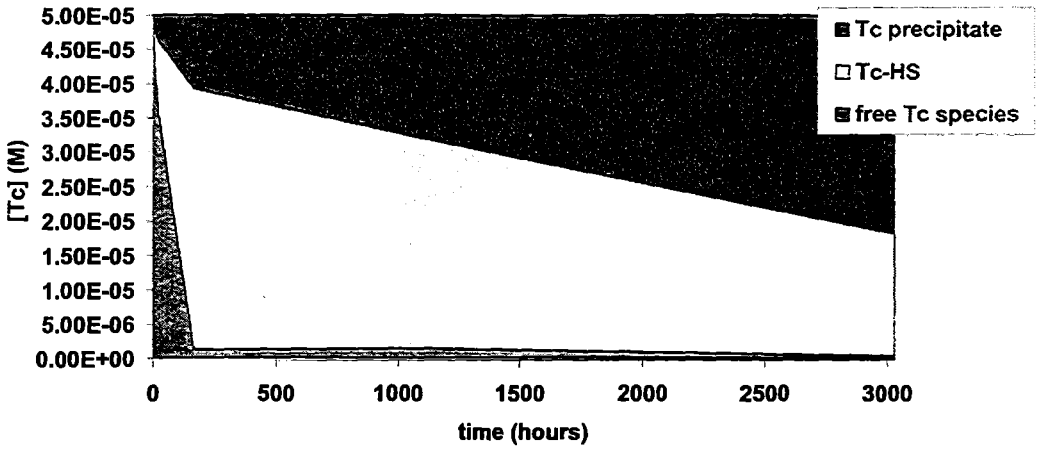

[Tc]initial = 5e-6 M, [HS] = 5e-4 Eq/l, pH = 9.5

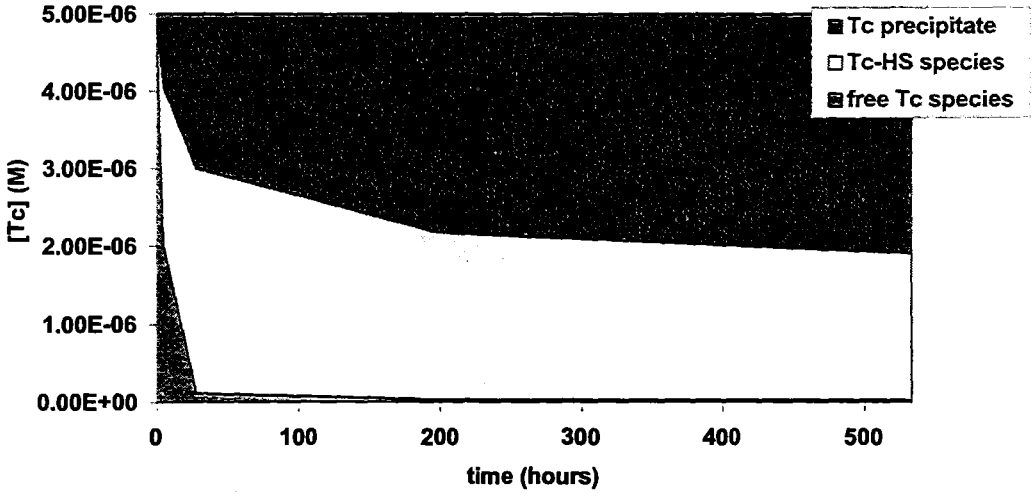

[Tc]initial = 1e-6 M, [HS] = 5e-4 Eq/l, pH = 9.8

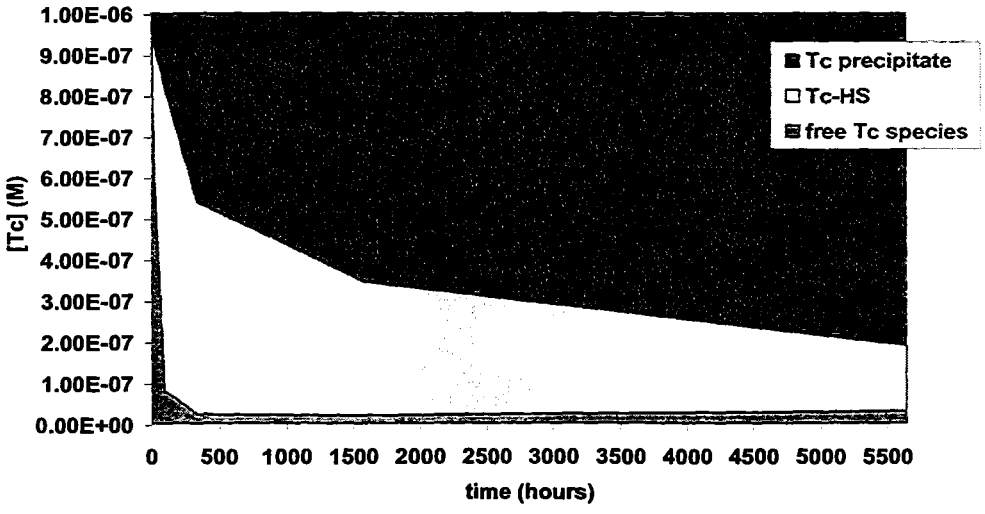

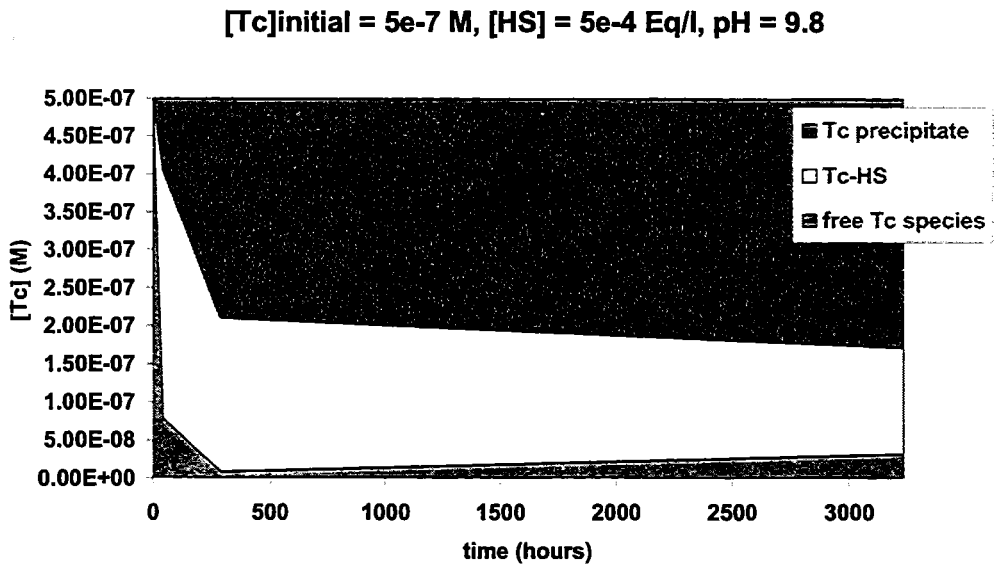

Figures 15abcd: Tc-speciation versus time in experiments with magnetite and Gorleben Water and for different initial TcO_4^- concentrations.

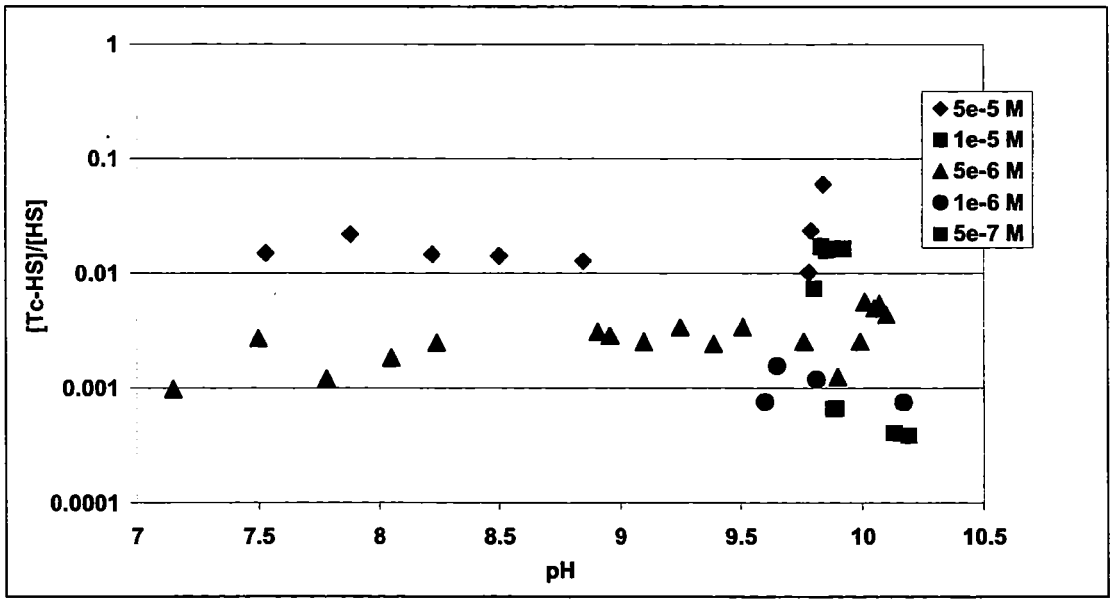

Figure 16: Demonstration of the dependency of the Tc-HS/HS ratio versus pH on the total Tc concentration in the synthetic (magnetite and Gorleben Water) and natural (Gorleben Sand and Gorleben Water) systems.

4. General conclusions

1) A new method to separate the Tc - humate fraction from the free Tc species was developed and verified with Gel Permeation Chromatography. This method is based on the fact that trivalent ions such as La^{3+} are able to precipitate organic matter.

2) The reducing phases magnetite, pyrite, siderite and Gorleben Sand behave similar with respect to the reduction of Tc(VII) into Tc(IV) and the interaction of Tc(IV) with humic substances

3) The distribution of Tc(IV) species between humic and fulvic acids was determined. For synthetic systems with magnetite as the reducing phase, a preference for the fulvic acids was measured. However in the case of natural systems (hence with Gorleben Sand and Gorleben groundwater) no preference could be identified.

4) The process of solubilisation of a TcO_2 precipitate due to Tc-humate formation is very slow compared with the time to reach equilibrium in reactions which simultaneously form the precipitate and Tc-HS complexes.

5) The previously [3] proposed reaction mechanism:

$$TcO^{2+} + HS \Leftrightarrow TcO^{2+}\text{-}HS$$

was found to linearly depend on pH. A new reaction mechanism involving the release of 2 H^+:

$$TcO^{2+} + HS \Leftrightarrow TcO^{2+}\text{-}HS + 2\ H^+$$

leads to constant KH values which are independent on the pH and HS concentration. However unexpectedly, the KH values depend on the total Tc concentration indicating that two or more additive processes occur together.

5. References

[1] Lieser, K. H., Bauscher, Ch. "Technetium in the Hydrosphere and in the Geosphere I. Chemistry of Technetium and Iron in Natural Waters and Influence of the Redox potential on the Sorption of Technetium", *Radiochimica Acta*, **42**:205-212 (1987)

[2] Cui, D., Eriksen, T. E. "Reduction of pertechnetate by ferrous iron in solution: influence of sorbed and precipitated Fe(II)", *Environ. Sci. Technol.*, **30**:2259-2262 (1996a)

[3] Maes, A., Vancluysen, J., Geraedts, K. "Studies on the Reduction of Tc(VII) and the formation of Tc-Humic Substance Complexes in Synthetic and Natural systems", In: Effects of Humic Substances on the Migration of Radionuclides: Complexation and Transport of Actinides, Second technical progress report of the EC-project No.: F14W-CT96-0027 Report FZKA 6324, Ed. G. Buckau (1999)

[4] Maes, A., Capon, L. "Reduction of Technetium in Solution: Influence of Ferrous Iron, Minerals Phases and Organic Matter", In: Effects of Humic Substances on the Migration of Radionuclides: Complexation and Transport of Actinides, First technical progress report of the EC-project No.: F14W-CT96-0027 Report FZKA 6124, Ed. G. Buckau (1998)

[5] Marquardt, C., Artinger, R., Zeh, P., Kim, J. I. "Redoxchemistry of Neptunium in a Humic Rich Groundwater", In: Effects of Humic Substances on the Migration of Radionuclides: Complexation and Transport of Actinides, First technical progress report of the EC-project No.: F14W-CT96-0027 Report FZKA 6324, Ed. G. Buckau (1999)

[6] Artinger, R., Kienzler, B., Schüssler, W., Kim, J. I. "Sampling and Characterization of Gorleben Groundwater/Sediment Systems for Actinide Migration Experiments", In: Effects of Humic Substances on the Migration of Radionuclides: Complexation and Transport of Actinides, First technical progress report of the EC-project No.: F14W-CT96-0027 Report FZKA 6124, Ed. G. Buckau (1998)

[7] Hummel, W. "Binding Model for Humic Substances", In: Modelling in Aquatic Chemistry, Ed. Grenthe, I., Puigdomenech, I. NEA-OECD (1997)

Annex 13

Transport Behavior of Pertechnetate and Technetium Humate Complexes in Gorleben Sand

(K. Geraedts, A. Maes and J. Vancluysen and (KUL))

3rd Technical Progress report

EC project

K.U.Leuven contribution to task 2 (complexation)

Effects of humic substances on the migration of radionuclides: complexation and transport of actinides

TRANSPORT BEHAVIOUR OF PERTECHNETATE AND TECHNETIUM - HUMATE COMPLEXES IN GORLEBEN SAND

K. Geraedts, A. Maes, J. Vancluysen

K.U.Leuven

Departement Interfasechemie
Laboratorium voor Colloïdchemie
Kardinaal Mercierlaan 92, B-3001 Heverlee

1. Introduction

In column experiments, using Gorleben groundwater (GoHy 2227) and Gorleben sand, the migration behaviour of Technetium-99 under deep geological conditions was investigated.

Under oxic conditions Tc-99 forms pertechnetate, a highly soluble, anionic aqueous species, that does not sorb significantly on minerals or sediments [1]. However technetium can be removed from solution by reduction of Tc(VII) to Tc(IV), when suitable conditions are met [2]: a precipitate $TcO_2.nH_2O$ with a low solubility is assumed to be formed. However in presence of organic matter, the solubility can be enhanced because soluble Tc(IV) species associate with mobile humic substances [3]. The migration behaviour of these Tc - Humic Substance complexes in Gorleben Sand was investigated.

2. Experimental

All experiments were carried out at ambient temperature (22°C) in a controlled atmosphere box (95% N_2, 5% H_2). The oxygen concentration in the glove box was maintained at less than 2 ppm by constant purification of the gas.

^{99}Tc was purchased form Amersham in 0.1 M NH_4OH aqueous solution. TcO_4^- solutions ($2x10^{-4}$ M) were prepared by diluting aliquots of a stock solution ($2x10^{-2}$ M) in a mixture of $NaHCO_3$ ($8x10^{-3}$ M) and NaCl ($3.2x10^{-2}$ M). This mixture is taken as representative for the inorganic composition of Gorleben groundwater. Gorleben Sand and Gorleben groundwater (GoHy 2227) were delivered from Forschungszentrum Karlsruhe and were used as obtained.

Flow through column experiments were performed using two different columns: firstly a relatively small column (217 mm long, and 27 mm in diameter) and secondly a column of 210 mm long and 55 mm in diameter prepared jointly (KUL, FZK) following the procedure of FZK. The columns were tightly packed with sand and equilibrated with groundwater. Periodically, pH, Eh and optical density of the groundwater were measured and equilibrium was assumed after 35 days for the first column and after 3 months for the second column.

The pH measurements were made by a Portatest 655 and a WTW SenTix 50 glass electrode. The redox potentials were monitored by a combined redox Toledo Mettler P14805-DXK-S8/120 electrode connected to the Portatest 655. To determine the concentration of humic substances in solution, the optical density was measured with an LKB UV-Vis spectrophotometer at 280 nm.

To determine the hydraulic properties of both columns ^{36}Cl was used as a conservative tracer.

Complexes of Tc with humic substances in natural Gorleben groundwater were prepared in batch experiments, before their injection into the column. Polypropylene vials with 10 g Gorleben Sand and 19 ml Gorleben groundwater were used. After a two week period of pre-equilibrium of sand and groundwater, a $^{99}TcO_4^-$ spike in 1 ml 10^{-2} M $NaHCO_3$ was added. The

initial TcO_4^- concentration was 10^{-5} M. The vials were turned slowly head over head to ensure good mixing. As extensively demonstrated in previous work [4,5], the pertechnetate was reduced to Tc(IV) and Tc-HS complexes were formed. To validate the formation of Tc-HS complexes, the samples were centrifuged (15 min, 7000 rpm) and the supernatant was analysed for ^{99}Tc in a Packard Liquid Scintillation Analyser using Ultima Gold Liquid Scintillation Cocktail (Packard). The amount of free Tc species and the concentration of the formed Tc-HS complexes were determined by a method based on induced flocculation of the organic matter with La^{3+} [4].

To investigate the influence of the pre-equilibrium period of Tc with the groundwater before injection into the column, the contact time between the sand and the Tc - Humic Substance complexes was varied from 4 days to 34 days.

An aliquot of the supernatant (1 ml) was then injected into the column. In order to obtain different retention times (between 4 and 66 hours) in the column, the pump speed was varied in different experiments. The collected samples were analysed for ^{99}Tc. In order to calculate the recovery, the speciation of Tc in the eluent fraction was made with the aforementioned La^{3+} flocculation method.

The third and last experiment in the first column, consisted in injecting 1 ml of $5x10^{-6}$ M pertechnetate present in the aforementioned mixture of $8x10^{-3}$ M $NaHCO_3$ and $3.2x10^{-2}$ M NaCl. The eluent was again measured for ^{99}Tc and speciation of the Tc was made.

3. Results

The main objectives of the column tests were to determine the migration behaviour of Tc-HS complexes on the one side and the behaviour of "pure" pertechnetate on the other side.

In total 7 different experiments were conducted with the two columns: 6 experiments with Tc-HS complexes and with variable Darcy velocities and variable contact times between the Tc - humate complexes and the sand and 1 experiment with pertechnetate.

3.1. Tc - Humic substance complexes

The pH, Eh, Darcy velocity and effective porosity for the 2 columns are shown in table 1. The Darcy velocity in the small column was kept constant at $5.71x10^{-4}$ cm/s, resulting in a retention time of the injected sample in the column of 4 hours. In the second column (large column) the Darcy velocity was varied between $2.75x10^{-7}$ and $1.26x10^{-6}$ cm/s corresponding to retention times between 66 and 16 hours.

Both the small (C1) and the large (C2) column- showed a analogous Tc-HS migration behaviour. All the results of the column experiments are gathered in table 2.

	pH	Eh	Darcy velocity (cm/s)	Effective porosity
Column 1 (C1)	8.9	-347	5.71×10^{-4}	0.346
Column 2 (C2)	8.7	-207	2.75×10^{-5} - 1.26×10^{-6}	0.314

Table 1: Working parameters for the small (column 1) and large (column 2) columns.

Column Experiment		Retention Time (hours)	Tc - HS pre-equilibrium period (days)	pH	Recovery R (%)	Retardation factor R_f
C1	1	4	4	9.0	97	0.98
	2	4	26	9.1	99.9	0.97
C2	1	16	8	8.8	55	0.99
	2	16	34	9.0	66	0.99
	3	32	4	8.9	44.5	1
	4	66	8	9.1	30	1

Table 2: Results of the column experiments with Tc - HS complexes.

The mobile Tc-HS fractions are transported with a retardation factor R_f, which varies between 0.97 and 1. This is illustrated in figures 1 and 2, which compares the migration of tetravalent Tc-humate at pH = 8.9, with the migration of the conservative tracer ^{36}Cl in both columns. A slightly faster migration of the Tc- HS complex compared to the groundwater movement is observed. This is probably due to size exclusion and/or anion exclusion of the mobile HS molecules. The Tc - humate complexes do not interact with the surrounding sand, because this would result in a slower migration of the complex compared with the inert tracer.

The recovery was calculated from the knowledge of the amount of Tc-HS complex in solution before injection and in the eluates.

In experiments with the first column - hence with a relatively short retention time - and after an equilibration period of 4 days, 97% of the injected Tc-HS complex was recovered. The recovery factor increased to 99.9% when the pre-equilibrium period increased to 26 days. Similar results were obtained with the second column: 55% recovery for a pre-equilibrium period of 8 days and increasing to 66% for a pre-equilibrium period of 34 days. These observations suggest that Tc will be more strongly bound to humic substances when the pre-equilibration time in the batch preparation of the Tc-HS complex is longer. Inspection of the table also reveals that for identical preconditioning time of the Tc-HS complexes, the recovery of

the Tc-HS decreases with increasing residence time in the column. This observation indicates that the kinetics of decomplexation (desorption of Tc from HS) is an important process in the transport behaviour of Tc-HS.

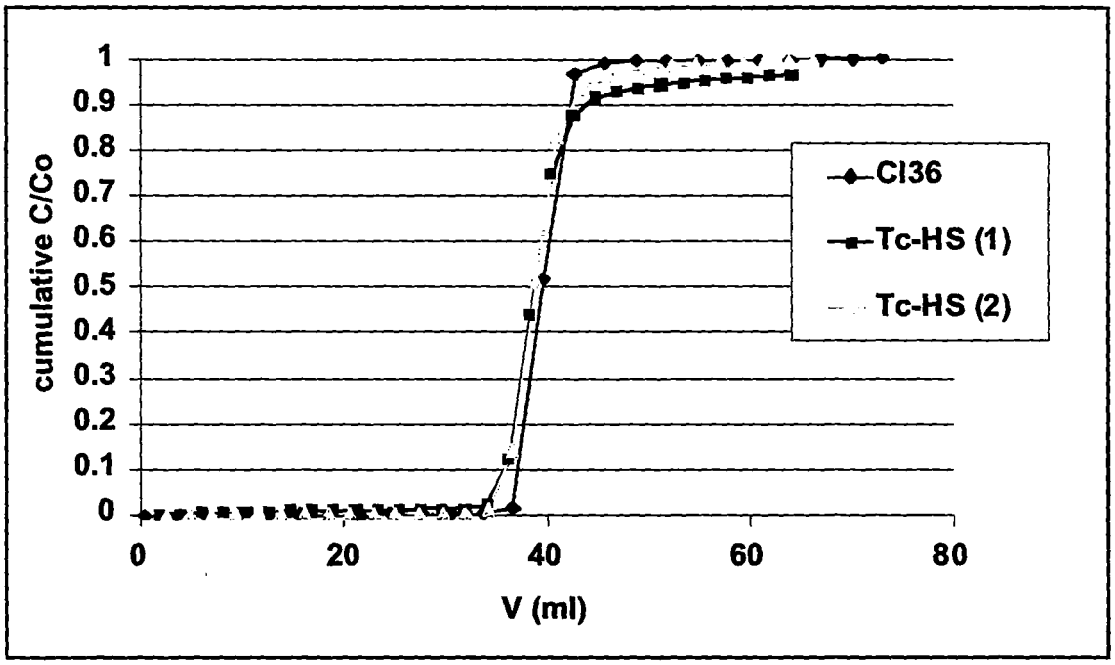

Figure 1: Cumulative breakthrough curves for the migration of ^{36}Cl and the two ^{99}Tc - humate complexes in column 1.

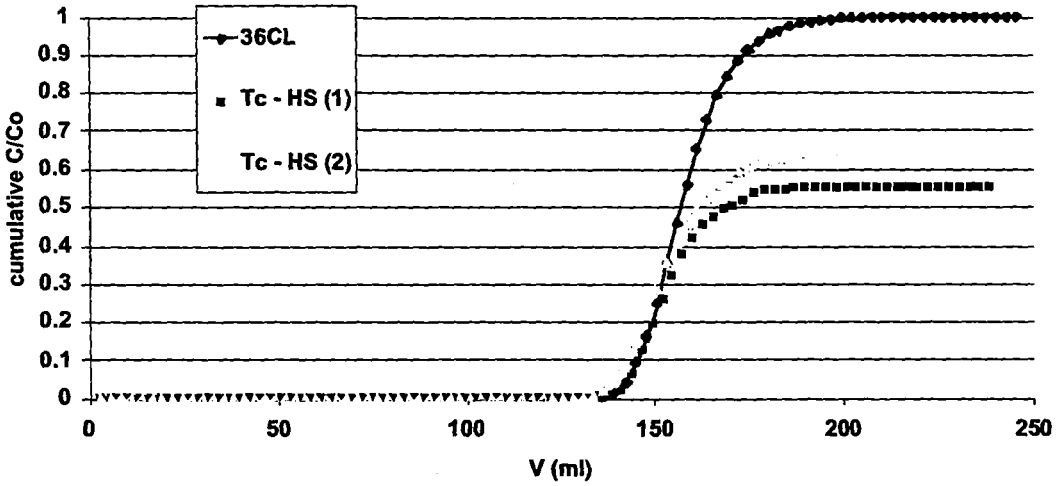

Figure 2: Cumulative breakthrough curves for the migration of ^{36}Cl and two ^{99}Tc - humate complexes in column 2.

the Tc-HS decreases with increasing residence time in the column. This observation indicates that the kinetics of decomplexation (desorption of Tc from HS) is an important process in the transport behaviour of Tc-HS.

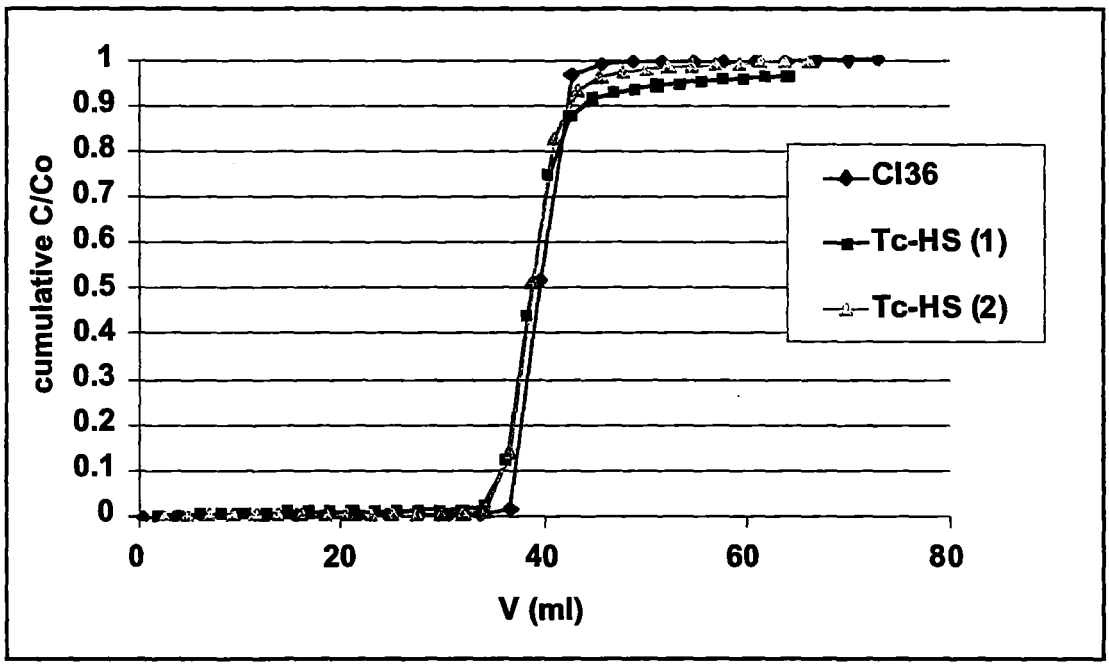

Figure 1: Cumulative breakthrough curves for the migration of ^{36}Cl and the two ^{99}Tc - humate complexes in column 1.

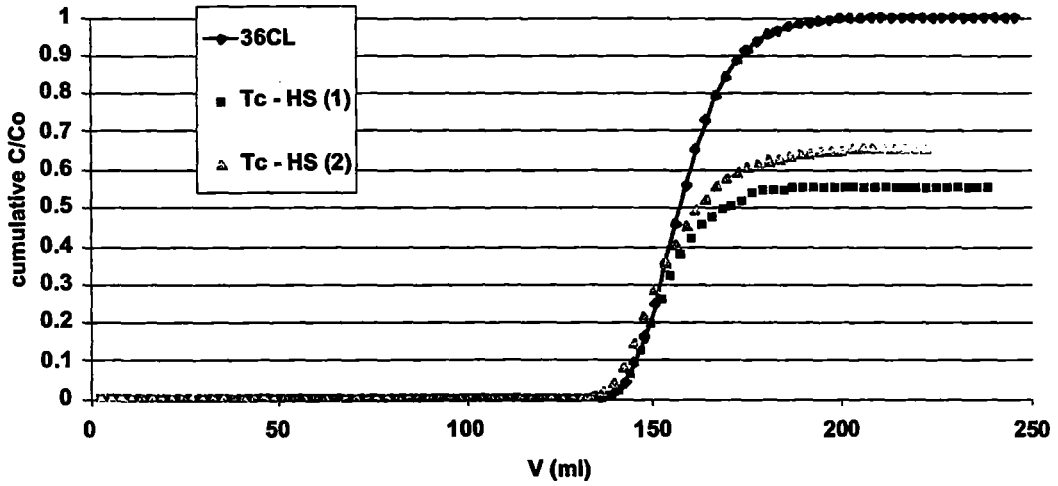

Figure 2: Cumulative breakthrough curves for the migration of ^{36}Cl and two ^{99}Tc - humate complexes in column 2.

Analogous results with Gorleben Sand, Gorleben groundwater and ^{241}Am were obtained by Artinger *et al.* [6] and were interpreted in the same way.

In order to estimate the expected recovery for "long" retention times, occurring in larger scale migration in the field, the obtained data are represented in figure 3, as the recovery versus the retention time. From this figure, it is not obvious whether the recovery will tend to zero at an "infinitive" retention time or will flatten at a low percentage recovery. The latter case would mean that Tc may be transported as Tc-HS colloids.

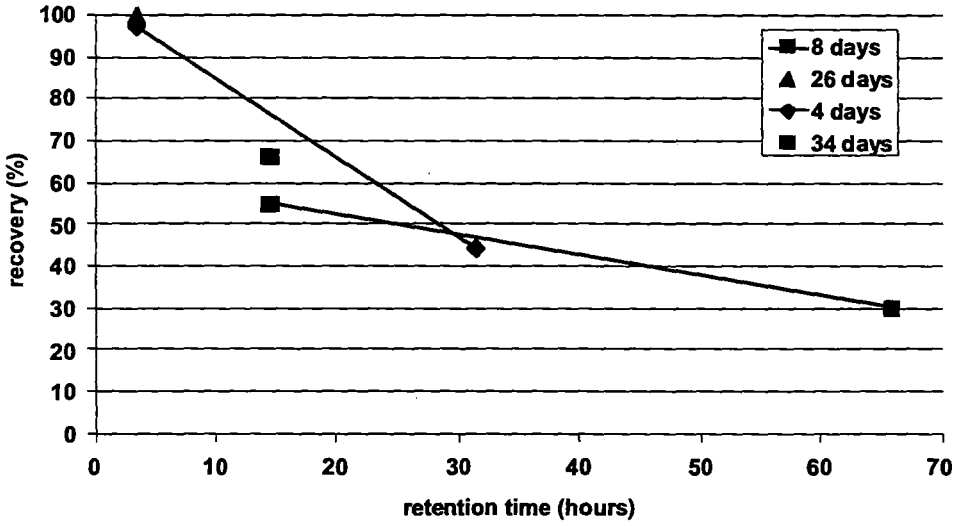

Figure 3: Recovery versus retention time for the different experiments.

3.2. Pertechnetate.

The Tc-HS injection experiments in column 1 were followed by injection of pertechnetate. The results are shown in figure 4, in which the breakthrough curve of ^{36}Cl is also displayed. A very low Tc recovery is noticeable. Only 0.3% of the injected Tc migrated with the same speed as the aforementioned Tc - HS complex. Speciation determination of the eluent indicated indeed that the Tc migrated as a Tc - HS complex which was formed in situ in the column.

After further pumping of groundwater through the column, occasionally some very small fractions of Tc were determined in the eluent (see figure 4), but no trend of a continuous bleeding could be deduced. After breakdown of the column, 99% of the Tc was found at the beginning of the column.

The experimental observations are ascribed to the reduction of Tc(VII) to Tc(IV) due to the reducing conditions in the column. The expected scenario is then the formation of a TcO_2 precipitate, which is in equilibrium with $3x10^{-8}$ M soluble Tc(IV) species, which in turn may

associate with the organic matter. Therefore recovery with tailing was expected. However only a tiny fraction of Tc moved as Tc-HS. Therefore the reduction must have lead either a) to the formation of a much less soluble TcS_2 precipitate or b) to the formation of surface associated Tc-HS complexes.

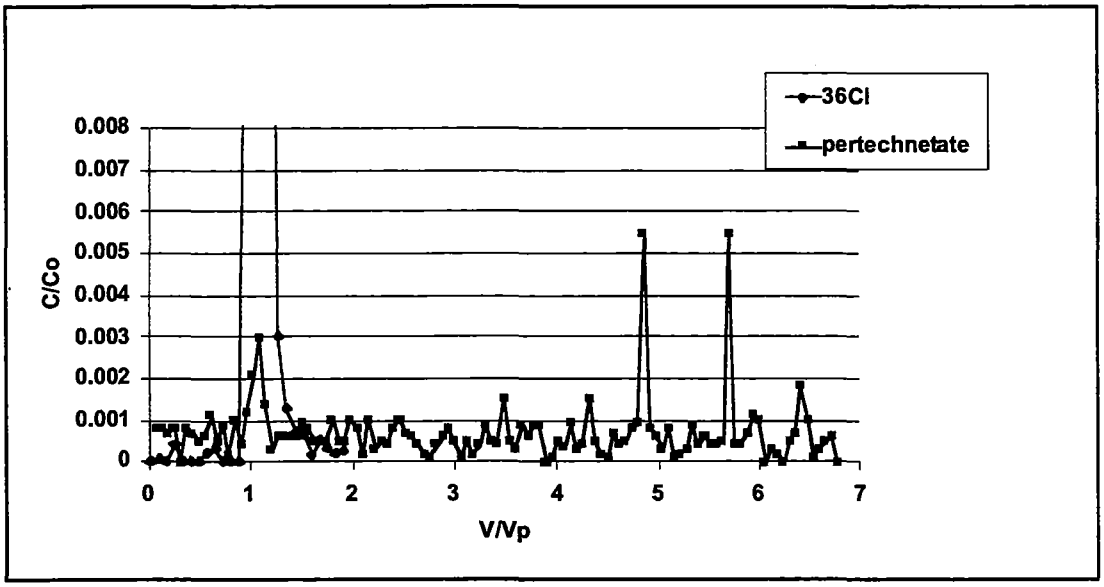

Figure 4. Results of the column experiment with pertechnetate

4. Conclusions

The findings on the migration of the tetravalent technetium humate complexes are similar to those observed at FZK for humate complexes fo U, Eu and Am:

1) Tc - HS complexes move slightly faster than does the inert tracer ^{36}Cl.
2) The recovery of humate bound Tc increases with increasing pre-conditioning prior to column injection
3) For identical pre-conditioning times, the recovery of humate bound Tc decreases with increasing residence time in the column.
4) Unlike the behaviour of tetravalent Tc humate complexes, 99% of the pertechnetate ion (which is not associated with humate) is found sorbed at the beginning of the column. Only a very small amount (0.3%) of Tc migrates with the same speed as the technetium humate complexes. From speciation techniques, it is shown that these Tc species are complexes formed in the column after reduction of the pertechnetate.

5. References

[1] Lieser, K. H., Bauscher, Ch. "Technetium in the Hydrosphere and in the Geosphere I. Chemistry of Technetium and Iron in Natural Waters and Influence of the Redox potential on the Sorption of Technetium" *Radiochimica Acta*, **42**:205-212 (1987)

[2] Cui, D., Eriksen, T. E. "Reduction of pertechnetate by ferrous iron in solution: influence of sorbed and precipitated Fe(II)", *Environ. Sci. Technol.*, **30**:2259-2262 (1996a)

[3] Van Loon, L., Stalmans, M. Maes, A., Cremers, A. "Technetium in the environment", eds. G. Desmet and C. Muyttenaere, Elsevier Appl. Sci. Pub., London, chap. 12 (1986)

[4] Maes, A., Capon, L. "Reduction of Technetium in Solution: Influence of Ferrous Iron, Minerals Phases and Organic Matter" In: Effects of Humic Substances on the Migration of Radionuclides: Complexation and Transport of Actinides, First technical progress report of the EC-project No.: F14W-CT96-0027 Report FZKA 6124, Ed. G. Buckau (1998)

[5] Maes, A., Vancluysen, J., Geraedts, K. "Studies on the Reduction of Tc(VII) and the formation of Tc-Humic Substance Complexes in Synthetic and Natural systems", In: Effects of Humic Substances on the Migration of Radionuclides: Complexation and Transport of Actinides, Second technical progress report of the EC-project No.: F14W-CT96-0027 Report FZKA 6324, Ed. G. Buckau (1999)

[6] Artinger R., Kienzler, B., Schüssler, Kim, J. I. "Effects of humic substances on the ^{241}Am migration in a sandy aquifer: column experiments with Gorleben groundwater/sediment systems", *Journal of Contaminant Hydrology*, **35**:261-275 (1998)

Annex 14

Kinetics of EuHS Dissociation

(P. Warwick, A. Hall, S.J. King and N. Bryan (LBORO and RMC-E))

3rd Technical Progress Report

EC Project:

Effects of humic substances on the migration of radionuclides: complexation and transport of actinides.

Project No.: F14W-CT96-0027

LU Contributions to Tasks 3 and 4

Kinetics of EuHS dissociation

P. Warwick[1], A. Hall[1], S. J. King[1] and N. Bryan[2].

January 2000

1. Department of Chemistry, Loughborough University, Loughborough, Leics. LE11 3TU, UK.

2. Department of Chemistry, University of Manchester, Oxford Road, Manchester M13 9PL, UK.

Kinetics of EuHS dissociation.

Authors: P. Warwick[1], A. Hall[1], S. J. King[1] and N. Bryan[2].

1. Department of Chemistry, Loughborough University, Loughborough, Leics. LE11 3TU, UK.

2. Department of Chemistry, University of Manchester, Oxford Road, Manchester, M13 9PL, UK.

Summary.

The effects of equilibration time, pH, temperature, metal loading, HS concentration and competing cations, on EuHS dissociation were investigated. Three consecutive, pseudo-first order, dissociation processes were invoked to describe the observations. The slowest step which is probably the most important with regard to radionuclidic transport had a half life of ~200 hours. The proportion of Eu entering the hindered sites (responsible for the slow dissociation step) was found to increase with pH, pre-equilibration time, FA concentration and humification (HA > FA).

The effect of temperature on the proportion of Eu entering the hindered sites was used to gain information on nature of the free energy difference between the hindered and exchangeable fractions (logβ, ΔG, ΔH and ΔS were calculated). The effect of temperature on the rate constant (for the slow dissociation step) was also used to gain information on the on the size and nature of the activation barrier (A, Ea, ΔG, and ΔS were calculated). This information was then used to further develop the mechanistic model of metal HS interactions.

Introduction.

There is concern that after disposal in underground repositories radionuclides may eventually come into contact with groundwaters containing humic substances at elevated temperatures. Many of these radionuclides are metallic, including radiologically significant actinide elements. The stability constants of many metal-humic substances (HS) complexes are high and hence these substances may have a significant effect on the migration of the metal ion in the environment.

For this reason considerable efforts are being made to model the interaction of metals, in particular the actinides, with natural organic matter [1]. However, previous column modelling work has shown that the transport behaviour of radionuclides in the presence of humic acid cannot be described using a model based on the assumption of local equilibrium [1]. Results showed that a particular fraction of the bound metal was very slow to de-sorb from the humic acid, this caused much faster transport than would otherwise be expected. The importance of including kinetic processes when modelling the experimental results of transport of radionuclides in the presence of radionuclides has also been reported by van de Weerd and Leijnse [3].

The rate at which metal humate complexes dissociate therefore may be a significant factor in understanding radionuclide transport in the environment. Various schemes have been developed and applied to the study of metal HS dissociation kinetics such as; ion exchange [3, 4]; competing ligand technique [5, 6 and 7], anodic stripping voltametry [8] and ion selective

electrodes [9]. In the current work EuHS dissociation kinetics were investigated using Dowex cation exchange resin. The method allowed the dissociation kinetics to be studied over long time intervals, at trace metal concentrations and, at different temperatures. Eu was used as an analogue of trivalent actinides.

The reaction between a metal humic substance complex MHS and resin can be expressed as

$$MHS + Resin = MRes + HS \qquad (1)$$

When the resin is present in excess the rate of formation of MRes is determined by the rate of dissociation of MHS.

Experiments were conducted to determine the rate of dissociation of europium humate and europium fulvate. It was found that the kinetics could be resolved into three first order pathways. The effect of resin weight, equilibration time, pH, metal loading, competing cations and temperature, on the rate (k_3) and amount of europium (Eu_{FIX}) dissociating by the longest lived pathway were investigated. The observed effects were used to gain an insight into the mechanism of metal binding to humic substances.

Experimental

Materials

Fulvic acid was extracted from Derwent reservoir, Derbyshire UK and characterised by BGS [10]. Sodium humate was supplied by Aldrich and purified by a method previously described [11]. Before use fulvic acid was filtered through a 0.45μm membrane (Fisher Scientific) to remove any microbes present. The rate of binding of europium was investigated at pH=4.5 and 6.5. Dowex 50x4, 100-200 mesh cation exchange resin was conditioned and dried at each pH by a method previously described [12]. For a resin weight of 0.5g the rate of Eu binding to the resin was found to be sufficiently fast, after 2 minutes i.e. >99% bound at pH=4.5 and >98% bound at pH=6.5. ^{152}Eu was obtained from Amersham International.

Method development

A batch procedure was developed to study the dissociation of EuFA. In the procedure 0.6 cm^3 of an Eu III solution (2.85×10^{-6} mol dm^{-3}), containing radioactive tracer quantities of Eu-152, were added to 14.4 cm^3 of fulvic acid (10.416 mg dm^{-3} in 0.1 mol dm^{-3} $NaClO_4$ at pH=4.5). The experiments were performed in duplicate in acid washed polysulfone centrifuge tubes (Nalgene).

In order to ensure the reaction was first order or pseudo first order various weights (0.5, 1.0, 1.5, 2.0 and 2.5g) of dry conditioned resin were used in separate experiments. Each experiment was performed in duplicate. The samples were left to equilibrate at 20°C for 26 days and were shaken in a thermostated water bath. At specific times shaking was stopped and the resin allowed to settle. A 0.5 cm^3 aliquot of the supernatant was then removed and counted for 1 minute in a clean vial in a Philips 4800 gamma spectrometer. To investigate the effect of removing aliquots and hence changing the volume of solution, one sample aliquot was replaced immediately after counting. The pH of each solution was checked regularly and any solution with a pH drift greater than 0.5 of pH unit was discarded from the final results.

The Eu-152 activity remaining in solution was used to calculate the concentration of EuFA present at a specific time. The stability constant for EuFA formation under these experimental conditions has been determined to be of the order of 10^8 dm^3 mol^{-1} [12]. The percentage of free europium at the time the resin is added is therefore assumed to be negligible.

Results and Discussion

Data analysis method

The second technical report [1] describes how the dissociation of Eu from the fulvic acid in the experiments described above was modelled. The presence of an equilibrium component and a series of first order rate processes were postulated, i.e. the amount of Eu remaining bound to the humic at time t, $Eu_B(t)$, was modelled using the expression:-

$$Eu_B(t) = Eu_{EQM} + \sum_{i=1}^{N_{Comp}} Eu_{FIX,i} e^{-k_i t} \qquad (2)$$

where: Eu_{EQM} is the equilibrium component, N_{comp} is the number of first order components; $Eu_{FIX,i}$ is the amount of component i. As already noted three first order components sufficed.

The contribution of the equilibrium component was found to decrease as the mass of resin increased. Eu_{EQM} became effectively zero above a resin mass of 1.5g, also $Eu_{FIX,i}$ and k_i were independent of the resin mass.

The first two processes were found to be relatively fast so the Eu involved is readily exchangeable. However the longer lived, more slowly dissociating component is more important from the point of view of facilitated transport. Therefore experiments were conducted to determine the effects of:- resin contact time, pre-equilibration period, filtering, pH, HS

concentration, metal loading, competing cations, ionic strength, and temperature on the slowly dissociating component (Eu_{FIX}) and the corresponding dissociation constant (k_3). The results are summarised in Table 1.

The studies were performed using a resin weight of 2.5g and Eu concentration of 1.14×10^{-7} mol dm^{-3}, unless stated otherwise. The control experiments showed that the removal of an aliquot from solution for counting had no effect on the dissociation kinetics. Also no Eu was observed to sorb to the vials and no humic substances were observed to sorb to the resin.

Effect of long contact times with resin

The dissociation constant k_3 was found to adequately account for the observed Eu dissociation in the range 1,000 - 20,000 minutes. Therefore an experiment was performed in order to determine whether further rate constants are required to describe the dissociation kinetics at longer time periods. Fulvic acid (10 and 60 mg dm^{-3}) and humic acid (10mg dm^{-3}) were equilibrated with Eu at $20^{o}C$ for 9 days before the addition of resin. The dissociation kinetics were followed until the pH drifted greater that 0.5 pH units, which occurred at 80,000 minutes at pH=4.5 and 30,000 minutes at pH=6.5. A plot of the natural log of $[EuFA]_t/[EuFA]_{t=0}$, i.e. LN[C]/[Co] versus time can be seen in Figure 2.1 for pH=4.5. A single k_3 value proved to be sufficient to describe the Eu dissociation kinetics after 1,000 minutes. The pH 6.5 behaviour was similar i.e. capable of being modelled using a single k_3 value.

The effect of equilibration time for the Eu-FA reaction on dissociation kinetics

The contact time for europium and fulvic acid (10 mg dm^{-3}), before addition of resin, was varied in order to investigate the time taken for the metal/fulvic acid reaction to reach equilibrium. It can be seen in Table 1 and Figure 2.2 that as the pre equilibration time increases the amount of europium remaining bound to the fulvic acid, $[Eu]_{FIX}$, increases. The effect of equilibration time is relatively slow, with no observable effect over small time variations.

At pH=4.5 the rate of increase in $[Eu]_{FIX}$ was found to be independent of temperature, $3.19 \pm 0.20 \times 10^{-11}$ mol per day on average. This suggests that there is no enthalpic contribution to the activation barrier at this pH. At pH=6.5 an effect of pre-equilibration time was observed at $20^{o}C$ and $40^{o}C$, with an increase in $[Eu]_{FIX}$ of 1.4×10^{-10} mol and 4.86×10^{-11} mol per day, respectively. After 150 days equilibrium had not been reached, which shows $[Eu]_{FIX}$ was still

undersaturated. The dissociation constant (k_3) was also unaffected by the equilibration time at both pH's.

The effect of equilibration time has also been shown to effect de-sorption of Cd and Co from soil clays and goethite [13]. It was found that as the sorption period increased, the proportions of metal that desorbed decreased substantially.

The effect of filtering

In order to assess whether microbes have a significant effect on the dissociation kinetics an experiment was performed at pH= 6.5 where the fulvic acid was not passed through 0.45μm membrane filter. It can be seen in Table 1 that at $40^{o}C$ and at an equilibration time of 64 days that no effect was observed. If any microbes were present they were not having an effect.

The effect of pH

Experiments were performed at pH=4.5 (no metal hydrolysis) and pH=6.5 (close to neutral pH, groundwater conditions). At pH=4.5 100% of the Eu is present as Eu^{3+}, but at pH=6.5 the aqueous species present are predicted by PHREEQE calculations to be Eu^{3+} (70.74%), $Eu(OH)^{2+}$ (3.47%) and $EuCO_3$ (25.7%). The effect of pH was investigated for 10 mg dm^{-3} FA, 60mg dm^{-3} FA and 10mg dm^{-3} HA which had been equilibrated with Eu for 8-12 days.

The amount of europium available for dissociation by the very slow pathway $[Eu]_{FIX}$ was found to increase with increasing pH. At $20^{o}C$ this effect was found to be comparable for 10 mg dm^{-3} FA, 60mg dm^{-3} FA and 10 mg dm^{-3} HA. On average 6.5 times more Eu was bound as $[Eu]_{FIX}$. A comparison is shown in Table 2a. This observed effect could be predicted by consideration of the degree of deprotonation of the acid functional groups. An increase in deprotonation increases the charge density that expands the macromolecule by electrostatic repulsion. The dissociation rate was observed to decrease slightly with increasing pH at $20^{o}C$. A comparison is shown in Table 2b. Similar responses to pH have been observed for FeFA [14], CuHA [7], NiFA [15, 16], UO_2HA [6] and ThHA [5].

The effect of Fulvic acid concentration

The effect of fulvic acid concentration was investigated by reacting Eu with 10 mg dm^{-3} and 60 mg dm^{-3} FA over a range of temperatures for equilibration times of 8-12 days. The effect of

increasing the fulvic acid concentration on $[Eu]_{FIX}$ and k_3 can be seen in Tables 3a and 3b for pH=4.5 and 6.5, respectively.

By increasing the FA concentration the amount of europium undergoing slow dissociation also increased, by a factor of 3.8 at pH=4.5 and 2.9 at pH=6.5 at 20°C. The increased proportion of Eu retained in the fulvic molecule reflects an increased number of sites.

It can be seen in Table 3b that at pH=6.5 for 60 mg dm^{-3} FA the amount of europium retained in $[Eu]_{FIX}$ is close to saturation. Hence, at this pH the magnitude of the effect of FA concentration on $[Eu]_{FIX}$ is not a true indication.

A decrease in the FA:Eu ratio, by decreasing the FA concentrations tended to decrease the rate of dissociation at both pH values studied. This effect has also been reported for CuFA [17], CuHA [7], PbFA, AlFA [18] and NiFA [15, 16].

Comparison of fulvic acid with humic acid

Europium was equilibrated with FA and HA (10 mg dm^{-3}) over a range of temperatures for 8-9 days. The difference between $[Eu]_{FIX}$ and k_3 for equivalent concentrations of humic and fulvic acid can be seen in Tables 4a and 4b for pH=4.5 and 6.5, respectively.

At 20°C the humic acid retained more Eu in the hindered sites than fulvic acid by a factor 2.1 at pH=4.5 and a factor of 2.4 at pH=6.5. Again this may not be a true indication of increase at pH=6.5 due to 90% of the Eu already retained in Eu_{FIX}. However, the difference between Eu_{FIX} retained by humic acid compared to fulvic acid did not remain constant across the temperature range and this observation is discussed later. No effect the dissociation constant at either pH was observed on average over the temperature range studied.

The proton exchange capacity (PEC) can be used to calculate the concentration of COOH groups hence the operational concentration of a humic substance. The PEC for Aldrich humic acid and Derwent fulvic acid were determined to be 5.43 meq g^{-1} [19] and 5.00 meq g^{-1} [10], respectively. The concentration of COOH groups for the humic and fulvic acid concentrations used in this study are therefore similar. It therefore appears that the greater proportion of Eu being retarded by humic acid cannot be explained by a greater number of sites. One of the differences between the humic and fulvic acid is size distribution. These have been determined for fulvic acid [1] to be 3995 (σ = 90) dalton and 5700 (σ = 320) dalton for humic acid [20] by

ultra-violet scanning analytical ultracentrifugation. Humics also tend to have a higher percentage aromatic composition (40-60%) compared to fulvics (20-50%) [21].

It is possible that the differences in size cause more Eu to become retarded in the coiled structure of humic acid. In order to be removed from the humic substance the Eu must be in a similar site to that on a fulvic acid molecule, hence no difference in the rate of dissociation between fulvic and humic acid.

The kinetics of Sm dissociation from size fractionated polyacrylic acid (PAA) and humic acid (HA) have been studied by Clark and Choppin [22]. Polyacrylic acid is a homogenous, linear polyelectrolyte with regularly spaced carboxylate groups and was used to gain insight into a description of metal binding. For PAA the large (450,000 daltons) and the small (18,100 daltons) fractions had equivalent carboxylate capacities. The dissociation kinetics for the large PAA was slower and more complicated than the kinetics observed for the small PAA fraction. The addition of a further rate constant to describe the dissociation of the large PAA makes comparison difficult. To compare these rate constants with those observed for HA, large (>300,000 daltons) and small (50,000-100,000 daltons) fractions of Bradford humic acid were prepared by ultrafiltration. The carboxylate capacity differed for the large and small fractions, 3.52 and 6.89 meq/g respectively and therefore, experiments were performed with equivalent carboxylate concentrations. The dissociation was found to be faster for the smaller HA fraction. Clark *et al* suggest that this reflects the role of decreased conformational change as the size decreases, (plus marginally more hindered) [22]. Similar observations have been reported for Cu(II) [23] and UO_2^{2+} [6]. These results are opposite to those reported here.

The effect of Metal Loading

In the batch procedure 0.6 cm^3 of Eu III solution ($2.85x10^{-6}$ mol dm^{-3}), containing radioactive tracer quantities of Eu-152, was equilibrated with 14.4 cm^3 of humic substance (10.416 mg/l). In order to investigate the effect of increased Eu concentrations a 0.15 cm^3 aliquot of inactive Eu was added to the tube in order to create final Eu concentrations of $6.84x10^{-7}$ mol dm^{-3} and $1.28x10^{-6}$ mol dm^{-3}. This aliquot was added immediately before the 0.6 cm^3 of ^{152}Eu solution.

The metal loading was determined by the ratio of total concentration of Eu added ($[Eu]_T$) to the concentration of [HS] determined from the PEC. The results are shown in Tables 1 and 5. From these results it can be seen that in general increasing the concentration of europium added

increases $[Eu]_{FIX}$, but there is no effect on k_3. This suggests that the sites on the humic substance available for long retention of Eu are not yet saturated.

At pH=4.5 the ratio of $[Eu]_{FIX}/[Eu]_T$ is constant for 60 mg dm^{-3} FA over the metal loading range studied. A similar effect was observed for 10 mg dm^{-3} FA at 60^oC. However, at 20^oC an increase in the Eu concentration by a factor of 10 decreased $[Eu]_{FIX}/[Eu]_T$ by about half. For 10 mg dm^{-3} HA a similar decrease was observed at both 20^oC and 60^oC. The effect of temperature on $[Eu]_{FIX}/[Eu]_T$ for 10 mg dm^{-3} FA is unknown. It appears therefore that above a metal loading of about 2.5 % for 10 mg dm^{-3} FA and HA the sites available for Eu binding start to become saturated.

At pH=6.5 increasing the metal loading decreases $[Eu]_{FIX}/[Eu]_T$ for both FA and HA (10 mg dm^{-3}). This suggests that at pH=6.5 the kinetically hindered sites are approaching saturation.

Choppin *et al* reported that the percentage of 'strongly bound' Eu^{3+} decreased with loading (2.5 to 9.5%) and an additional long-lived dissociation pathway appeared in the kinetic spectrum at high humate loading. This is consistent with metals binding to progressively weaker sites as the metal loading increases. When Eu^{3+} in excess of 10% of the carboxylate capacity of the humic acid was added, coagulation and precipitation occurred [6].

The effect of Competing cations

In the batch procedure 0.6 cm^3 of Eu III solution ($2.85x10^{-6}$ mol dm^{-3}), containing radioactive tracer quantities of Eu-152, was equilibrated with 14.4 cm^3 of fulvic or humic acid (10.416 mg dm^{-3}). In order to investigate the effect of competing cations a 0.15 cm^3 aliquot of Ca, Mg, Al and/or Fe containing solution was added to the tube. The effect on the Eu dissociation reaction was studied in the presence of Ca and Mg ($1.0x10^{-4}$ mol dm^{-3}), and/or Al and Fe ($1.0x10^{-6}$ mol dm^{-3}) at pH=4.5. (At pH=4.5 the speciation of Al is Al^{3+} (35.45%), $Al(OH)^{2+}$ (18.1%), $Al(OH)_2^+$ (26.68%), $Al(OH)_3$ (1.69%)).

At pH=6.5, only Ca and Mg were studied because of possible changes in the solubility of Al and Fe at this pH. The results can be seen in Table 1 and 6. Overall no significant effect was observed on $[Eu]_{FIX}$ and k_3.

Competition for sites will only occur if the sites are the same for both cations and the cation concentration exceeds the number of sites. Previous experiments have investigated the effect of competing cations on the total binging strength of metals to humic substances. Norden *et al* [24]

performed ion exchange distribution experiments to investigate the competing effects of Fe, Al and Sr on Eu complexation with FA. In Norden's experiments, the concentration of HS ($5.6x10^{-4}$ mol/l) and Eu ($5.0x10^{-9}$ mol/l) remain constant and the pH and competing metal concentration were varied. Only a slight effect on the EuFA stability constant was observed for Al, Fe and Sr ($1.0x10^{-4}$ mol/l). It was suggested that due to it being known that Eu^{3+} forming stronger complexes with FA than Al^{3+} and Fe^{2+} that the high concentration of metal required is not surprising. It was also stated that it might be possible for these metals to have different binding sites [24]. However, the pKa values used by Tipping in PHREEQEV suggest that the order of binding strength is for humic acid

$$Fe^{2+} > Eu^{3+} = Al^{3+} > Fe^{3+} > Ca^{2+} = Mg^{2+}$$

and for fulvic acid

$$Fe^{2+} > Eu^{3+} = Al^{3+} > Fe^{3+} > Ca^{2+} = Mg^{2+}$$

The competition by Al for Eu binding sites has been investigated by Bidoglio *et al* [25] by TRLFS at pH=5.5. It was found that Al only competed for sites provided Al:Eu ratio was greater than 10. (At this pH the speciation of Al is Al^{3+} (1.16%), $Al(OH)^{2+}$ (3.93%), $Al(OH)_2^{+}$ (58.12%), $Al(OH)_3$ (36.67%) and $Al(OH)_4^{-}$ (0.12%)).

In the case of calcium Moulin *et al* [26] found that a competition occurred with trivalent elements for calcium concentrations starting from 0.01M.

It is interesting to note that in the previous section an increase in the Eu concentration to 2.5% loading had a significant effect on Eu_{FIX}. However, an increase in the total metal concentration to 5% metal loading by the addition of aluminium and iron had no effect on Eu_{FIX}. This suggests that the sites for binding of Eu are not the same as those for Al and Fe or that it is possible for both equilibria to be satisfied and Eu binds more strongly. Further work is required in which the bound Al and Fe are measured.

Ionic Strength

The effect of ionic strength was not investigated for EuHS dissociation. However, the effect of ionic strength has been investigated on CuHA [7] and NiFA [16] dissociation. Rate *et al* [7] varied the added $NaNO_3$ concentration to investigate ionic strength using a competing ligand spectrophotometric technique. It was found that an increased proportion of the Cu underwent

slow dissociation and the slow rate constant increased with increasing ionic strength. Cabaniss *et al* [16] found that increasing the ionic strength increased the overall rate of complex dissociation for NiFA. Proposing that only the more rapidly dissociating complexes responded to changes in the electrolyte concentration.

Temperature effects:-Total Free Energy Changes

To gain information on the nature of the free energy difference between the exchangeable (that able to reach equilibrium) and kinetically controlled fractions, we must compare $[Eu]_{FIX}$ values. The data allows an estimation of the magnitude of the free energy change. Assuming that the exchange between the equilibrium and kinetically controlled fractions is first order in both the forward and backward directions

$$M_{Eq} \Leftrightarrow M_{FIX} \tag{3}$$

the equilibrium constant will be given by

$$K = \frac{M_{FIX}}{M_{Eq}} \tag{4}$$

The Gibbs free energy can be calculated

$$\Delta G = -RT\ln K \tag{5}$$

The enthalpy of the complexation reaction of metal and HS is given by

$$-\frac{\Delta H}{R} = \frac{d\ln K}{d(1/T)} \tag{6}$$

and deduced from the slope of a plot of lnK against 1/T.

The entropy change is derived from

$$\Delta S = (\Delta H - \Delta G)/T \tag{7}$$

The temperature dependence of lnK for 10 mg dm^{-3} FA, 60 mg dm^{-3} FA and 10 mg dm^{-3} HA at pH=4.5 and 6.5, for pre equilibration times of 8-12 days, can be seen in Figure 2.3 and 2.4, respectively. The thermodynamic parameters ΔH, ΔG and ΔS are shown in Table 7a.

At pH=4.5 temperature had no observable effect on $[Eu]_{FIX}$ for 10 mg dm^{-3} HA. However, the enthalpy change for 10 and 60 mg dm^{-3} FA was similar, i.e. exothermic and small. The entropy change is negative for both HA and FA. This suggests that for the europium to bind to the $[Eu]_{FIX}$ site there is some restructuring of the molecule required. It is this unfavourable entropy which leads to the free energy change in going from the exchangeable to the kinetically controlled to be small but positive.

At pH=6.5 the change in enthalpy was endothermic for 10 mg dm^{-3} HA and FA. There appears to be no temperature dependence of $[Eu]_{FIX}$ for 60 mg dm^{-3} FA. This is possibly due the errors associated with measuring a change in $[Eu]_{FIX}$ when the majority (>90%) of the Eu is bound to these sites.

The change in entropy is positive for 10 mg dm^{-3} HA and 10 mg dm^{-3} FA. This reflects an increase in disorder for Eu entering a more "open" HS structure at this higher pH. It can be seen in Table 7b that for 10 mg dm^{-3} FA the change in entropy is approximately a fifth of that for the equivalent concentration of HA. This may be due to the smaller structure of FA compared to HA and hence less disorder created when Eu enters $[Eu]_{FIX}$.

For 10 mg dm^{-3} HA, $T\Delta S$ is sufficiently large to cause the free energy change to be negative. The amount of europium that desorbs slowly is the majority of the total europium added. For fulvic acid, however, the change in free energy depends on the fulvic acid concentration. At 10 mg dm^{-3} FA the change in free energy is positive, due to the smaller entropy change. At the higher concentration of FA the change in free energy is negative.

Activation energies and Entropies

From the effect of temperature upon the rate constant, it is possible to gain information on the size and nature of the activation energy from the dependence of the k upon T using the Arrhenius equation:

$$k = Ae^{\frac{-Ea}{RT}} \qquad (8)$$

where k is the rate constant, Ea is the activation energy, and A is the pre exponential factor. Hence, a plot of ln k versus 1/T will result in a straight line of slope -Ea/R and intercept ln A. In the case of the pH=6.5 data there appears to be a significant dependence. The plots of ln k versus 1/T are shown in Figure 2.5 for 10mg dm^{-3} FA, 60 mg dm^{-3} FA and 10 mg dm^{-3} HA. By

extrapolation, it is possible to calculate a value for A, although due to the fairly narrow range of temperatures over which data were taken this value carries a large uncertainty.

For a first order reaction, the activation energy, ΔS, is related to A via the equation,

$$A = e^{\frac{RT}{N_A h}} e^{\frac{\Delta S}{R}} \qquad (9)$$

The values derived for Ea, A and S are shown in Table 7b. It can be seen that the height of the activation barrier is very similar for fulvic and humic acid (≈ 40 kJ/mol), and is independent of fulvic acid concentration. Despite the large uncertainty in the extrapolated value of A both FA and HA have a similar activation entropy ≈ -250 J/K/mol. This is also similar to the activation entropy determined by Choppin *et al* for Th-HA, as discussed below.

As can be seen in Figure 2.6, in which the results from each duplicate experiment are plotted, K does not systematically depend on temperature at pH=4.5. Rather than an average k_3 the result from each duplicate is plotted. As can be seen, the experimental scatter does not account for the observed results. The enthalpic contribution to the activation barrier must be negligible. Hence the barrier must be entirely entropic in origin.

Cacheris and Choppin measured the dissociation kinetics of Th from humic acid by a ligand exchange technique. Arsenazo III was used as a competitive ligand in place of ion exchange resin and the concentration of Th-arsenzo was determined spectrophotometrically. For all pathways, increasing temperature increased the rate of dissociation slightly (ThHA); however, the longer-lived dissociation processes were noticeably more sensitive to temperature changes than the shorter lived processed [5]. A similar response was observed for UO_2^{2+}HA using a similar ligand exchange technique [6].

Activation energies and entropies were obtained by measuring the dissociation at 2°C, 25°C and 40°C, for ThHA at pH=4.2. For the faster processes the change in temperature is within error for the calculation of the rate constants and corresponds to an activation energy of less than 6 kJ/mol and between -230 and -270 J/mol/K activation entropy. Dissociation by the slower processes required between 20 and 30kJ/mol activation energy and between -200 and -230J/mol/K activation entropy [5].

Cacheris and Choppin suggest that the greater activation energies for the slower pathways are consistent with the assignments of the two classes of binding. Dissociation of thorium from a site within the coiled structure of the humic acid (a slower pathway) would be expected to have larger

positive activation energies while dissociation of territorially bound and surface bound thorium should have smaller activation energies [5]. It is also suggested that the negative values for the activation entropy of the dissociation of the surface bound thorium reflect the restructuring of water molecules around individual charged groups on the macro ion as the thorium leaves. The more negative activation entropies associated with the surface bound thorium (as compared to those for internal binding) may indicate differences in water structure and that of the binding groups in the macro ion [5].

Forward rate constants

It is possible to also calculate the forward rate constant from the equilibrium constant and the backward rate constant k_b (where $k_b=k_3$). Table 8 shows tabulated results for k_f and k_b for these Eu resin experiments with analogous values for Am determined by Schussler *et al* [27] and Co determined during transport modelling [10].

The effect of 2-(N-Morpholino)ethansulphonic acid (MES) buffer

It was found that investigating kinetics at pH=6.5 for long equilibration times and contact times with the resin were problematic due to pH drift. Experiments were performed to compare the effect of MES on the dissociation kinetics of fulvic and humic acid. Solutions were prepared of fulvic and humic acid (10 mg dm^{-3}) at pH=6.5, buffered with 10^{-3} mol dm^{-3} MES. Resin was also conditioned with 10^{-3} mol dm^{-3} MES. The results are shown in Table 9.

The results for humic acid showed that the use of MES buffer decreased the proportion of Eu in the strongly retarded site by approximately a third. No significant effect was observed on the rate of dissociation due to the addition of MES. The results obtained for fulvic acid were not so conclusive and were not performed in duplicate. The proportion of Eu in the strongly retarded site appeared to decrease in comparison to the control sample, but not in comparison to the whole data set. Also no rate constants could be determined from these data. The results indicate that the use of a buffer could interfere with the retention of Eu but further experiments are required to confirm this effect.

Conclusions

Kinetic modelling has been able to reproduce the behaviour observed in long term desorption experiments, and has enabled the determination of activation energies and entropies, and also the

free energy change associated with the conversion from the exchangeable to the kinetically controlled fractions [1].

Mechanistic modelling by Bryan *et al* has shown that the uptake of metals into the exchangeable fraction may be explained in terms of the dehydration of the cation and the relaxation of the humic double layer. The model predicts that the reaction is driven almost entirely by the entropy changes associated with the loss of water molecules from the cation and the release of cations from the double layer.

The results show that the amount of Eu entering the site undergoing slow dissociation increases with increasing equilibration time, increasing pH, increasing fulvic acid concentration, increasing Eu concentration and humification (humic acid>fulvic acid). The rate of dissociation decreased with increasing pH and increasing fulvic acid concentration.

The effect of temperature at pH 4.5 and 6.5 showed large differences in the humic and fulvic acid behaviour. This is matched by differences in $[Eu]_{FIX}$; greater at pH=6.5 than at pH=4.5. The physical state of the humic substance is likely to be very different at the two pH values. Adopting the penetrable gel model of humic substances the humic would be expected to be much more 'open' at higher pH [1].

References.

[1] N.D. Bryan. A modelling study of humate mediated metal transport. In Effects of Humic Substances on the Migration of Radionuclides: Complexation and Transport of the Actinides. pp 245-262 Ed. G. Buckau. Wissenschaftliche Berichte (FZKA 6124, ISSN 0947-8620), Forschungszentrum Karlsruhe Technik and Umwelt, Karlsruhe, Germany (1998).

[2] H. Van de Weerd and A. Leijnse. Assessment of the effect of kinetics on colloid facilitated radionuclide transport in porous media. Journal of Contaminant Hyrdology, 26, 245-256, (1997).

[3] J.C. Rocha, I.A.S. Toscano and P. Burba. Lability of heavy metal species in aquatic humic substances charcterized by ion exchange with cellulose phosphate. Talanta, 44, 69-74, (1997).

[4] C.L. Chakrabarti, Y. Lu, D.C. Gregoire, D.C. Back and W.H. Schroeder. Kinetic studies of metal speciation using Chelex cation exchange resin: Application to cadmium, copper and lead speciation in river water and snow. Environ. Sci. Technol., 28, 1957-1967, (1994).

[5] W.P. Cacheris and G.R. Choppin. Dissociation kinetics of Thorium-Humate complex. Radiochimica Acta, 42, 185-190, (1998).

[6] G.R. Choppin. and S.B.Clark. The kinetic interactions of metal ions with humic acids. Marine Chemistry, 36, 27-38, (1991).

[7] A.W. Rate, R.G. McLaren and R.S. Swift. Response of copper (II)-humic acid dissociation Kinetics to factors influencing complex stability and macromlecular conformation. Environ. Sci. Technol., 27, 1408-1414, (1993).

[8] H.K.J. Powell and R.M. Town. Interaction of humic substances with hydrophobic metal complexes: a study by stripping voltammetry and spectrophotometry. Analytica Chimica Acta, 248, 95-102, (1991).

[9] H.M.V.M. Soares and M.T.S.D. Vasconcelos. Study of the lability of copper(II)-fulvic acid complexes by ion selective electrodes and potentiometric stripping analysis. Analytica Chimica Acta, 293, 261-270, (1994).

[10] J.J. Higgo *et al.*. Extraction, Purification and Characterization of Fulvic Acid. In Effects of Humic Substances on the Migration of Radionuclides: Complexation and Transport of the Actinides. pp 103-128 Ed. G. Buckau. Wissenschaftliche Berichte (FZKA 6124, ISSN 0947-8620), Forschungszentrum Karlsruhe Technik and Umwelt, Karlsruhe, Germany (1998).

[11] P. Warwick, A. Hall, J. Zhu, P.W. Dimmock, R. Robbins, L. Carlsen and P. Lassen. Effect of temperature on the nickel humic acid equilibrium reaction. Chemosphere, (1998).

[12] S.J. King and P. Warwick. Studies of Metal Complexation with Humic and Fulvic Acid. In Effects of Humic Substances on the Migration of Radionuclides: Complexation and Transport of the Actinides. pp 217-244 Ed. G. Buckau. Wissenschaftliche Berichte (FZKA 6124, ISSN 0947-8620), Forschungszentrum Karlsruhe Technik and Umwelt, Karlsruhe, Germany (1998).

[13] R.G. McLaren, C.A. Backes, A.W. Rate and R.S. Swift. Cadmium and Cobalt desorption kinetics from soil clays: Effect of sorption period. Soil Sci Soc Am J. 62, 332-337, (1998).

[14] F. Rey, E. Calle and J. Casado. Study of the effects of concentration and pH on the dissociation kinetics of Fe(II)-fulvic acid complexes. International Journal of Chemical Kinetics, 30, 1, 63-67, (1998).

[15] J.A. Lavigne, C.H. Langford and M.K.S. Mak. Kinetic study of speciation of nickel (II) bound to a fulvic acid. Anal. Chem. 59, 2616-2620, (1987).

[16] S.E. Cabaniss. pH and ionic strength effects on Nickel-Fulvic acid dissociation kinetics. Environ Sci Tech, 24, 583-588, (1990).

[17] Y. Lu, C.L. Chakrabarti, M.H. Back, D.C. Gregoire, and W.H. Schroeder. Kinetic studies of metal speciation using inductively-coupled plasma mass spectrometry. J. Environ. Anal. Chem. 60, 313-337, (1995).

[18] A.L.R. Sekaly, M.H. Back, C.L. Chakrabarti, D.C. Gregoire, J.Y. Lu and W.H. Schroeder. Measurements and analysis of dissociation rate constants of metal fulvic acid complexes in aqueous solutions. Part II: measurement of decay rates by inductively-coupled plasma mass spectrometry and determination of rate constants for dissocaition. Spectrochimica Acta Part B, 53, 847-858, (1998).

[19] J.I. Kim, G. Buckau, E. Bryant and R. Klenze. Complexation of Americium(III) with Humic Acid. Radiochimica Acta, 48, 135-143, (1989).

[20] A. J. Fairhurst. The role of colloids in the transport of toxic metals through the environment. Ph. D. Thesis, Loughborough University, UK (1996).

[21] G.R. Aiken, D.M. McKnight, R.L. Wershaw and P. MacCarthy. Humic substances in soil sediment and water. Wiley.

[22] S.B. Clark and G.R. Choppin. A comparison of the dissociation kinetics of rare earth element complexes with synthetic polyelectrolytes and humic acid. ACS Symposium Series, 651, 207-219, (1996).

[23] D.L. Olson and M.S. Shuman. Copper dissociation from estuarine humic materials. Geochimica Cosmochimica Acta, 49, 1371-1375, (1985).

[24] M. Norden, J.H. Ephraim and B. Allard. Europium complexation by an aquatic fulvic acid-effects of competing ions. Talanta, 44, 781-786, (1997).

[25] G. Bidoglio, N. Omenetto and P. Robouch. Kinetic Studies of Lanthanide Interactions with Humic Substances by Time Resolved Laser Induced Fluorescence. Radiochimica Acta, 52/53, 57-63, (1991).

[26] V. Moulin, J. Tits and G. Ouzounian. Actinide Speciation in the Presence of Humic Substances in Natural Water Conditions. Radiochimica Acta, 58/59, 179-190, (1992).

[27] W. Schussler, *et al.* Modelling of Humic Colloid Mediated Transport of Americium(III) by a kinetic approach. In Effects of Humic Substances on the Migration of Radionuclides: Complexation and Transport of the Actinides. pp 245-262 Ed. G. Buckau. Wissenschaftliche Berichte (FZKA 6124, ISSN 0947-8620), Forschungszentrum Karlsruhe Technik and Umwelt, Karlsruhe, Germany (1998).

Table 2.1. $[Eu]_{FIX}$ and k_3 determined for different conditions.

[HS]	$[Eu]_T$	Equilibration time	$[Eu]_{FIX}$	k_3	
mg dm^{-3}	mol dm^{-3}	(days)	mol dm^{-3}	(min^{-1})	
20°C, pH=4.5					
FA/HA concentration					
10 (FA)	1.14E-07	9	5.29E-09	1.50E-05	
60 (FA)	1.14E-07	9	1.99E-08	8.50E-06	
10 (HA)	1.14E-07	9	1.10E-08	1.50E-05	
Equilibration Time					
10 (FA)	1.14E-07	7	5.15E-09	2.80E-05	
10 (FA)	1.14E-07	9	5.29E-09	1.50E-05	
10 (FA)	1.14E-07	26	3.40E-09	6.90E-05	
10 (FA)	1.14E-07	35	5.24E-09	2.17E-05	
10(FA)	1.14E-07	133	8.79E-09	3.10E-05	
Competing cations					
10 (FA)	1.14E-07	7	5.15E-09	2.80E-05	
10 (FA)	1.14E-07	7	5.25E-09	1.10E-05	Ca,Mg
10 (FA)	1.14E-07	7	5.48E-09	5.00E-05	Al,Fe
10 (FA)	1.14E-07	7	5.24E-09	3.30E-05	Al,Fe,Ca, Mg
10 (HA)	1.14E-07	7	1.55E-08	2.90E-05	
10 (HA)	1.14E-07	7	1.41E-08	3.90E-05	Al,Fe,Ca, Mg
Europium concentration					
10 (FA)	1.14E-07	9	5.29E-09	1.50E-05	
10 (FA)	1.28E-06	8	2.58E-08	4.60E-05	
10 (HA)	1.14E-07	9	1.10E-08	1.50E-05	
10 (HA)*	1.31E-07		7.50E-08	6.10E-05	
10 (HA)	6.84E-07	8	5.80E-08	6.62E-05	
10 (HA)	1.28E-06	8	6.79E-08	3.20E-05	
Resin weight					
10 (FA)	1.14E-07	26	3.40E-09	7.20E-05	

[HS]	[Eu]T	Equilibration time	[Eu]FIX	k3	
mg dm-3	mol dm-3	(days)	mol dm-3	(min-1)	
20°C, pH=6.5					
FA/HA concentration					
10 (FA)	1.14E-07	9	3.55E-08	1.30E-05	
60 (FA)	1.14E-07	9	1.03E-07	5.30E-06	
10 (HA)	1.14E-07	9	8.29E-08	1.40E-05	
Equilibration Time					
10 (FA)	1.14E-07	9	3.55E-08	1.30E-05	
10 (FA)	1.14E-07	131	5.23E-08	9.20E-06	
Competing cations					
10 (FA)	1.14E-07	7	3.91E-08	5.00E-06	
10 (FA)	1.14E-07	7	4.27E-08	6.00E-06	Ca+Mg
10 (HA)	1.14E-07	7	9.17E-08	1.10E-05	
10 (HA)	1.14E-07	7	9.38E-08	6.30E-06	Ca+Mg
Europium Concentration					
10 (FA)	1.14E-07	9	3.55E-08	1.30E-05	
10 (FA)	6.84E-07	8	1.71E-07	1.80E-05	
10 (FA)	1.28E-06	8	2.67E-07	2.00E-05	
10 (HA)	1.14E-07	9	8.29E-08	1.40E-05	
10 (HA)	6.84E-07	8	3.71E-07	1.20E-05	
10 (HA)	1.28E-06	8	5.69E-07	1.00E-05	
Buffer					
10 (HA)	1.14E-07	7	9.25E-08	3.60E-06	No MES
10 (HA)	1.14E-07	7	6.30E-08	1.80E-05	MES

[HS]	[Eu]T	Equilibration time	[Eu]FIX	k3
mg dm-3	mol dm-3	(days)	mol dm-3	(min-1)
40°C, pH=4.5				
FA/HA concentration				
60 (FA)	1.14E-07	12	1.65E-08	5.80E-05
10 (HA)	1.14E-07	8	1.45E-08	1.10E-04
Equilibration Time				
10 (FA)	1.14E-07	2	2.90E-09	7.20E-05
10 (FA)	1.14E-07	8	3.36E-09	1.20E-04
10 (FA)	1.14E-07	12	3.16E-09	8.20E-05
10 (FA)	1.14E-07	41	4.33E-09	7.80E-05
10 (FA)	1.14E-07	161	8.33E-09	1.10E-04
40°C, pH=6.5				
FA/HA concentration				
10 (FA)	1.14E-07	8	3.95E-08	2.70E-05
60 (FA)	1.14E-07	6	1.10E-07	1.50E-05
10 (HA)	1.14E-07	6	1.04E-07	3.20E-05
Equilibration Time				
10 (FA)	1.14E-07	3	3.69E-08	2.90E-05
10 (FA)	1.14E-07	8	3.95E-08	2.70E-05
10 (FA)	1.14E-07	64	3.63E-08	3.10E-05
10 (FA)	1.14E-07	183	4.67E-08	3.80E-05
Filtering				
10 (FA)	1.14E-07	64	3.63E-08	3.10E-05
10 (FA) UF	1.14E-07	64	3.64E-08	3.00E-05

[HS]	[Eu]T	Equilibration time	[Eu]FIX	k3
mg dm-3	mol dm-3	(days)	mol dm-3	(min-1)
60°C, pH=4.5				
FA/HA concentration				
10 (FA)	1.14E-07	8	1.70E-09	6.10E-05
60 (FA)	1.14E-07	8	8.01E-09	4.80E-05
10 (HA)	1.14E-07	8	1.12E-08	6.10E-05
Equilibration Time				
10 (FA)	1.14E-07	8	1.70E-09	6.10E-05
10 (FA)	1.14E-07	15	2.18E-09	4.10E-05
10 (FA)	1.14E-07	61	3.76E-09	5.30E-05
10 (FA)	1.14E-07	176	6.84E-09	1.90E-04
Europium Concentration				
10 (FA)	1.14E-07	8	1.70E-09	6.10E-05
10 (FA)	6.84E-07	7	8.02E-09	5.90E-05
10 (FA)	1.28E-06	7	1.74E-08	4.00E-05
60 (FA)	1.14E-07	8	8.01E-09	4.80E-05
60 (FA)	6.84E-07	8	4.53E-08	5.70E-05
60 (FA)	1.28E-06	8	9.94E-08	5.70E-05
10 (HA)	1.14E-07	8	1.12E-08	6.10E-05
10 (HA)	1.28E-06	7	7.09E-08	4.90E-05
60°C, pH=6.5				
FA/HA concentration				
10 (FA)	1.14E-07	9	4.54E-08	1.11E-04
60 (FA)	1.14E-07	9	1.06E-07	4.10E-05
10 (HA)	1.14E-07	9	1.03E-07	8.70E-05

Table 2.2a. The effect of pH on $[Eu]_{FIX}$ at different temperatures.

[HS]	[Eu]FIX	[Eu]FIX	Ratio
mg dm-3	pH=4.5	pH=6.5	
20°C			
10 (FA)	5.30E-09	3.55E-08	6.71
60 (FA)	2.00E-08	1.03E-07	5.18
10 (HA)	1.10E-08	8.29E-08	7.54
Average			6.47
40°C			
10 (FA)	3.36E-09	3.95E-08	11.76
60 (FA)	1.65E-08	1.10E-07	6.67
10 (HA)	1.45E-08	1.04E-07	7.17
Average			8.53
60°C			
10 (FA)	1.70E-09	4.54E-08	26.71
60 (FA)	8.01E-09	1.06E-07	13.23
10 (HA)	1.12E-08	1.03E-07	9.2
Average			16.38

Table 2.2b. The effect of pH on k_3 (min^{-1}) at different temperatures.

[HS]	k3	k3	Ratio
mg dm-3	pH=4.5	pH=6.5	
20°C			
10 (FA)	1.50E-05	1.30E-05	0.87
60 (FA)	8.50E-06	5.30E-06	0.62
10 (HA)	1.50E-05	1.40E-05	0.93
Average			0.81
40°C			
10 (FA)	1.20E-04	2.70E-05	0.23
60 (FA)	5.80E-05	1.50E-05	0.26
10 (HA)	1.10E-04	3.20E-05	0.29
Average			0.26
60°C			
10 (FA)	6.10E-05	1.11E-04	1.82
60 (FA)	4.80E-05	4.10E-05	0.85
10 (HA)	6.10E-05	8.70E-05	1.43
Average			1.37

Table 2.3a. The effect of fulvic acid concentration on $[Eu]_{FIX}$ and k_3 at pH = 4.5.

[HS]	20°C	40°C	60°C	Average
mg dm-3				
[Eu]FIX				
10 (FA)	5.30E-09	3.36E-09	1.70E-09	
60 (FA)	2.00E-08	1.65E-08	8.01E-09	
60:10:00	3.76	4.91	4.71	4.46
k3				
10 (FA)	1.50E-05	1.20E-04	6.10E-05	
60 (FA)	8.50E-06	5.80E-05	4.80E-05	
60:10:00	0.57	0.48	0.79	0.61

Table 2.3b. The effect of fulvic acid concentration on $[Eu]_{FIX}$ and k_3 at pH = 6.5.

[HS]	20°C	40°C	60°C	Average
mg dm-3				
[Eu]FIX				
10 (FA)	3.55E-08	3.95E-08	4.54E-08	
60 (FA)	1.03E-07	1.10E-07	1.06E-07	
60:10:00	2.9	2.78	2.33	2.67
k3				
10 (FA)	1.30E-05	2.70E-05	1.11E-04	
60 (FA)	5.30E-06	1.50E-05	4.10E-05	
60:10:00	0.41	0.56	0.37	0.44

Table 2.4a. A comparison of $[Eu]_{FIX}$ and k_3 for HA and FA at pH = 4.5.

[HS]	20°C	40°C	60°C	Average
mg dm-3				
[Eu]FIX				
10 (FA)	5.30E-09	3.36E-09	1.70E-09	
10 (HA)	1.10E-08	1.45E-08	1.12E-08	
HA:FA	2.08	4.32	6.59	4.33
k3				
10 (FA)	1.50E-05	1.20E-04	6.10E-05	
10 (HA)	1.50E-05	1.10E-04	6.10E-05	
HA:FA	1	0.92	1	0.97

Table 2.4b. A comparison of $[Eu]_{FIX}$ and k_3 for HA and FA at pH = 4.5.

[HS]	20°C	40°C	60°C	Average
mg dm-3				
[Eu]FIX				
10 (FA)	3.55E-08	3.95E-08	4.54E-08	
10 (HA)	8.29E-08	1.04E-07	1.03E-07	
HA:FA	2.34	2.63	2.27	2.41
k3				
10 (FA)	1.30E-05	2.70E-05	1.11E-04	
10 (HA)	1.40E-05	3.20E-05	8.70E-05	
HA:FA	1.08	1.19	0.78	1.02

Table 2.5. The effect of changing the total Eu concentration on $[Eu]_{FIX}$ and k_3.

[HS]	$[Eu]_T$	Temp	$[Eu]_{FIX}$	k_3	$[Eu]_{FIX}/[Eu]_T$	Metal
mg dm-3	mol dm-3	°C	mol dm-3	min-1		Loading
pH=4.5						
10 (FA)	1.14E-07	20	5.29E-09	1.50E-05	0.046	2.30E-03
10 (FA)	1.28E-06	20	2.58E-08	4.60E-05	0.02	2.60E-02
10 (HA)	1.14E-07	20	1.10E-08	1.50E-05	0.096	2.10E-03
10 (HA)	6.84E-07	20	5.80E-08	6.62E-05	0.085	1.30E-02
10 (HA)*	1.31E-07	20	1.44E-08	6.10E-05	0.11	2.40E-03
10 (HA)	1.28E-06	20	6.79E-08	3.20E-05	0.053	2.40E-02
10 (FA)	1.14E-07	60	1.70E-09	6.10E-05	0.015	2.30E-03
10 (FA)	6.84E-07	60	8.02E-09	5.90E-05	0.012	1.40E-02
10 (FA)	1.28E-06	60	1.74E-08	4.00E-05	0.014	2.60E-02
60 (FA)	1.14E-07	60	8.01E-09	4.80E-05	0.07	3.80E-04
60 (FA)	6.84E-07	60	4.53E-08	5.70E-05	0.066	2.30E-03
60 (FA)	1.28E-06	60	8.23E-08	4.00E-05	0.064	4.30E-03
10 (HA)	1.14E-07	60	1.12E-08	6.10E-05	0.098	2.10E-03
10 (HA)	1.28E-06	60	7.09E-08	4.90E-05	0.055	2.40E-02
pH=6.5						
10 (FA)	1.14E-07	20	3.55E-08	1.30E-05	0.311	2.30E-03
10 (FA)	6.84E-07	20	1.71E-07	1.80E-05	0.25	1.40E-02
10 (FA)	1.28E-06	20	2.67E-07	2.00E-05	0.209	2.60E-02
10 (HA)	1.14E-07	20	8.29E-08	1.40E-05	0.727	2.10E-03
10 (HA)	6.84E-07	20	3.71E-07	1.20E-05	0.542	1.30E-02
10 (HA)	1.28E-06	20	5.69E-07	1.00E-05	0.445	2.40E-02
10 (FA)	1.14E-07	60	2.57E-08	9.50E-05	0.225	2.30E-03
10 (FA)	1.28E-06	60	1.96E-07	9.80E-05	0.153	2.60E-02
60 (FA)	1.14E-07	60	7.72E-08	6.80E-08	0.677	3.80E-04
60 (FA)	6.84E-07	60	3.39E-07	7.10E-05	0.496	2.30E-03

Table 2.6. The effect of cations on $[Eu]_{FIX}$ and k_3 at 20°C.

[HS]	[Eu]FIX	k_3	Cation added
mg dm^{-3}	mol dm^{-3}	min^{-1}	
pH=4.5			
10 (FA)	5.15E-09	2.80E-05	
10 (FA)	5.25E-09	1.10E-05	Ca, Mg
10 (FA)	5.48E-09	5.00E-05	Al, Fe
10 (FA)	5.24E-09	3.30E-05	Al, Fe, Ca, Mg
10 (HA)	1.55E-08	2.90E-05	
10 (HA)	1.41E-08	3.90E-05	Al, Fe, Ca, Mg
pH=6.5			
10 (FA)	3.91E-08	5.00E-06	
10 (FA)	4.27E-08	6.00E-06	Ca, Mg
10 (HA)	9.17E-08	1.10E-05	
10 (HA)	9.38E-08	6.30E-06	Ca, Mg

Table 2.7a. Determination of K, ΔG_{KIN}. ΔH_{KIN} and ΔS_{KIN} from $[Eu]_{FIX}$.

[HS]	K	ΔG_{KIN}	ΔH_{KIN}	ΔS_{KIN}
mg dm^{-3}		kJ/mol	kJ/mol	J/K/mol
pH=4.5				
10(FA)	0.05	7.4	-24.2	-107
60(FA)	0.21	3.8	-19.4	-78
10(HA)	0.11	5.5	0.24	-18
pH=6.5				
10(FA)	0.45	2	7.9	20
60(FA)	9.36	-5.5	7.8	45
10(HA)	2.67	-2.4	26.1	97

Table 2.7b. Determination of E_a, A, ΔS_{ACT} and ΔG_{ACT} from k_3.

[HS]	Ea	A	?SACT	?GACT
mg dm-3	kJ/mol		J/K/mol	kJ/mol
pH=6.5				
10 (FA)	41.7	5.35	-239	70
60 (FA)	41.5	2.1	-247	72
10 (HA)	37	0.86	-254	75

Table 2.8. Sorption and de-sorption rate constants for several metals.

	[HS]	kb	kf
	mg dm-3	(s-1)	(s-1)
LBORO (Eu)	pH=4.5		
	10 (FA)	2.50E-07	1.20E-08
	60 (FA)	1.40E-07	3.00E-08
	10 (HA)	2.50E-07	2.70E-08
	pH=6.5		
	10 (FA)	2.20E-07	9.80E-08
	60 (FA)	8.80E-08	8.30E-07
	10 (HA)	2.30E-07	6.20E-07
BGS (Co)		1.30E-06	2.90E-07
FZK (Am)		1.10E-06	5.90E-07

Table 2.9. The effect of 0.001M MES buffer on dissociation of EuHS.

[HS]	Equilibration time	$[Eu]_{FIX}$	k_3		R_2
mg dm^{-3}	(days)	(M)	(min^{-1})		
pH=6.5					
FA concentration					
10 (FA)	9	3.55E-08	1.30E-05		0.91
Competing cations					
10 (FA)	7	3.91E-08	5.00E-06		0.61
10 (FA)	7	4.27E-08	6.00E-06	Ca+Mg	0.91
Buffer					
10 (FA)	7	5.13E-08		No MES	
10 (FA)	7	3.88E-08		MES	
HA concentration					
10 (HA)	9	8.29E-08	1.40E-05		0.97
Competing cations					
10 (HA)	7	9.17E-08	1.10E-05		0.79
10 (HA)	7	9.38E-08	6.30E-06	Ca+Mg	0.72
Buffer					
10 (HA)	7	9.25E-08	3.60E-06	No MES	0.5
10 (HA)	7	6.30E-08	1.80E-05	MES	0.9

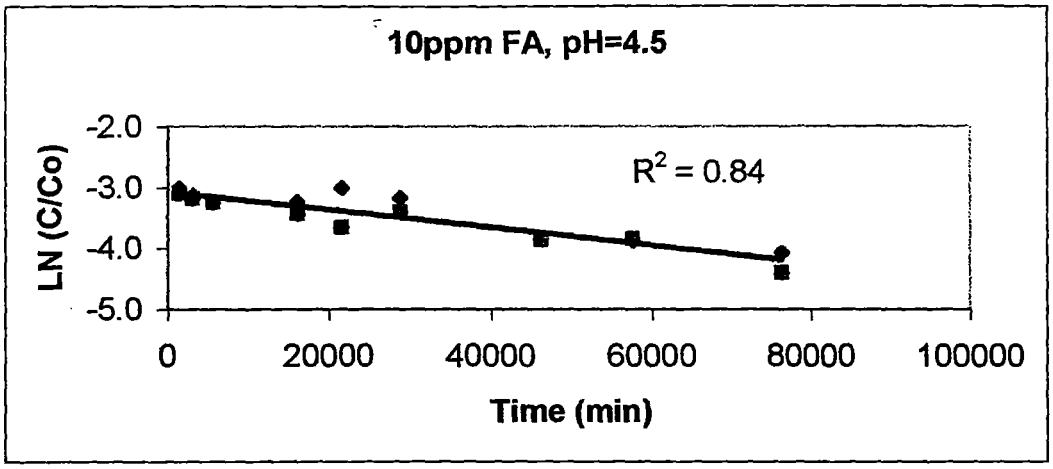

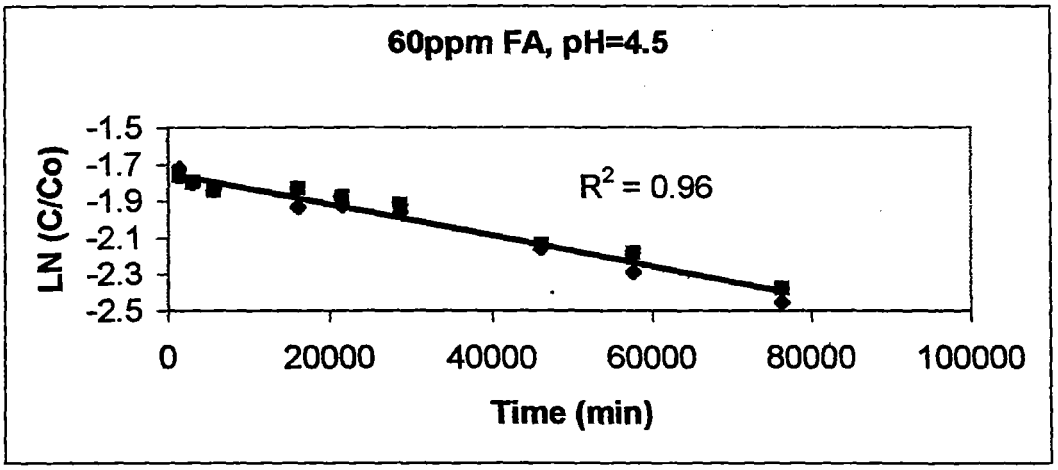

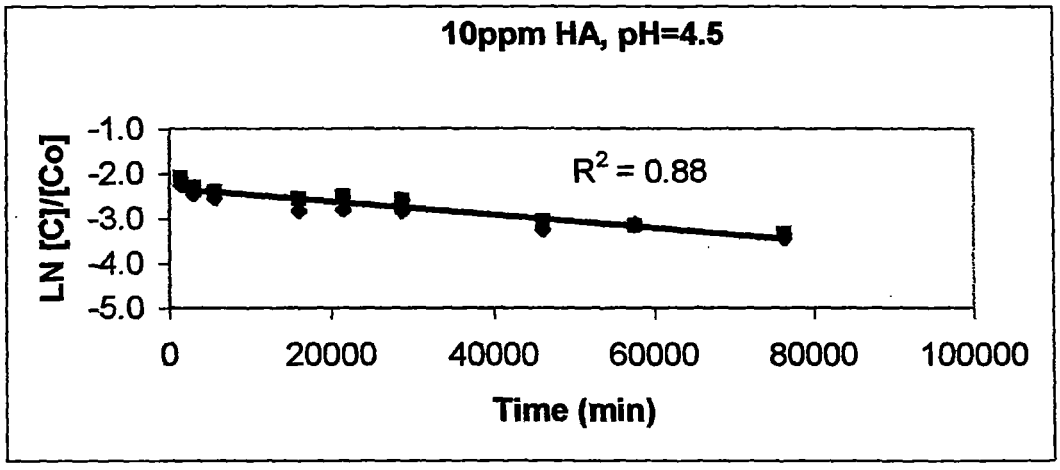

Figure 2.1 $\ln[EuFA]_t$ / $[EuFA]_{t=0}$ versus time for long resin contact times (pH = 4.5, T = 20°C)

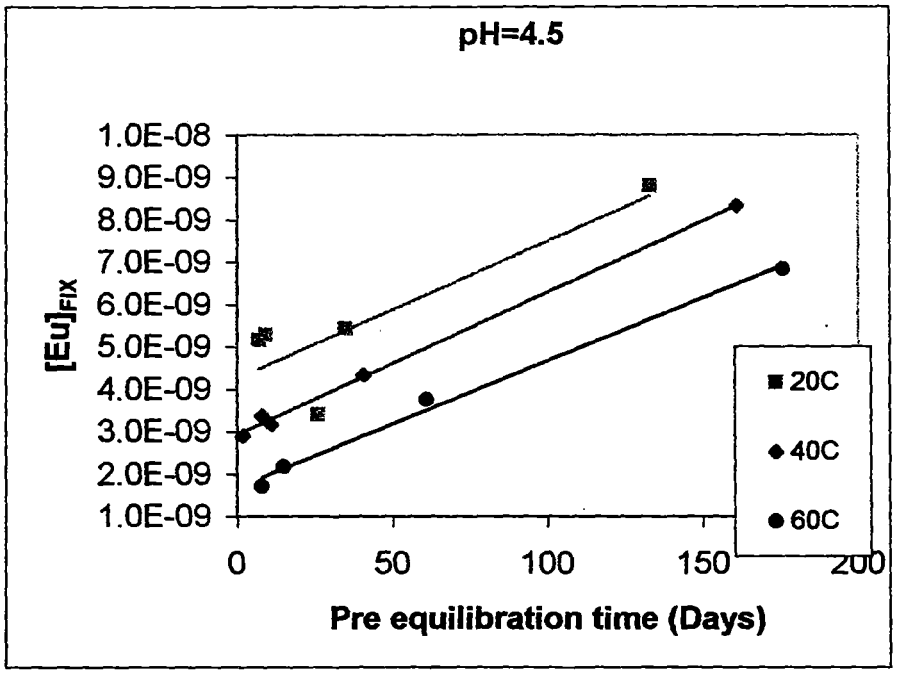

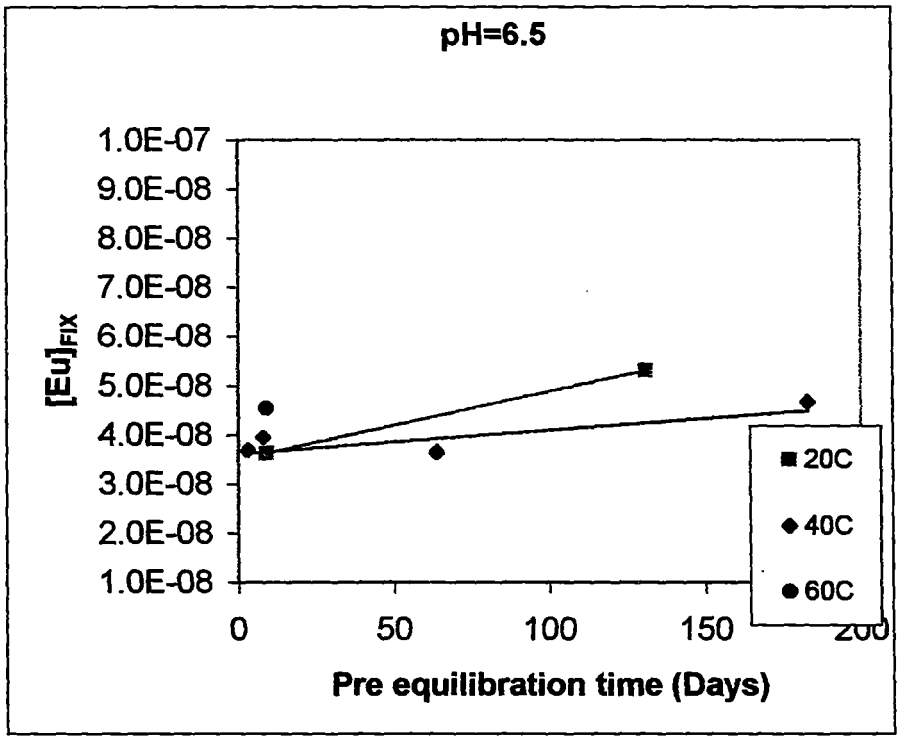

Figure 2.2 The effect of equilibration time on $[Eu]_{FIX}$

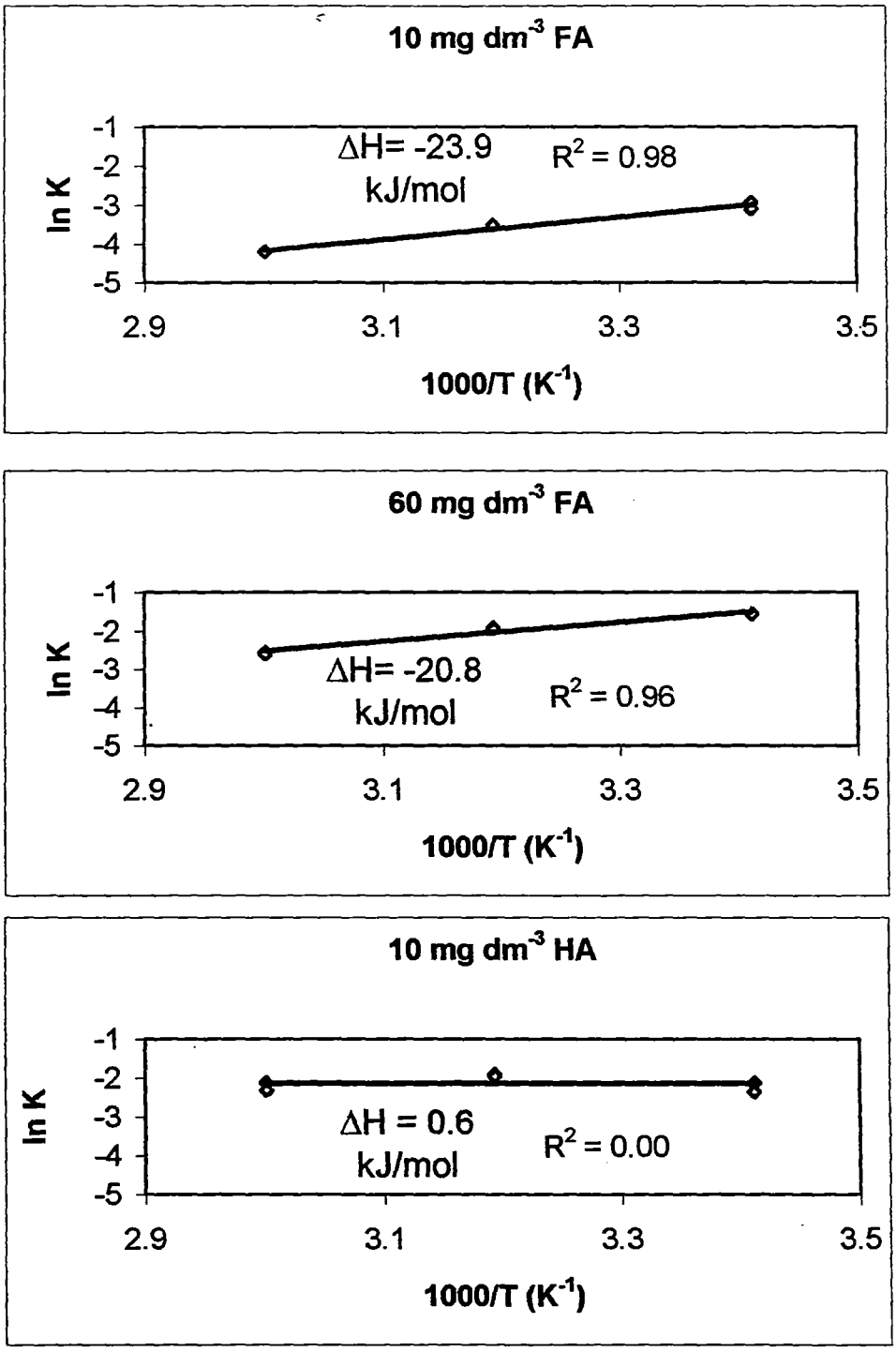

Figure 2.3. The temperature dependence of log β at pH = 4.5.

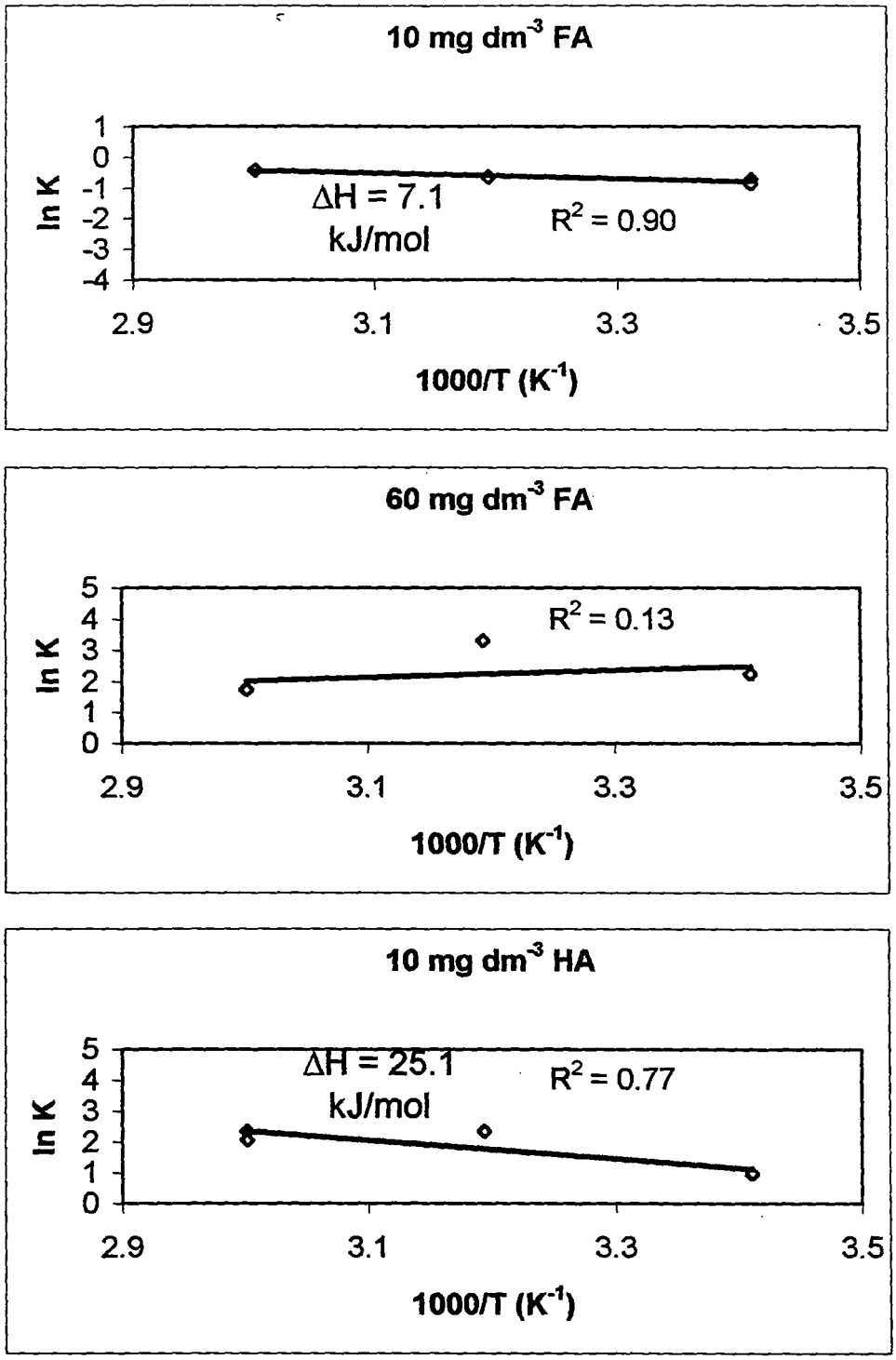

Figure 2.4. The temperature dependence of log β at pH = 6.5.

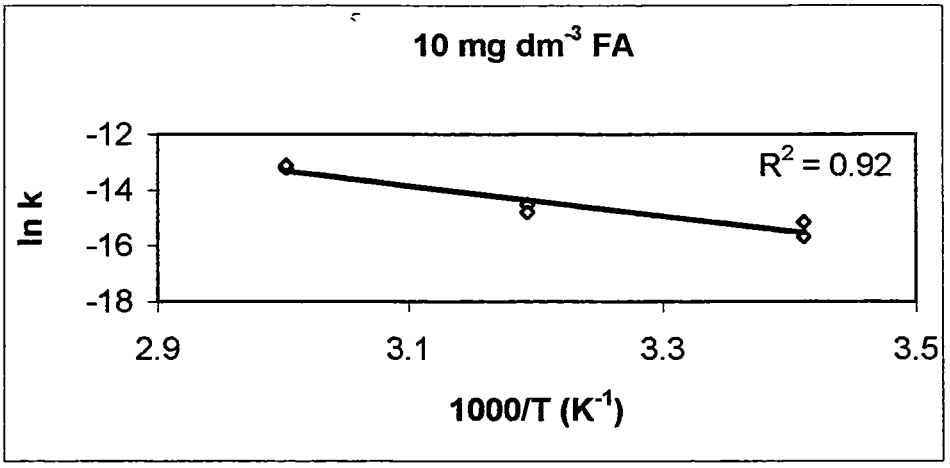

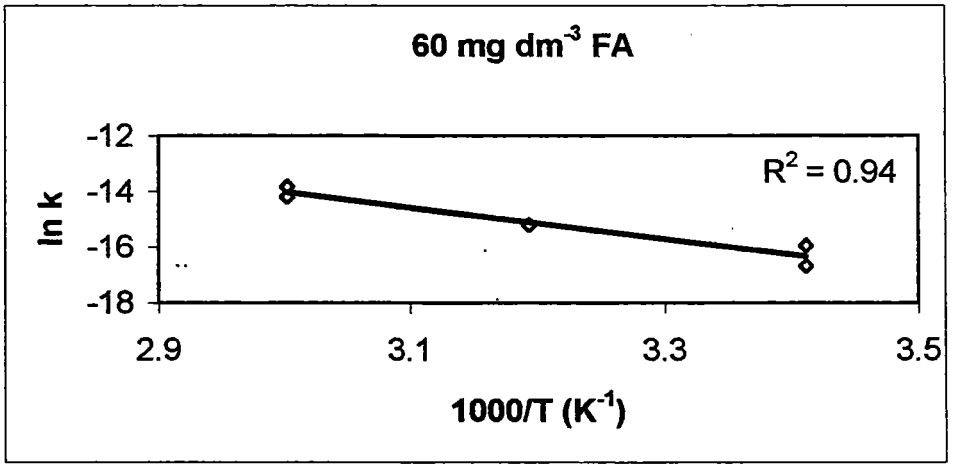

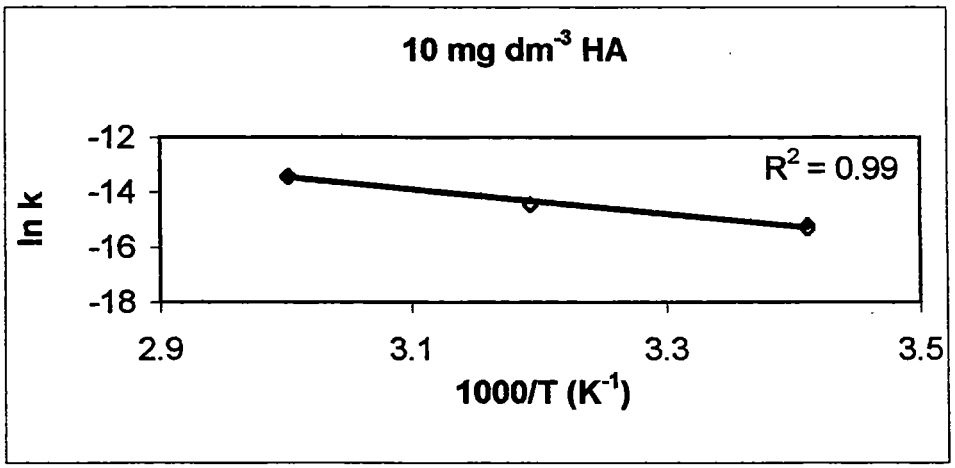

Figure 2.5. Determination of activation barrier at pH = 6.5

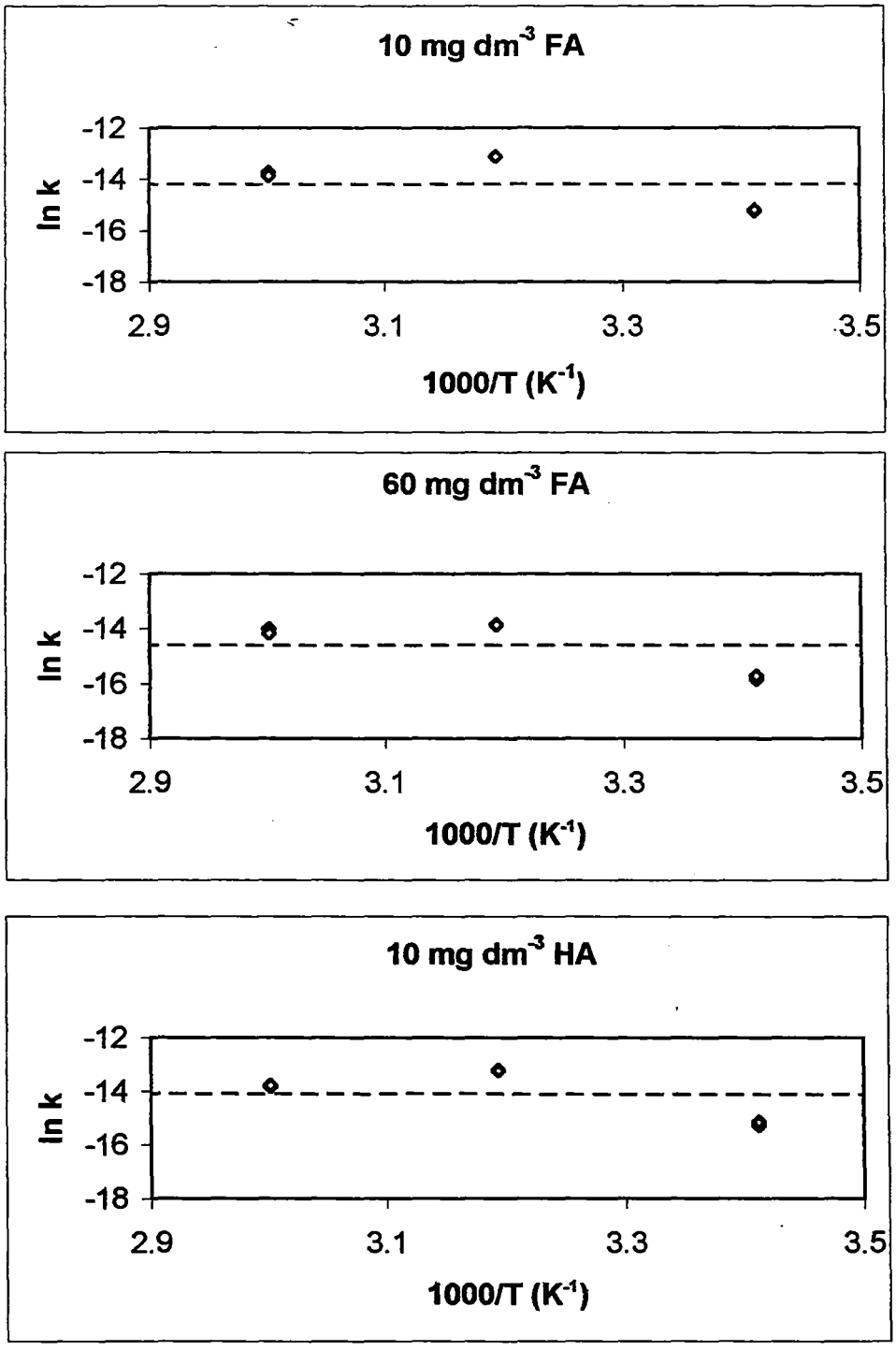

Figure 2.6 Determination of Activation Barrier at pH = 4.5

Annex 15

Investigations of Mixed Complexes

(P. Warwick, A. Hall, S.J. King and N. Bryan (LBORO and RMC-E))

3rd Technical Progress Report

EC Project:

Effects of humic substances on the migration of radionuclides: complexation and transport of actinides.

Project No.: F14W-CT96-0027

LU Contribution to Task 2

Investigation of mixed complexes

P. Warwick[1], A. Hall[1], S. J. King[1] and N. Bryan[2].

January 2000

1. Department of Chemistry, Loughborough University, Loughborough, Leics. LE11 3TU, UK.

2. Department of Chemistry, University of Manchester, Oxford Road, Manchester M13 9PL, UK.

Investigation of mixed complexes

Authors: P. Warwick[1], A. Hall[1], S. J. King[1] and N. Bryan[2].

1. Department of Chemistry, Loughborough University, Loughborough, Leics. LE11 3TU, UK.

2. Department of Chemistry, University of Manchester, Oxford Road, Manchester, M13 9PL, UK.

Summary.

Zetapotential measurements were performed on HA, before and after reaction with Eu in the presence and absence of excess carbonate, under alkaline conditions. The aim was to establish whether complexation resulted in a loss or gain of negative charge.

The magnitude of the negative zetapotential in the $NaHCO_3$ system decreased in direct contrast to the predicted increase in negative charge due to $EuHA(CO_3)_2^{-2}$ formation. Unexpectedly in the NaCl system, where mixed carbonate complexation was impossible, the same decrease in zetapotential was observed. The observations raise questions regarding the correctness of the reported stoichiometry and/or log β value of the mixed complex.

Introduction.

Metal ions (M) react with humic acids (HA) to form complexes (MHA). The general reaction can be represented as

$$M + HA \Leftrightarrow MHA$$

However under certain conditions several workers have reported the formation of mixed complexes involving HA and other ligands such as OH^- and CO_3^{-2} [1, 2, 3]. For example Maes et al [3] postulated that the ternary complex $EuHA(CO_3)_2$ forms under alkaline conditions in the presence of excess carbonate viz:-

$$Eu + HA + 2CO_3 \Leftrightarrow EuHA(CO_3)_2$$

(Charges are ignored at this stage.)

Assuming metal ions bind predominantly at carboxyl sites on the HA molecules binary and ternary interactions will generate different localised electrical charges. For example the net

charge at a site where $EuHA(CO_3)_2$ has formed due to the combination of a single COO^- function, one Eu^{3+} ion and 2 CO_3^{-2} ions will be –2. Whereas one Eu^{3+} ion combined with a single COO^- confers a local +2 charge. Therefore Zetapotential measurements were performed on HA, before and after reaction with Eu in the presence and absence of excess carbonate, under alkaline conditions. The aim being simply to establish whether complexation resulted in a loss or gain of negative charge and thereby to provide evidence for or against the existence of $EuHA(CO_3)_2$. However a number of assumptions were necessary. Firstly the non-availability of a rigorous mathematical relationship between surface charge and zetapotential [4] was deemed not to be a problem, since only relative and not absolute changes required to be determined. Secondly HA molecules, with molecular dimensions of around 1nm, are generally regarded as being too small for successful zetapotential measurements. However in this study credible values were observed. Association of HA molecules was inferred. Association is an accepted HA phenomenon [6] and during electrophoresis, the resulting metastable flocculated HA species [7] would be capable of producing the light scattering effects needed to deduce mobilities and hence zetapotentials. Therefore the technique as employed in the Malvern Instruments Zetamaster [5], was successful. Finally the postulated agglomeration was assumed not to affect the underlying relationship between charge density and zetapotential.

Experimental.

Aldrich NaHA (0.05 g) was dissolved in deionised H_2O (1.0 dm^3) and adjusted to pH = 9.0 to give a 50 mg dm^{-3} stock solution.

A.R. $Eu(NO_3)_3.5H_2O$ (0.4282g) was dissolved in deionised H_2O (100cm^3) to give a 1.0×10^{-2} M stock solution.

A.R. NaHCO3 (1.6796g) was dissolved in deionised H_2O (100cm^3) and adjusted to pH = 9.0 to provide a 2.0×10^{-1} M stock solution.

A.R. NaCl solution (0.5845g) was dissolved in H_2O (100cm^3) and adjusted to pH = 9.0 to provide a 2.0×10^{-1} M stock solution.

These stock solutions were used to prepare the mixtures specified in Table 5. The mixtures were prepared with and without Eu (1×10^{-4}M), in either 0.1 M $NaHCO_3$ or 0.1M NaCl. HA was present at a concentration of 20 mg dm^{-3} and small amounts of NaOH were added to adjust the

final pH values to 9.0. The mixtures were equilibrated for two weeks at room temperature. Afterwards the HA zetapotentials were determined using a Malvern Instruments' Zetamaster [5].

Results and discussion.

The width of the diffuse part of the electrical double layer surrounding charged particles varies with ionic strength [4]. Hence zetapotentials which are considered to be located at the shear plane also vary. For example in water, containing a very small amount of NaOH, the zetapotential of a 20.0 mg dm^{-3} solution was determined to be –43.3 (+5.1) mV, whereas in 0.1 M NaCl at pH = 9.0, the potential was –32.9 (+7.4) mV. Therefore all the measurements were carried out under constant ionic strength conditions in either 0.1 M $NaHCO_3$ or 0.1 M NaCl.

As noted above formation of $EuHA(CO_3)_2^{-2}$ from HA should lead to an increase in the magnitude of the negative charge. The anticipated increase was calculated by predicting the speciation of Eu in $NaHCO_3$ and NaCl containing solutions, using Maes et al's [3] log β value of 16.5 for $EuHA(CO_3)_2^{-2}$ and the PHREEQE speciation code [8]. For completeness Maes et al's log β value of 18 (-10 PHREEQE format) for $EuHA(OH)_2^0$ was also included. The resulting predictions for the species of interest are given in Tables 1 and 2.

The HA-COOH groups (represented as HA^-) were assumed to be fully dissociated, since the experiments were conducted at pH = 9.0. In the $NaHCO_3$ system 49% were predicted to react with Eu to form the mixed carbonato complex. $EuHA(OH)_2^0$ formation was not significant. In the NaCl system $Eu(OH)_3$ precipitation was predicted, along with 42% $EuHA^{+2}$ and 6% $EuHA(OH)_2^0$ formation. In both systems 51% of free HA^- remained. It may be noted that the quoted concentrations were obtained in molalities, however they can be treated as molarities, since the differences are not significant.

In order to compare the results with an accepted modelling approach, not incorporating mixed HA carbonate complexes, the speciation was also predicted using PHREEQEV [9]. PHREEQEV contains an implementation of Tipping's humic acid Model V [10] and therefore does include mixed hydroxo species i.e. in this case $EuHA(OH)^+$. Also the approach has been used

successfully by the authors in previous metal humic acid studies [11]. The predictions obtained in this study are given in Tables 3 and 4. It must be noted that convergence problems encountered using PHREEQEV, when attempting to equilibrate the system with $Eu(OH)_3$, did not affect the outcome of the study, either in terms of the inferences or the conclusions. The resulting lack of a precise quantitative description of the system simply highlighted limitations with regard to the current implementation of Model V within PHREEQE.

The species information was then used to calculate the HA charge in each situation. The predicted charges are listed alongside the measured zetapotentials in Table 5. For the reader's convenience certain features of the anticipated and observed behaviour are conceptualised in Figure 1. It will be noted from Table 5 that the experimental precision was poor. Nevertheless due to the large number of observations involved (>20) the quoted averages are believed to be reliable i.e. accurate.

The results may be summarised as follows:-
(i) The magnitude of the negative zetapotential exhibited by the HA in the $NaHCO_3$ system decreased on addition of Eu,
(ii) The zetapotential decreased in the $NaHCO_3$ and NaCl systems to the same extent.
(iii) A brown coloured precipitate was produced in the NaCl system but not in the $NaHCO_3$ system.

With regard to the change in the magnitude of the negative zetapotential upon addition of Eu, neither model predicted the observed 19% decrease in the $NaHCO_3$ system. Model V predicted no change in the negative charge, whilst the mixed complex approach predicted a 51% increase (Table 5). Model V indicated that the HA dissociation was approximately 66%. Consequently the assumption of complete HA dissociation in the mixed ligand approach probably contributed to an overestimate of mixed complex formation. However a 33% reduction in COOH dissociation would not have obscured an increase in negative charge resulting from $EuHA(CO_3)_2^{-2}$ formation.

In the $NaHCO_3$ system, Model V predicted virtually 100% $Eu(CO_3)_2^-$ formation and therefore complete solubility as observed. However formation of $Eu(CO_3)_2^-$ alone would not have affected the zetapotential and the zetapotential decrease certainly indicated some interaction between HA and Eu. The mixed ligand approach predicted 51% $Eu(CO_3)_2^-$ and 49% $EuHA(CO_3)_2^{-2}$ but this would have increased the magnitude of the negative zetapotential. Also the solubility of this amount of mixed complex is an open question. In the NaCl system both models predicted substantial amounts of $Eu(OH)_3$ precipitation. Unfortunately neither model incorporates a solubility product for EuHA. Clearly there was no possibility of mixed carbonate complexation in the NaCl system. However the re-suspended particulates displayed the same zetapotential as the colloidal HA in the Eu - $NaHCO_3$ system. If the precipitate in the NaCl system was as predicted i.e. $Eu(OH)_3$ and not simply EuHA, then co-precipitation of HA can be inferred due to the brown colour of the precipitate and the loss of colour from the solution phase. This sorbed HA carried bound Eu, so it is postulated that the surface exhibited the same charge density as the colloidal agglomerates in the $NaHCO_3$ system.

Concluding remarks.

Neither the mixed ligand approach nor PHREEQEV predictions are compatible with the observed zetapotential changes. At the very least the results suggest a reappraisal of the postulated $EuHA(CO_3)_2$ complex. Either the mixed HA carbonate stoichiometry, the log β value or both are incorrect. The similarity of the zetapotential decrease in the $NaHCO_3$ and NaCl systems strongly suggests that an equal but limited amount of Eu HA interaction occurred in both cases. The decrease rather than an increase indicates that the HA charge was partially neutralised. Possibly mixed hydroxo complexes were formed in both systems. However if mixed $EuHA(OH)_x$ species were involved, it follows that neither model currently employs the correct parameters for these species.

References.

1. P. Panak, R. Klenze and J. I. Kim. A study of ternary complexes of Cm(III) with humic acid and hydroxide or carbonate in neutral pH range by Time Resolved Laser Fluoresence Spectroscopy. Radiochimica Acta 74, 141 – 146 (1996).

2. M. A. Glaus, W. Hummel and L. r. Van Loon. Stability of mixed-ligand complexes of metal ions with humic substances and low molecular weight ligands. Environ. Sci. Technol. 29, 2150 – 2153 (1995).

3. A. Dierckx, A. Maes and J. Vancluysen. Mixed complex formation of Eu^{3+} with humic acid and a competing ligand. Radiochimica Acta 66/67, 149 – 156 (1994).

4. W. Stumm and J. J. Morgan., Aquatic Chemistry. (3^{rd} Edition), John Wiley and Sons, Inc., New York. (1996).

5. Zetamaster instruction manual. Malvern Instruments. Malvern Worcester, UK.

6. M. B. H. Hayes. Humic substances: Progress towards more realistic concepts of structures, in Humic substances, structures, uses and properties. G. Davies and E. A. Ghabbour. (Eds.). The Royal Society of Chemistry, MPG Books Ltd., Bodmin, Cornwall, UK. (1998)

7. M. J. Vold and R. D. Vold. Colloid chemistry. Chapman and Hall Ltd., London (1964).

8. D. L. Parkhurst, D. C. Thorstenson and L. N. Plummer, PHREEQE – A computer program for computer calculations. U.S. Geological Survey, Water Resources Investigations, 80 – 96, 210 (1980).

9. M. B. Crawford, PHREEQEV; The incorporation of Model V into the speciation code PHREEQE to model organic complexation in dilute solutions. British Geological Survey, Keyworth, Nottinghamshire, UK. NERC Technical Report, WE/93/19 (1993).

10. E. Tipping and M. A. Hurley. A unifying model of cation binding by humic substances. Geochim. Cosmochim. Acta. 56, 3627 - 3641 (1992).

11. P. Warwick, A. Hall and D. Read. A comparative evaluation of metal humic and fulvic predictive models. Radiochimica Acta 73, 11 – 19 (1996).

Table 1. Predicted concentrations of selected Eu and HA species in 0.1 M $NaHCO_3$ solution at pH 9.0, using PHREEQE [5] and Maes at al's log β values (see text) for mixed ligand complexes.

Species	Concentration /(mol kg^{-1})
HA^-	5.102×10^{-5}
$EuHA(CO_3)_2^{-2}$	4.898×10^{-5}
$EuHA(OH)_2^0$	1.277×10^{-9}
$Eu(CO_3)_2^-$	5.099×10^{-5}

Table 2. Predicted concentrations of Eu and HA species in 0.1 M NaCl solution at pH 9.0, using PHREEQE [5] and Maes at al's log β value for the $EuHA(OH)_2^0$ species.

Species	Concentration /(mol kg^{-1})
HA^-	5.131×10^{-5}
$Eu(OH)^{+2}$	7.535×10^{-8}
$Eu(OH)_2^+$	1.062×10^{-8}
$Eu(OH)_3$	1.585×10^{-9}
$EuHA^{+2}$	4.251×10^{-5}
$EuHA(OH)_2^0$	6.186×10^{-6}
$Eu(OH)_3$ precipitate	5.086×10^{-5}

Table 3. Predicted concentrations of important Eu and HA species in 0.1 M $NaHCO_3$ solution at pH 9.0, using PHREEQEV [9].

Species	Concentration /(mol kg^{-1})
HA^-	7.697×10^{-5}
HAH	2.203×10^{-5}
$EuHA^{+2}$	7.215×10^{-9}
$EuHA(OH)^+$	1.749×10^{-9}
$Eu(CO_3)_2^-$	9.998×10^{-5}

Table 4. Predicted concentrations of important Eu and HA species in 0.1 M NaCl solution at pH 9.0, using PHREEQEV [9].

Species	Concentration* /(mol kg^{-1})
HA^-	6.847×10^{-5}
HAH	3.799×10^{-5}
$EuHA^{+2}$	2.440×10^{-9}
$EuHA(OH)^+$	2.339×10^{-9}
$Eu(OH)_3$ precipitate	7.055×10^{-5}

*The values are approximate due to convergence problems and a slight reduction in pH, when equilibrating the solution with the $Eu(OH)_3$ solid phase.

Table 5. Predicted charges and measured zetapotentials of HA (20mg dm^{-3}) , in the presence and absence of Eu (1 x 10^{-4}M) and carbonate (0.1M) or NaCl (0.1M), at pH = 9.0.

System	Model V charge predictions /(mol g^{-1})	Mixed complex charge predictions /(mol g^{-1})	Zetapotential /(mV)
HA + $NaHCO_3$	-3.85 x 10^{-3}	-5.0 x 10^{-3}	-30.9 (±7.3)
HA + $NaHCO_3$ + Eu (III)	-3.85 x 10^{-3}	-7.6 x 10^{-3}	-25.2 (±2.5)
HA + NaCl	-3.82 x 10^{-3}	-5.0 x 10^{-3}	-32.9 (±7.4)
HA + NaCl + Eu(III)	-1.04 x 10^{-3}	+1.8 x 10^{-3}	-25.5 (±3.8)

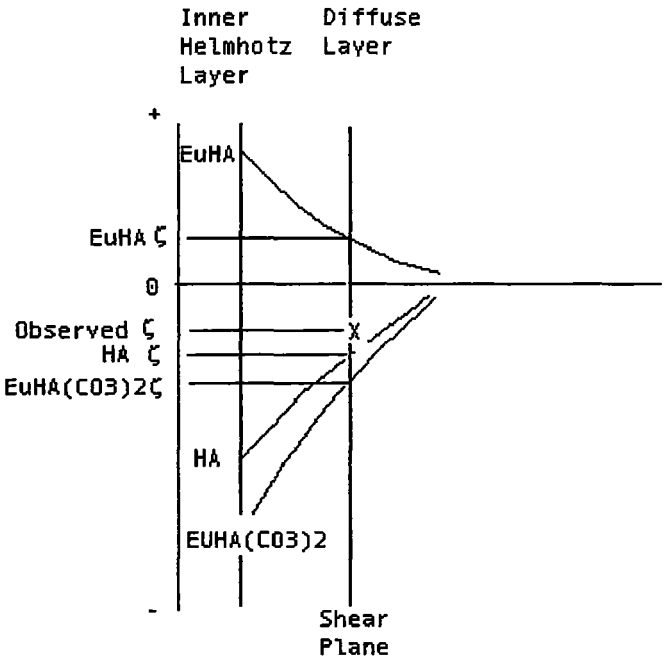

Figure 1. A schematic representation (not to scale) of the changes in electrical potential upon approaching pure HA, EuHA and EuHA$(CO_3)_2$ surfaces, facilitating a visual comparison between the anticipated zetapotentials (ζ) and the observed zetapotential (X) at the shear plane.

Annex 16

Effects of HA on the Transport of Eu through Sand

(P. Warwick, A. Hall, S.J. King and N. Bryan (LBORO and RMC-E))

3rd Technical Progress Report

EC Project:

Effects of humic substances on the migration of radionuclides: complexation and transport of actinides.

Project No.: F14W-CT96-0027

Further LU Contribution to Task 3

Effects of HA on the transport of Eu through sand

P. Warwick[1], A. Hall[1], S. J. King[1] and N. Bryan[2].

January 2000

1. Department of Chemistry, Loughborough University, Loughborough, Leics. LE11 3TU, UK.

2. Department of Chemistry, University of Manchester, Oxford Road, Manchester M13 9PL, UK.

Effects of HA on the transport of Eu through sand.

Authors: P. Warwick[1], A. Hall[1], S. J. King[1] and N. Bryan[2].

1. Department of Chemistry, Loughborough University, Loughborough, Leics. LE11 3TU, UK.

2. Department of Chemistry, University of Manchester, Oxford Road, Manchester, M13 9PL, UK.

Summary.

The effects of HA and silica colloids on Eu transport, through sand, were investigated at LU, by means of batch and column experiments during the parallel CARESS project. The Eu recoveries and elution profiles were used by Partner 9 to aid development and testing of a 1-d transport model.

Introduction.

The EC funded CARESS project (1996 – 1999) addressed the questions, "Do colloids have critical impact upon the transport and retention of radionuclides in the geosphere?" and if they do, "how should radionuclides associated with mobile colloids be treated in performance assessment calculations?"

The influence of organic colloids (HA) on the transport properties of inorganic iron and silica colloids was investigated at LU, by means of batch and column experiments. The silica / HA column results were used by Partner 9 in the development of an HA transport model. A full account of the experiments can be found in the CARESS literature [1]. However for the reader's convenience essential details of the relevant column experiments are repeated here.

Experimental.

A glass column was slurry packed with ~100g of pure sand (BDH), rinsed beforehand with 0.01M $NaClO_4$ to remove fines. The homogeneity and porosity of the column was determined using tritiated water (HTO) injections, in 0.1M $NaClO_4$. The HTO acted as a conservative tracer. Having verified the behaviour of the column the following sequence of mobile phases, all at pH = 6.5, were pumped through the column. Minimal interuptions to the flow (~10 cm^3 $hour^{-1}$) occurred at each changeover.

First mobile phase: 0.01M $NaClO_4$ containing 500 mg dm^{-3} SiO_2 colloid.

Second mobile phase: 0.01M $NaClO_4$ containing 500 mg dm^{-3} SiO_2 colloid and 10^{-8}M Eu solution, with a radioactive tracer quantity of ^{152}Eu (γ emitter, $t_{1/2}$ = 12.5 years) added.
Third mobile phase: 0.01M $NaClO_4$ containing 500 mg dm^{-3} SiO_2 colloid.
Fourth mobile phase: 0.01M $NaClO_4$.
Each phase was continued for sufficient time, usually several days, for equilibrium conditions to become established.
The whole experiment was repeated twice using mobile phases containing 1 x 10^{-7}M and 1 x 10^{-6}M Eu.
The eluates were fraction collected and the Eu recovery monitored by measuring the γ activity of each fraction.
To determine the effect of HA, parallel experiments were conducted but HA (10 mg dm^{-3}) was included in each mobile phase, including the pre-conditioning $NaClO_4$ solution. The sand was thereby pre-coated with HA.
The complete elution profiles are presented in the original report but the equilibrium Eu recoveries (100 x $[Eu]_{eluate}/[Eu]_{input}$) observed during the Eu elution phases, in the presence and absence of HA, are listed in Table 1. A control experiment was also performed in which the silica colloids and HA were omitted. No Eu was detected in the eluate during the Eu elution phase in the absence of HA and silica colloids.

Discussion of results.

The dramatic effect of HA can be seen by inspecting Table 1. In the presence of HA the Eu recoveries and elution profiles indicated that mobile EuHA formation dominated.

References.

[1] CARESS report in preparation (2000).

Table 1. Effect of HA (10 mg dm^{-3}) on Eu elution from sand columns (diameter 2.6 cm; length 13 – 14 cm), in the presence of silica colloids (500 mg dm^{-3}), in $NaClO_4$ (0.01M) solution, at pH = 6.5, flowing at 10 cm^3 $hour^{-1}$.

Eu concentration $[Eu]_{input}$ / (M)	Conditions	Percentage recovery (100 x $[Eu]_{eluate}/[Eu]_{input}$)
1.0×10^{-8}	HA absent	~50
1.0×10^{-8}	HA present	~100
1.0×10^{-7}	HA absent	~40
1.0×10^{-7}	HA present	~100
1.0×10^{-6}	HA absent	~25
1.0×10^{-6}	HA present	~100

Annex 17

A Methodology for Inclusion of Humic Substances in Performance Assessment

(N. Bryan, D. Griffin and L. Regan (RMC-E))

3rd Technical Progress Report

EC Project:

"Effects of Humic Substances on the Migration of Radionuclides: Complexation and Transport of the Actinides"

Project No.: FI4W-CT96-0027

RMC-E Contribution to Task 5 (Performance Assessment)

A Methodology for the Inclusion of Humic Substances in Performance Assessment

N.D. Bryan[1,2], D. Griffin[1], L.Regan[1]

[1]RMC Ltd, Suite 7, Hitching Court, Abingdon Business Park, Abingdon, Oxfordshire, OX14 1RA, United Kingdom

[2]Department of Chemistry, University of Manchester, Oxford Rd., Manchester, M13 9PL, United Kingdom

1. INTRODUCTION

Recently, models have been developed that can describe the behaviour of humic substances and radionuclides in laboratory column experiments (Bryan et al 1999; Warwick et al 2000). Previously, the results of these experiments could not be modelled satisfactorily using the existing local equilibrium assumption, or Kd, codes. The major modelling advance, therefore, has been the realisation that the humic/radionuclide complex behaviour is dominated by kinetics and rate constants, and not by equilibria and stability constants. It has already been shown that the chemical kinetics observed in the laboratory may have serious implications for the transport of metallic pollutants in the environment (Bryan et al 1999b).

However, there are still significant areas of uncertainty. For example, there is evidence that the desorption rate constants observed in the laboratory may not be the same as those observed in the environment (Geckeis et al 1999). In fact, there is evidence that desorption may be significantly slower in metal-humate samples which have been allowed to age for long periods of time. Clearly, this observation will have implications for future performance assessment studies. In addition, there is still uncertainty about the effect of humic sorption to mineral surfaces: i.e., do humic substances, and their complexes, move as conservative tracers in the environment, or are they retarded by sorption to mineral surfaces? It has been demonstrated that humic kinetics have implications for field scale migration studies (Bryan et al 1999b). However, calculations that include chemical kinetics are computationally expensive, and hence, should be avoided if at all possible. Also, all current codes used for Performance Assessment (P.A.) are 'equilibrium only', and therefore, to include kinetics would not be immediately feasible. Therefore, although it has been shown that chemical kinetics have an important effect, it is important to identify exactly when it is necessary to include them explicitly in mathematical calculations.

In this work, the importance of the relationship between chemical rate constants, and the residence time of the complex in the water column has been studied. Rules have been developed that predict when, and in what manner, humic chemical kinetics must be included in field scale studies. In addition a number of approximation methods have been developed, which allow an estimate of the effect of kinetics, but without the need to include them explicitly. In

addition, the effects of various uncertainties and variables have been investigated. Finally, the implications of slow, or even pseudo-irreversible, natural kinetics have been studied.

2. UP-SCALING ISSUES

In P.A. studies conducted so far, humics have either been completely ignored, or have been included at the most basic level, for example with very simple, local equilibrium, 'Kd-type' parameters. This is primarily because the controlling reactions and processes were not properly understood. Following recent advances, the next stage is to produce a set of instructions, which would enable humics to be included effectively in a P.A. exercise.

One important aspect is to appreciate the problems which the recent mechanistic and column modelling work (Bryan et al 1999a; Bryan 1998; Schussler et al 1998; Schussler et al 1999) has presented to performance assessors. P.A. studies are for the most part carried out using Kd values to describe the sorption of radionuclides to surfaces. However, it has been demonstrated that humic reactions are often very slow, and hence there is bound to be some incompatibility with a local equilibrium assumption approach. Modelling work has shown that rate constants are the most effective way to describe humic behaviour in laboratory experiments (e.g. Bryan et al 1999a). However, the use of rate constants is expensive in terms of computing time, and so wherever possible performance assessors will want to use equilibria to describe these reactions. More than this, all current P.A. models are based solely upon equilibria. Therefore, one major contribution would be to determine the limits of the validity of an approach based upon equilibria. In a previous study (Bryan et al 1999b), it has been suggested that one might still be able to use a simple Kd code, defining a 'best Kd' to use. However, it was found that such an approach was of limited use, since the best Kd was very sensitive to system conditions; flow rate, column length, time of simulation etc.

In order to be useful to P.A. studies, it is not sufficient merely to produce a model and a set of parameters, which can describe column experiments. It is necessary to explore the specific implications, which this model has for the field scale migration of radionuclides. It fact, it is not even sufficient to develop a model that is capable of including chemical kinetics in field scale problems. It is also important to consider when it is absolutely necessary to use that model, and

when a reasonable result may be achieved with a simpler, quicker model. Finally, it is important to estimate the uncertainties in the final prediction, and attempt to minimise them.

Central to this whole process is the conceptual model of metal-humate interactions, which has been developed from laboratory modelling studies. In this model (see Figure 1), humics have a range of metal binding modes ranging from instantly exchangeable to very kinetically hindered, pseudo irreversible. The figure shows the humic having a series of interconnected, successively more kinetically hindered, metal binding sites. Which of the sites any given metal ends up in will depend upon the chemistry of the metal and the equilibration time. Current evidence suggests that occupation of the non-exchangeable metal binding sites is highest for metals of high valency, e.g. Th, and that metals become progressively more 'fixed' within the humic structure as equilibration time proceeds. Although, the system is clearly complex, there are many aspects which allow generalisation. For example, although different metals show different degrees of fixation within the humic, and also some small differences in desorption rate constants, thus far, they may all be described with the same conceptual model. Therefore, the methodology is common to all metals (and humic substances also).

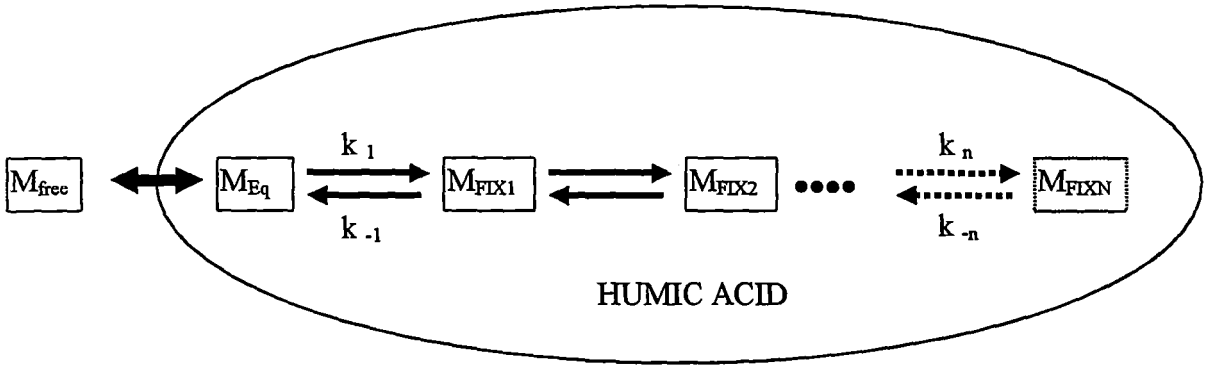

FIGURE 1: CONCEPTUAL MODEL OF HUMIC ACID

This model is deceptively simple. However, to calculate the occupancy of each box with time is actually mathematically complex and computationally expensive. It would be very difficult to include such a model into a P.A. code. Therefore, one task is to examine the conceptual model above and to determine how it could be simplified, without the introduction of significant inaccuracy.

The most obvious avenue for simplification lies in examining the values of the rate constants. The distinction between equilibrium and kinetic reactions is always artificial, since it depends upon the time scale of the observation: a reaction which is 'equilibrium' over periods of hours, may well be slow on the time scale of seconds. For a given set of physical conditions, e.g. flow rate, distance travelled and total time of interest, it should be possible to reduce the series of reactions in the conceptual model to just three groups:

(1) Those reactions which are sufficiently fast to be treated as equilibria.
(2) Those which are sufficiently slow that they effectively do not take place.
(3) Those reactions which can only accurately be described via the use of rate equations.

This will be true regardless of the number of binding sites in the series, and will also hold true if the binding sites are not in series, as shown in the figure. At this point it is important to appreciate that we have a special concern, because we are developing a methodology for P.A.. Scenarios (1) and (2) above advocate the use of an approximation to obtain a reasonable estimate: such approximations are common in science. However, there is a special requirement in P.A. studies that any approximations must lead to **conservative** estimates, i.e., they must over-estimate radionuclide migration.

3. UNCERTAINTIES

In a preliminary study into the implications of humic kinetics for P.A. (Bryan et al 1999b), two areas of potential uncertainty were identified: the initial state of the metal-humate complex at the upper boundary, and the humic sorption reaction.

Although more is now known about the behaviour of humics towards radionuclides, one significant area of uncertainty has been the interaction of the humic substances with the mineral surface. In the past, this area has been given less attention, since, in the case of an equilibrium description of metal binding, it has little effect upon the outcome of the prediction. However, if a metal is hidden inside the humic structure, then for transport purposes it will behave like a humic, and hence it becomes much more important to know how the humic will behave. In the case of the BGS columns, the humic, and its complexes, were retarded by sorption, and this

behaviour was described with an equilibrium constant. However, the situation in those column experiments was artificial, since the solid phase was not pre-equilibrated with the humic concentration used in the experiment. Of course, in the environment, all of the surfaces should be in equilibrium with the ambient concentration of humic material. The main area of uncertainty is the nature of the interaction. Is it an equilibrium reaction? Once the surface has reached maximum sorption, is any further humic material ignored, or does it replace material already on the surface? This distinction is potentially important, since it will make the difference between the kinetically hindered nuclide being retarded, or being transported effectively as a conservative tracer. There is currently insufficient evidence to indicate which of these will be the case in the environment. However, a recent study using the k1d model to simulate a large set of column experiments that used natural packing material fully equilibrated with the humic concentration used in the experiments, showed no evidence of humic retardation by sorption. To assume no humic sorption produces a conservative prediction. Since we have direct evidence that in experiments using natural solid phases and in situ groundwater, there was no retardation, we must assume, until there is conclusive evidence to the contrary, that, in the environment, humics will **not** be retarded.

Another important factor is the initial state of the humic/radionuclide complex, i.e., what is the initial occupancy of each of the metal binding sites? When modelling a column experiment, this information is provided by the pre-equilibration time. In a P.A. exercise, this will not be easy to estimate, but will have a large influence on the final prediction. It will depend crucially upon whether or not humic substances are able to penetrate into the near field and carry radionuclides out into the far field. Or, will radionuclides only encounter humics at the boundary of the near and far fields; the 'local field'? This is potentially one of the largest sources of uncertainty. In this case, unfortunately, there is no new evidence. Previous calculations (Bryan et al 1999b) have shown that the maximum migration is observed in the case where the non-exchangeable humic binding sites are fully occupied. The effect of this uncertainty is discussed later.

A further, new source of uncertainty, which needs to be considered, is the magnitude of the rate constants. There is now no doubt that the behaviour of these systems are heavily influenced by chemical kinetics, and we have a conceptual model of metal-humate interactions

(Figure 1). However, there is now uncertainty about the absolute magnitude of the rate constants that would be observed in the environment. Desorption experiments carried out at FZK-INE (Geckeis et al 1999) have idicated that the desorption rate constants for certain fractions of humate-bound metal are an order of magnitude slower than those observed in artificial systems. More than that, there is also evidence that some of the metal may be 'pseudo-irreversibly' bound, at least on practicable laboratory timescales (years). The importance of humic chemical kinetics has only been recognised for a very short time, and clearly, there is a great deal of work that still needs to be done to determine which rate constants will be observed in post-closure scenarios. In time, studies may be able to provide the magnitudes of the environmental rate constants, and therefore, a methodology has been developed that is independent of the magnitude of the rate constants. Until such evidence is available, in order to achieve a conservative approximation, one should assume 'pseudo-irreversible' behaviour in field scale calculations. It would have been possible to develop a methodology based wholly upon the assumption that humic substances bind metals pseudo-irreversibly: indeed, that would have been very easy. However, such a procedure would only have been useful until the correct magnitude of the natural desorption rate constants were identified. Therefore, we have developed a methodology that treats chemical kinetics explicitly, and does not depend upon the magnitude of the rate constants. At present, the only numbers, which we have to work with, are those observed in lab systems, coupled with the observation that some desorption rate constants for natural systems are an order of magnitude slower. Therefore, the calculations discussed below are based upon these '*lab*' and '*natural*' rate constants.

There will of course be other sources of uncertainty, for example, the temperature of the system, which will affect the magnitude of any rate and equilibrium constants. In addition, there will be all of the other 'non-humic' uncertainties (hydrology etc.). However, these are beyond the scope of this study, and will not be considered here.

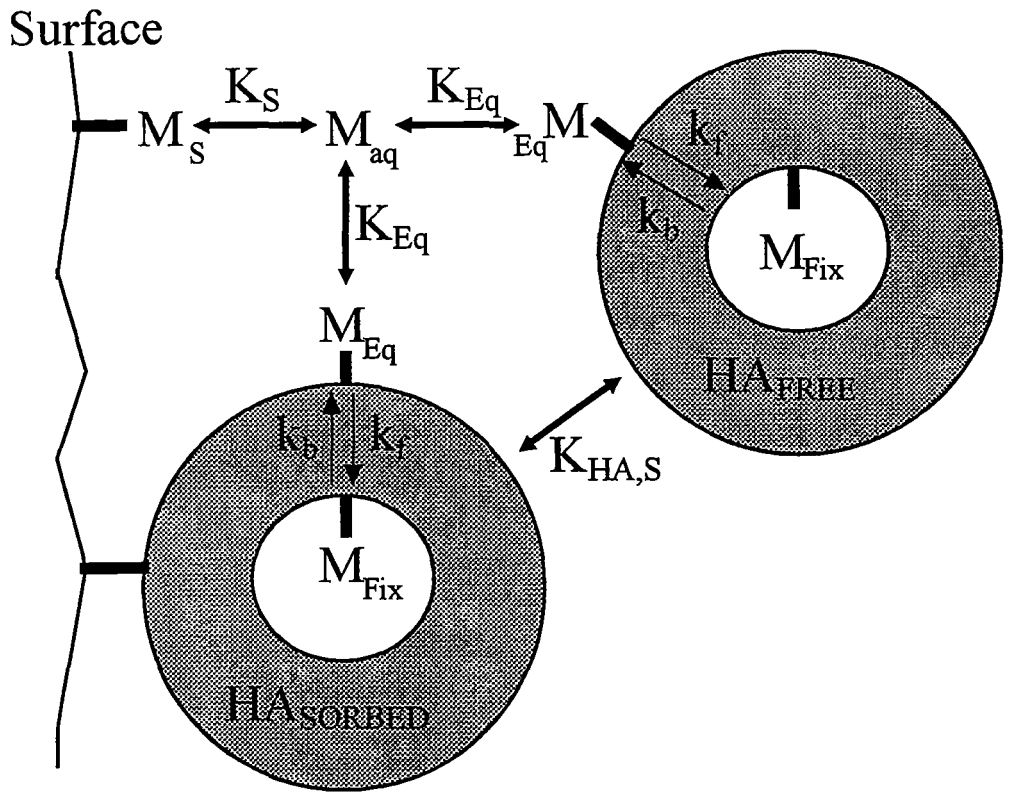

K_S= 1.0E7; $K_{HA,S}$= 10.0; K_{EQ}= 5.0E8; k_f= 0.029; k_b= 0.041

$[HA_{EQ}]$=1 mmol/g; $[HA_{FIX}]$=0.31 mmol/g; [S]=0.1

FIGURE 2: SYSTEM USED TO MODEL COLUMN EXPERIMENTS

4. PREVIOUS WORK

Previous work (Bryan et al 1999b) has shown the effect of humic kinetics on field scale migration studies. These calculations were performed using the system of equations and parameters shown in Figure 2. These were obtained directly from the modelling of the BGS columns (Bryan et al 1999a). Note, like all calculations discussed in this work, they were performed using the k1D transport code (Bryan et al 1999a; Schussler et al 1999). Figure 3 shows the results obtained using the column experiment parameters, for a hypothetical 100m column, a $1x10^{-5}$ ms^{-1} flow rate, a total simulation time of $5x10^6$ s, and assuming that the kinetically hindered site, M_{FIX}, is in equilibrium with the exchangeable, M_{Eq} , at the upper boundary.

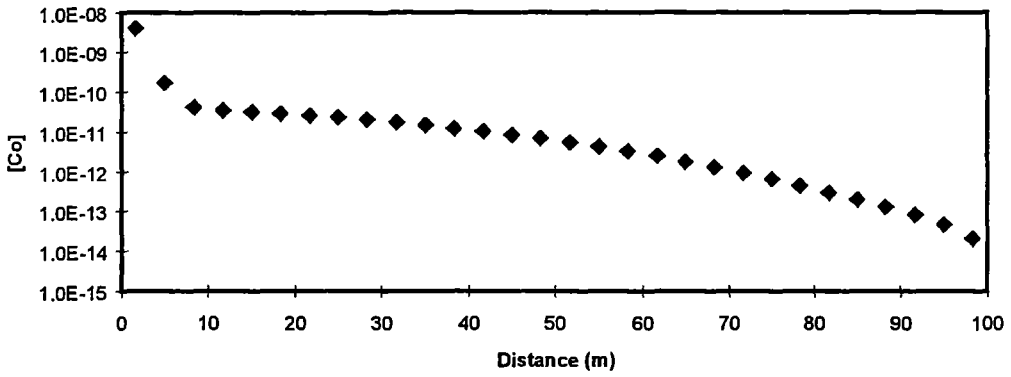

FIGURE 3: [CO] PROFILE OBTAINED USING BGS MODELLING PARAMETERS ($[Co]_o=1x10^{-10}$ M)

From Figure 3, the two distinct types of Co behaviour are clearly discernible. The Co held in the exchangeable site is very easily removed by the sand. This is responsible for the sharp fall in the Co concentration at short distances. Hence, the vast majority of the metal has not moved past the top of the column (note the log scale in Figure 3). However, it is clear that the non-exchangeable metal fraction has been transported much further down the column: this is responsible for the long shallow curve in the profile at medium to long distances. For the purposes of their migration, it is possible to treat the two fractions as essentially independent, once they are exposed to the sand surface. Similar behaviour is obtained if parameters for other column experiments or metals are used.

In addition, a series of calculations were performed keeping all other parameters constant, but varying the values of k_f and k_b, whilst keeping the ratio between them constant. Figure 4 shows the profiles obtained: the 'true' behaviour, that achieved with the column experiment derived parameters, is shown as a line.

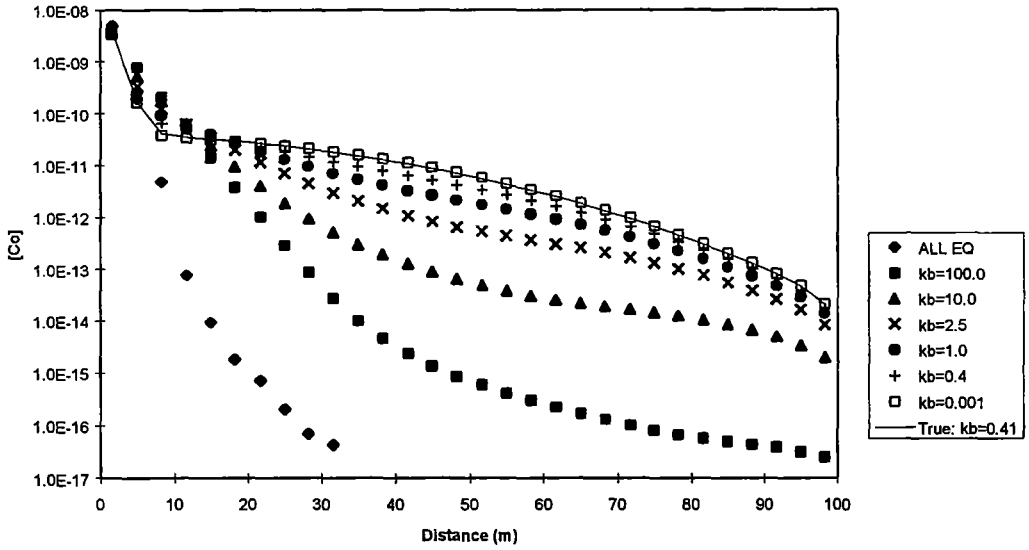

FIGURE 4: EFFECT OF CHANGING DESORPTION CONSTANT ON THE CO PROFILE

As expected, as the rate constant, k_b, for the desorption reaction increases, the extent of Co migration decreases, and as k_b falls the behaviour seems to tend to some limit. Note that the true value (0.041) produces virtually identical behaviour to that with k_b=0.001.

It is clear that, as k_b increases, the non-exchangeable Co behaves increasingly like the exchangeable. Indeed, for $k_b > 100$, the kinetic Co appears to behave very much like the exchangeable fraction. Conversely, as k_b decreases, its behaviour tends towards that of the humic itself.

The calculations were repeated, but with the non-exchangeable site empty at the upper boundary. The results are shown in Figure 5. There is, in general, less migration than for the initial case (Figure 4). However, whereas before, the change in the profile was fairly simple, this time it is much more complex. The maximum migration is obtained for k_b=1.0. This is because both the forward and backward rate constants increase and decrease together. Initially, as k_b falls from 100 the rate of desorption falls, and the kinetic Co is able to travel slightly further. However, as k_b continues to fall, so does the forward reaction rate, and hence the Co finds it increasingly difficult to get into the hindered site. The profile is a result of a balance between these two, producing a maximum migration for k_b=1.

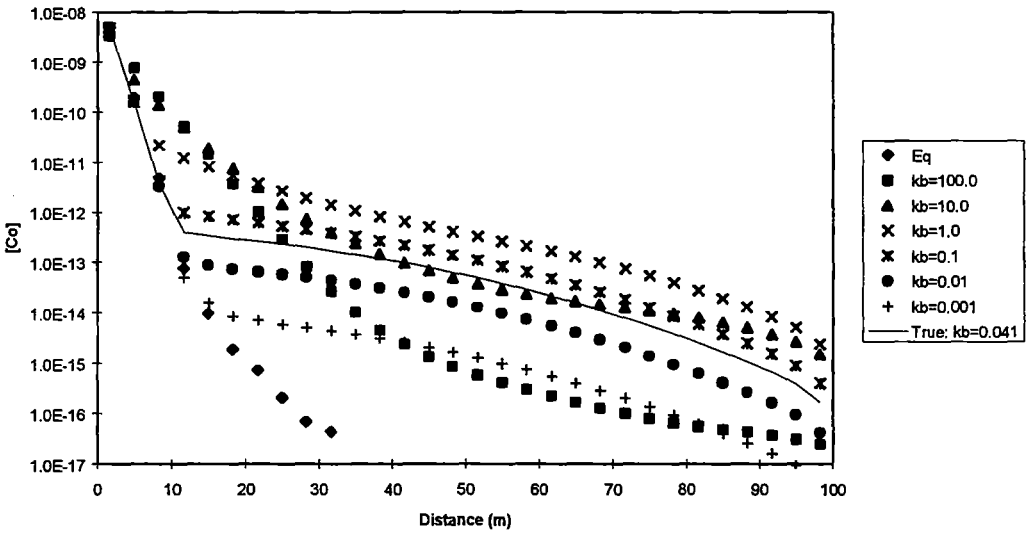

FIGURE 5: CO PROFILES OBTAINED WITH KINETICALLY HINDERED SITE EMPTY AT THE UPPER BOUNDARY

A complete description of these calculations may be found in Bryan et al (1999b). The main conclusion is that humic chemical kinetics may have a very significant effect upon the migration of radionuclides in the environment. Having established this fact, the next stage is to investigate when it is necessary to include them explicitly in mathematical calculations.

5. DAMKOHLER NUMBERS

Damkohler numbers were used by Jennings and Kirkner (1984) to examine sorption kinetics during column experiments. The Damkohler number for a system, D, is defined by,

$$D = \frac{L}{V_H} k$$

where, L is the length of the column, k is the chemical (first order) rate constant, and V_H is the flow rate. The Damkohler number for a system is a dimensionless parameter, which may be used to judge the impact of chemical kinetics. Jennings and Kirkner (1984) used them to decide at what point a slow surface sorption reaction could not be approximated by an equilibrium assumption. They developed a set of rules,

D > 100: Equilibrium gives an **excellent** approximation

100 > D > 10: Equilibrium gives a **reasonable** approximation

10 > D > 1: Equilibrium gives a **poor** approximation

D < 1: Equilibrium approximation cannot be used.

Now, the situation here is slightly different. Firstly, the slow kinetic reaction takes place within a solution phase colloid, and not at the solid surface. As a result, we must redefine one of the variables slightly: for our systems, V_H must be the **effective velocity** of the humic colloid through the water column, including the effects of any sorption or pore exclusion etc. Note, in all subsequent sections, unless otherwise stated, the rate constant used to define Damkohler numbers in this work is the desorption rate constant, k_b (Figure 2). Secondly, the work of Jennings and Kirkner was not directed at P.A. with its requirement for conservative approximations. Therefore, what may have been satisfactory there, may require caution here.

The most significant result of Jennings and Kirkner was the discovery that systems with a single kinetic reaction and with the same 'D-number' show the same behaviour, regardless of the particular physical conditions. In this work, we have defined a second dimensionless number, T,

$$T = \frac{t V_H}{L}$$

where, t is the total elapsed (simulation) time. The combination of D and T numbers are sufficient to define uniquely the behaviour of our systems. Any system with the same D and T numbers will show the same profile along a column. Note: the term 'column' here is used to define the distance over which any calculation is based, whether that is in the laboratory (real column) or the field (hypothetical column). Figure 6 shows the calculated distribution of metal from a non-exchangeable site, plotted as the ratio compared to the concentration at the upper boundary, ignoring the contribution from the exchangeable site, for a range of D numbers, and for T=0.5. These results are independent of column length, flow rate, chemical concentrations etc.

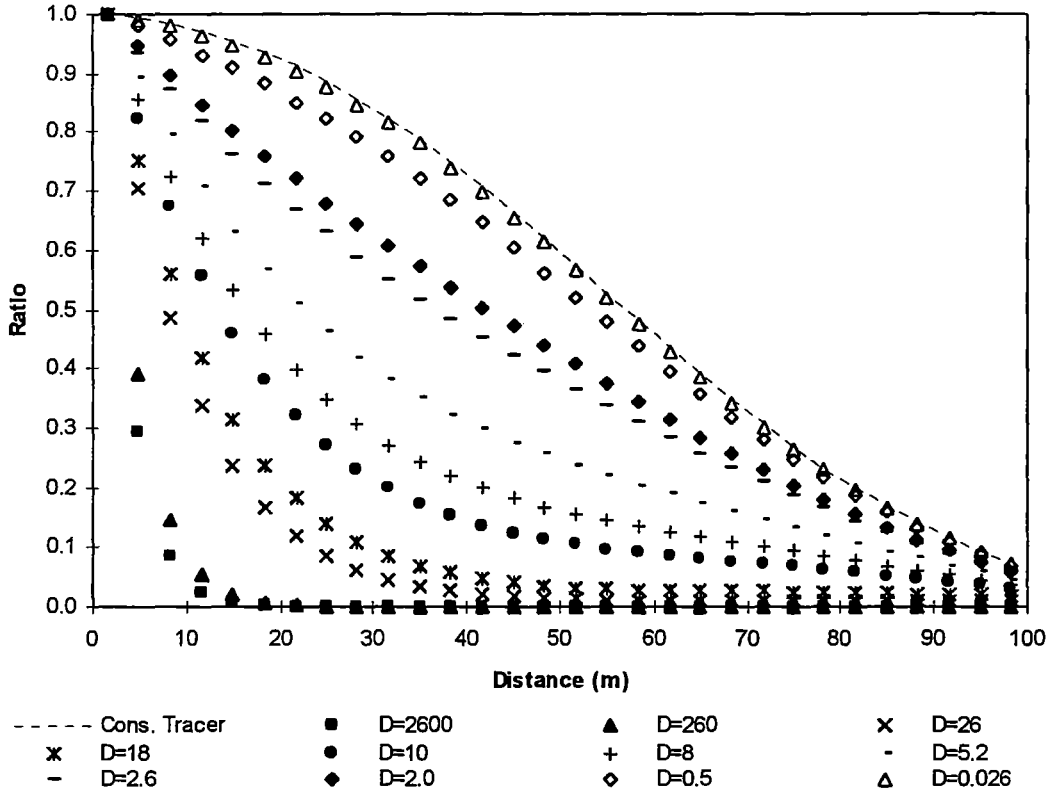

FIGURE 6: EFFECT OF DAMKOHLER NUMBERS ON MIGRATION (T=0.5)

This dimensionless approach works for these systems for 2 reasons. Firstly, the non-exchangeable metal fraction is isolated from all other chemical interactions. In fact, the only chemical reaction open to it is the desorption step, defined by k_b. Secondly, the forward and backward rate constants, k_b and k_f, have approximately the same magnitude (Bryan et al 1999a). Hence, approximately the same D-number would be obtained if either rate constant were used to define D.

Jennings and Kirkner (1984) have defined their own set of rules for the use of local equilibrium assumption models. However, these are not directly applicable to our own case. To define a set of operating instructions, we must consider the 3 scenarios described in section 2, i.e., 2 limiting behaviours and the intermediate. When the desorption reaction is fast, i.e. D-number large, then the behaviour tends towards that of an equilibrium. Therefore, as D increases, an equilibrium approximation will become increasingly realistic. At the other extreme, as the rate constant deceases, and the D-number falls, the rate of desorption falls, and we may eventually assume that it does not take place. This is illustrated in Figure 6: as D increases, the profile

does tend to some limit, i.e. an equilibrium assumption, and as D falls, it tends towards the conservative tracer. Therefore, when considering approximations to our conceptual model, we must take account of these types of behaviour.

Jennings and Kirkner (1984) propose a sliding scale for the applicability of the equilibrium approach (see above). However, it is clear already that we will need to define two separate limits. Therefore, for the purposes of this study we have defined single values of D to define these limits: i.e., 50 and 1/50. If D is greater than 50, then an equilibrium approach may be considered, whilst if it less than 1/50, then it may be possible to assume that the reaction does not take place. Of course, any such limits will be subjective, and the correct limits will depend upon the acceptable margin of error. This issue will be discussed further below.

6. APPROXIMATIONS

6.1 Equilibrium

Of all of the approximations, the equilibrium assumption model is the simplest to use, since this is the approach used in all current field scale models. One simply replaces the rate constants and rate equations with equilibria, i.e. assume that all desorption from the humic occurs instantaneously.

There is one major problem with the equilbrium approach: it is not conservative. The main influence of humic kinetics is to increase migration. Therefore, any approximation that assumes that kinetics do not exist, must be non-conservative. Figure 7 shows an example based upon the rate constants derived from Am columns (Schussler et al 1999). The D-number for this calculation is 30,000, which is well into the region where one would expect an equilibrium assumption to be valid. However, even in this case, the equilibrium assumption has underestimated the extent of migration, and as D decreased, the effect would become progressively more pronounced. It is possible that the difference between the exact and approximate value is not significant. That would depend upon the magnitude of the upper boundary concentration of Am. In terms of the total Am, the difference between the two plots is certainly small, representing less than a 1% error. However, that error is highest at the leading edge of the plume, which is the most important region in terms of P.A. How much of a

problem this would be in the case of a real P.A. exercise would depend upon the individual circumstances. It is clear that care must be taken when using an equilibrium approximation.

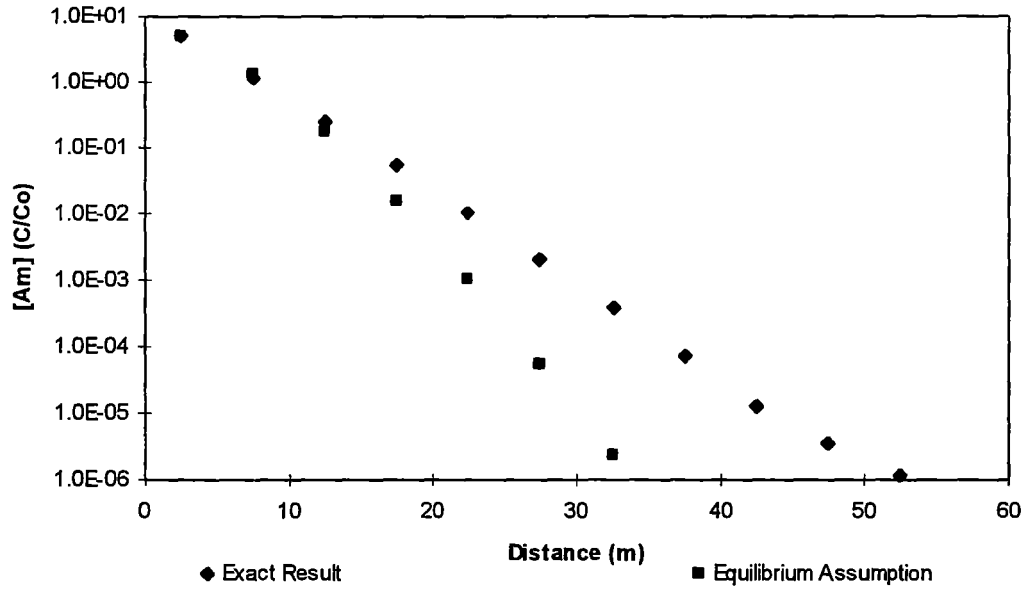

FIGURE 7: EQUILIBRIUM ASSUMPTION, Am PARAMETERS, D=30,000

6.2 Decoupled approximation

After local equilibrium, the other limiting case is to assume that the desorption reaction does not take place. Therefore, an approximation based upon this limiting case would ignore the existence of the desorption reaction. That is, the two humic metal fractions are 'decoupled'. In terms of geochemical modelling, two master species are defined for the radionuclide. The first represents the exchangeable fractions, i.e., using the nomenclature of Figure 2, M_{Eq}, M_S M_{aq} plus any other solution phase complexes, precipitates etc. These would interact with each other in exactly the same way as for the exact calculation. The second would represent the non-exchangeable fraction only, i.e., M_{FIX}. No interaction between the two is permitted during the calculations. The result is that the metal trapped within the humic is assumed to be isolated completely from the solution chemistry, and is transported with exactly the same characteristics as the humic colloid. In other words, the metal is pseudo-irreversibly bound by the humic. The advantage of this system is that it is inherently conservative, since it does not allow any retardation due to sorption.

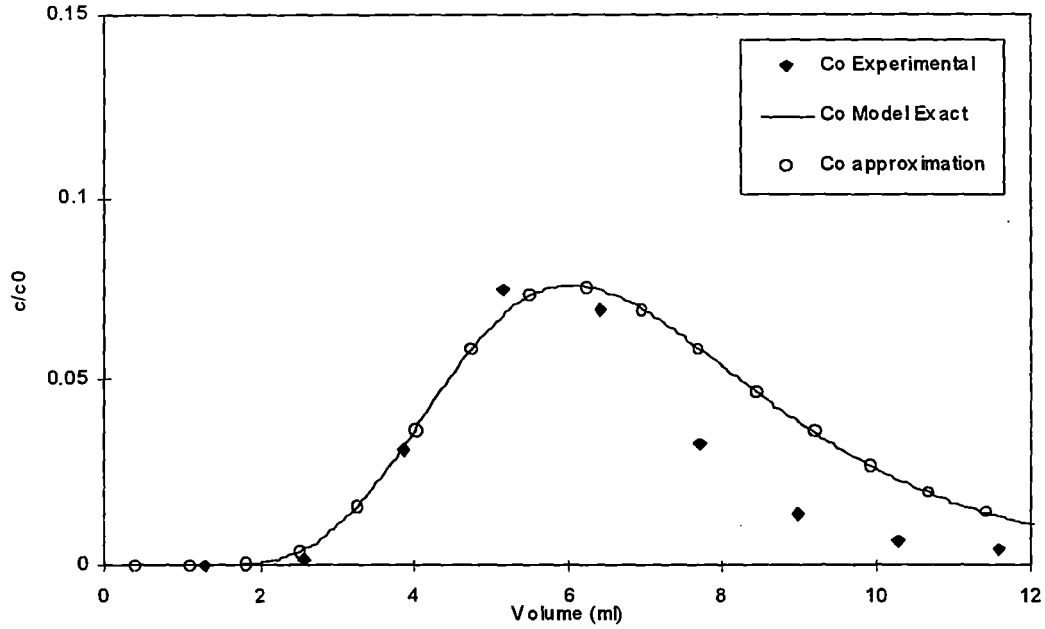

FIGURE 8: DECOUPLED APPROXIMATION TO BGS CO COLUMNS

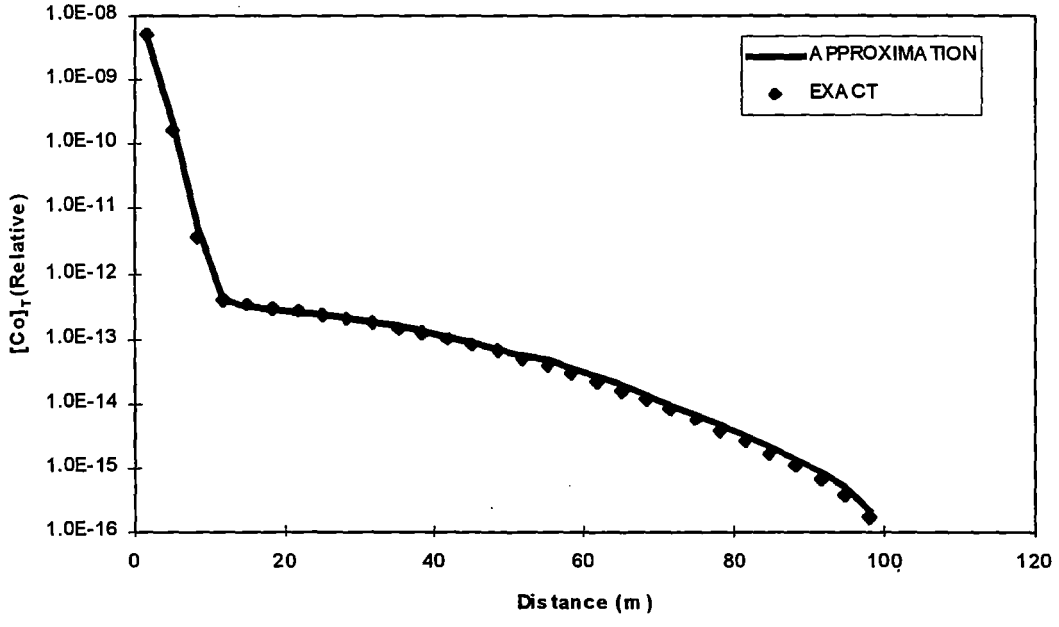

FIGURE 9: EXAMPLE OF DIMENSIONLESS APPROXIMATION METHOD

Figure 8 shows the application of the decoupled approximation to the BGS Co columns. Because of their short length, these lab experiments have very low D-numbers; 0.004 – 0.0004 depending upon the flow rate. The figure shows that the decoupled approximation provides an

excellent estimate of the exact solution, and also of the true behaviour of the (humic bound) Co.

6.3 Dimensionless approximation

The equilibrium and decoupled approaches can provide approximations to the exact solution for systems with either very large, or very small numbers. However, they cannot be used at intermediate values of D ($50 > D > 0.02$). In fact, there is no simple approximation method that may be used in this region. However, there is one alternative, which can provide an estimate of migration, without the need to perform a full calculation. As discussed above (section 5), systems with the same D and T numbers are expected to behave in the same way. Therefore, the result of a calculation for a given pair of D and T numbers will serve as an estimate for another with the same values, even if the real physical parameters are completely different. Figure 9 shows an example of this approach. The modelling system and parameters used to model the BGS Co column experiments were used in an exact calculation where the upper boundary concentration of the hindered site was zero (i.e. one of the plots in Figure 5: k_b=0.041). The resulting profile is shown as points in Figure 9. An approximation was obtained by using a different set of physical parameters that had the same D and T numbers, but still using the set of equations shown in Figure 2. The results of the approximation are shown as a full line in Figure 9. This result suggests that it should be possible to use this method to provide estimates of exact solutions.

This first example has used an estimate based upon the same set of equations as the exact calculation. However, that is not strictly necessary. As a further test, the dimensionless approximation approach was used to obtain estimates for some of the FZK-INE column experiments. These columns have already been successfully modelled using the k1D/KICAM approach (Schussler et al 1999). This time a set of very simple calculations were made based upon a column of length 1m and area $1m^2$ and a flow rate of 1 m day^{-1}. Two chemical species, A and B, and one chemical reaction were included:

$$A \xrightarrow{k} B$$

The upper boundary concentrations were, $[A]_o$=1 and $[B]_o$=0. The value of the first order rate constant, k, was varied so that the D number of the approximation calculation was the same as that of the column experiment. The calculations were performed over the same range of T

values as the experiment. Figure 10 shows an example for a column experiment with D=0.04. The real experimental data are shown as points, whilst the approximation is shown as a line. It is clear from the figure that, despite the fact that the approximation calculation was based on a column with completely different physical and chemical characteristics, it has still produced a surprisingly good fit to the data. Similar result were obtained for a number of different column experiments (data not shown).

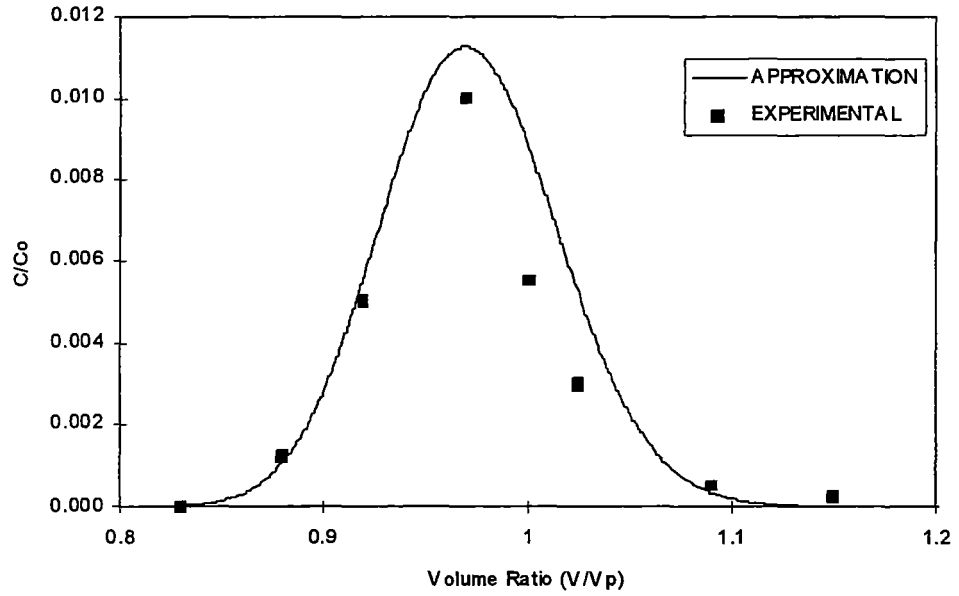

FIGURE 10: DIMENSIONLESS APPROXIMATION TO FZK Am COLUMN, D=0.04

At first sight, the fact that this approach works at all seems amazing. However, the success may be explained as follows. In the column experiments, despite the complexity of the system, there is only **one** important process/reaction, which determines the amount of Am in the effluent, i.e. the desorption of the Am from the humic colloid. Other chemical processes play a part. For example, as Am desorbs from the humic, it is immediately sorbed by the surface. However, the precise magnitude of the interaction constant between the Am and the surface is not critical, provided of course that it is high enough to remove all exchangeable Am from solution. Therefore, the only process determining how much Am appears in the effluent is the desorption step from the humic. That is why it is possible to achieve a good approximation with our simple, one reaction system: because only one significant real chemical reaction has a significant effect upon the real result.

These results suggest that the dimensionless approach to approximation might prove to be useful. The big advantage of the approach is that, although it was developed to fill the gap between the equilibrium and decoupled approximations, it is in fact valid at all values of D. It is of course much more cumbersome to use than the two limiting cases, and hence, by choice one would still probably use it only in the region where D>50, or D<0.02.

It might be possible to construct a database of profiles that could be used to provide a quick estimate of the impact of metal-humate interactions without the need for a full calculation including chemical kinetics. Figure 11 shows an example of database calculations. Figure 11a shows calculations at constant D (=1) for T ranging from 1 to10, whilst Figure 11b shows calculations at constant T (=10) for D ranging from 0.05 to 100. To obtain an estimate, one would merely need to calculate the D and T values, corresponding to the case study, and then consult the plot whose D and T values most closely matched.

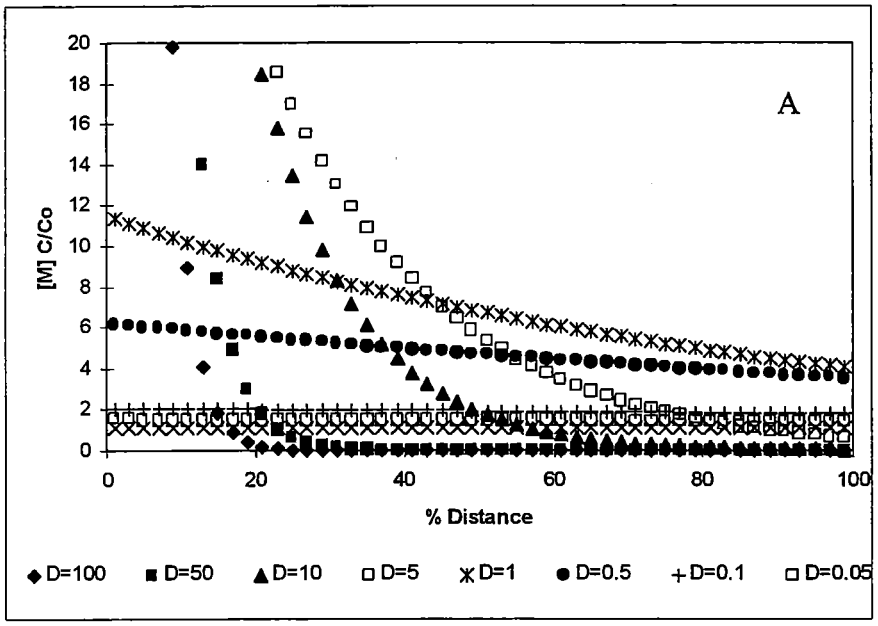

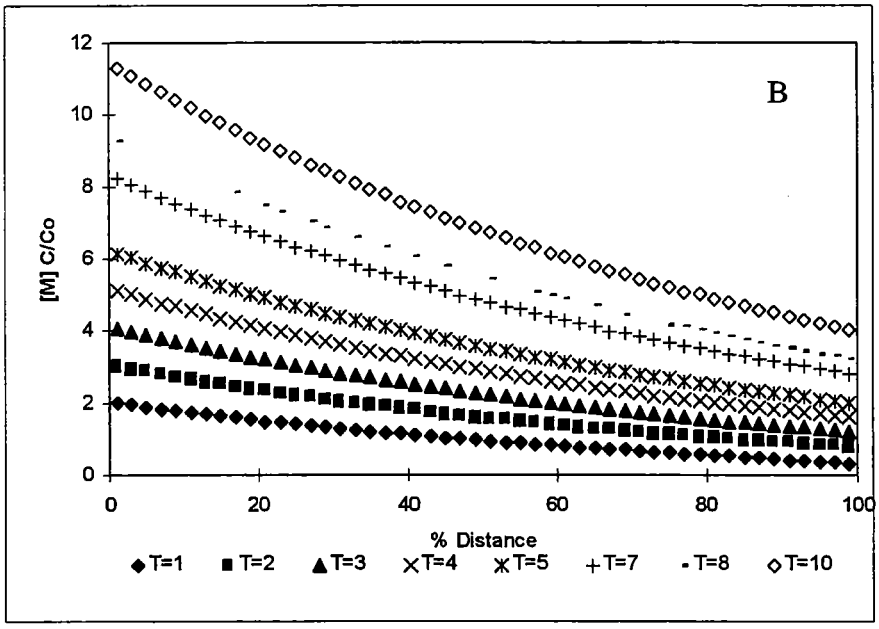

FIGURE 11: DAMKOHLER DATA BASE, (A) PROFILES AT CONSTANT T (=10), (B) PROFILES AT CONSTANT D (=1)

6.4 Ranges of validity

We now have three methods for obtaining estimates to the exact solution, and we can define their limits of validity. The equilibrium approach should only be used for systems with $D > 50$. However, this method will always underestimate migration, and should be treated with care. In the region $50 > D > 0.02$, only the dimensionless approach will give an accurate approximation, although it may be used at all values of D. Finally, for $D < 0.02$, the decoupled approach gives the best approximation. The decoupled approach is inherently conservative, since it will always overestimate migration.

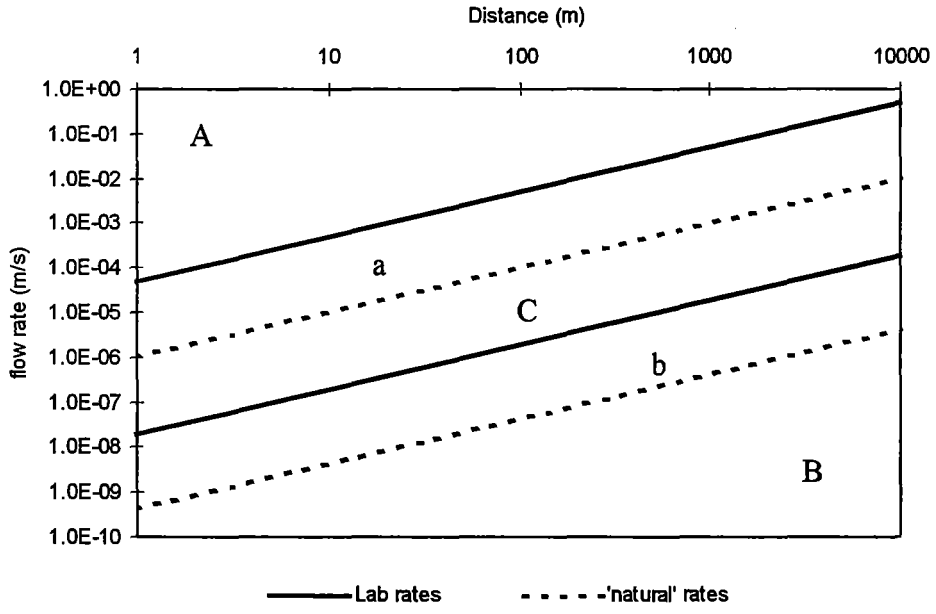

FIGURE 12: MODEL RANGES OF VALIDITY, (A) – Decoupled approximation valid, (a) - Decoupled approximation valid with care, (B) - Equilibrium valid with care, (b) - Equilibrium valid with extra care, (C) – Dimensionless approach valid.

We have had to define our ranges in terms of D, because the magnitude of the first order desorption rate constant, k, observed in the environment is uncertain. At present, we have two possible values for k. That observed in 'artificial', man-made systems, and that, an order of magnitude slower, observed in some studies of 'natural' systems. Over and above this, there is also the possibility that some natural systems display even slower rates. Therefore, at present, it is not possible to make concrete predictions about whether or not humic kinetics will be

important for field studies with a particular length and flow rate. Only when the true, in situ rates have been identified will that be possible. In the meantime, of course, the only conservative approach is to assume that the binding is pseudo-irreversible, i.e., the decoupled method, which will provide a conservative estimate. However, such estimates may represent gross over-estimates, since they will assume that the humic bound metal effectively moves as a conservative tracer. This clearly has implications for P.A. studies, and further research is needed to provide concrete values for these rate constants.

When these values have been obtained, it will be possible to define regions where different approaches will be valid. Figure 12 shows an example of this concept based on values of k from laboratory experiments, and also initial studies on natural materials.

7. SENSITIVITY

There are a large number of possible uncertainties in field scale migration studies. It is an essential part of any study such as this to identify them, and also to determine the sensitivity of the final result to them. Great advances have been made in our understanding of humic substances and their interaction with metals. However, with this increased knowledge has come new areas of uncertainty. In particular, the discovery of the importance of kinetics has lead to new areas of uncertainty. Most of the important uncertainties concern the 'kinetic' aspects of the system. This is not surprising, since humic kinetics can potentially lead to the transport of metal fractions as conservative tracers. We will deal with each of the areas of uncertainty in turn.

7.1 Temperature

Temperature has long been identified as a potential sorce of uncertainty in calculations. A great deal of effort has been spent, measuring and collating reaction enthalpies in order to take account of temperature effects. In the case of kinetic reactions, the important parameter is the activation energy. In fact the activation energy of the desroption step is known only for the Eu/humic acid system (King et al 1999, Bryan et al 1999a). This value has been used, along with lab rate constants derived from batch experiments, in a series of calculations to investigate the effect of temperature. Calculations were performed in the region from 20 - 60°C, since this

was the range studied in the lab. Hence, we may be confident of the results. Figure 13 shows typical results, for a simulated field scale study.

A problem when investigating the effect of uncertainties upon our system is that, unlike equilibrium systems, the effect of any uncertainty in either the rate constants, or in the amount of metal in the non-exchangeable site, will depend very strongly upon the flow rate of the system. For this reason, it is not possible to make clear-cut, generalised decisions about the importance of variables. The inter-relation of uncertainty and flow rate is discussed later (section 7.5). A distance of 100m and a flow rate of $5x10^{-5}$ ms^{-1} were used. This rate was chosen, because the desorption rate constant at 40°C is $\approx 5x10^{-7}$ s^{-1}, giving D=1. At this D value, the system will be most sensitive to variations in the rate constant. Hence, the differences shown here will represent a maximum expected influence.

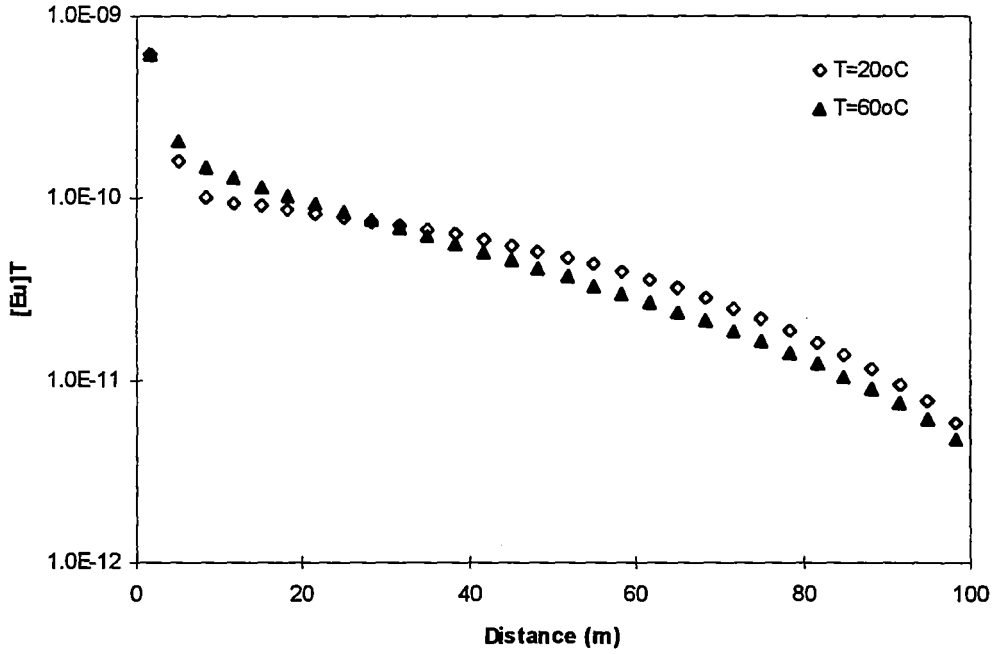

FIGURE 13: EFFECT OF TEMPERATURE.

The figure shows that, as the temperature increases, the metal migrates less, because the desorption rate constant increases with temperature. However, the difference between the two plots is relatively small, despite the fact that the temperature difference is large (40°C), and that this system is expected to be most sensitive. Hence, the calculations suggest that temperature will probably not be a major uncertainty.

7.2 Rate constants

Although laboratory systems are now well understood and characterised, there is still significant uncertainty about the magnitude of desorption rate constant that will be observed in the environment. The problem is that we have very little data for natural systems, other than the observation that they are probably significantly different. Preliminary experiments have shown that some of the desorption rates observed in natural systems are an order of magnitude slower than those in the lab. However, this probably represents a best-case scenario, since there is also evidence, for even slower desorption of some metal fractions. In fact, the desorption is so slow in some cases that it has not been possible to measure the rate constant in the time scale of this project. The problem is that P.A. calculation must be conservative, and as rate constants decrease, migration increases. Therefore, since these desorption reactions cannot be assigned values, because they are too slow, we must for the moment assume that they do not take place, i.e., that they are 'irreversibly bound'. Of course, in reality, true irreversibility does not exist, and reaction rates never actually equal zero. However, while there is no defined lower limit, we must assume that the metal remains locked inside the humic, once it has been transferred to the non-exchangeable site.

Clearly, further research is needed to determine natural rate constants. However, we may still demonstrate the likely effect of the differences between lab and natural systems, by investigating the difference in behaviour between calculations using lab rate constants, and those using rates an order of magnitude slower (remember, preliminary experiments have already found natural systems with these sort of rates). Figure 14 shows the results of a series of predictions made for Am based upon lab rate and surface interaction constants determined from column experiments (Schussler et al 1999) and 'natural' rate constants an order of magnitude slower. The total distance of the simulation was 300 m, the flow rate was $1x10^{-6}$ ms^{-1} (D=300 w.r.t. lab rate), the simulation time was 100 years, and the exchangeable and non-exchangeable sites were in equilibrium at the upper boundary. 4 separate predictions are shown: the first assumes no humic to be present; the second uses an equilibrium approximation; the third uses the lab rate constants; the fourth uses the 'natural' ones. As expected, the 3 predictions that assume the presence of humic show more migration than the other. Also as expected, the equilibrium assumption plot shows less then those including

kinetics. In fact, the equilibrium plot is not very different from the no humic plot. Therefore, if all the reactions were equilibria, then humics would not be expected to be a significant factor. However, the main point is that there is a significant difference between the predictions using the lab and the natural rate constants. Figure 15 shows an identical set of calculations based upon data for tetravalent actinide ions (labelled Pu).

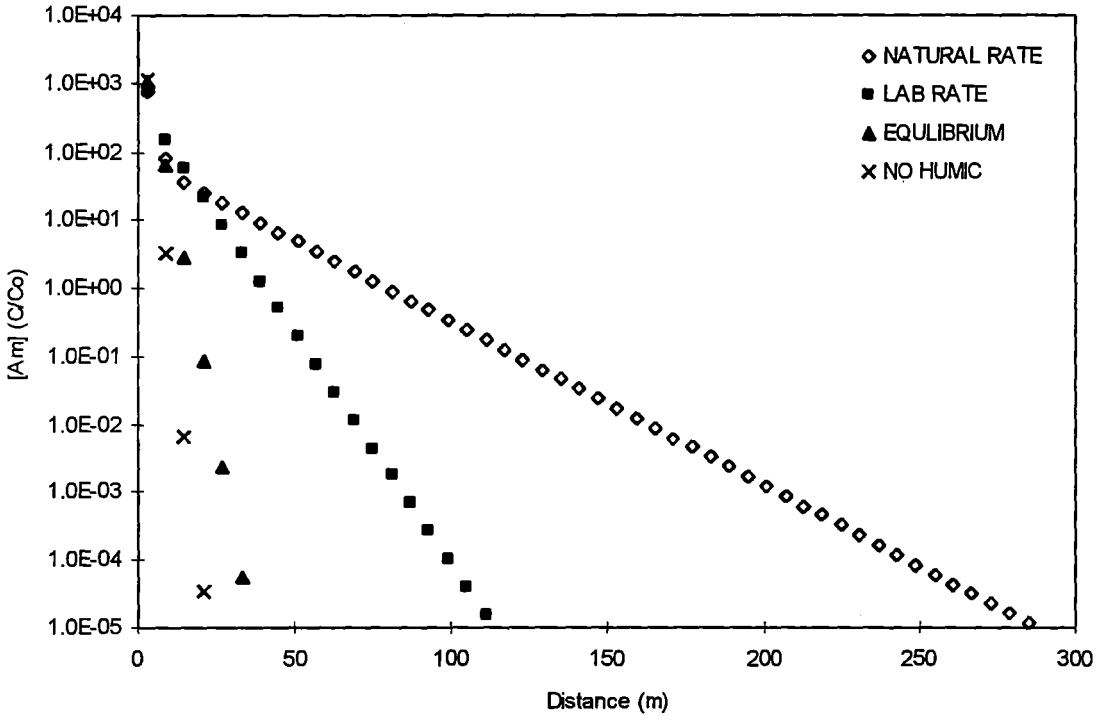

FIGURE 14: EFFECT OF UNCERTAINTY IN RATE CONSTANTS FOR Am

Once again, the same general effects are observed. However, this time the difference between the lab and natural predictions is even higher. In fact, the model predicts significant breakthrough at the end of the 300m column within 100 years. This result has potentially serious implications, because these natural rate constants used in the calculation probably represent a best possible case scenario. We have evidence that at least some natural rate constants are even slower than this.

Figures 14 and 15 clearly demonstrate the importance of the uncertainty in the rate constants. In fact, it currently dominates over all other uncertainties.

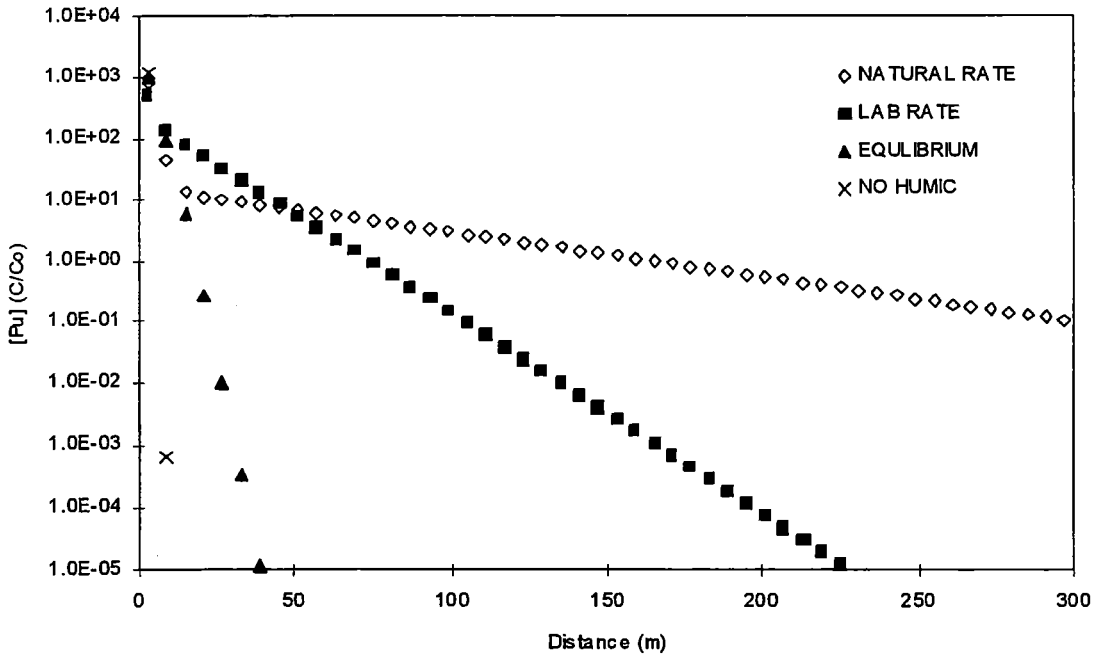

FIGURE 15: EFFECT OF UNCERTAINTY IN RATE CONSTANTS FOR Pu

7.3 Pre-equilibration time

In column experiments, the pre-equilibration time prior to injection is well defined, and hence, it is possible to predict the amount of metal that will enter the column bound in the non-exchangeable form. However, in P.A.-type calculations it is very poorly defined. We do not know at present whether metals will emerge from the near-field already complexed to humic substances, or whether humic substances will be significant only after the metal has entered the far field. This area was identified as a potential source of uncertainty in earlier, preliminary studies (Bryan et al 1999b). To investigate the effect, calculations were performed using the same parameters as for figure 14, but this time for the lab and natural cases, two sets of calculations were performed, the first with the exchangeable and non-exchangeable fractions in equilibrium (non-exchangeable site 'full'), i.e. the same as in figure 14, and the second with the non-exchangeable site empty at the upper boundary. The results are shown in figure 16.

The calculations show that the effect of this uncertainty depends upon the magnitude of the rate constants. For the lab rate constants, there is virtually no difference between the two situations, whereas for the natural system, there is. Ironically, the uncertainty in the magnitude of the rate constants means that we cannot be certain of the effect of this other uncertainty.

Given that the 'natural calculations' represent a more realistic representation of the real system, the results do suggest that, once the true rate constants have been defined, this uncertainty may become very significant.

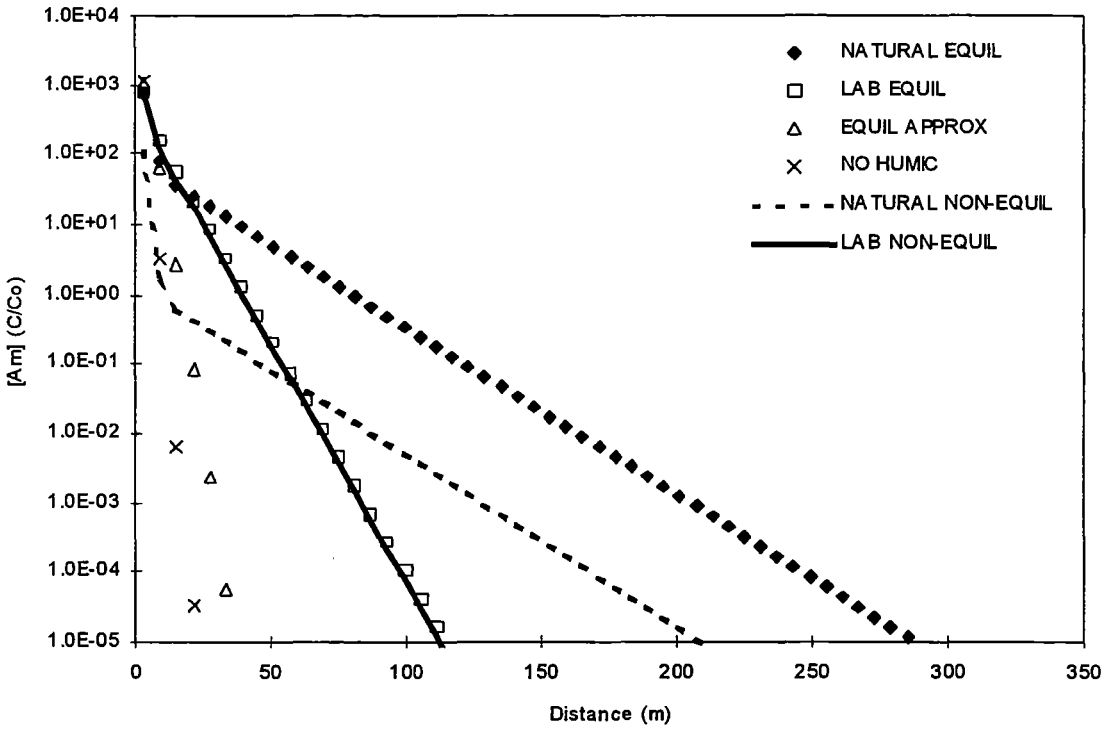

FIGURE 16: EFFECT OF UNCERTAINTY IN PRE-EQUILIBRATION TIME

7.4 Equilibrium parameters

Although aspects of these systems require a kinetic description, there are other parameters that necessarily do not. For example, the interaction of the metal, both with the solid surface, and with the humic exchangeable site, which are treated here with equilibrium constants. The effects of variations in these parameters have been studied, and the results have been found to be surprisingly insensitive. Figure 17 shows typical results of test calculations: once again the 'natural' system was used as the base case (plotted as symbols). A second calculation was performed, this time with the surface interaction constant (K_s, figure 2) increased by a factor of ten, whilst the non-exchangeable constant (K_{Eq}, figure 2) was kept constant. In a simple equilibrium-only calculation, this change would have had a significant effect. However, the figure shows that, in this case, there is almost no difference. Hence, we can see that

uncertainties in the equilibrium parameters are not expected to be significant compared to the uncertainties in the rate constants, and in the source term.

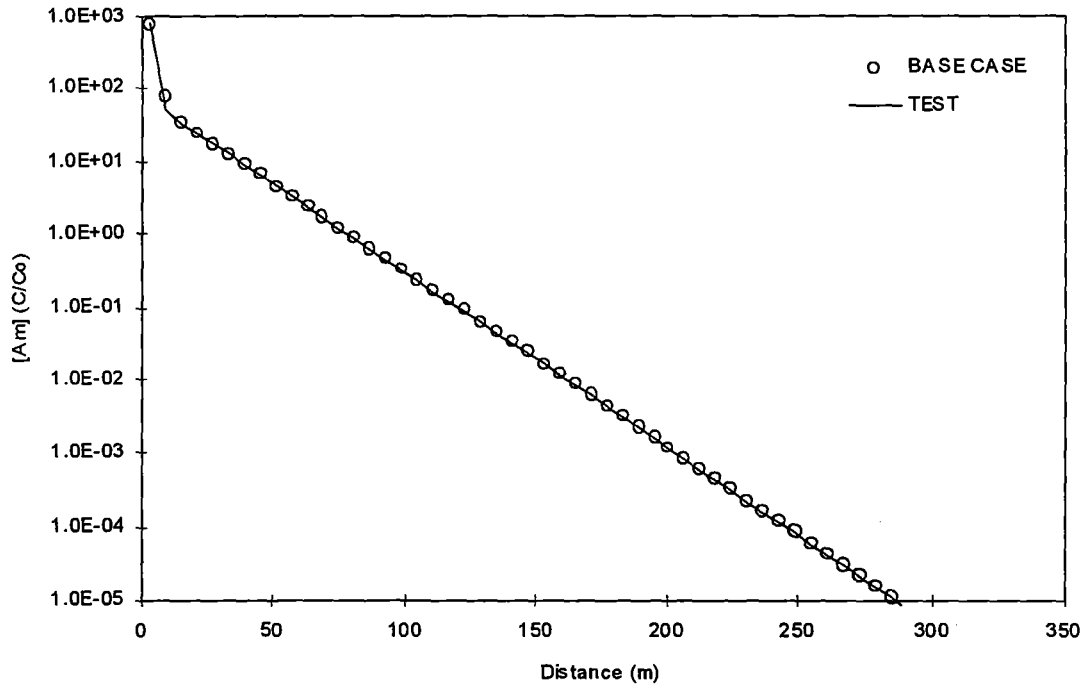

FIGURE 17: SENSITIVITY OF RESULT TO EQUILIBRIUM PARAMETERS

7.5 Effect of flow rates on sensitivity

One of the most significant problems introduced by chemical kinetics is that flow rate becomes a critical parameter. Not only will flow rate be a factor in the amount of migration, but it will also affect the sensitivity of the result to different parameters: i.e., an uncertainty that has very little impact at one flow rate may well become significant at a different rate. Because of the uncertainty in the magnitude of the natural rate constants, it is hard to make concrete predictions about the exact impact of flow rates. However, it is possible to demonstrate the likely effects.

Calculations were performed for best and worst case scenarios. The best-case scenario used the fastest measured rate constant for any metal, assumed that the non-exchangeable site was empty at the upper boundary and that the temperature was 60°C. The worst case used the slowest measured rate, assumed that the non-exchangeable site was in equilibrium with the exchangeable at the upper boundary, and used a temperature of 20°C. Two sets of calculations

were performed over a distance of 100m for two different flow rates; $1x10^{-4}$ and $1x10^{-6}$ ms^{-1}. The results (T=0.5) are shown in Figures 18 and 19.

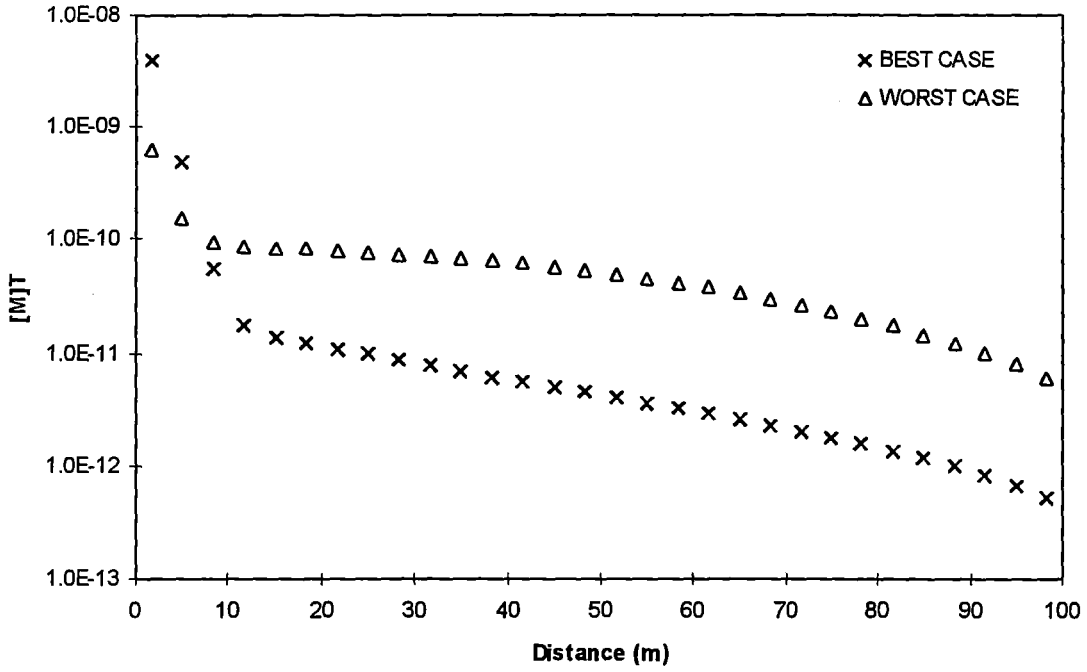

FIGURE 18: BEST AND WORST CASE SCENARIOS FOR $V_H = 1x10^{-4}$ ms^{-1}, T = 0.5.

The fact that there is a significant difference between the best and worst case scenarios is not surprising: that is expected. However, the most significant result here is that the difference between the best and worst case scenarios depends upon the flow rate, and is greatest for the slower (probably more realistic) flow rate. Here, we have chosen overall best and worst case scenarios for all metals, based on current data, and therefore, the effect shown here is the maximum currently expected. That said, similar, if less pronounced, behaviour will be observed for any sensitivity study where either the concentration or the desorption rate constant of the non-exchangeable site are affected.

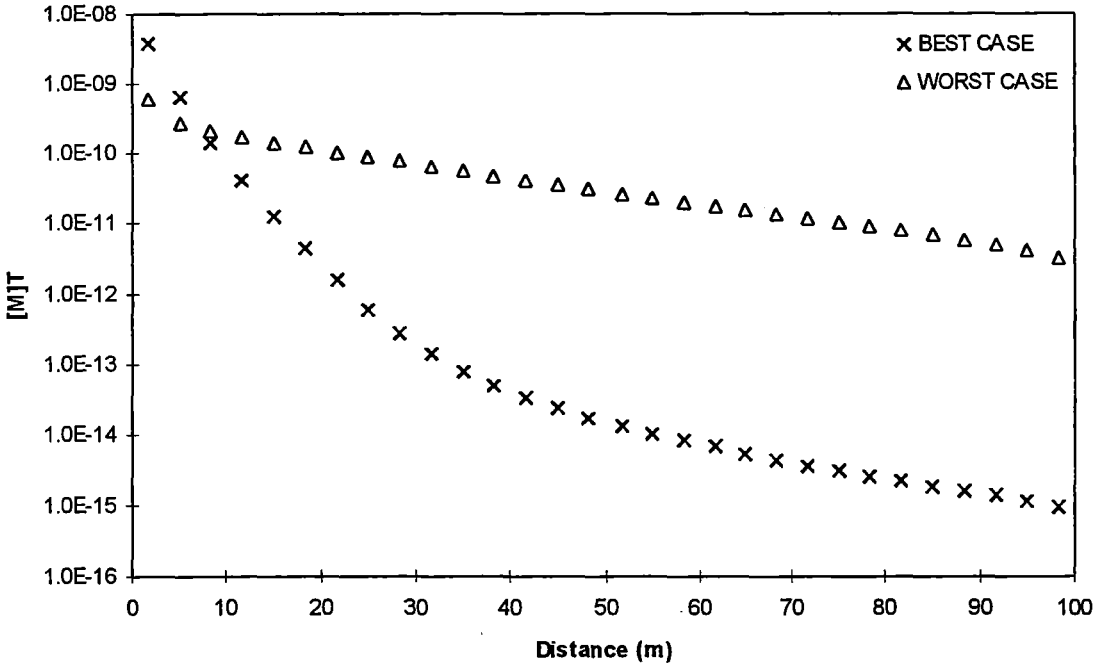

FIGURE 19: BEST AND WORST CASE SCENARIOS FOR $V_H = 1x10^{-6}$ ms^{-1}, T = 0.5.

8. CONCLUSIONS

This report has focussed mainly upon sources of uncertainty, and those areas where we still have insufficient data. However, it is important not to loose sight of the large amount of progress that has been made over the last few years. Three years ago laboratory column experiments could not be modelled, and the important processes controlling the behaviour of the system were not known. We were still using simple equilibrium transport codes to attempt to reproduce the observed behaviour, and failing. We can now model column experiments, and more than that, for the first time we have a model that can explain both batch and column experiments using the same parameters. We know that humic kinetics are vitally important in controlling the behaviour of metal-humate interactions. The problem is that this new understanding has lead to new questions and new uncertainties. However, the new uncertainties are different in character to the previous ones. The most important difference is that we can now identify precisely what parameters are not sufficiently well defined, whereas before, we simply did not understand how the system worked.

More research is required in order to reduce the remaining uncertainty. In particular, it is crucial that the true values of the rate constants observed in the environment are determined. In the mean time, the only conservative approach is to assume that the non-exchangeable metal is irreversibly sorbed. When the true rate constants have been positively identified, we have presented a methodology that will be able to take them into account.

At present, the uncertainty in the rate constants is dominating the system. However, when that is resolved, the uncertainty in the source term will probably start to dominate. It will be more difficult to remove this area of uncertainty, because it is likely to vary from case to case.

The general conclusion of this work is that humic substances are expected to have a significant impact upon the transport of actinides, fission products and other toxic metals in the environment.

9. REFERENCES

N.D. Bryan A Modelling study of humate mediated metal transport. In *Effects of Humic Substances on the Migration of Radionuclides: Complexation and Transport of the Actinides.* pp 245 - 262 Ed. G. Buckau. Wissenschaftliche Berichte (FZKA 6124, ISSN 0947-8620), Forschungszentrum Karlsruhe Technik und Umwelt, Karlsruhe, Germany (1998).

Bryan N.D., Jones D., Griffin D., Regan L., King S., Warwick P., Carlsen L. and Bo P. 1999 Combined mechanistic and transport modelling of metal humate complexes. In *Effects of Humic Substances on the Migration of Radionuclides: Complexation and Transport of the Actinides.* pp 301 - 338, Ed. G. Buckau. Wissenschaftliche Berichte (FZKA 6324, ISSN 0947-8620), Forschungszentrum Karlsruhe Technik und Umwelt, Karlsruhe, Germany (1999a)

Bryan N.D., Griffin D. and Regan L. Implications of Humic Chemical Kinetics for Radiological Performance Assessment. In *Effects of Humic Substances on the Migration of Radionuclides: Complexation and Transport of the Actinides.* pp 339 - 356, Ed. G. Buckau. Wissenschaftliche Berichte (FZKA 6324, ISSN 0947-8620), Forschungszentrum Karlsruhe Technik und Umwelt, Karlsruhe, Germany (1999b)

Geckeis H., Rabung T., Kim J.I. Kinetic Aspects of Metal Ion Binding to Humic Substances. In *Effects of Humic Substances on the Migration of Radionuclides: Complexation and Transport of the Actinides.* pp 47 - 58, Ed. G. Buckau. Wissenschaftliche Berichte (FZKA 6324, ISSN 0947-8620), Forschungszentrum Karlsruhe Technik und Umwelt, Karlsruhe, Germany (1999)

Jennings A.A. and Kirkner D.J. Instantaneous Equilibrium Approximation Analysis. *Journal of Hydraulic Engineering (A.S.C.E.)*, 1984, **110**, 1700 – 1717.

King S., Warwick P., Bryan N.D. A Study of Metal Complexation with Humic and Fulvic Acid: The effect of Temperature on Association and Dissociation. In *Effects of Humic Substances on the Migration of Radionuclides: Complexation and Transport of the Actinides.* pp 277 - 300, Ed. G. Buckau. Wissenschaftliche Berichte (FZKA 6324, ISSN 0947-8620), Forschungszentrum Karlsruhe Technik und Umwelt, Karlsruhe, Germany (1999)

Schussler W., Artinger R., Kienzler B. and Kim J.I. Modelling of Humic Colloid Mediated Transport of Amercium(III) by a kinetic approach. In *Effects of Humic Substances on the Migration of Radionuclides: Complexation and Transport of the Actinides.* pp 245 - 262 Ed. G. Buckau. Wissenschaftliche Berichte (FZKA 6124, ISSN 0947-8620), Forschungszentrum Karlsruhe Technik und Umwelt, Karlsruhe, Germany (1998).

Schussler W., Artinger R., Kim J.I., Bryan N.D., Griffin D. Modelling of Humic Colloid Borne Americium (III) Migration in Column Experiments Using the Transport/Speciation Code k1-D and the KICAM Model, Paper presented at MIGRATION 99, Chemistry and Migration Behaviour of Actinides and Fission Products in the Geosphere, Lake Tahoe, California, September 26 - October 1, 1999.

Annex 18

The Influence of Humic Substances on the Interaction between Mineral Surfaces and Europium

(L. Carlsen, P. Lassen and E. Tønning (NERI))

3rd Technical Progress Report

EC Project:

"Effects of Humic Substances on the Migration of Radionuclides: Complexation and Transport of Actinides"

Project No.: FI4W-CT96-0027

The Influence of Humic Substances on the Interaction Between Mineral Surfaces and Europium

L. Carlsen, P. Lassen and E. Tønning

National Environmental Research Institute, Department of Environmental Chemistry,
Dk-4000 Roskilde, Denmark

THE INFLUENCE OF HUMIC SUBSTANCES ON THE INTERACTION BETWEEN MINERAL SURFACES AND EUROPIUM

Lars Carlsen[1], Pia Lassen and Erik Tønning

National Environmental Research Institute, Department of Environmental Chemistry
DK-4000 Roskilde, Denmark

([1]Corresponding author: e-mail LC@dmu.dk)

Abstract

The influence of humic substances on the interaction between europium and selected mineral surfaces has been investigated at neutral pH (6-7). The minerals included were γ-alumina, in the form of boemite, kaolinite, in its sodium form, and goethite. It appeared that in all cases the presence of humic substances in solution significantly reduced the sorption of europium to the mineral surfaces. The investigations comprise the ternary mineral (S) - humic substances (HS) - europium (Eu) system and three different starting conditions, i.e. the reaction systems HA-Eu + S, HA-S + Eu and Eu-S + HA, respectively, were studied. It turned out that the amount of europium bound to each mineral surfaces at equilibrium is independent of the starting conditions, i.e. identical equilibrium situations are reached. However, the equilibrium situation apparently is reached somewhat more slowly in the case of boemite compared to kaolinite and goethite.

Introduction

Humic substances interact with polyvalent metal ions and organic pollutants thereby altering the migration and sorption properties of the ions and pollutants (Carlsen, 1989, 1992; Randall et al., 1996). In addition the interaction between humic substances and mineral surfaces may also play a crucial role in determining the fate of pollutants in e.g. the soil/ground water system due to significant changes in surface characteristics as a consequence of the surface coating with organic material (Haas and Horowitz, 1986; Keoleian and Curl, 1989; Takahashi et al., 1996; Kretzschmar et al., 1997, Takahashi et al., 1999). The sorption of metal ions to mineral surfaces has been described in numerous reports (cf. Bo and Carlsen, 1981). In the case of europium these interactions can be described by the reactions summarized in Fig. 1, where HS denoted humic substances, Eu is europium ions and $\mathbb{S}$ a binding site on a mineral surface. The above equations represent a complex chemical system and in order to simplify this system, usually, only one or a maximum of two of the above equations are experimentally investigated at a time.

1: $\mathbb{S}$ + HS <=> $\mathbb{S}$ -HS

2: $\mathbb{S}$ + Eu <=> $\mathbb{S}$ -Eu

3: HS + Eu <=> HS/Eu

4: $\mathbb{S}$ + HS/Eu <=> $\mathbb{S}$ -HS/Eu

5: $\mathbb{S}$ -HS + Eu <=> $\mathbb{S}$ -HS/Eu

6: $\mathbb{S}$ -Eu + HS <=> $\mathbb{S}$ + HS/Eu

7: $\mathbb{S}$ -HS/Eu + HS <=> $\mathbb{S}$ -HS + HS/Eu

8: $\mathbb{S}$ -HS/Eu + HS' <=> $\mathbb{S}$ -HS' + HS/Eu

Figure 1: Reactions involved in the ternary system. Mineral surface ($\mathbb{S}$), Humic Substances (HS) and Europium ions (Eu)

We have previously studied the interaction between humic acids and various minerals (Carlsen et al., 1995a, 1995b, 1999; Lassen et al., 1996). In the present paper we report on the reactions 4, 5 and 6 (Fig. 1), in all cases, however, HS is present in excess corresponding to the natural situation.

Experimental

The study have included 3 mineral, i.e. γ-alumina, Na-kaolinite and goethite. Characterization of the minerals was performed by X-ray diffraction using a Siemens D5000 diffractometer.

γ-alumina (Al_2O_3) was purchased from Hopkin and Williams Ltd, UK ("CAMAG M.F.C., 100-250 mesh), and used without further purification.

Based on diffractometry the γalumina was characterized as boemite (γ-alumina monohydrate: AlOOH). The sample investigated contained probably minor amounts of an amorphous material as indicated by a relative high background in the diffractometric investigation.

The specific surface area of the γ-alumina used was found to be 144 m^2/g.

Preparation of Na-kaolinite:
Kaolinite on Na-form was prepared by washing kaolinite with 1 M NaCl for 1 hour. The kaolinite was subsequently isolated by centrifugation and washed with 10^{-3} M NaCl 4 x 1 h corresponding

to equilibrium (i.e. no change in the aqueous concentration), isolated by centrifugation and filtration. The final product was air-dried and stored in a closed container.

Based on diffractometry the identity of Na-kaolinite was verified. Based on the diffractometric study it appeared that the sample investigated contained minor amounts of a mica mineral, probably muscovite (white mica).

The specific surface area of the Na-kaolinite used was found to be 6 m^2/g.

Preparation of goethite:
A solution of 1 M $Fe(NO_3)_3$ was added 5 M KOH (ratio 1: 1.8) under stirring. The solution was diluted approximately 5 times with water and left for a minimum of 60 h at 70°C. During this period ferrihydrite was converted to goethite. The precipitate was isolated by centrifugation and washed with water until the supernatant was colorless. The goethite was isolated by centrifugation and air dried. The final product was the pulverized and stored in a closed container.

Based on diffractometry the identity of the synthesized goethite was verified. The sample investigated appeared to be virtually pure goethite.

The specific surface area of the goethite used was found to be 34 m^2/g.

Humic acid solutions:
Stock solution of humic acids: 1.000 mg/L humic acids (obtained as sodium salt form Aldrich Co.) were dissolved in water and filtered through a 0.45 μm filter. pH was adjusted to a pH of 6.4 with 0.1 M HCl.

Humic acid solutions, in the appropriate concentrations, were made by dilution of the stock solution of the humic acid in 0.01 M NaCl, pH 6.

The concentrations in the humic acid solutions were determined by electronic absorption spectroscopy at 400 nm.

Europium solutions:
Europium was applied as Europium nitrate (Merck). The variations in europium concentrations were followed, using $^{152/154}Eu$ spiked solutions (in saturated sodium chloride), by γcounting (Kontron MR252 Automatic Gamma Counting System; Counting: 1 min.; 90-1500 keV).

Sorption isotherms for humic substances to the mineral surfaces in the presence of europium

Humic acid solutions, in the concentrations of 0, 20, 40, 100, 200 400, and 600 mg/L, were brought into contact with 25 mg of the mineral in 5 mL aqueous solution (the concentrations of 400 and 600 mg/L were only applied in the case of goethite). The mixtures were left for 6 days. Subsequently 0.1 mL 5.24 x 10^{-4} M Eu in 1.1 M NaCl were added and the mixtures was left for further 24 h followed by centrifugation, the eventual HS concentration in solution being determined. The concentration of HS sorbed to the mineral surface was determined by subtraction.

Sorption isotherms for europium to the mineral surfaces

Total Eu concentrations of 5, 10, 49, 204, and 979 μM, respectively were brought into contact with 25 mg of the mineral in 5.1 mL 0.01 M NaCl, pH 6. The mixtures were shaken for 24 h or 35 days, respectively, followed by centrifugation, the eventual Eu concentration in solution being determined. The concentration of Eu sorbed to the mineral surface was determined by subtraction.

Europium sorption in the ternary system

The sorption of europium to the solid material was studied in three different approaches, corresponding to different starting conditions as reflected in the reactions 4, 5, and 6, respectively (Fig. 1). Common for all three cases were a mixing of 0.1 mL 1.1 M NaCl exhibiting a Eu concentration of 5.24 x 10^{-4} M and 25 mg of the minerals and concentrations of humic substances of 0, 20, 40, 100, 400, and 600 mg/L, respectively, in 5 mL, the resulting Eu and Na concentrations being 10.27 μM, and 0.03 M, respectively.

Reaction 4: Mineral interaction with pre-equilibrated HS-Eu mixtures.

Eu and HS in various concentrations were left for 8 d. The mineral was added, the mixture being further shaken for 24h or 5 d, respectively, followed by centrifugation. The resulting Eu concentration in the supernatant was determined.

Reaction 5: Europium sorption to pre-equilibrated mineral-HS mixtures.

Mineral and HS in various concentrations were shaked for 6 days or more. Eu was added, the mixture being further shaken for 24h or 5 d, respectively, followed by centrifugation. The resulting Eu concentration in the supernatant was determined. In the case of boemite prolonged experiments (40 days) were also carried out in order to obtain equilibrium.

Reaction 6: HS sorption to pre-equilibrated mineral-Eu mixtures.

Mineral and Eu were shaked for 24h. HS in various concentrations were added, the mixture being further shaken for 24h or 5 d, respectively, followed by centrifugation. The resulting Eu concentration in the supernatant was determined. The resulting Eu concentration in the supernatant was

determined. In the case of boemite prolonged experiments (40 days) were also carried out in order to obtain equilibrium.

Results and Discussion

The sorption of humic substances (Aldrich Humic acid) and europium (III) to the three mineral surfaces was studied. Thus the minerals were left into contact with solutions of humic acids for 7 days whereas the mineral-europium interactions were monitored following 24 h or 35 days of contact, respectively. In Figures 2 - 4 the resulting sorption isotherms are depicted.

The sorption of humic substances to the minerals has previously been studied (Lassen et al., 1996; Carlsen et al., 1999). The overall picture developed in the present study are in agreement with those obtained in our previous investigations. Thus, the presence of europium only caused minor changes in the HA sorption.

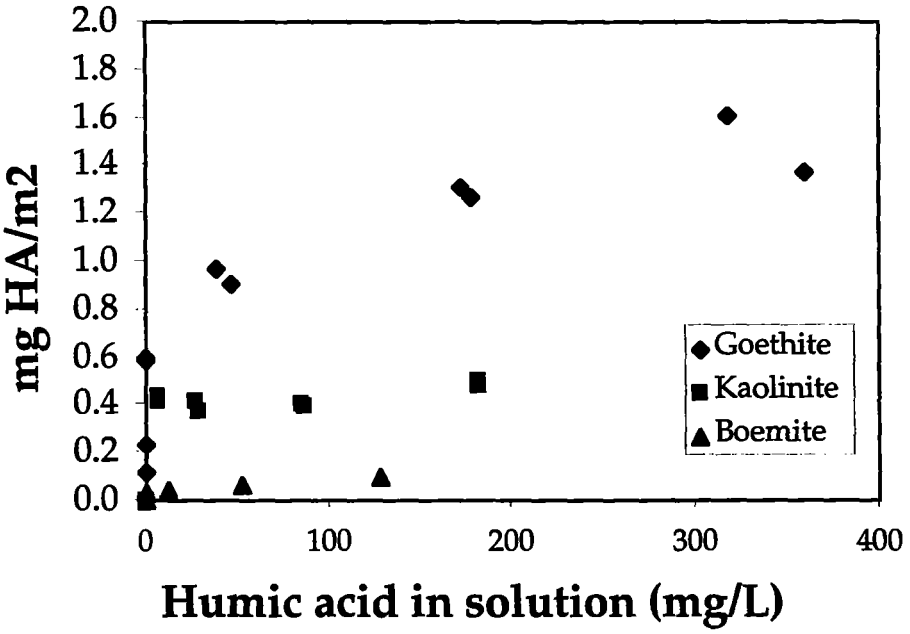

Figure 2: Humic acids sorption isotherms to kaolinite, goethite and boemite in the presence of europium following 7 days contact time.

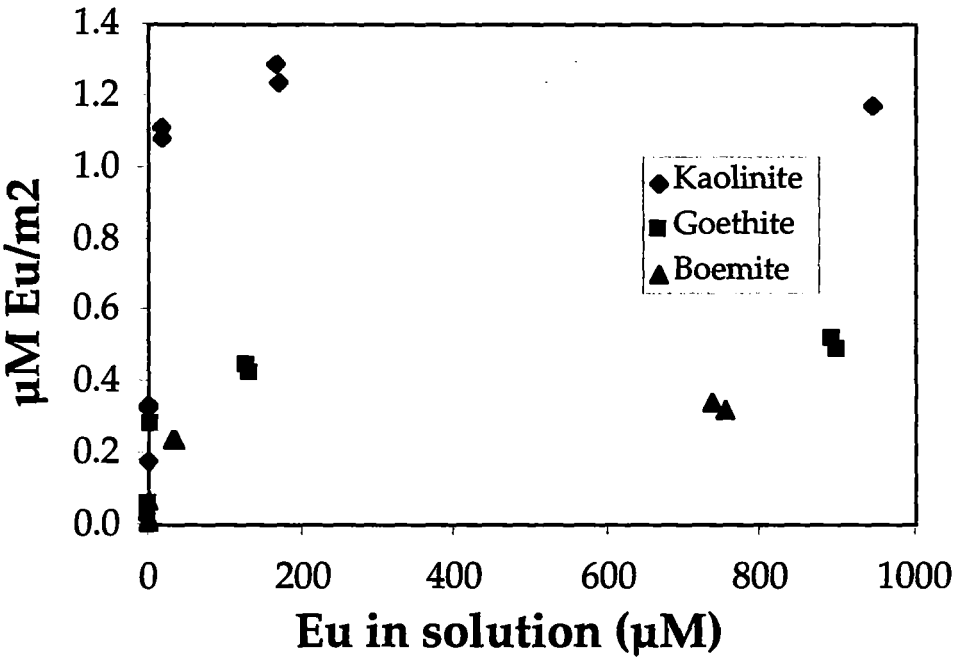

Figure 3: Europium sorption isotherms to kaolinite, goethite and boemite following 24 h contact time.

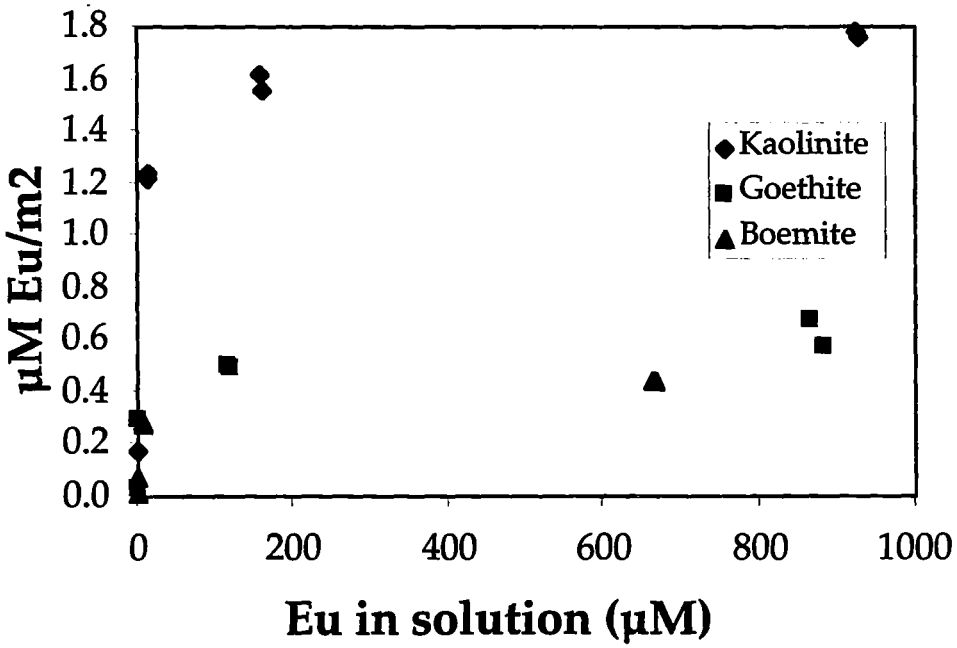

Figure 4: Europium sorption isotherms to kaolinite, goethite and boemite following 35 days contact time.

It is immediately seen that in the case of goethite and boemite the equilibrium situations were virtually reached following 24 h of contact time, whereas an approximate increase in europium sorption to kaolinite was noted following 35 days of contact time compared to a contact time of 24 h, only. In the ternary systems contacts times for the single systems for 24 h and 5 days, respectively, and in the case of boemite in addition 40 days, before measuring the eventual europium concentrations in the supernatants. In the following the single ternary systems, corresponding to reactions 4, 5 and 6 (cf. Fig. 1), are treated separately for each mineral.

Kaolinite

In Table 1 the percentage of Eu(III) sorbed to kaolinite are shown for the reaction system HA-Eu + S (reaction 4), HA-S + Eu (reaction 5) and Eu-S + HA (reaction 6), respectively.

It is immediately noted that the equilibrium situation in all three cases virtually is reached following 24 h contact time as only minor increase in the amount of sorbed Eu(III) was noted following 5 days contact time. It is further noted that the amount of Eu(III) in solution at equilibrium appears virtually independent of the actual starting conditions.

Table 1a: Percentage of Eu(III) sorbed following 24 h contact time with kaolinite as function of Humic Acid concentration (mg/L)

[HA]	HA-Eu+S	HA-S+Eu	Eu-S+HA
0	93.4	93.4	93.4
20	92.0	93.8	90.6
40	40.7	48.5	46.7
100	17.5	16.8	

Table 1b: Percentage of Eu(III) sorbed following 5 days contact time with kaolinite as function of Humic Acid concentration (mg/L)

[HA]	HA-Eu+S	HA-S+Eu	Eu-S+HA
0	93.4		93.4
20	96.5		95.7
40	46.4	51.8	49.3
100	18.4	18.1	18.4

Goethite

In Table 2 the percentage of Eu(III) sorbed to goethite are shown for the reaction system HA-Eu + S (reaction 4), HA-S + Eu (reaction 5) and Eu-S + HA (reaction 6), respectively.

Table 2a: Percentage of Eu(III) sorbed following 24 h contact time with goethite as function of Humic Acid concentration (mg/L)

[HA]	HA-Eu+S	HA-S+Eu	Eu-S+HA
0	99.9	99.9	99.9
20	99.7	99.5	99.9
400	84.9	79.4	85.9
600	67.3	61.4	71.7

Table 2b: Percentage of Eu(III) sorbed following 5 days contact time with goethite as function of Humic Acid concentration (mg/L)

[HA]	HA-Eu+S	HA-S+Eu	Eu-S+HA
0	99.9		99.9
20	100	99.8	99.8
400	88.6	80.5	87.3
600	71.1	62.9	71.6

As was the case with kaolinite (vide infra) it appears that the equilibrium situation in all three cases virtually is reached following 24 h contact time, although a slight increased sorption was noted following 5 days contact time in the HA-Eu + S (reaction 4) reaction system, probably reflecting the decreased affinity, measured as $\mu mol/m^2$, for sorption of Eu(III) to goethite compared to kaolinite (cf. Fig. 2 and 3) and thus the ability to compete with the humic acids for the europium. Likewise it is noted that the amount of Eu(III) in solution at equilibrium appears virtually independent of the actual starting conditions.

Boemite

In Table 3 the percentage of Eu(III) sorbed to boemite are shown for the reaction system HA-Eu + S (reaction 4), HA-S + Eu (reaction 5) and Eu-S + HA (reaction 6), respectively.

Table 3a: Percentage of Eu(III) sorbed following 24 h contact time with boemite as function of Humic Acid concentration (mg/L)

[HA]	HA-Eu+S	HA-S+Eu	Eu-S+HA
0	99.9	99.9	99.9
20	73.0	99.8	91.9
40	62.2	71.5	85.0
100	43.2	44.3	77.2

Table 3b: Percentage of Eu(III) sorbed following 5 days contact time with boemite as function of Humic Acid concentration (mg/L)

[HA]	HA-Eu+S	HA-S+Eu	Eu-S+HA
0	99.9		99.9
20	95.6		98.8
40	85.3	83.0	89.9
100	62.7	62.0	73.9

In the case of boemite it is noted that in the cases of HA-Eu + S (reaction 4) and HA-S + Eu (reaction 5) a distinctly increased sorption prevails following 5 days contact time compared to 24 h contact time, whereas in the case of the Eu-S + HA system, this effect was not be found. It further appears, assuming identical equilibrium situations independent of the starting conditions, as noted in the case of kaolinite and goethite, that the two mentioned systems (reactions 4 and 5) the equilibrium situation is not reached completely even after 5 days contact time, whereas equilibrium was noted following 40 days contact time.

In order to explain these observations we turn to the sorption isotherms (Fig.'s 2 - 4). First of all it can be noted that both in the case of HA sorption and Eu(III) sorption the affinity, measured as function of specific surface area, of boemite is significantly lower than is the case for kaolinite and goethite. Consequently the elimination of Eu from the strong HA-Eu complex (Carlsen, 1989) by the boemite surface (reaction 4) will be kinetically unfavorable. In the case of reaction 5, i.e. the HA-S + Eu system, the reason may be sought for in the fact that probably the sorption of HA and Eu(III) to the surface involves the same sites, such as S-OH. Thus, the Eu will sorb only slowly due to the lack of available free sites. On the other hand in the case of reaction 6, i.e. the Eu-S + HA system, the formation of the strong Eu-HA complexes can be expected to control the reaction rate, thus leading to a rapidly reached equilibrium situation.

Conclusions

Based on the above described investigations the following main conclusions can be drawn:

1° The presence of humic substances in solution significantly reduces the sorption of europium to the mineral surfaces.

2° The amount of europium bound to the mineral surfaces involved in the present study at equilibrium is independent of the starting conditions, i.e. reactions 4, 5 and 6 lead to identical equilibrium situations.

3° The equilibrium situation apparently is reached more slowly in the case of boemite compared to kaolinite and goethite.

References

Bo, P. and Carlsen, L. (1981) "Ion exchange properties of soil fines", *European Appl.Res.Rept.-Nucl.Sci.Technol* , **3**, 813-873

Carlsen, L. (1989) "The role of organics in the migration of radionuclides in the geosphere", Report: EUR-12024 EN, Commision of the European Communities, Nuclear Science and Technology, Luxembourg, 76 pages

Carlsen, L. (1992) "Migration chemistry. Chemical and physico-chemical processes influencing the migration behaviour of pollutants", NERI Technical Report No. 52, National Environmental Research Institute, Roskilde, 70 pages

Carlsen, L., Lassen, P. and Warwick, P. (1995a) "Sorption of humic acids to alumina: Size effects", HUMUS - Nordic Humus Newsletter, **2**, 25-32

Carlsen, L., Lassen, P. and Warwick, P. (1995b) "Sorption of humic acids to alumina: Temperature effects", HUMUS - Nordic Humus Newsletter, **2**, 33-38

Carlsen, L., Lassen, P. and Volfing, M.-B. (1999) "Sorption of humic acids to kaolinite and goethite", in: Effects of Humic Substances on the Migration of Radionuclides: Complexing and Transport of Actinides. Second technical progress report', G. Buckau, ed., Wissenschaftliche Berichte FZKA 6324, Forschungzentrum Karlsruhe, Nukleare Entsorgungstechnik, 1999, pp. 359-372

Haas, C.N. and Horowitz, N.D., (1986) "Adsorption of cadmium to kaolinite in the presence of organic material", *Water, Air, and Soil Pollut.*, **27**, 131-140

Keoleian, G.A. and Curl, R.L., (1989) "Effect of humic acid on the adsorption of tetrachlorobiphenyl by kaolinite", in Adv.Chem. vol. 219, I.H. Suffet and P. McCarthy, Eds, ACS, Washington DC, Ch. 16, 231-250

Kretzschmar, R., Hesterberg, D. and Sticher, H. (1997) "Effects of adsorbed humic acid on surface charge and flocculation of kaolinite", SoilSci.Soc. Am.J. 61, 101-108

Lassen, P., Carlsen, L. and Warwick, P. (1996) "The interaction between humic acids and γ-Al_2O_3" Theophrastus' Contributions to Advanced Studies in Geology, **1**, 3-16

Randall, A., Warwick, P., Carlsen, L. and Lassen, P. (1996) "Fundamental studies on the interaction of humic materials", EUR-16865 EN, Commision of the European Communities, Nuclear Science and Technology, Luxembourg, 220 pages

Takahashi, Y., Minai, Y, Ambe S., Maeda, H., Ambe, F. and Tominaga, T. (1996) "Multitracer study of the influence of humate formation on the adsorption of various ions on kaolinite and

silica gel", RIKEN Review No. 13: Focused on The Multitracer, Its Application to Chemistry, Biochemistry and Biology 11

Takahashi, Y., Kimura, T., Kato, Y. and Minai, Y. (1999) "Speciation of europium(III)) sorbed on a montmorillonite surface in the presence of polycarboxylic acid by laser-induced fluorescence spectroscopy", *Environ.Sci.Technol.* **33**, 4016-4021

Annex 19

^{152}Eu Migration Experiments with Different Sediments and Flow-Velocities

(D. Klotz and M. Wolf (GSF-IfH))

3rd Technical Progress Report

EC Project:

"Effects of Humic Substances on the Migration of Radionuclides:
Complexation and Transport of Actinides"

GSF Contribution to Task 3 (Actinide Transport)

^{152}Eu Migration Experiments with Different Sediments and Flow Velocities

D. Klotz and M. Wolf

GSF-National Research Center for Environment and Health, Institute of Hydrology

D-85764 Neuherberg, Germany

Objectives

The objectives are to determine the humate mediated migration behavior of lanthanide and actinide ions in non-tenacious loose sediments of variable grain size. For this purpose, columns experiments are carried out with different sediments and groundwater flow-velocities. Prior to performing migration experiments, columns were conditioned with groundwater over several months (Klotz, 1999). All migration experiments of ^{152}Eu have been carried out with the humic rich Gorleben groundwater Gohy 2227.

Experimental

Five columns with non-tenacious loose sediments of varying grain size from Lower Saxony (Gorleben) and Bavaria (Dornach and Oberpfalz) were prepared and installed in an inert gas box (Klotz and Wolf, 1998). Properties of these columns are described in Klotz (1999). The ^{152}Eu migration experiments were carried out at different flow velocities (filter velocities v_f) of approx. 0.008 to 0.88 m/d. The ^{152}Eu spiked humate solution (0.37 MBq) were conditioned for at least three months prior to migration experiments. Preconditioning was done for six weeks with a synthetic groundwater, followed by conditioning for 37 weeks with the Gorleben groundwater Gohy 2227 (flow velocities v_f about 2×10^{-4} cm/s $\approx$ 0.2 m/d). Tracer experiments (tritiated water) were used to monitor the hydrological properties during conditioning (Klotz 1999) .

Results and Discussion

The migration results are presented in Table 1 and include also the migration experiment carried out with a flow velocity (v_f) of approx. 0.20 m/d (Klotz, 1999). The results show that Eu humate is transported more or less without retardation (mean retardation factors 0.95 to 1.08). The recovery as a measure of the physical migration of the Eu humate particles decrease with lower flow velocity or higher residence time of ^{152}Eu in the column, respectively. If the ^{152}Eu recovery is plotted vs. the ^{152}Eu residence time in the columns (Fig. 1), it is shown that after a fast decrease within the first hours a relatively slow decrease in ^{152}Eu recovery follows (fast and slow kinetics). A good approximation of the measured data is possible with a kinetic model (cf. Schüßler et al. 1998 and Geckeis et al. 1999) assuming two first order reactions with fast and slow kinetics for the loss of ^{152}Eu from the solution (eq. 1).

$$^{152}Eu \text{ recovery } [\%] = F_1 \exp(-K_1 t) + F_2 \exp(-K_2 t) \qquad (1)$$

In this equation F_1 and F_2 are two estimated fractions of the Eu-humate colloids (given in %) which dissociate with two different reaction rates K_1 and K_2 (given in h^{-1}). The estimated parameters for some different column experiments are summarized in Table 2. The results of

the estimations show, that all data of the column experiments can not be modelled with one set of parameters but with individual parameters for each column experiment. The minor fractions F_1 (19 to 32 %) react with much higher reaction rates than the major fractions F_2 (68 to 81 %) and the reaction rates K_1 are more than one order of magnitude higher than the reaction rates K_2. This behavior can be explained by the Kinetically Controlled Availability Model (Schüßler et al. 1998) together with an influence of the sediment type and surface on the kinetic parameters.

Table 1: Results of ^{152}Eu migration experiments in columns with different sediments and flow velocities (filter velocities v_f) carried out with the humic rich groundwater Gohy 2227.

Column No.:	1	2	3	4	5	v_f (m/d)
			Sediments			
Origin	Dornach/ Bavaria	Gorleben/ Lower Saxony	Gorleben/ Lower Saxony	Gorleben/ Lower Saxony	Oberpfalz/ Bavaria	
Type	Sandy pebbles/ gravel	Fine sand I	Fine sand II	Medium course sand I	Course sand	
^{152}Eu recovery (%)	85.5	82.9	83.1	83.1	91.9	0.88
	82.9	77.8	78.8	82.4	82.8	0.20
	75.3	74.2	>63.2*	79.3	79.8	0.04
	67.3	68.9	65.6	>62.7*	74.1	0.008
Retardation factor	0.94	0.97	0.98	1.01	0.97	0.88
	0.94	0.96	0.97	1.00	1.03	0.20
	1.07	1.02	1.06	1.08	1.13	0.04
	0.83	0.96	0.92	0.95	1.18	0.008
Mean value	0.95	0.98	0.98	1.01	1.08	

* These data can be given only as minimum values due to possible losses during ^{152}Eu injection

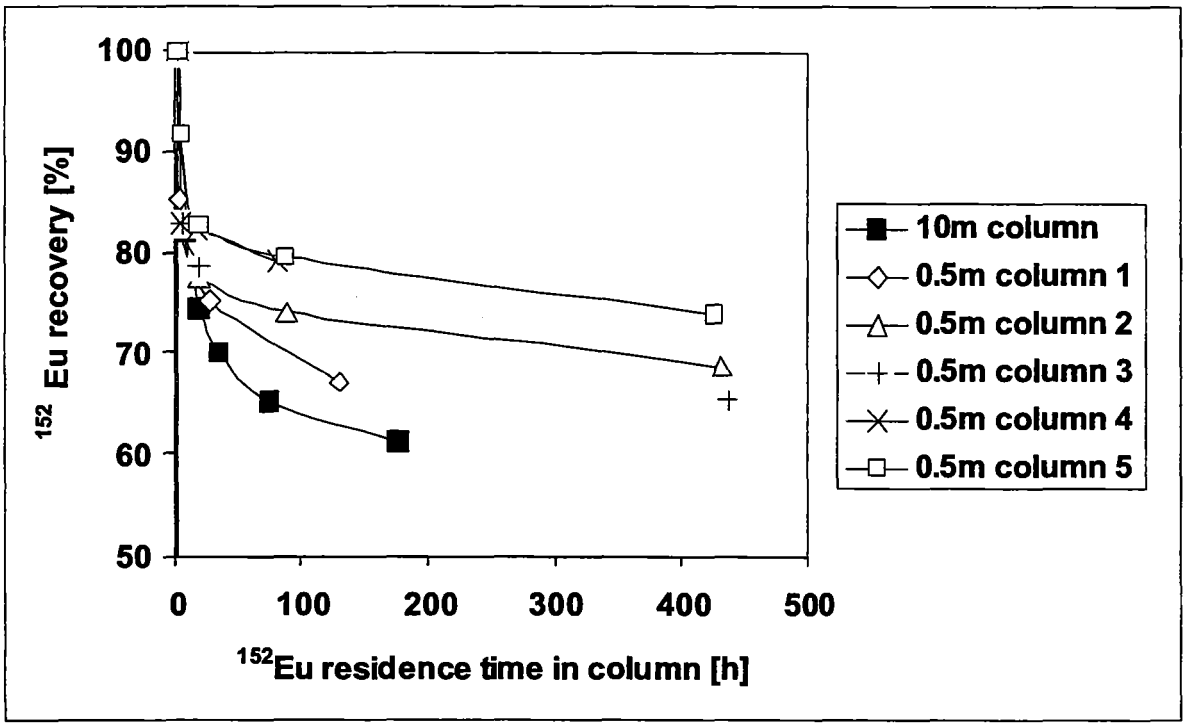

Fig. 1: ^{152}Eu recovery vs. ^{152}Eu residence time in different columns.

Table 2: Estimated kinetic model parameters for some migration experiments.

Column No./Type:	1	2	5	10 m column
		Sediments		
Origin	Dornach/ Bavaria	Gorleben/ Lower Saxony	Oberpfalz/ Bavaria	Gorleben/ Lower Saxony
Type	Sandy pebbles/ gravel	Fine sand I	Course sand	Fine sand III
F_1 [%]	23	24	19	32
F_2 [%]	77	76	81	68
K_1 [h^{-1}]	0.88	0.31	0.15	0.09
K_2 [h^{-1}]	0.0011	0.0002	0.0002	0.0006

References

Geckeis, H., Rabung, Th., Kim, J.I. (1999): Kinetic Aspects of the Metal Ion Binding to Humic Substances. In: Effects of Humic Substances on the Migration of Radionuclides: Complexation and Transport of Actinides (Ed. G. Buckau), Second Technical Progress Report FZKA 6324, Research Center Karlsruhe, 45-58

Klotz, D. (1999): Conditioning of Columns and ^{152}Eu Migration Experiments. In: Effects of Humic Substances on the Migration of Radionuclides: Complexation and Transport of Actinides (Ed. G. Buckau), Second Technical Progress Report FZKA 6324, Research Center Karlsruhe, 373-380

Klotz, D. and Wolf, M. (1998): Effects of Humic Substances on the ^{152}Eu Migration in a Sandy Aquifer: First Results from Column Experiments with 10 m Flow Distance. In: Effects of Humic Substances on the Migration of Radionuclides: Complexation and Transport of Actinides (Ed. G. Buckau), First Technical Progress Report FZKA 6124, Research Center Karlsruhe, 269-278

Schüßler, W., Artinger, R., Kienzler, B., Kim, J.I. (1998): Modeling of Humic Colloid Mediated Transport of Americium (III) by a Kinetic Approach. In: Effects of Humic Substances on the Migration of Radionuclides: Complexation and Transport of Actinides (Ed. G. Buckau), First Technical Progress Report FZKA 6124, Research Center Karlsruhe, 91-101

Annex 20

Complementary Information on the Characterization of Material Used within the Project

(P. Hooker (BGS))

(L. Carlsen, M. Thomson and P. Lassen K. (NERI))

(K. Schmeide (FZR-IfR))

(C. Barbot and J. Pieri (GERMETRAD))

3rd Technical Progress Report
EC-Project

"Effects of Humic Substances on the Migration of Radionuclides: Complexation and Transport of Actinides"

Complementary Information on the Characterization of Material Used within the Project

Part 1: **Introduction and Summary of Characteristic Properties of Humic Substances**
(P.J. Hooker (BGS))

Part 2: **Characterization of Humic Substances at NERI**
(L. Carlsen, M. Thomson and P. Lassen)

Part 3: **Characterization of Natural and Synthetic Humic Substances, Rock Material and Minerals at FZR-IfR (K. Schmeide)**

Part 4: **Silica Gel Coated with Humic Acid and Specific Functional Groups at GERMETRAD (C. Barbot and J. Pieri)**

BGS: British Geological Survey, Nottingham, NG12 5GG, UK
NERI: National Environmental Research Institute, Department of Environmental Chemistry, Dk-4000, Roskilde, Denmark
FZR-IfR: Forschungszentrum Rossendorf, Institute of Radiochemistry, P.O. Box 510 119, D-01314 Dresden, Germany
GERMETRAD: Universite de Nantes, Laboratory for Biochemistry and Radiochemistry, 2 Rue de la Houssiniere, F-44322 Nanes Cedex 03, France

Part 1: Introduction and Summary of Characteristic Properties of Natural Humic Substances

(P.J. Hooker (BGS))

Introduction

The objective of the project is to provide the scientific basis, models and codes for predictive modeling of the impact of humic colloid mediated actinide transport on the long-term safety of radioactive waste disposal and contaminated sites. For this purpose, a large number of designed and near-natural systems are investigated in order to provide input data and process understanding. In this context, characterization of material used and adequate documentation of relevant properties is required. Characterization data are given in various contributions within this and the two foregoing technical progress reports of the project, as well as in numerous publications resulting from the project activities. In these individual contributions not all characterization data are given. Furthermore, these data are scattered over a large number of papers. Therefore, in this section a summary of selected important data is given for humic substances and sediments/minerals used within the project. Below a summary of important characteristic data for natural humic and fulvic acids are discussed. In section 2, principle component analysis of eight natural humic substances by NERI is given. In part 3, characteristic data of natural and synthetic humic substances and mineral/sediment material by FZR-IfR are presented. Finally, in part 4, the generation and characteristic properties of silica gel covalently coated with humic acid and specific functional groups are found.

Natural Humic Substances

Most of the basic properties were measured by more than one method. Although the use of different methods was encouraged, it was also important that some properties were determined on all the relevant humic materials using the same method.

Within the project, aqueous fulvic and humic acids were sampled and prepared from two new sites, namely the "Kleiner Kranichsee" Bog in Saxony, Germany, and the Derwent Reservoir, Derbyshire, UK. In addition, other site-specific humic and fulvic acids from the Gorleben groundwater Gohy-573 were used. Furthermore, purified Aldrich humic acid was used for different investigations and serves as a reference.

The fundamental properties of the humic and fulvic acids sampled and studied under this project were determined. These included elemental compositions, trace impurities and the proton exchange capacities of the carboxylic acid and phenolic groups (Higgo et al.1998; Schmeide et al. 1998). The FZR group also characterised the Derwent Reservoir fulvic acid,

the Kranichsee fulvic and humic acids and the Aldrich humic acid by means of FTIR spectroscopy and capillary zone electrophoresis (Schmeide et al. 1999).

Results

Tables 1 to 3 summarize the elemental compositions, trace impurities and proton exchange capacities of the humic and fulvic acids. Data for humic material from Gorleben and Aldrich humic acid are included in these Tables (Kim et al. 1990). The data show some significant variations. These reflect the very different origins of the humic substances; the Derwent and Kranichsee materials were taken from surface waters whereas the Gorleben organics were collected from deep groundwater. See summary discussions in Buckau (1998) and Buckau (1999) for comments on the methods and results.

Important parameters are the size distribution and molecular weights. Both the U.V. Scanning Ultracentrifugation method (carried out by Nick Bryan at Manchester University) and the Flow-Field Flow Fractionation (Flow-FFF) method (carried out by Ngo Manh Thang and H. Geckeis at FZK/INE) gave similar results for the Derwent fulvic acid. The derived size-average value of ~ 4000 Dalton, relative to calibration standards used, for the Derwent FA is within the range expected for fulvic acids (see Higgo et al. 1998). Both techniques showed a wide size distribution of molecular size for the Derwent FA. This feature of size dispersion was also observed for the Gorleben fulvic acid (Gohy-573-FA) and humic acid (Gohy-573-HA) using gel permeation chromatography (Kim et al. 1990). The number-average molecular size of Gohy-573-FA (9400 Dalton), and Gohy-573-HA (9100 Dalton), were significantly higher than the Derwent FA value (2200 Dalton), reflecting differences in reference calibration standards.

Table 1. Elemental compositions

Element	Fulvic	Fulvic	Fulvic	Fulvic	Humic	Humic	Humic	Humic	Humic
	Derwent ϕ	Kranichsee +	Gohy-573 *	Literature *	Kranichsee +	Gohy-573 *	Aldrich *	Aldrich +	Literature *
C (wt%)	49.1	48.8	57.2	40-50	49.9	56.3	55.2	58.7	50-60
H	4.2	2.6	4.9	4-6	3.5	4.52	4.48	3.3	4-6
N	0.6	0.6	1.14	1-3	1.8	1.69	0.32	0.8	2-6
S	0.32	0.5	1.44	0-2	0.5	1.73	2.33	4.1	0-2
O	45.8	39.1	35.4	44-50	33.4	35.8	37.64	24.8	30-35
H/C	1.02	0.63	1.02	1.02	0.84	0.98	0.97	0.67	0.94
O/C	0.69	0.60	0.46	0.51	0.50	0.48	0.51	0.32	0.50

ϕ Data from Higgo et al. (1998); + Data from Schmeide et al. (1998); * Data from Kim et al. (1990).

Table 2. Impurities (mg/kg or ppm)

	Fulvic Derwent Reservoir ϕ	Fulvic Kranichsee +	Fulvic Gohy-573 *	Humic Kranichsee +	Humic Gohy-573 *	Humic Aldrich Purified +	Humic Aldrich Purified *	Humic Aldrich Unpurified *
Na	36.1	10 095	2 196	1 670	19.0	226	270	75 116
K	<12	701		324		36		
Ca	<12	487	437	708	22.6	611	31.7	9 931
Mg	<24	87	44	35	4.0	19	5.6	698
Al	61.3	41		149	39.3	93	35	2 950
Si	18.0	290	1 196	656	68	137	15	3 333
Fe	168	296	52.9	1 018	277	863	360	12 207
Co	<2.4		0.24		2.5		0.33	2.5
Ce	0.06		0.1		1.1		4.1	23.0
Eu	<0.12		0.01		0.05		0.24	0.66
Th	0.17	Not detected	0.23	2	7.4	1	1.53	2.0
U	0.05	2		4	2.2	1	0.23	0.65

ϕ Data from Higgo et al. (1998); + Data from Schmeide et al. (1998).; * Data from Kim et al. (1990).

Table 3. Proton exchange capacities of functional groups

	METHOD	TOTAL meq/g	Carboxylic meq/g	Phenolic meq/g
FULVIC ACIDS				
Derwent FA ϕ	Titration and curve fitting	8.1	5.0	3.1[a]
Kranichsee FA +	Ca–acetate		6.05	
Kranichsee FA +	Radiometric	8.82	3.98	4.84
Kranichsee FA +	Titration		5.60	
Gohy-573 FA *	Titration		5.70	
HUMIC ACIDS				
Kranichsee HA +	$Ba(OH)_2$ & Ca–acetate	10.17	4.20	5.97[a]
Kranichsee HA +	Radiometric	7.75	3.88	3.87
Kranichsee HA +	Titration		4.83	
Gohy-573 HA *	$Ba(OH)_2$ & Ca–acetate	6.61	4.75	1.86[a]
Gohy-573 HA *	Titration		5.38	
Aldrich HA *	$Ba(OH)_2$ & Ca–acetate	7.06	4.80	2.26[a]
Aldrich HA *	Titration		5.43	
Aldrich HA +	$Ba(OH)_2$ & Ca–acetate	7.12	4.41	2.71[a]
Aldrich HA +	Radiometric	7.4	3.9	3.4
Aldrich HA +	Titration		5.06	

[a] Calculated from the difference between the Total and Carboxylic values. ϕ Data from Higgo et al. (1998).
+ Data from Schmeide et al. (1998). * Data from Kim et al. (1990).

References

Buckau G. (1998) "Executive Summary", In *First Technical Progress Report of the EC project 'Effects of Humic Substances on the Migration of Radionuclides: Complexation and Transport of Actinides'* (ed. G. Buckau). Forschungszentrum Karlsruhe Report FZKA 6124, pp. 1-21.

Buckau G. (1999) "Executive Summary", In *Second Technical Progress Report of the EC project 'Effects of Humic Substances on the Migration of Radionuclides: Complexation and Transport of Actinides'* (ed. G. Buckau). Forschungszentrum Karlsruhe Report FZKA 6324, pp. 1-20.

Carlsen L., Lassen P. and Volfing M-B. (1999) "Sorption of humic acids to kaolinite and goethite", In *Second Technical Progress Report of the EC project 'Effects of Humic Substances on the Migration of Radionuclides: Complexation and Transport of Actinides'* (ed. G. Buckau). Forschungszentrum Karlsruhe Report FZKA 6324, pp. 357-372.

Fleury C., Barbot C., Pieri J., Durand J.P. and Goudard F. (1999) "Influence of the organic coating and calcium ions on the sorption of europium on a silica gel", In *Second Technical Progress Report of the EC project 'Effects of Humic Substances on the Migration of Radionuclides: Complexation and Transport of Actinides'* (ed. G. Buckau). Forschungszentrum Karlsruhe Report FZKA 6324, pp. 137-153.

Higgo J.J.W., Davis J.R., Smith B. and Milne C. (1998) "Extraction, purification and characterization of fulvic acid", In *First Technical Progress Report of the EC project 'Effects of Humic Substances on the Migration of Radionuclides: Complexation and Transport of Actinides'* (ed. G. Buckau). Forschungszentrum Karlsruhe Report FZKA 6124, pp. 103-128.

Kim J.I., Buckau G., Li G.H., Duschner H. and Psarros N. (1990) "Characterization of humic and fulvic acids from Gorleben groundwater", *Fresenius J. Anal. Chem.* **338**, 245-252.

Schmeide K., Zänker H., Heise K.H. and Nitsche H. (1998) "Isolation and characterization of aquatic humic substances from the bog 'Kleiner Kranichsee'", In *First Technical Progress Report of the EC project 'Effects of Humic Substances on the Migration of Radionuclides: Complexation and Transport of Actinides'* (ed. G. Buckau). Forschungszentrum Karlsruhe Report FZKA 6124, pp. 161-195.

Schmeide K., Zänker H., Hüttig G., Heise K.H. and Bernhard G. (1999) "Complexation of aquatic humic substances from the bog 'Kleiner Kranichsee' with uranium (VI)", In *Second Technical Progress Report of the EC project 'Effects of Humic Substances on the Migration of Radionuclides: Complexation and Transport of Actinides'* (ed. G. Buckau). Forschungszentrum Karlsruhe Report FZKA 6324, pp. 177-197.

Part 2: Characterization of Humic Substances at NERI
(L. Carlsen, M. Thomson and P. Lassen)

The following information can be found in more detail in:

M. Thomsen, S. Dobel, P. Lassen, L. Carlsen, B.B. Mogensen, and P.-E. Hansen, Investigation of the Complex Formation between Esfenvalerate and Dissolved Humic Matter of different Origin, Submitted.

The origin of the eight humic substances investigated is given in Table 1. A principle component analysis is conducted, based on data obtained by UV-VIS spectroscopy, size exclusion chromatography, ^{13}C-NMR and elemental analysis (Figs. 1-4).

Table 1. Types and origin of the Humic Substances used in this study.

Humic Substances	Names	Origin
Humic Acid		
	Purified Aldrich HA	Commercial
	Kranichsee HA	From the raised bog, Kleiner Kranichsee, Saxony
	Gohy-573-HA(H)II	From groundwater in Gorleben
Fulvic acid	DE72	From Derwent Reservoir, Derbyshire, UK
	FA-surface	-
Humic substances	Aldrich HA	Commercial
	Gohy-573-HS-(H)II	From groundwater in Gorleben
	water pond HS	From an artificial water pond at NERI, Roskilde

The first principal components t_1 and p_1

•Polarity descriptors:
High contents of substituted aliphatics (amino groups, carbohydrates), carboxylic acids/ester groups and ketonic/aldehyde carbons, as well as %O and the (N+O)/C ratio are characteristic for humic substances with high t_1 scores (water pond HS, FA-surface, and Gohy-573-HII).

• Aromaticity:
High aromaticity is quantified through the original variables: 272 nm absorptivity, aromatic/phenolic carbons, and %C. These descriptors are characteristic for humic substances with high negative score values (Gohy-573-HAII, Purified Aldrich HA and Kranichsee HA). The E2/E3 values, i.e. the absorbance at 250 nm divided by the absorbance at 365 nm, as well as the H/C ratio have high positive loading values, i.e., are inversely related to the other aromaticity descriptors, further underlining decreased aromaticity of the fulvic acids with respect to the humic acids.

• Average molecular weight:
The E4/E6 ratio, i.e. the absorbance at 465 nm divided by the absorbance at 665 nm, is assumed to quantify the size distribution of the humic substances, i.e., is inversely related to the average MW. Its high positive loading value is in agreement with an average MW of fulvic acids significantly smaller than the average MW of humic acids.

The descriptor A(top2) is the area of the low molecular weight peak in the size exclusion chromatogram. On the face of it the low molecular size fraction should be more predominant for fulvic acids than for humic acids. However, the systematic variation in the area of the integrated low molecular weight peaks, are best described by the variation of the 272 nm absorbances of the humic substances.

The second principal components t_2 and p_2

• Aliphatics:
The high loading of the unsubstituted aliphatic carbon descriptor in $\mathbf{p}_2$ reflects high aliphatic contents of the fulvis acid FA-surface. HA Aldrich has the lowest content of aliphatic structures, in agreement with the well-known high aromatic content of this humic substance.

The most significant original variables of $\mathbf{p}_3$ are %N and the ketonic and aldehyde C descriptors. The third latent variable shows that DE72 and Kranichsee has the lowest content of nitrogen, and the DEP72 differ from the rest of the humic substances by a significantly higher content of aldehyde/ketonic groups.

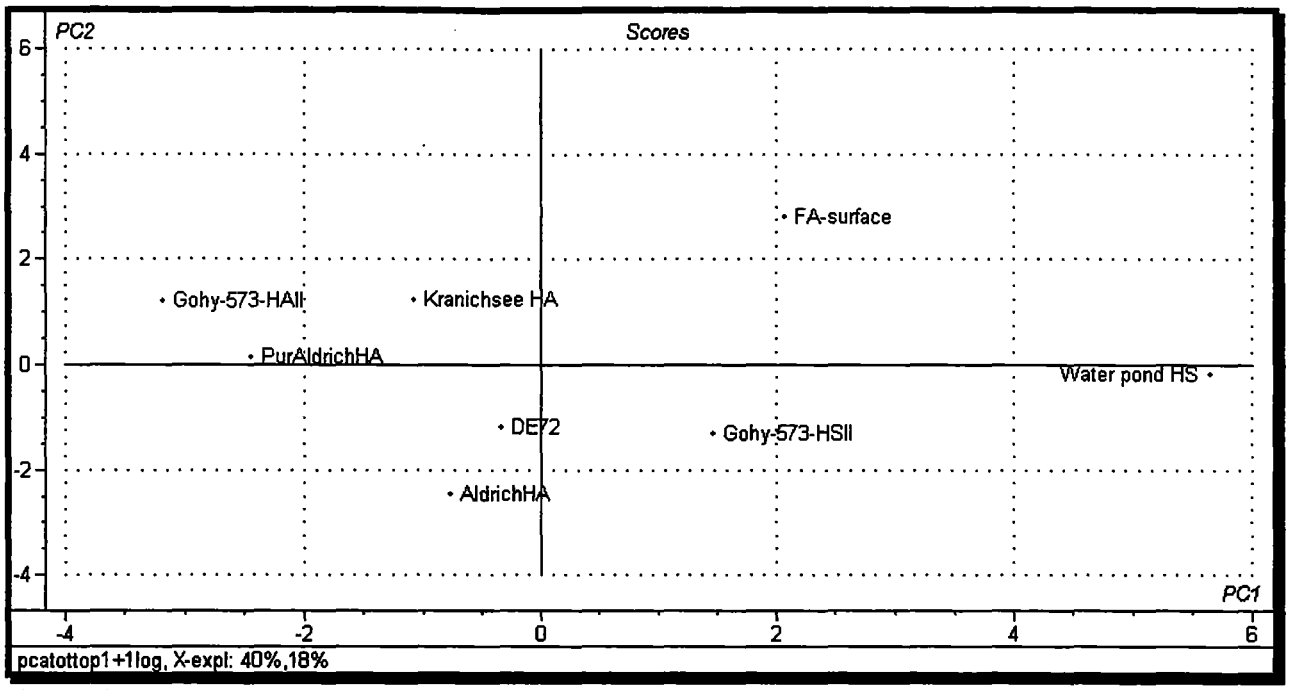

Figure 1. Score plot (t_2 versus t_1) of the humic substances.

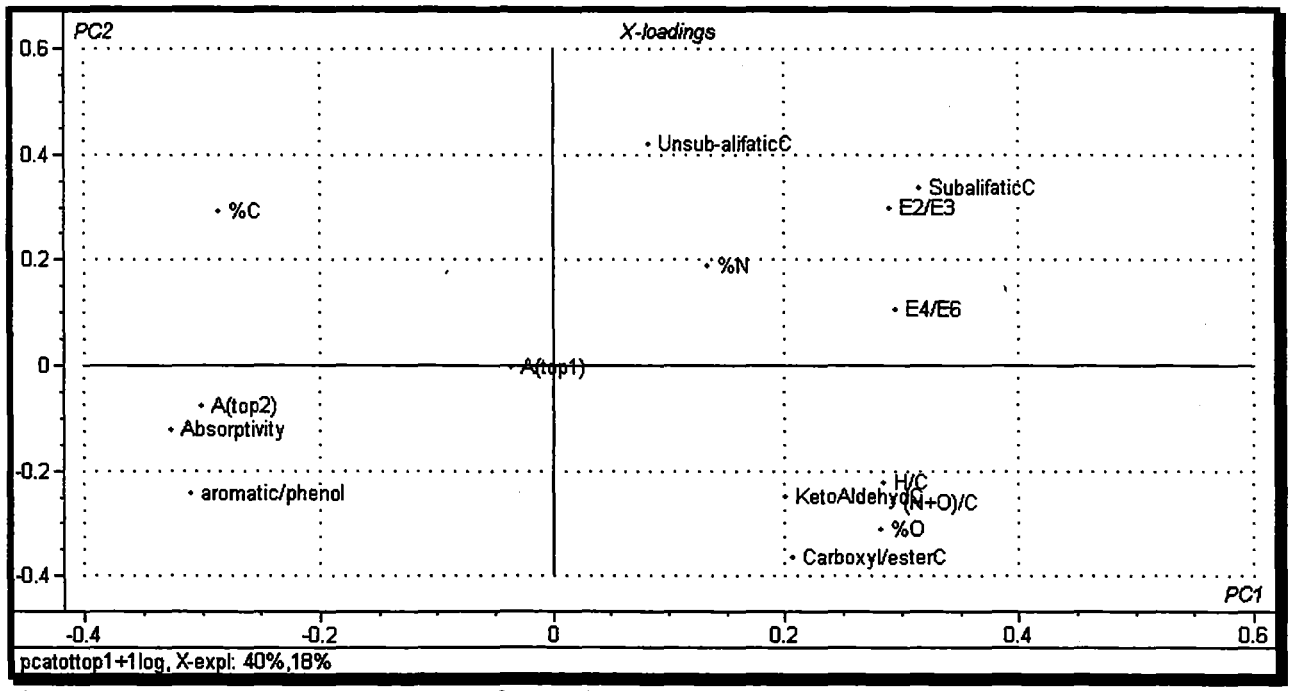

Figure 2. Loading plot (p_2 versus p_1) for the humic substances explaining 40 % and 18 % of the total X-variance, respectively.

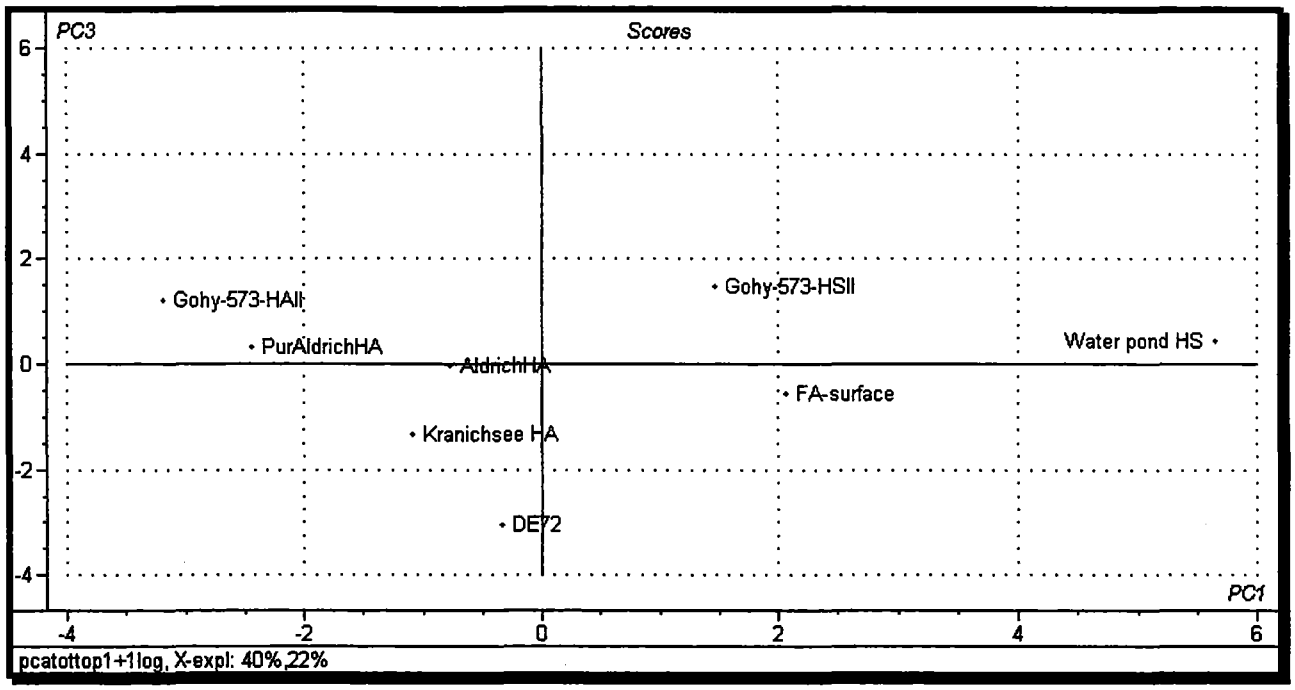

Figure 3. Score plot (t_3 versus t_1) of the humic substances.

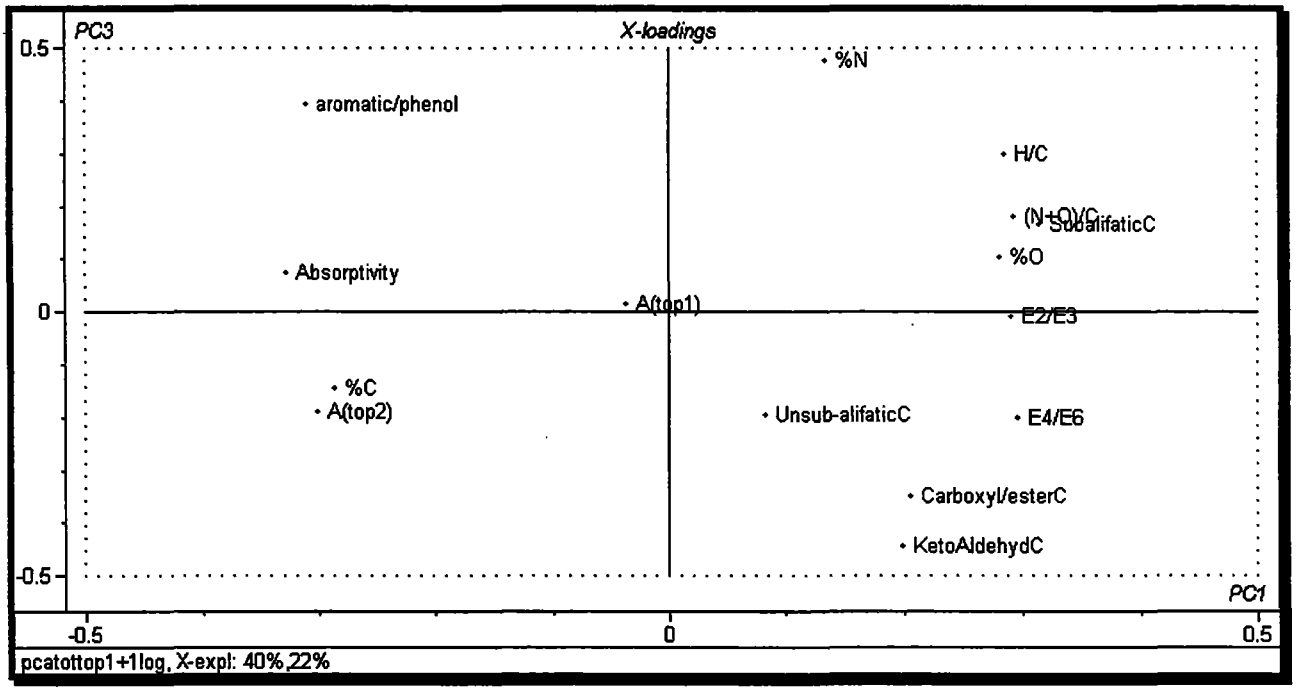

Figure 4. Loading plot (p_3 versus p_1) for the humic substances, the third latent variable explaining 22 % of the total X-variance.

Part 3: Characterization of Natural and Synthetic Humic Substances, Rock Material and Minerals at FZR-IfR

(K. Schmeide)

If not otherwise stated, then data given to Kranichsee humic and fulvic acid and Aldrich humic acid are from:

Schmeide K., Zänker H., Heise K.H., and Nitsche, H. (1998) Isolation and Characterization of Aquatic Humic Substances from the Bog 'Kleiner Kranichsee'. In: *FZKA 6124, Wissenschaftliche Berichte*, (G. Buckau, ed.). Forschungszentrum Karlsruhe, 161.

Schmeide K., Zänker H., Hüttig G., Heise K.H., and Bernhard G. (1999) Complexation of Aquatic Humic Substances from the Bog 'Kleiner Kranichsee' with Uranium (VI). In: *FZKA 6324, Wissenschaftliche Berichte*, (G. Buckau, ed.). Forschungszentrum Karlsruhe, 177.

and data for ^{14}C-M1 are from:

Pompe S., Bubner M., Schmeide K., Heise K.H., Bernhard G., and Nitsche H. (2000) Influence of Humic Acids on the Migration Behavior of Radioactive and Non-Radioactive Substances under Conditions Close to Nature. Synthesis, Radiometric Determination of Functional Groups, Complexation. Report: FZR-290, Wissenschaftlich-Technische Berichte, Rorschungszentrum Rossendorf.

Kranichsee humic acid (HA) and fulvic acid (FA) were isolated from the mountain bog "Kleiner Kranichsee" near Johanngeorgenstadt. The isolation procedure is described in Schmeide et al. 1998. The Kranichsee humic substances were primarily used for studies of the complexation with uranyl ions and for batch sorption experiments where the influence of humic acid on the uranium sorption onto the rock material phyllite was studied. The commercially available natural HA from Aldrich (Steinheim, Germany) was purified according to Kim and Buckau (1988) and used for comparison. Furthermore, a ^{14}C-labeled synthetic humic acid type M1 (^{14}C-M1) was used. It is synthesized from xylose, phenylalanine, and [2-^{14}C]glycine (Bubner et al. 1998) and has a specific activity of 59 MBq/g. Its concentration in solution can be easily determined by liquid scintillation counting (LSC). Furthermore, it is possible to determine directly the uptake of the ^{14}C-labeled humic acid onto rock materials by LSC measurements after combustion of the samples. Therefore, this ^{14}C-M1 was used for kinetic experiments investigating the sorption of uranium and humic acid onto rock materials and minerals.

All humic acids were comprehensively characterized by different analytical methods.

I. Natural and Synthetic Humic Substances

I.a Ash and Moisture Content

Thermoanalysis was used to determine the ash and moisture contents of humic substances (Table 1) (TG/DTA thermoanalyzer STA 92, Setaram, Lyon, France).

Table 1: Moisture and ash content in Kranichsee HA and FA, Aldrich HA and ^{14}C-M1 determined by thermoanalysis

Sample	Kranichsee HA	Kranichsee FA	Aldrich HA [a]	^{14}C-M1
Moisture content [%] (up to 110°C)	7.8	6.4	7.95	2.8
Ash content [%] (up to 800°C)	3.1[b]	2.0	0.5	0.7

[a] Aldrich humic acid, purified according to Kim and Buckau (1988).
[b] The oxidation residue is of brown color, similar to Fe_2O_3.

I.b Elemental Composition

Carbon, hydrogen, nitrogen and sulfur were analyzed by an elemental analyzer (Model CHNS-932, Leco, St. Joseph, MI, USA). The elemental composition of the humic substances is normalized to an ash- and moisture-free basis (100 % organic components). The oxygen content is calculated from the difference to 100 % (Table 2).

Table 2: Elemental composition of Kranichsee HA and FA, Aldrich HA and ^{14}C-M1 in comparison to literature data

Element [a] [%]	Kranichsee HA	Aldrich HA	^{14}C-M1	Literature [d] HA	Kranichsee FA	Literature [d] FA
C	49.9 ± 0.3	58.7 ± 0.6	63.9 ± 0.7	50 - 60	48.8 ± 0.06	40 - 50
H [b]	3.5 ± 0.4	3.3 ± 0.1	4.8 ± 0.3	4 - 6	2.6 ± 0.1	4 - 6
N	1.8 ± 0.1	0.8 ± 0.1	5.3 ± 0.1	2 - 6	0.6 ± 0.005	1 - 3
S	0.5 ± 0.01	4.1 ± 0.03	-	0 - 2	0.5 ± 0.02	0 - 2
O [c]	33.4 ± 0.3	24.8 ± 0.6	22.5 ± 0.5	30 - 35	39.1 ± 0.1	44 - 50
H/C	0.84	0.67	0.90	0.94 ± 0.12	0.63	1.02 ± 0.11
O/C	0.50	0.32	0.26	0.50 ± 0.03	0.60	0.51 ± 0.10

[a] Calculated on an ash- and moisture-free basis (100 % organic components); [b] Corrected for water content of samples; [c] Calculated as difference to 100 %; [d] according to Stevenson (1982)

The Kranichsee humic substances have a similar carbon and sulfur content. The hydrogen and especially the nitrogen content of the Kranichsee FA are lower than those of Kranichsee HA. A lower nitrogen content of fulvic acids compared to that of corresponding humic acids is also reported in the literature (Aiken et al. 1985; Rhee 1992).

The Kranichsee FA has a higher oxygen content than the Kranichsee HA and thus, a higher O/C atomic ratio. These values are typical of those compiled in the literature (Stevenson 1982; Kim et al. 1995).

The Aldrich HA has a somewhat different elemental composition than the Kranichsee humic substances which can be attributed to its different origin.

Table 2 also shows that the elemental compositions of the analyzed humic substances are similar to the average elemental compositions of humic substances given in the literature.

The elemental composition of ^{14}C-M1 is also close to the average literature values. ^{14}C-M1 does not contain sulfur since sulfur-free amino acids were used. The carbon and nitrogen content is higher and the oxygen content is slightly lower than those of Kranichsee HA and Aldrich HA.

I.c Major Inorganic Constituents

Inorganic constituents of humic substances were determined by atomic absorption spectrometry (AAS) and by inductively coupled plasma mass spectrometry (ICP-MS). The low concentrations of inorganic components, listed in Table 3, show that the Kranichsee humic substances were successfully purified.

I.d Functional Groups

The proton exchange capacity is determined by different methods. They are:

- Barium hydroxide method: The total proton exchange capacity (as sum of carboxylic and phenolic groups) is determined as the barium exchange capacity in alkaline medium (pH > 13). (Schnitzer and Khan 1972; Aiken et al. 1985)
- Calcium acetate method: The number of carboxylic groups is determined as the calcium exchange capacity in neutral medium (Schnitzer and Khan 1972; Aiken et al. 1985).
- The phenolic groups, as a measure of weak acidic groups, are calculated from the difference between the total acidity and the carboxylic group content.
- Direct titration: The content of proton exchanging functional groups that are deprotonated at the turning point of the titration curve in the neutral pH range (Aiken et al. 1985). The values fall between the carboxylic group capacities determined by the calcium acetate

method and the total proton exchange capacities. It is assumed that mainly the carboxylic groups and a small part of phenolic groups (acidic OH groups) are determined by this method.

- Radiometric method: The carboxylic, phenolic OH and ester groups are determined radiometrically by methylation with [^{14}C]-diazomethane according to the scheme shown in Figure 1 (Bubner and Heise 1994).

The results of the different methods are summarized in Table 4.

Table 3: Major inorganic components of Kranichsee HA and FA, Aldrich HA and ^{14}C-M1 determined by ICP-MS and AAS-F

Element	Kranichsee HA [ppm]	Kranichsee FA [ppm]	Aldrich HA [ppm]	^{14}C-M1 [ppm]
Na	1670 ± 20	10095 ± 268	226 ± 14	2451 ± 698
Mg	35 ± 12	87 ± 2	19 ± 3	206 ± 104
Al	149 ± 21	41 ± 11	93 ± 18	204 ± 179
K	324 ± 40	701 ± 28	36 ± 15	
Ca	708 ± 367	487 ± 130	611 ± 124	886 ± 604
Cr	9 ± 1	7 ± 0.5	32 ± 0.5	
Si	1780 ± 467	786 ± 131	372 ± 61	205 ± 128
Fe	1018 ± 30	296 ± 20	863 ± 40	< 250
Zn	16 ± 4	40 ± 27	n.d.	
Th	2 ± 0.2	n.d.	1 ± 0.1	
U	4 ± 0.3	2 ± 0.3	1 ± 0.2	

n.d.: not detected

According to the radiometric analysis, the total acidity and the carboxylic group content of the Kranichsee FA are only slightly higher than those of the Kranichsee HA. However, the carboxylic group content of the Kranichsee FA determined by Ca-exchange (6.05 meq/g) is much higher than the carboxylic group content determined radiometrically (3.98 meq/g). It is also higher than the proton exchange capacity determined by direct titration (5.6 meq/g). It can be assumed that the carboxylic group content of the FA determined by Ca-exchange is too high. One reason could be an incomplete filtration of FA during the calcium acetate method because it may contain acidic OH groups (Stevenson 1982) or other acidic protons that could also take part in the Ca exchange.

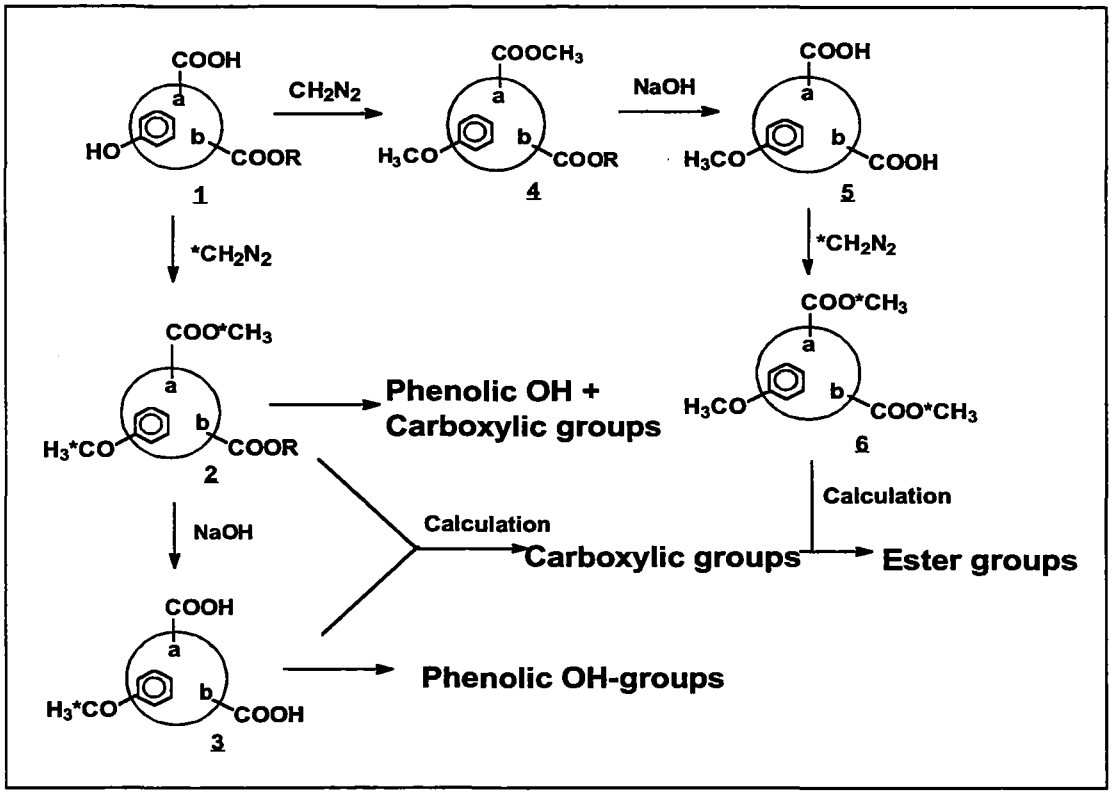

Figure 1: Determination of functional groups of humic substances by methylation with [^{14}C]diazomethane (*C = ^{14}C) (Bubner and Heise 1994)

The Aldrich humic acid contains more COOH and fewer phenolic OH groups than the Kranichsee HA.

The amount of functional groups, and especially the amount of carboxylic groups, determined for ^{14}C-M1 is lower than that of the natural humic acids.

I.e Capillary Zone Electrophoresis

Kranichsee HA and FA, Aldrich HA and Dervent FA were studied by capillary zone electrophoresis (P/ACE 2050 Beckman Instruments, Palo Alto, CA, USA). The separation conditions of the measurements were:

Buffer: 40 mM Na_2HPO_4, 20 mM H_3BO_3, pH 8.17; temperature 30 °C; separation voltage 15 kV, I: 84 µA; detection 214 nm; 15 s injection by means of pressure; fused silica capillary, 57 cm total length, 50 cm effective length, 75 µm inner diameter.

In Fig. 2, the electropherograms of the humic substances are shown. The peak shapes of the different humic substances are similar but there are differences in their migration time and in

their UV absorption. The longer migration time of the Kranichsee FA compared to that of Kranichsee HA is caused by its smaller molecular size and its somewhat higher number of dissociated functional groups. This confirms the results of the functional group determination. That means, the longer migration time of Kranichsee FA is caused by its higher charge-to-size ratio. Furthermore, the FA shows a slightly higher UV absorption.

Table 4: Functional groups of Kranichsee HA and FA, Aldrich HA and ^{14}C-M1

Determination method	Humic Acid	COOH + Phenolic OH	COOH [meq/g]	Phenolic OH
Barium hydroxide method	Kranichsee HA	10.17 ± 0.5	-	-
	Kranichsee FA	-	-	-
	Aldrich HA	7.12 ± 0.25	-	-
Calcium acetate method	Kranichsee HA	-	4.20 ± 0.17	5.97 ± 0.39 [a]
	Kranichsee FA	-	6.05 ± 0.31	-
	Aldrich HA	-	4.41 ± 0.11	2.71 ± 0.34 [a]
	^{14}C-M1	-	1.34 ± 0.05	
Radiometric method	Kranichsee HA	7.75 ± 0.35	3.88 ± 0.41	3.87 ± 0.52
	Kranichsee FA	8.82 ± 0.48	3.98 ± 0.25	4.84 ± 0.65
	Aldrich HA	7.4 ± 0.4	3.9 ± 0.1	3.4 ± 0.4
	^{14}C-M1			2.4 ± 0.1
Direct Titration [b]	Kranichsee HA		4.83 ± 0.18	
	Kranichsee FA		5.60 ± 0.12	
	Aldrich HA		5.06 ± 0.17	
	^{14}C-M1		1.69 ± 0.10	

[a] Calculated from the difference of total acidity (barium hydroxide method) and carboxylic group content (calcium acetate method).

[b] Proton Exchange Capacity

Aldrich HA exhibits both a longer migration time and a higher UV absorption intensity than the Kranichsee HA. This can also be attributed to a higher charge-to-size ratio. Presuming that both HA's have comparable molecular masses, a different amount of charge carriers must exist. According to the calcium acetate and the radiometric method, the COOH-content of Aldrich HA is higher than that of Kranichsee HA. Thus, the longer migration time of the Aldrich HA is caused by a larger amount of charge carriers. The higher UV absorption intensity could be caused by a greater number of UV-active groups (chromophores, such as conjugated double bonds, aromatic rings, phenolic functional groups).

Comparing both fulvic acids, it becomes obvious that the peak of Derwent FA is broader than that of Kranichsee FA. This can be attributed to a larger distribution of the charge-to-size ratio

of Derwent FA. Thus, the molecule fraction of the Kranichsee FA is more homogeneous than that of Derwent FA. Furthermore, the migration time of Derwent FA is slightly larger indicating a somewhat smaller molecular size and/or a higher amount of charge carriers due to a higher COOH content. The latter is confirmed by COOH determinations.

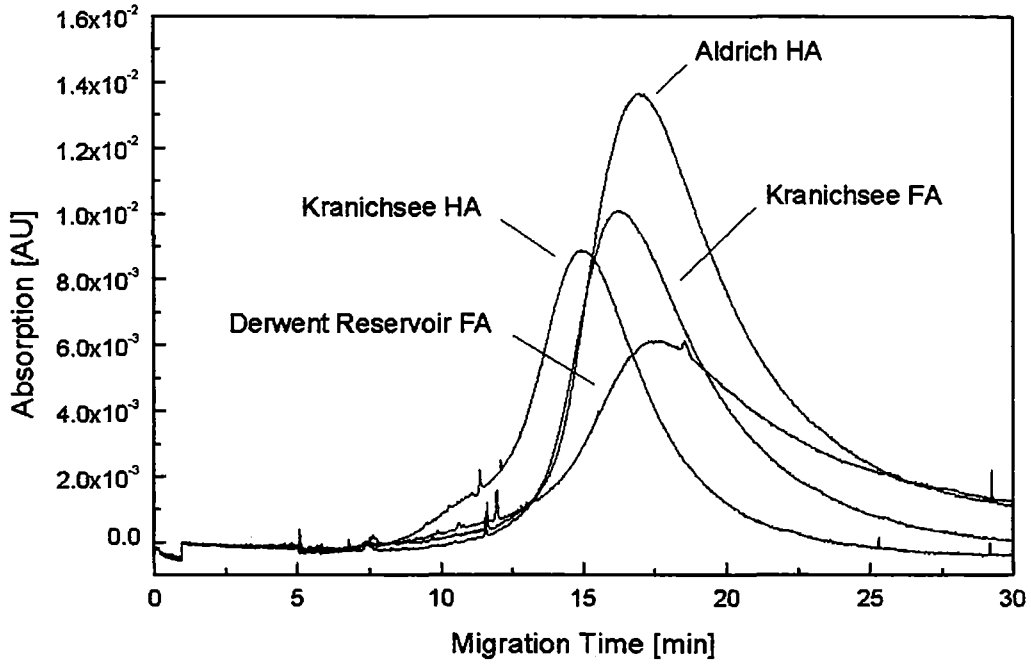

Figure 2: Electropherograms of Kranichsee HA and FA, Aldrich HA and Derwent HA. Buffer: 40 mM Na_2HPO_4, 20 mM H_3BO_3, pH 8.17.

From the electropherogram of the synthetic humic acid type M1 (not shown here) it is concluded that M1 is more homogeneous (smaller charge-to-size ratio distribution) than the natural humic acids. The shorter migration time of M1 is explained by a smaller charge-to-size ratio caused by a larger molecular size and a smaller number of dissociated functional groups. This corresponds to the lower total amount of functional groups as shown in Tab. 4. The larger molecular size of M1 compared to Aldrich HA was also determined by size exclusion chromatography.

I.f IR Spectroscopy

The results of IR spectroscopy of Kranichsee HA and FA, Aldrich HA and Derwent FA (Fig. 3) are discussed in detail in Schmeide et al. 1999. The IR absorption bands of M1 (not shown) are characteristic of natural humic acids. However, M1 has a greater amount of mono-substituted aromatic carbon structures than the natural humic acids. These structural elements

are caused by the use of phenylalanine as precursor. The lower content of carboxylic groups of M1 is also visible in the IR spectra.

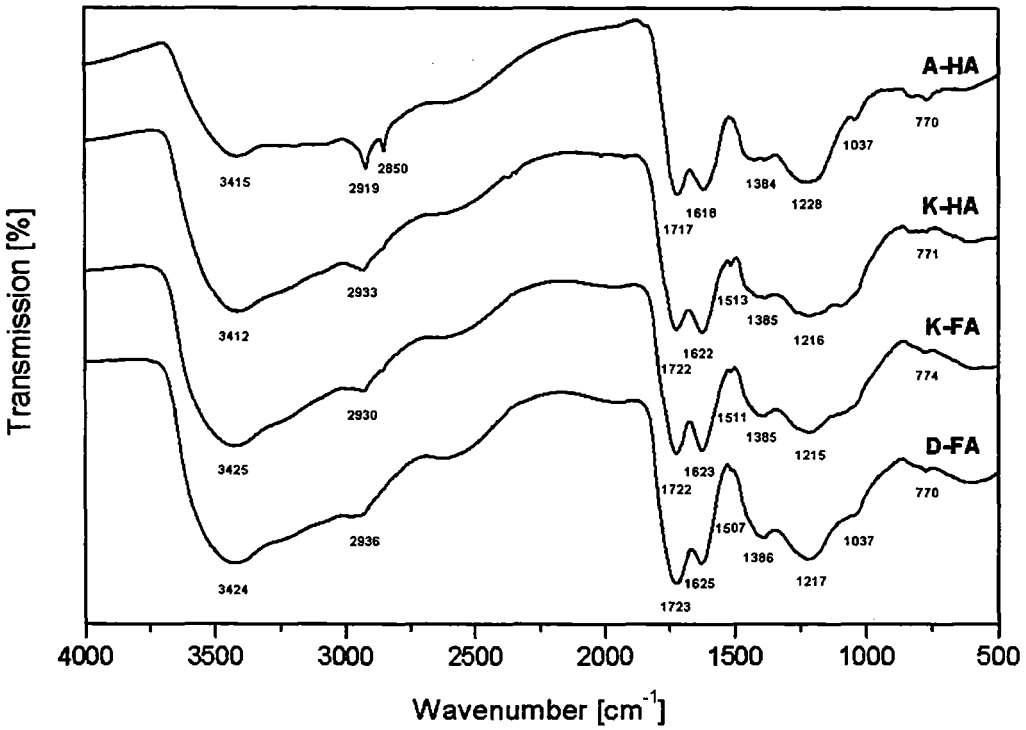

Figure 3: IR spectra of Kranichsee HA (K-HA), Kranichsee FA (K-FA) and Derwent FA (D-FA) compared to Aldrich HA (A-HA)

II. Rock Materials and Minerals

The following overview of the characterization of rock materials and minerals used for steady-state sorption and kinetic sorption experiments is extracted from:

Schmeide, K., Pompe, S., Bubner, M., Heise, K.H., Bernhard, G., and Nitsche, H. (2000) Uranium(VI) Sorption onto Phyllite and Selected Minerals in the Presence of Humic Acid, *Radiochim. Acta.* in press.

The rock material phyllite, and the minerals quartz, chlorite, muscovite, albite and ferrihydrite were used for sorption experiments.

The light-colored phyllite was obtained from the uranium mine 'Schlema-Alberoda' near Aue in Western Saxony, Germany. It was collected at a depth of 540 m. The phyllite is composed of 48 vol.% quartz, 25 vol.% chlorite, 20 vol.% muscovite, 5 vol.% albite, and 2 vol.% brownish opaqueous material, identified as Ti- and Fe-oxides (Arnold et al. 1998).

Quartz (SiO_2) was a commercially available fine-grained quartz (Merck, p.a.). Muscovite ($KAl_2[(OH)_2/Si_3AlO_{10}]$), chlorite ($(Mg,Fe)_3[(OH)_2/(Al,Si)_4O_{10}]\cdot(Mg,Fe,Al)_3(OH)_6$) and albite ($Na[AlSi_3O_8]$) were obtained as geological specimen. The 63 to 200 µm grain size fractions of the solids were applied for sorption experiments. The chlorite fraction was smaller than 40 µm. The specific surface areas, determined by the BET method, are 0.2 m^2/g for quartz, 0.2 m^2/g for albite, 1.4 m^2/g for muscovite, 1.6 m^2/g for chlorite and 4.0 m^2/g for phyllite. A more detailed characterization of the minerals is given elsewhere (Arnold et al. 1998).

Ferrihydrite ($Fe_2O_3\cdot H_2O$ (Dzombak and Morel 1990)) was precipitated from $1\cdot10^{-3}$ M iron(III) nitrate solution by slowly raising the pH to 7 (Cornell and Schwertmann 1996). This suspension was aged for 60 min before the pH was lowered to 5 and the ionic strength was adjusted to 0.1 M $NaClO_4$. The specific surface area of ferrihydrite is 600 m^2/g (Dzombak and Morel 1990).

References

Aiken G.R., McKnight D.M., Wershaw R.L. and MacCarthy P. (1985) *Humic Substances in Soil, Sediment and Water-Geochemistry, Isolation and Characterization.* John Wiley & Sons, New York, pp. 70, 191 and 199.

Arnold T., Zorn T., Bernhard G., and Nitsche H. (1998) Sorption of Uranium(VI) onto Phyllite. *Chemical Geology* 151, 129.

Bubner M. and Heise K.H. (1994) Characterization of Humic Acids. II. Characterization by Radioreagent-Derivatization with [^{14}C]Diazomethane. In: *Annual Report 1993*, Forschunszentrum Rossendorf, Institute of Radiochemistry, FZR-43, 22.

Bubner M., Pompe S., Meyer M., Heise K.H. and Nitsche H. (1998) Isotopically Labelled Humic Acids for Heavy Metal Complexation. *J. Labelled Compounds and Radiopharmaceuticals* XLI, 1017.

Cornell R.M., Schwertmann U.: *The Iron Oxides.* VCH, Weinheim 1996.

Dzombak D.A., Morel F.M.M.: *Surface Complexation Modeling –Hydrous Ferric Oxide.* John Wiley & Sons, New York 1990.

Kim J.I. and Buckau G. (1988) Characterization of Reference and Site Specific Humic Acids. In *RCM-Report 02188*, TU München, Institute of Radiochemistry.

Kim J.I., Artinger R., Buckau G., Kardinal Ch., Geyer S., Wolf M., Halder H. and Fritz P. (1995) Grundwasserdatierung mittels ^{14}C-Bestimmungen an gelösten Humin- und Fulvinsäuren. In *Abschlußbericht - RCM 00895*, TU München, Institut für Radiochemie, 86-92.

Pompe S., Bubner M., Schmeide K., Heise K.H., Bernhard G. and Nitsche H. (2000) Influence of Humic Acids on the Migration Behavior of Radioactive and Non-Radioactive Substances under Conditions Close to Nature. Synthesis, Radiometric Determination of Functional Groups, Complexation. Report: FZR-290, Wissenschaftlich-Technische Berichte, Forschungszentrum

Rossendorf.

Rhee D.S. (1992) Komplexierungverhalten der Huminstoffe mit dreiwertigen Aktinoidelementen in aquatischen Systemen, Dissertation, TU München.

Schmeide K., Zänker H., Heise K.H. and Nitsche H. (1998) Isolation and Characterization of Aquatic Humic Substances from the Bog 'Kleiner Kranichsee'. In: *FZKA 6124, Wissenschaftliche Berichte*, (G. Buckau, ed.). Forschungszentrum Karlsruhe, 161.

Schmeide K., Zänker H., Hüttig G., Heise K.H. and Bernhard G. (1999) Complexation of Aquatic Humic Substances from the Bog 'Kleiner Kranichsee' with Uranium (VI). In: *FZKA 6324, Wissenschaftliche Berichte*, (G. Buckau, ed.). Forschungszentrum Karlsruhe, 177.

Schmeide K., Pompe S., Bubner M., Heise K.H., Bernhard G. and Nitsche H. (2000) Uranium(VI) Sorption onto Phyllite and Selected Minerals in the Presence of Humic Acid., *Radiochim. Acta*, in press.

Schnitzer M., Khan S.U. (1972) *Humic substances in the environment.* (A.D. McLaren, ed.), Marcel Dekker, Inc., New York.

Stevenson F.J. (1982) *Humus Chemistry, Genesis, Composition, Reactions*. John Wiley & Sons, New York.

Part 4:
Silica Gel Coated with Humic Acid and Specific Functional Groups at GERMETRAD (C. Barbot and J. Pieri)

Humic acid coated silica gel is generated by covalent binding of purified Aldrich humic acid on activated epoxy silica. This system may be used to mimic the interaction of actinides with surface bound humic acid. For the purpose of studying the actinide humate interaction, this system also allows for easy separation between humic bound and free ions. Different organic substances are also attached to silica gel by covalent binding in order to study the interaction of different surface bound functional groups with actinide ions.

The coating process consists of two major steps, namely:
-silanization of the silica surface by reacting with glycidoxypropyltrimethoxysilane
-nucleophilic acid of the phenolic groups on epoxy silica groups.

Synthesis of humic gels

Humic acids purification

Humic acids, purchased from Aldrich on the form Na^+ have been purified by the method of Kim [1]:

- Humic acid is dissolved in 0.1 M NaOH and 0.2 g/g HA NaF in order to remove the silicates. The mixture is reacted 10 min and the pH is decreased to pH 7 with 6 M HCl, to prevent humic acid from degeneration by oxidation in contact with air oxygen.
- Humic acid is precipitated at pH 1, by acidification with 6 M HCl, and the supernatant is removed after centrifugation at 10 000 g for 30 min.
- Humic acid is redissolved in 0.1 M NaOH and precipitated again (pH 1).
- After three cycles of precipitation/redissolution, humic acid is washed with several times 0.1 M HCl.
- The purified and protonated humic acid is freeze-dried.

Epoxy activation of silica

Silica Sorbsil C500 40/60H, BET surface 320 m^2/g, pore volume 1.5 mL, is used as support for grafting glycidoxypropyltrimethoxysilane. After covalent binding, the epoxy gel is washed with organic solvents.

Humic acids grafting procedure on silica

- Humic acid is washed with distilled water and dried.
- In a Petri dish, epoxy silica is covered by humic acids solution dissolved in an organic solvent and dried at ambient temperature for at least 60 h.
- Humic gel thus obtained is washed with 0.1 M Tris and slightly acidic distilled water to remove physically adsorbed HA.
- This grafting procedure is repeated once again.

Characterization of the coated phases

Elementary analysis is performed at CNRS Vernaison.

I.R spectra are conducted on a IRTF Nicolet 510, detector DTGS window KBr, separatrice Ge/KBr, assisted by NICIR program for Mac. Spectra are recorded at a resolution of 2 cm^{-1}, averaging 200 scans.

BET surface was measured on ASAP 2010.

The proton exchange capacity of the humic gel is examined by pH titration with 0.1 M NaOH. The titration is performed with a Metrohm 726 titrator system. Prior to the titration, the electrode is calibrated with pH 4, 7 and 10 buffer. In a 100 mL vessel, humic gel is added to 50 mL 0.1 M $NaClO_4$. The vessel is sealed and Ar is bubbled into the solution for 1 hour prior to equilibration. The 0.1 M NaOH titrant is added in 0.05 mL increments every 10 minutes.

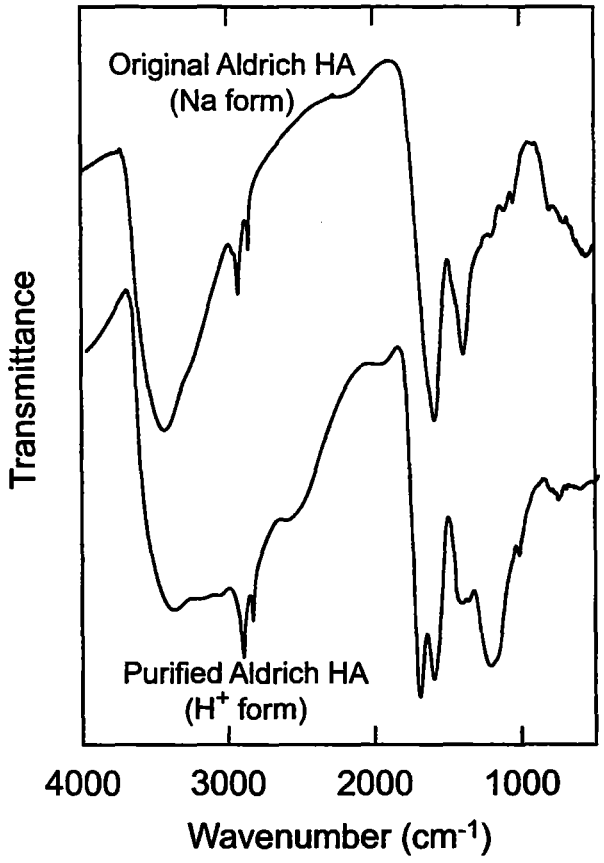

Fig 1: IR spectra of non-purified Aldrich humic acids on the form Na^+(dashed line) and purified humic acids (solid line)

Characterization of humic gel

The elementary composition (C: 54.24 %, H: 4.9 %, N: 0.7 %) and IR spectra (Fig. 1) of the purified humic acid show that purification was successful (cf. Kim 1998).
Two humic gels with different humic acid surface coating density were obtained (6.75 and 12.9 mg HA/g resin).
The pure silica original material has a BET surface of 320 m^2/g. After silanization as well as humic coating, the BET surface is 91-93 m^2/g.
The proton exchange capacity (PEC) of the two humic gels was measured by potentiometric pH titration. From the first derivative of the titration curve, average values of PEC are found to be 2.90 10^{-2} meq/g and 7.12 10^{-2} meq/g gel, for the 6.75 and 12.9 mgHA/g gel, respectively.

Synthesis of selected molecules on silica gel:

Silica gel coated with selected molecules were prepared to mimic different functional groups expected to be important for humic acid metal ion interaction. These gels are schematically described in Fig. 2 and some important properties are given in Table 1. An amino silica is reductively alkylated with an excess of glutaraldehyde. The use of cyanoborohydride reduces the intermediate Schiff base and then the product is reacted with the small molecules by the way of their amino groups for coupling.

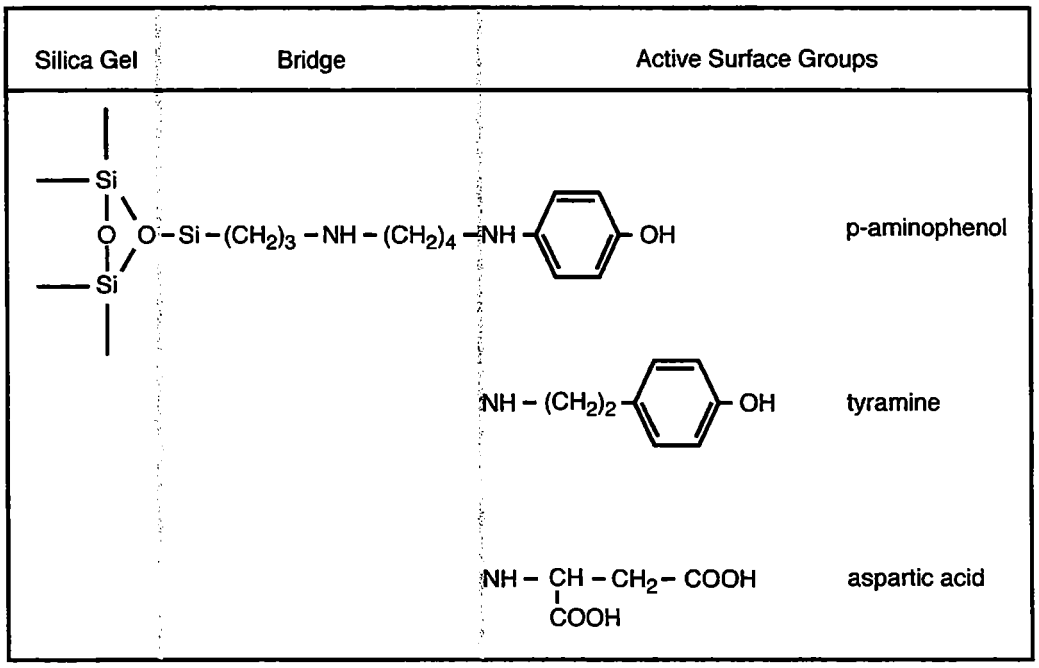

Fig. 2: Silica gels with specific functional group coating (GERMETRAD).

Table 1: Properties of silica gels with specific functional group coating (GERMETRAD).

	Gel:		
	Aminophenol	Tyramine	Aspartic acid
BET Surface area (m^2/g)	263	227	282
Carbon content in coating (%)	15.3	16.3	14.7
Surface coating (mg/g gel)	76.1-106	109-151	85.7-119
Molecule surface density ($\mu mol/m^2$)	1.55-1.83	1.76-2.07	1.43-1.69

References

Kim J.I. (1998) "Geochemistry of Actinides and Fission Products.", In: *Natural Aquatic systems*, CEC report EUR 11589 EN, ed. B. Come, 1988, p1-57